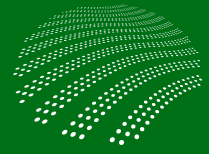


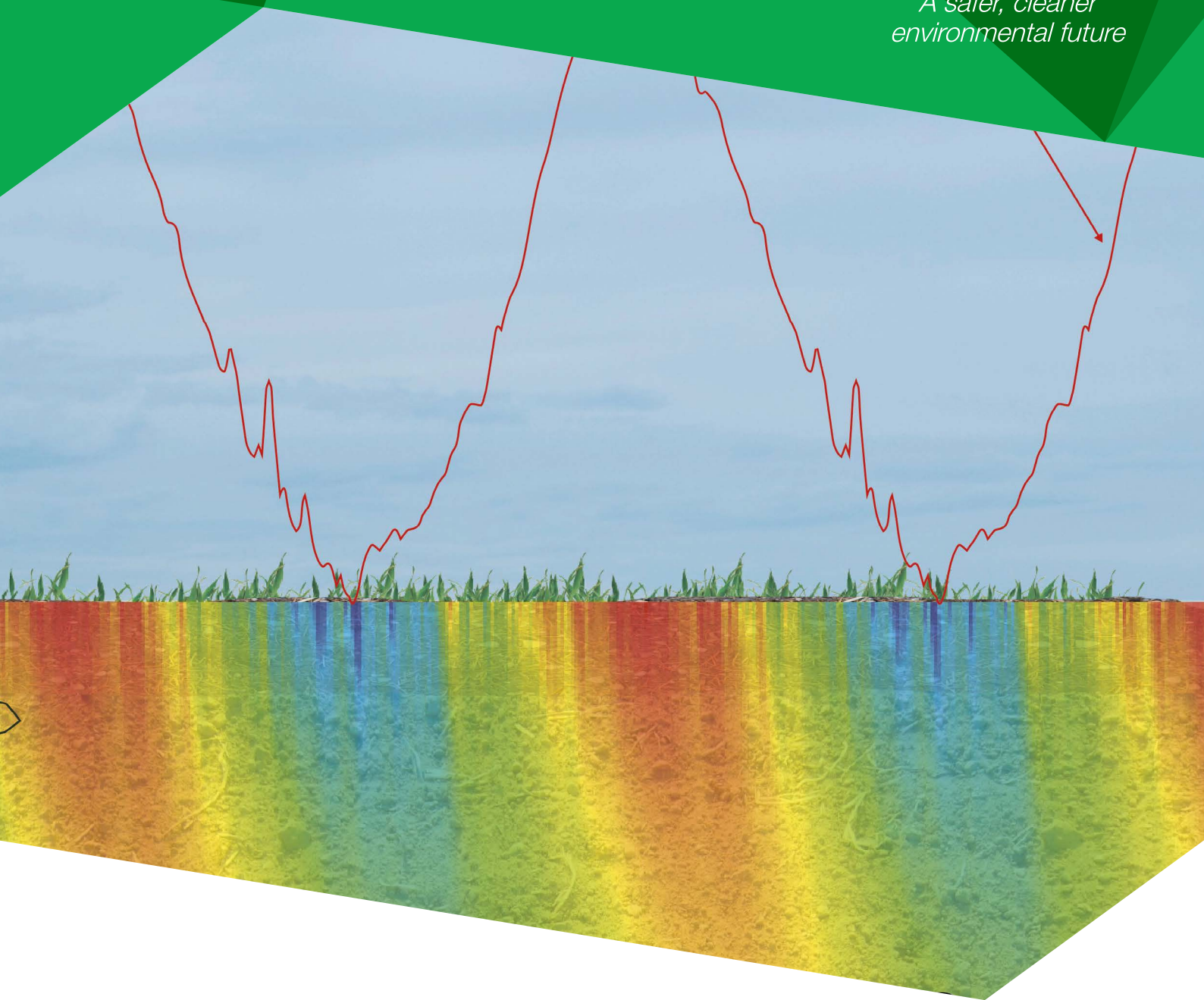
Cooperative Research Centre for **Contamination
Assessment and Remediation of the Environment**

www.crccare.com



CRCCARE

*A safer, cleaner
environmental future*



TECHNICAL REPORT NO. 44

Technical measurement guidance for LNAPL natural source zone depletion

Cooperative Research Centre for Contamination Assessment and Remediation of the Environment, Technical Report series, no. 44

August 2018

Copyright © CRC CARE Pty Ltd, 2018

This book is copyright. Except as permitted under the Australian Copyright Act 1968 (Commonwealth) and subsequent amendments, no part of this publication may be reproduced, stored or transmitted in any form or by any means, electronic or otherwise, without the specific written permission of the copyright owner.

ISBN: 978-1-921431-63-0

Enquiries and additional copies:

CRC CARE, C/- Newcastle University LPO, PO Box 18, Callaghan NSW, Australia 2308

Tel: +61 (0) 2 4985 4941

Fax: +61 (0) 8 8302 3124

admin@crccare.com

www.crccare.com

This report should be cited as:

CRC CARE 2018, *Technical measurement guidance for LNAPL natural source zone depletion*, CRC CARE Technical Report no. 44, CRC for Contamination Assessment and Remediation of the Environment, Newcastle, Australia.

Disclaimer:

This publication is provided for the purpose of disseminating information relating to scientific and technical matters. Participating organisations of CRC CARE do not accept liability for any loss and/or damage, including financial loss, resulting from the reliance upon any information, advice or recommendations contained in this publication. The contents of this publication should not necessarily be taken to represent the views of the participating organisations.

Acknowledgement:

CRC CARE acknowledges the contributions made by Tom Palaia and Luke Clements of Jacobs Engineering Group, Inc. towards the writing and compilation of this report.

Funding acknowledgement:

This work was supported by the Cooperative Research Centre for Contamination Assessment and Remediation of the Environment (CRC CARE), whose activity in this case was funded by National Energy Resources Australia (NERA), which is one of the Australian Government's Industry Growth Centres.

Cover image:

E-Flux LLC., USA.

CRC for Contamination Assessment and Remediation of the Environment

Technical Report no. 44

**Technical measurement guidance for LNAPL natural
source zone depletion**

August 2018



Executive summary

Natural source zone depletion (NSZD) is a term used to extend the traditional understanding of natural attenuation to the light non-aqueous phase liquid (LNAPL) source zone. It describes the collective, naturally occurring processes of dissolution, volatilisation, and biodegradation that result in mass losses of LNAPL petroleum hydrocarbon constituents from the subsurface. This document provides practical guidance on the measurement of NSZD rates using various available methods, including the following:

- Aqueous methods using dissolved contaminant concentration trends and natural attenuation indicator parameter (NAIP) mass budgeting analysis
- Soil gas flux methods using concentration gradients, passive flux traps, and the dynamic closed chamber (DCC)
- Biogenic heat method based on soil temperatures, and
- LNAPL compositional change method based on chemical analysis of the oil.

Significant advances have been made in the methods using gas flux and biogenic heat processes to measure NSZD. Traditional methods of measuring natural degradation rates using groundwater and LNAPL samples also remain viable. Monitoring the chemical changes in the LNAPL and applying this to NSZD rate estimates is an emerging method. Using the information contained herein, practitioners have what they need to select a method and implement NSZD monitoring at their site.

The main objective of this document is to provide a knowledge base and procedures for consistency in the measurement of NSZD in Australia. It leverages materials previously developed by the Cooperative Research Centre for Contamination Assessment and Remediation of the Environment (CRC CARE), as well as work from Commonwealth Scientific and Industrial Research Organisation (CSIRO), the United States (US) Interstate Technology & Regulatory Council (ITRC), US Geologic Survey (USGS), the American Petroleum Institute (API), and various universities. It captures the state of the practice and is useful as a guide to develop site-specific plans.

Like many environmental remediation monitoring methodologies, this is an evolving field, and the practical portions of the document are subject to change as new approaches evolve. Place the information in this document into proper context using a project team that is well-versed in site conditions and project data quality and need objectives.

This guidance is generally applicable to a wide range of environmental remediation sites containing petroleum hydrocarbon impacts in the subsurface. Its use is appropriate at sites that have a need for theoretical, qualitative, or quantitative understanding of NSZD processes.

API (2017) and Garg *et al* (2017) summarise emerging science related to method modifications (e.g. use of radiocarbon ^{14}C for background correction of the gradient and DCC measurements) and future research needs in NSZD measurement technology. The reader is advised to consult current literature for more recent advances and method improvements.

As NSZD is an evolving approach for managing the LNAPL source zones, it is critical that practitioners liaise closely with the regulator and/or auditor (if applicable) at the early stages of the project to obtain acceptance of the approach, and during implementation to ensure that the information generated is robust, defensible and useful for making decisions regarding site clean-up and (perhaps) closure.

Acknowledgements

Authors of technical report

Tom Palaia	Jacobs
Amy Jimmo	Jacobs
Nick Mahler	Jacobs
Consuelo Molinari	Jacobs
Luke Clements	Jacobs

Technical working group

Dennis Monahan	Chair
Anne Northway	VIC EPA
Janet Macmillan	WA DWER
Greg Davis	CSIRO Land and Water
Rod Lukatelich	CRC CARE/BP Australia Pty Ltd
Prashant Srivastava	CRC CARE

Project advisory group

Dennis Monahan	Chair
Janet Macmillan	WA DWER
Anne Northway	VIC EPA
Andrew Miller	WA DWER
Andrew King	BP Australia Pty Ltd
Brian Priestly	Monash University
Christopher Coombes	NT EPA
Colin Roberts	Caltex Australia Petroleum Pty Ltd
Craig Barnes	Air Services Australia
Daniel Walters	ACT EPA
Garbis Avakian	Australian Department of Defence
Holly Ainslie	Department of Infrastructure, Regional Development and Cities
Joanne Stuart	NSW EPA

Mirella Goetzmann	WA Department of Health
Paul Barrett	Australian Institute of Petroleum (AIP)
Peter Gniel	AIP
Rebecca Hughes	SA EPA
Rod Lukatelich	CRC CARE/BP Australia Pty Ltd
Tanya Astbury	Viva Energy Australia
Tony Bradshaw	Queensland Department of Environment and Science
Damien Davidson	Caltex Australia Petroleum Pty Ltd
Damien Home	Viva Energy Australia
Dave Thomas	Chevron Energy Technology Pty Ltd
John Mikac	ExxonMobil Environmental Services Company
Stuart Rhodes	Rio Tinto
Jack Ng	CRC CARE/University of Queensland
Prashant Srivastava	CRC CARE
Ravi Naidu	CRC CARE

Technical review

Greg Davis	CSIRO Land and Water
Andrew King	BP Australia Pty Ltd
John Raynor	CSIRO Land and Water
Trevor Bastow	CSIRO Land and Water
Julio A. Zimbron	E-Flux, LLC
Sanjay Garg	Shell Global Solutions (US) Inc.
Robert Sweeney	Environmental & Petroleum Geochemistry
Ean Warren	U.S. Geological Survey
Eric M. Nichols	Substrata LLC

Abbreviations

°C	Degrees Celsius
°K	Degrees Kelvin
°K/m	Degrees Kelvin per metre
%	Percent
%RE	Percent reference emitter
µmol/m ² /s	Micromoles per square metre per second
Acc-BP	Electron acceptors and by products
AMS	Accelerator mass spectrometry
API	American Petroleum Institute
AST	Aboveground storage tank
BTEX	Benzene, toluene, ethylbenzene, and xylenes
¹⁴ C	Carbon 14
C	Concentration
C ₈ H ₁₈	Octane
CH ₄	Methane
cm	Centimetre
CO ₂	Carbon dioxide
COC	Chemical of concern
CRC CARE	Cooperative Research Centre for Contamination Assessment and Remediation of the Environment
CSIRO	Commonwealth Scientific and Industrial Research Organisation
cv	Coefficient of variation
d	Day
dC	Change in concentration
dC/dz	Soil gas concentration gradient
DCC	Dynamic closed chamber
DEMDEL	Diethyl dimethyl lead
DIPE	Diisopropyl ether
D _{LNAPL}	Specific volume of in situ LNAPL
DO	Dissolved oxygen

$D_{m_{COC}}$	Change in mass content
D_v^{eff}	Effective vapour diffusion coefficient
EC	Electrical conductivity
EDB	Ethylene dibromide
E-Flux	E-Flux, LLC
EIC	Extracted ion chromatogram
EPH	Extractable petroleum hydrocarbons
ETBE	Ethyl tert-butyl ether
Fe	Iron
Fe^{2+}	Ferrous iron
Fe^{3+}	Ferric iron
g_{COC}/g_{LNAPL}	Grams of chemical of concern per grams of LNAPL
g_{COC}/m^3	Grams of chemical of concern per cubic metre
$g_{COC}/m^2/yr$	Grams of chemical of concern per square metre per year
GC-FID	Gas chromatograph-flame ionisation detector
GC/MS	Gas chromatograph/mass spectrometer
$g/m^2/d$	Grams per square metre per day
g/m^3-m	Gram per cubic metre by gram
$g/m^2/s$	Grams per square metre per second
$g/m^2-soil/s$	Grams per square metre of soil per second
$g/m^2/yr$	Grams per square metre per year
$g/m^3/yr$	Grams per cubic metre per year
H_2	Hydrogen
HC	Hydrocarbon
He	Helium
H_2O	Water
H_2S	Hydrogen sulphide
IRGA	Infrared gas analyser
ITRC	Interstate Technology & Regulatory Council
J	Flux
$J_{background}$	NSR-related flux
J_{NSZD}	NSZD-related gas flux

J_{total}	Total flux
$J/m^2\text{-soil/s}$	Joules per square metre of soil per second
$J/m/s/^\circ K$	Joules per metre per second per degree Kelvin
k	Bulk attenuation rate
kg/d	Kilogram per day
$kg/m^2/d$	Kilogram per square metre per day
$kg/m^2/yr$	Kilogram per square metre per year
kg/yr	Kilogram per year
kJ/g	Kilo Joules per gram
k_{point}	Point attenuation constant
L	Litre
L/d	Litre per day
$L/m^2/d$	Litre per square metre per day
LCSM	LNAPL conceptual site model
L/yr	Litre per year
LDRM	LNAPL distribution and recovery model
LIF	Laser-induced fluorescence
LNAPL	Light non-aqueous phase liquid
m	Metre
m^2	Square metre
m^3	Cubic metre
m^3/m^2	Cubic metre per square metre
m^3/m^3	Cubic metre per cubic metre
$m^3/m^2/yr$	Cubic metre per square metre per year
m^2/s	Square metre per second
m^3/yr	Cubic metre per year
MADEP	Massachusetts Department of Environmental Protection
MB	Mass budgeting
mbg	Metres below grade
mbtoc	Metres below top of casing
$mg/m^2/hr$	Milligrams per square metre per hour
MMT	Methylcyclopentadienyl manganese tricarbonyl

Mn	Manganese
Mn ²⁺	Soluble manganese
MNA	Monitored natural attenuation
m _r	Stoichiometric molar ratio of hydrocarbon degraded
MS-SIM	Mass spectrometer-select ion method
MtBE	Methyl tert-butyl ether
MTEL	Methyltriethyl lead
MW	Molecular weight
N ₂	Nitrogen
NA	Natural attenuation
NAIPs	Natural attenuation indicating parameters
nm	Nanometre
NO ₃	Nitrate
NRC	National Research Council
NSR	Natural soil respiration
NSZD	Natural source zone depletion
NWTPH	Northwest total petroleum hydrocarbon
O ₂	Oxygen
ORP	Oxidation reduction potential
PAH	Polycyclic aromatic hydrocarbon
PIANO	Paraffins, isoparaffins, aromatics, naphthenes, and olefins
PPE	Personal protective equipment
ppmv	Parts per million by volume
PVC	Polyvinyl chloride
QA	Quality assurance
QC	Quality control
q _H	Steady-state conductive heat flux
r ²	Coefficient of determination
R _{aq}	Aqueous reaction rate
RGB	Red green blue
RPD	Relative percent difference
s	Seconds

SIM	Select ion method
SO ₄ ²⁻	Sulphate
SOP	Standard operating procedure
SVE	Soil vapour extraction
SVOC	Semivolatile organic carbon
SW	US EPA methods from <i>Test Methods for Evaluating Solid Waste: Physical/Chemical Methods (SW-846)</i>
TBA	Tert-butyl alcohol
TEA	Terminal electron acceptor
TEL	Tetraethyl lead
TIC	Tentatively identified compound
TML	Tetramethyl lead
TPHCWG	Total Petroleum Hydrocarbon Criteria Working Group
US	United States
US EPA	United States Environmental Protection Agency
USGS	United States Geological Survey
UST	Underground storage tank
VOC	Volatile organic compound
VPH	Volatile petroleum hydrocarbons
yr	Year
z	Depth

Parameters

ΔH°	Heat of reaction or enthalpy (J/mol)
ΔT	Change in temperature ($^\circ\text{K}$)
$\Delta T/\Delta z$	Temperature gradient ($^\circ\text{K}/\text{m}$)
Δz	Change in distance (m)
A_c	Cross sectional area (m^2)
A_o	Amplitude of the sinusoidal curve ($^\circ\text{K}$)
b	Intercept coefficient of regression equation ($\text{g}/\text{m}^3/\text{yr}$)
C	Current chemical of concern concentration ($\text{g}_{\text{COC}}/\text{m}^3$)
C_0	Initial chemical of concern concentration ($\text{g}_{\text{COC}}/\text{m}^3$)
$C_{\text{clean-up}}$	Clean-up concentration (mg/L)
C_{max}	Initial concentration of gas injected, also referred to as the maximum concentration (ppb _v)
D	Biogenic heat method parameter equal to $\frac{2*\alpha^{0.5}}{w}$
d_1	Diameter of annulus (m)
d_2	Diameter of casing (m)
D_{air}	Molecular diffusion coefficient of air (cm^2/s)
$D_{\text{O}_2}^{\text{air}}$	Molecular diffusion coefficient for O ₂ in air (0.205 cm^2/s)
$D_{\text{tracer}}^{\text{air}}$	Molecular diffusion coefficient for the tracer gas in air (He = 0.703 cm^2/s ; SF ₆ = 0.089 cm^2/s)
dm_{coc}	Change in chemical content in the LNAPL ($\text{g}_{\text{COC}}/\text{g}_{\text{LNAPL}}$)
dC/dz	Soil gas concentration gradient ($\text{g}/\text{m}^3\text{m}$)
$D_{\text{O}_2}^{\text{eff}}$	Effective O ₂ vapour coefficient (m^2/s)
$D_{\text{tracer}}^{\text{eff}}$	Effective diffusion coefficient for the tracer gas (m^2/s)
dt	Change in time (d)
D_v^{eff}	Effective vapour diffusion coefficient (m^2/s), also known as effective diffusivity, that is specific to the soil and gas being measured
dz	Change in depth (m)
F_{sample}	Fraction of the fossil fuel based carbon in the sample (unitless)
F_{atm}	Fraction of the modern carbon in the contemporary living material (unitless)

$F_{m_{\text{fossil}}}$	Fraction of modern carbon the fossil base carbon (unitless)
$F_{m_{\text{sample}}}$	Fraction of the modern carbon in the sample (unitless)
h_1	Height of water column from base of well (m)
h_2	Length of filter pack (m)
h_{gw}	Saturated thickness of the plume (m^3/m^2)
i	Hydraulic gradient (m/m)
J	Steady state diffusive flux ($\text{g}/\text{m}^2\text{-soil}/\text{s}$)
$J_{\text{Background}}$	Flux associated with natural soil respiration processes ($\mu\text{mol}/\text{m}^2/\text{s}$)
J_{NSZD}	Background corrected soil gas flux ($\mu\text{mol}/\text{m}^2/\text{s}$)
J_{O_2}	O_2 flux ($\mu\text{mol}/\text{m}^2/\text{s}$)
J_{Total}	Total flux ($\mu\text{mol}/\text{m}^2/\text{s}$)
K	Average hydraulic conductivity of the plume (m/s)
k	Bulk attenuation rate, first order rate constant used in NA studies ($\text{g}/\text{m}^3/\text{yr}$)
k_{point}	Point attenuation rate constant ($\text{g}/\text{m}^3/\text{yr}$), first order rate constant (1/yr)
K_T	Thermal conductivity of the soil ($\text{J}/\text{m}/\text{s}/^\circ\text{K}$) that is specifying to the soil within the hydrocarbon oxidation zone
M	Mass (g)
m_r	Stoichiometric molar ratio (unitless)
MW	Molecular weight of the representative hydrocarbon (g/mol)
N	Effective porosity (m^3/m^3)
P	Period of the sinusoidal curve (s)
P_0	Initial pressure (kPa)
q_H	Steady state conductive heat flux ($\text{J}/\text{m}^2\text{-soil}/\text{s}$)
R	Universal gas constant ($\text{atm}\cdot\text{m}^3/(\text{kmol}\cdot\text{K})$)
R_{aq}	Aqueous reaction rate (g/d)
R_{COC}	Chemical-specific NSZD rate
$R_{\text{COC-aq}}$	Chemical of concern specific NSZD rate ($\text{g}_{\text{COC}}/\text{m}^2/\text{yr}$) calculated using aqueous methods
$R_{\text{COC-LNAPL}}$	Chemical of concern-specific NSZD rates in LNAPL ($\text{g}/\text{m}^2/\text{d}$)
R_{NSZD}	Total hydrocarbon degraded or NSZD rate ($\text{g}/\text{m}^2/\text{d}$)
S	Soil surface area (m^2)

T	Time (d or yr)
t_0	Initial time (yr)
T	Ambient temperature ($^{\circ}\text{K}$)
$T_{(z,t)}$	Soil temperature ($^{\circ}\text{K}$) at depth z and time t
T_0	Initial air temperature ($^{\circ}\text{K}$)
\bar{T}	Mean annual ambient temperature ($^{\circ}\text{K}$)
T_1	Background corrected soil temperature at the upper control point ($^{\circ}\text{K}$)
T_2	Background corrected soil temperature at the lower control point ($^{\circ}\text{K}$)
$t_{\text{clean-up}}$	Time required to reach the clean-up goal (year)
t_s	Duration of time between tracer injection and extraction (s)
V	Volume of the chamber headspace above ground surface (m^3)
V_D	Darcy velocity of groundwater flow (m/d, also known as the specific discharge)
V_o	Volume of the injected gas (m^3)
V_s	Volume of vapour extracted at the end of the test (m^3)
W	Angular frequency (s^{-1}) equal to $\frac{2\pi}{P}$
Y	Average LNAPL width (m)
YZ	Area perpendicular to groundwater flow (m^2)
Z	Average LNAPL thickness (m)
z_1	Depth at upper control point (m)
z_2	Depth at lower control point (m)
B	Tracer test parameter
H	Fraction of mass recovered during tracer test (unitless)
θ_T	Total porosity of the vadose zone soil within and above the hydrocarbon oxidation zone ($\text{m}^3\text{-pore}/\text{m}^3\text{-soil}$)
θ_v	Air-filled porosity ($\text{cm}^3\text{-vapour}/\text{cm}^3\text{-soil}$ or $\text{m}^3\text{-vapour}/\text{m}^3\text{-soil}$)
θ_w	Water filled porosity (m^3/m^2)
Λ	Biodegradation rate (1/yr)
ρ_{LNAPL}	LNAPL density (g/mL)
Ψ	Phase shift curve parameter (s)
α	Thermal diffusivity of the soil (m^2/s)

Table of contents

Executive summary	i
1. Introduction	1
1.1 Guidance objectives	1
1.2 Technical context and significance	1
1.3 Interrelation with other CRC CARE and industry guidance	2
1.4 Extension of natural attenuation concept	3
1.5 Overview of NSZD processes	4
1.6 Relevant site conditions	6
1.7 Measurement challenges	7
2. Measurement preparation	10
2.1 Establishing data use objectives and measurement scope	10
2.2 Review of the LNAPL conceptual site model (LCSM)	13
2.3 Measurement locations and relationship to LNAPL distribution	14
2.4 Effects of LCSM on NSZD rates	19
2.5 Characterisation for LCSM validation	20
2.5.1 Soil Gas Survey	20
2.5.2 Subsurface temperature	21
2.5.3 Chemical composition of LNAPL	21
2.6 Theoretical assessment	23
2.6.1 Analytical calculations and preparing a type curve	23
2.7 Overview of methods and guidance for method selection	23
2.8 Quality assurance/quality control documentation	24
3. Rate measurement using aqueous data	28
3.1 Use of dissolved contaminant concentration trends	28
3.2 Use of geochemical indicators of NSZD in groundwater	30
3.2.1 Natural attenuation indicating parameters (NAIPs)	31
3.2.2 Mass budgeting	33
3.3 Aqueous-based NSZD measurement quality assurance/quality control	34
3.4 Aqueous-based NSZD measurement considerations	36
4. Rate measurement using soil gas flux data	37
4.1 Stoichiometric calculation of NSZD rates using gas flux measurements	37
4.2 Common procedures using soil gas data	39
4.2.1 Background correction	39

4.2.2	Monitoring frequency	40
4.2.3	Ambient monitoring	40
4.2.4	Quality control and quality assurance	40
4.3	Gradient method	41
4.3.1	Gradient method key assumptions	41
4.3.2	Gradient method process	42
4.3.3	Gradient method quality assurance/quality control	45
4.3.4	Gradient method considerations	45
4.4	Passive flux trap method	46
4.4.1	Passive flux trap key assumptions	48
4.4.2	Passive flux trap method measurement process	48
4.4.3	Passive flux trap quality assurance/quality control	50
4.4.4	Passive flux trap method considerations	51
4.5	Dynamic closed chamber method	51
4.5.1	Dynamic closed chamber method key assumptions	52
4.5.2	DCC method measurement process	53
4.5.3	DCC quality assurance/quality control	56
4.5.4	DCC method considerations	57
5.	Rate measurement using temperature data	59
5.1	Biogenic heat method	59
5.1.1	Biogenic heat method key assumptions	59
5.1.2	Biogenic heat method process	61
5.1.3	Biogenic heat method quality assurance/quality control	67
5.1.4	Biogenic heat method considerations	67
6.	Rate measurement using LNAPL compositional change data	69
6.1	LNAPL weathering mechanisms	69
6.2	LNAPL compositional change method key assumptions	72
6.3	LNAPL compositional change method process	72
6.3.1	LNAPL sampling from in-well or soil samples	74
6.3.2	Laboratory analysis of LNAPL and soil	74
6.3.3	Regression analysis of chemical content in LNAPL	76
6.3.4	Calculation and mapping of LNAPL specific volume	76
6.3.5	Calculate the NSZD rate	77
6.4	NSZD emerging science	77
6.5	LNAPL compositional change method quality assurance/quality control	78

6.6 LNAPL compositional change method considerations	78
7. Conclusions	79
7.1 Summary of primary NSZD measurement guidance	80
8. References	82

Appendices

Appendix A. Overview of NSZD processes	89
Appendix B. NSZD rate measurement checklists	97
Appendix C. Procedures to measure the aqueous portion of NSZD	115
Appendix D. Gradient method-based NSZD evaluation procedures	139
Appendix E. Passive flux trap-based NSZD evaluation procedures	176
Appendix F. Dynamic closed chamber-based CO ₂ NSZD evaluation Procedure	219
Appendix G. Biogenic heat method-based NSZD evaluation procedures	239

Boxes

Box 2.1. Type curve construction for NSZD rate assessment	25
Box 3.1. Measurement of the aqueous portion of NSZD	35
Box 4.1. Gradient method of NSZD rate calculation	43
Box 4.2. Passive flux trap method of NSZD rate calculation	47
Box 4.3. Dynamic closed chamber method of NSZD rate calculation	54
Box 5.1. Biogenic heat method of NSZD rate calculation	62
Box 6.1. LNAPL composition change for chemical-specific NSZD rates	75

Tables

Table 1. Interrelationship between CRC CARE guidance on natural attenuation processes	3
Table 2. Summary of site conditions that physically or logistically affect vapour phase-related NSZD monitoring	8
Table 3. Typical NSZD monitoring data use objectives and scopes of work	11
Table 4. Key elements of the LCSM and how they relate to NSZD measurement	13
Table 5. Laboratory analytical options for whole-oil and forensic evaluation of LNAPL mass losses	22
Table 6. Summary of key attributes of NSZD measurement methods	26

Table 7.	Summary of first-order rate constants for natural attenuation studies	29
Table 8.	Evaluation of geochemical indicators (NAIPs) and preferable biodegradation reactions	32
Table 9.	Aqueous method uncertainty and variability considerations	36
Table 10.	Example representative hydrocarbons and CO ₂ stoichiometric conversion factors	38
Table 11.	Parameter units involved in estimating NSZD rates from gas flux measurements	38
Table 12.	Gradient method uncertainty and variability considerations	45
Table 13.	Passive flux trap method uncertainty and variability considerations	51
Table 14.	Dynamic closed chamber method uncertainty and variability considerations	58
Table 15.	Biogenic heat method uncertainty and variability considerations	67

Figures

Figure 1.	Extension of natural biological process monitoring from groundwater to vadose zone	4
Figure 2.	Comprehensive conceptualisation of petroleum hydrocarbon natural source zone depletion processes	6
Figure 3.	Decision logic flowchart for selection of NSZD measurement data quality levels	12
Figure 4.	NSZD monitoring locations at a site with LNAPL release into clean sands	14
Figure 5.	NSZD monitoring locations at a site with LNAPL release into fill	15
Figure 6.	NSZD monitoring locations at a site with LNAPL release into granite or igneous rock	16
Figure 7.	NSZD monitoring locations at a site with LNAPL release into interbedded sand and silt/clay	17
Figure 8.	NSZD monitoring locations at a site with LNAPL release into marine clays	18
Figure 9.	NSZD monitoring locations at a site with LNAPL release into limestone	19
Figure 10.	Hypothetical soil gas concentration profiles for background, low-moderate, and high NSZD rates	20
Figure 11.	Decay rate estimate using dissolved contaminant concentrations (benzene) and the regression function	30

Figure 12.	Example X-Y scatter plots of geochemical indicators (NAIPs) of biodegradation	32
Figure 13.	Schematic of gradient method soil gas monitoring setup	42
Figure 14.	Schematic and actual trap side-by-side comparison	48
Figure 15.	LI-COR 8100A dynamic closed chamber (DCC) soil gas flux system	52
Figure 16.	Example output from a CO ₂ efflux measurement using a DCC soil flux system	55
Figure 17.	Schematic of a biogenic heat method monitoring setup and a typical background-corrected NSZD temperature profile	60
Figure 18.	Annual average temperature profiles at a site and background corrected temperature profile	61
Figure 19.	Soil temperature variability at a site with a warm climate	63
Figure 20.	Soil temperature (°C) variability at a site with a temperate climate	64
Figure 21.	Laser-induced fluorescence log in condensate LNAPL source zone	70
Figure 22.	Change in gasoline, diesel fuel, and Bunker C composition during biodegradation	71
Figure 23.	Change in gasoline, diesel fuel, and Bunker C composition during biodegradation	72
Figure 24.	Linear regression analysis on the change in total BTEX content in LNAPL over time	77

1. Introduction

The Cooperative Research Centre for Contamination Assessment and Remediation of the Environment (CRC CARE) has released a series of technical reports on the assessment, management, and remediation of light non-aqueous phase liquid (LNAPL) petroleum hydrocarbons in the subsurface. These technical reports summarise comprehensive research on the strategies to assess and remediate LNAPL, as well as on the treatment of the vapour and dissolved-phase components attributable to the LNAPL source.

This technical report is intended as a practical guide for measuring natural source zone depletion (NSZD) in Australia. NSZD is an emerging management strategy for LNAPL source zones. This guide is intended to be the primary technical resource for a consistent, robust approach to the measurement of NSZD across Australia for the ultimate purpose of improving decision making at petroleum hydrocarbon remediation sites.

1.1 Guidance objectives

This guidance contains practical materials that environmental remediation practitioners planning and implementing NSZD monitoring will find immediately useful. To keep the guidance in this document focused on practical content, it includes essential theory referencing other technical resources for further details (API 2017 and ITRC 2018). The document contains checklists that Australian auditors and regulators can use to ensure appropriate measurement and data analysis quality assurance (QA)/quality control (QC). It also contains information boxes and appendices that practitioners can pull out and drop into a work plan, for example. The appendices are intended to be procedures that can be directly followed to meet the minimum QA/QC requirements stated on the checklists.

With respect to the content of this guidance, the following factors were considered to decide whether to include certain technical information (or exclude if not met):

1. Published in peer-reviewed literature
2. Well-developed with established industry-accepted field and analytical procedures, and
3. Gaining acceptance by the regulatory community.

1.2 Technical context and significance

It is well-established that after an oil release into the environment, petroleum hydrocarbon constituents in the oil (also known as LNAPL) undergo biodegradation (Kostecki & Calabrese 1989; NRC 2000; Johnson *et al* 2006; Garg *et al* 2017). A new scientific term, NSZD, has emerged over the past decade that better explains these biological processes. NSZD is a term used to describe the collective naturally occurring processes that result in mass losses of LNAPL (ITRC 2009). These processes physically degrade the LNAPL by mass transfer of chemical components to the

aqueous and gaseous phases, waterborne biodegradation, and direct-contact oil biodegradation (Ng *et al* 2014).

Traditional methods of NSZD monitoring (i.e. monitored natural attenuation (MNA) of dissolved-phase contaminants in groundwater) have focused on biodegradation processes that manifest themselves as changes in the groundwater. Aerobic respiration, denitrification, iron and manganese reduction, sulphate reduction, and methanogenesis each support hydrocarbon degradation. Through stoichiometric conversion of the mass of electron acceptor loss and by-product formation, the aqueous portion of NSZD can be estimated using traditional methods (Beck & Mann 2010).

However, understanding of the often significant gaseous expression of NSZD processes has recently improved. A large advance occurred with respect to the measurement and quantification of the gases that are produced from petroleum hydrocarbon biodegradation processes, predominantly methanogenesis. In summary, NSZD processes occurring within the subsurface manifest themselves as changes to both the aqueous and gaseous phases. Emerging best practice for quantifying the total NSZD rate is now a summation of the petroleum hydrocarbon stoichiometric mass loss equivalents from both phases.

Quantifying site-specific NSZD rates is important for various reasons:

1. NSZD forms an important part of the LNAPL conceptual site model (LCSM); the written and/or illustrative representation of the physical, chemical and biological processes that control the transport, migration, and actual/potential impacts of contamination. Within the LCSM, NSZD establishes a remediation baseline and supports interpretation of contaminant delineation and concentration trends.
2. NSZD rates typically range from 2,000 to 30,000 litres of LNAPL degraded per hectare per year and can be larger than engineered remedies (Palaia 2016; Garg *et al* 2017).
3. Measured NSZD rates can also form the basis for remediation technology selection, design, and optimisation. For example, comparing LNAPL mass removal rates from NSZD to other current or future potential remedial action and using NSZD rates as an endpoint for active remediation. Throughout the remediation life cycle, measured NSZD rates can be used for a variety of decision-making purposes, ranging from technology selection to system shutdown or site closure.

1.3 Interrelation with other CRC CARE and industry guidance

This guidance was prepared to relay relevant new science on natural attenuation of petroleum hydrocarbons, a historical topic of interest to CRC CARE. As such, it overlaps with several prior documents. Table 1 lists the CRC CARE technical reports that discuss natural processes and states whether this new guidance supersedes, supports, or augments the existing information.

In general, this guidance augments existing documents, including *CRC CARE Technical Report 15, A technical guide for demonstrating monitored natural attenuation of petroleum hydrocarbons in groundwater* (Beck & Mann 2010).

Table 1. Interrelationship between CRC CARE guidance on natural attenuation processes

Publication date	Report number	Title	Relevance
December 2006	3	<i>Natural attenuation: a scoping review</i> (McLaughlan <i>et al</i> 2006)	Supersedes
March 2009	12	<i>Biodegradation of petroleum hydrocarbon vapours</i> (Davis <i>et al</i> 2009a)	Supports
September 2010	15	<i>A technical guide for demonstrating monitored natural attenuation of petroleum hydrocarbons in groundwater</i> (Beck & Mann 2010)	Augments
September 2010	18	<i>Selecting and assessing strategies for remediating LNAPL in soils and aquifers</i> (Johnston 2010)	Augments
July 2013	23	<i>Petroleum hydrocarbon vapour intrusion assessment: Australian guidance</i> (CRC CARE 2013)	Supports
February 2015	34	<i>A practitioner's guide for the analysis, management and remediation of LNAPL</i> (CRC CARE 2015)	Augments

Additionally, this guidance draws on the wealth of literature on NSZD and on the documented experience of remediation practitioners. Of particular importance are prior guidance documents written by the CRC CARE, United States (US) Interstate Technology & Regulatory Council (ITRC), and the American Petroleum Institute (API) whom are cited in this document. Relevant content from all the aforementioned documents is referenced to highlight connections between documents where appropriate.

1.4 Extension of natural attenuation concept

Knowledge of the existence of the comprehensive set of NSZD processes was recognised in the 1990s (Revesz *et al* 1995; Stout & Lundegard 1998; Wiedemeier *et al* 1999; Hers *et al* 2000; Chaplin *et al* 2002; Amos *et al* 2005). However, the large magnitude of its contribution to LNAPL depletion and its methods of measurement were not well understood. For example, *CRC CARE Technical Report 15* mentions methanogenesis and methane gas production, but does not recommend monitoring it (Beck & Mann 2010). It is postulated that NSZD processes have historically been underestimated due to inadequate connectivity between research and practice and imperceptions of importance to remediation decision making. Recent work from the Commonwealth Scientific and Industrial Research Organisation (CSIRO), University of Waterloo, University of British Columbia, US Geological Survey (USGS), Arizona State University and Colorado State University has changed that (Davis *et al* 2005; Amos *et al* 2005; Johnson *et al* 2006; Sihota *et al* 2011; McCoy *et al* 2014).

NSZD is considered an extension of the natural attenuation concept. As shown in figure 1, where MNA formerly measured biodegradation processes in groundwater, NSZD now extends monitoring to within and above the source (LNAPL) zone, again, where no previous natural attenuation monitoring was recommended.

NSZD is not considered a new remediation technology. The overall conceptualisation of the source zone (i.e. free, trapped, and dissolved phases in the case of figure 1) and

the occurrence of biological degradation processes are the same. What has changed is the understanding of the biodegradation by-products overlying the source zone and their import to the total quantification of natural losses. These are described in more detail in the following section.

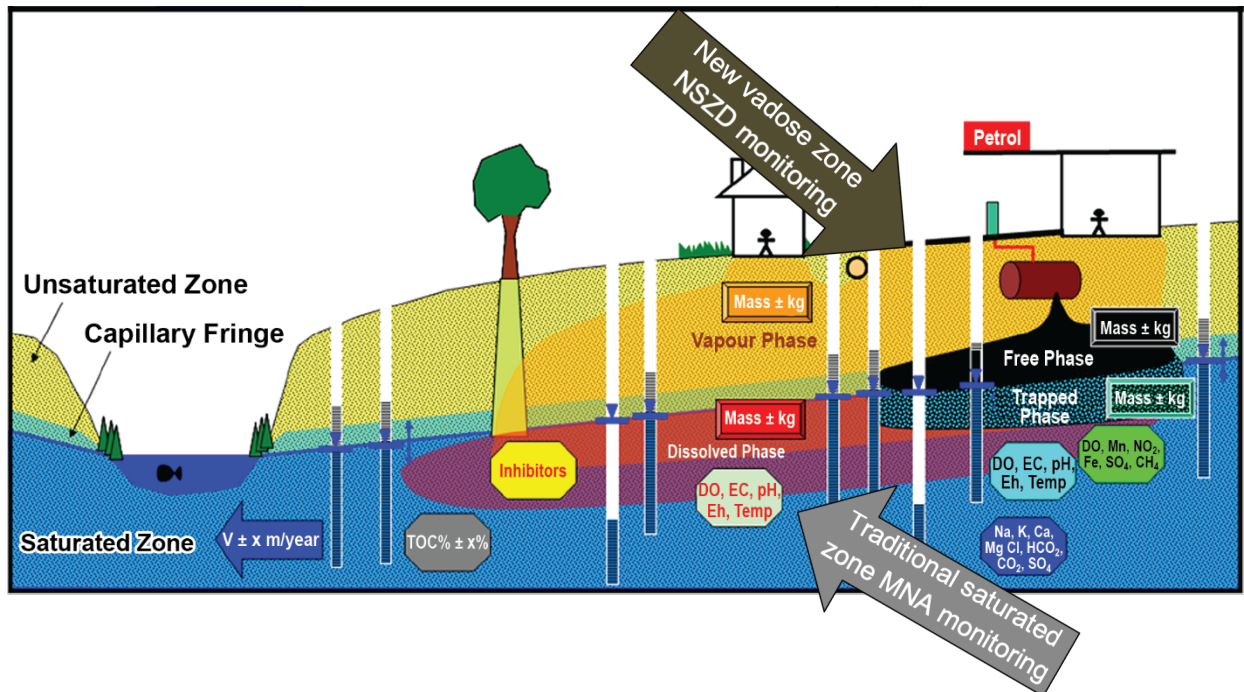


Figure 1. Extension of natural biological process monitoring from groundwater to vadose zone.
 Modified from Figure 9 of CRC CARE Technical Report 15, Beck & Mann (2010).

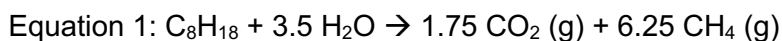
1.5 Overview of NSZD processes

The microbial communities present in soil and groundwater at LNAPL release sites adapt and acclimate as the LNAPL degrades over time. For example, as the more volatile hydrocarbon constituents leave the LNAPL during the early stages of a release, volatilisation rates decrease, and the most significant mass loss mechanism transitions to biodegradation (Chaplin *et al* 2002). The bioactivity in the source zone changes to acclimate to sequentially less thermodynamically favourable conditions (i.e. methane (CH₄) producing), and may ultimately result in methanogenic conditions in zones where electron acceptors are depleted. For the purposes of conceptualisation, it is assumed that a microbial population associated with NSZD of an LNAPL body in a middle- to late-stage (i.e. the LNAPL is stable and largely near residual saturation) stabilises and achieves a pseudo-steady state. The subsequent discussion is based upon this assumption.

Emerging research has recently improved the understanding of the gaseous expression of NSZD processes (Davis *et al* 2005; Amos *et al* 2005; Johnson *et al* 2006; Sihota *et al* 2011; McCoy *et al* 2014). A large advance occurred with respect to the quantification of the gases that are produced from petroleum hydrocarbon

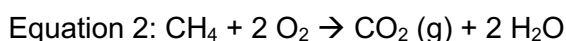
biodegradation processes, predominantly methanogenesis. At the Bemidji site¹ in the US, the gaseous expression of NSZD (i.e. the CH₄) has been shown to account for greater than 70 percent (%) of the hydrocarbon biodegradation that occurs in the subsurface (Molins *et al* 2010)².

Gases are produced in both the saturated and vadose zones where LNAPL biodegradation is occurring. Under anaerobic conditions, methanogenic organisms consume hydrocarbons to create CH₄ gases as demonstrated by the summary reaction in equation 1.



Degassing of excess CH₄ occurs along with the outgassing effects of direct-contact oil biodegradation because of the relatively low solubility of CH₄ within the highly reduced saturated zone and overlying capillary fringe (Garg *et al* 2017). CH₄ is subsequently transported up into the vadose zone along with smaller amounts of carbon dioxide (CO₂) (from the reaction in equation 1) and volatile organic compounds (VOCs) from residual volatilisation processes, if persisting.

Counter-current to the upward transport of CH₄ and VOCs is the downward transport of oxygen (O₂) from atmosphere. Where the CH₄ and O₂ meet in the vadose zone, a relatively thin hydrocarbon oxidation zone exists where CO₂ is generated according to equation 2.



Within the vadose zone where the gases meet, heat is also created via the exothermic oxidation reaction. A new composite conceptualisation of these vapour transport-related NSZD processes that are occurring at petroleum release sites is shown in figure 2.

The various discussed signatures of NSZD can be exploited to quantify petroleum hydrocarbon mass loss rates. The methods are aligned with the following three ways in which NSZD manifests itself:

- aqueous (dissolved by-product-related)
- gaseous (vapour by-product-related), and
- heat (vapour by-product-related).

The total NSZD rate is a summation of the reaction by-products that include both dissolved and vapour changes. The aqueous methods account for the dissolved by-products. The vapour by-products can be accounted using either the gaseous method or the biogenic heat method. Each is described in detail in appendix A.

It is important to note that NSZD rates are expected to decline as LNAPL source mass is depleted over the multiple decades of time that it will persist in the subsurface

¹ Several research sites have been critical to the understanding of NSZD and facilitated application to other petroleum hydrocarbon-impacted sites. Since 1983, significant research has taken place at the USGS Bemidji Crude-Oil Research Project site, near Bemidji, Minnesota, US.

² Research concerning NSZD processes began in the early 2000s. At 47°28'25" north latitude (Melbourne is 37°48'49" south latitude), it is situated in a temperate/subarctic climate zone with short warm summers, long cold winters, an annual average daily high temperature of 10 degree Celsius (°C), and an average annual precipitation of 68 centimetres (cm). The 1,700 cubic metres (m³) crude oil pipeline release occurred in glacial outwash soils consisting of sand and gravel with thin fine sand and silt interbeds (mn.water.usgs.gov/projects/bemidji/index.html; en.wikipedia.org/wiki/Bemidji,_Minnesota).

(Revesz *et al* 1995). Biodegradation results in significant changes to the composition of petroleum after its release with the compound types altered in an apparent stepwise depletion of compounds in a specific order, based on their susceptibilities to biodegradation (Volkman *et al.*, 1984 and Kaplan *et al.*, 1996), possibly due to the compounds undergoing biodegradation at different rates. However, there is no published data on the change in NSZD rates at sites over a period greater than 30 years. Recent publications, with data records less than 30 years, suggest that NSZD rates could be zero order (the same rate year over year) (Garg *et al* 2017). The practitioner is advised to keep abreast of current research on this important topic.

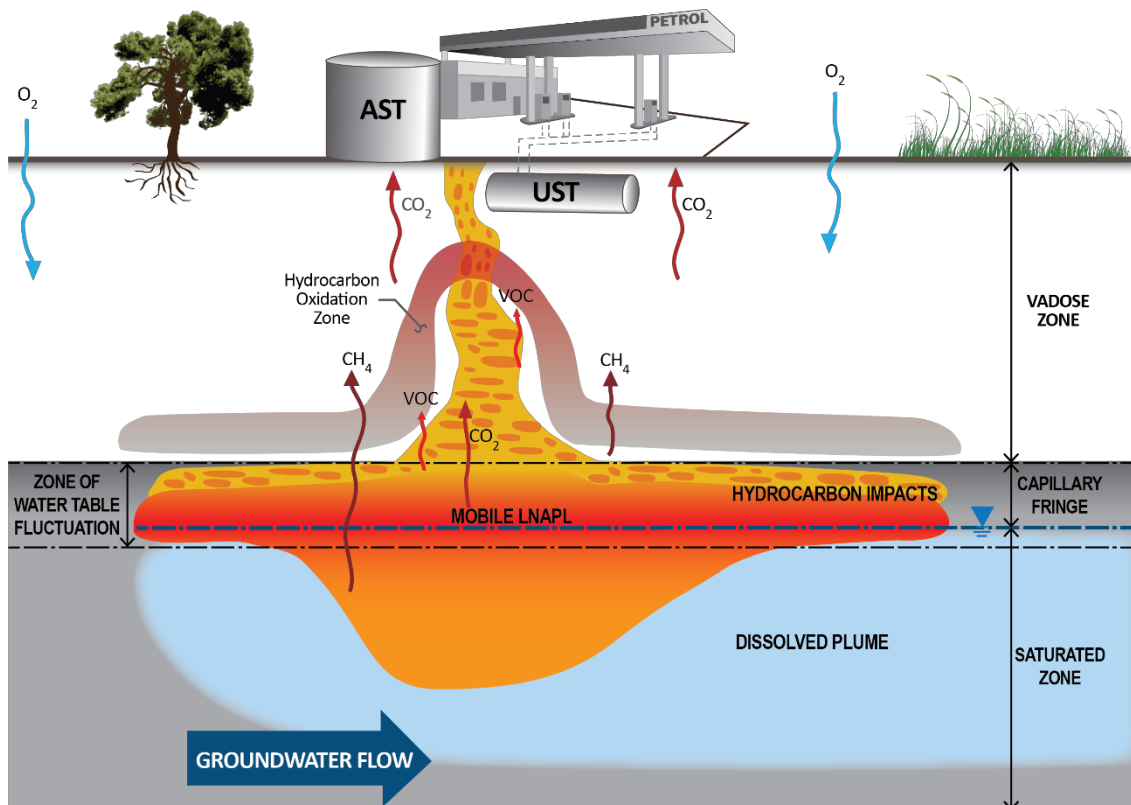


Figure 2. Comprehensive conceptualisation of petroleum hydrocarbon natural source zone depletion processes.

1.6 Relevant site conditions

NSZD measurement is applicable to a wide range of environmental remediation sites because petroleum hydrocarbon biodegradation is ubiquitous. Experience dictates that it is rarely irrelevant (e.g. no LNAPL or vadose zone). However, some site conditions may cause logistical or physical issues and hinder the monitoring methods. The practitioner is advised to review table 2 prior to proceeding with NSZD measurement as an initial pre-screening step that will provide necessary information for early planning and coarse adjustment of the NSZD monitoring program. It presents a comprehensive listing of the site conditions, the effect on NSZD monitoring, and adaptations to consider prior to proceeding with a monitoring program.

1.7 Measurement challenges

As is typical with environmental monitoring, measurement and interpretation of NSZD rates can be challenging. Each measurement method has unique inherent assumptions and potential biases due to equipment and ambient factors (e.g. short- or long-term measurement, soil moisture, wind effects, background). Specific factors that may affect each method individually are discussed in sections 4, 5, and 6. For this reason, NSZD measurement results from different methods at the same location rarely match.

Hydrogeochemical heterogeneities and confounding background effects are common factors that contribute to temporal and geospatial measurement variability in all methods.

In general, consider NSZD rate measurements at individual locations with one order-of-magnitude precision. The variability between measurement locations can be high because of the combined effects of the dynamics associated with soil gas and surface and subsurface soil heterogeneities that impart compounding potential biases in the measurement. However, when data from a network of monitoring locations are integrated across a site and are considered and evaluated collectively, the results become more meaningful and useful for decision-making purposes.

As indicated previously, NSZD is an emerging management strategy for LNAPL source zones, and this guide is a technical resource for a consistent approach to the measurement of NSZD in order to improve decision making at petroleum hydrocarbon remediation sites. The evolving nature of the NSZD approach means that it is critical that at the planning stage of each project, practitioners liaise closely with regulators and/or auditor (if applicable) to obtain acceptance of the approach. References are made throughout this document (particularly in appendix B) to the need for early engagement with the regulator and/or auditor. Liaison with regulators and/or auditor throughout the project will assist in ensuring that the information generated is sufficiently robust, defensible and useful for making decisions regarding site clean up and (perhaps) closure.

Table 2. Summary of site conditions that physically or logistically affect vapour phase-related NSZD monitoring. *Modified with permission from API (2017).*

Site condition	Effect on NSZD	Monitoring program adaptation
Vadose zone <2-foot thick	The methods discussed herein require a minimum vadose zone thickness for vapour transport to occur and some require adequate vertical space for probe installation. Additionally, gaseous byproducts from NSZD of shallow petroleum hydrocarbon-impacted soils may not completely oxidise within the small vadose zone.	Use a ground surface-based method (i.e. passive flux trap or DCC) and consider monitoring both CO ₂ and CH ₄ efflux and add stoichiometric conversions of both CO ₂ and CH ₄ to estimate the total NSZD rate (see section 4.1 for details).
Large measurable concentrations of CH ₄ near ground surface (e.g. percent-level as measured in a shallow probe using a landfill gas meter)	Atmospheric O ₂ exchange is insufficient to oxidise CH ₄ and convert to CO ₂ and renders the CO ₂ efflux methods of limited accuracy.	Methods discussed within this guidance must be adapted to estimate NSZD rates for sites where majority of CH ₄ is not converted to CO ₂ . Consider monitoring both CO ₂ and CH ₄ efflux and add stoichiometric conversions of both CO ₂ and CH ₄ efflux to estimate the total NSZD rate (see section 4.1 for details). If the CH ₄ is suspected to be an anomaly and potentially related to hydrocarbon impacts shallower than the bulk of the hydrocarbon mass (e.g. within the LNAPL smear zone), then another option is to relocate the NSZD monitoring location to assess the lateral extent of CH ₄ efflux.
Lack of lateral LNAPL delineation	Lack of lateral LNAPL delineation does not preclude NSZD monitoring. However, if a sitewide estimate of the NSZD rate is a data objective, then an estimate of the aerial footprint is required.	Use cost-effective means to delineate the LNAPL. For example, the DCC method can be used concurrent with the CO ₂ efflux survey to delineate the lateral LNAPL extent (Sihota <i>et al</i> 2016).
Intermittently flooded areas	Inundation of the ground surface and underlying vadose zone will restrict and may cut off soil gas transfer.	Design the NSZD monitoring efforts to occur during dry times and consider discounting the annual estimate of NSZD if flooding is routine.
Presence of large quantities of natural organic carbon in soils such as peat and loam	Natural soil respiration may have significant effects on the soil gas profiles and gas flux. In some situations, organic matter may even create CH ₄ , in addition to consuming O ₂ and creating CO ₂ .	If organic rich zones are discontinuous over the LNAPL footprint, then avoid NSZD monitoring in zones containing it. Otherwise, utilise advanced background correction methods such as ¹⁴ C.
Ground cover such as asphalt, concrete, compacted soil, or geotextiles	These types of ground cover restrict O ₂ exchange with the subsurface and, if significant enough, will limit CH ₄ oxidation. Additionally, they limit applicability of ground surface-based methods such as the passive flux trap and DCC. Penetration will create a chimney effect that will disturb natural soil gas patterns and result in high-biased efflux results.	Verify the soil gas concentration profile to demonstrate that ample O ₂ is penetrating the subsurface through diffusion gradients. If elevated CH ₄ is present in shallow soils above the hydrocarbon impacts, then include CH ₄ flux monitoring and add stoichiometric conversions of both CO ₂ and CH ₄ flux to estimate the total NSZD rate (see section 4.1).

Active ongoing remediation using soil vapour extraction (SVE)	SVE significantly alters the soil gas transport regime through advection resulting in a net inflow of gases at the ground surface. This, in turn, disturbs the soil gas profiles above the petroleum hydrocarbon-impacted soils and invalidates assumptions with the all NSZD monitoring methods.	Shut down the SVE system for a period of time necessary to allow re-equilibration of soil gas concentration profiles. After a series of routine field measurements verifies stability, then the NSZD monitoring can begin. Note that the duration for re-equilibration can vary greatly, from days to months.
Regionally elevated CH ₄ and/or CO ₂ flux from deep geologic fossil-based sources	Background sources of CH ₄ and/or CO ₂ flux can also include deep petroleum or natural gas reservoirs underlying the LNAPL source zone of concern. Modified correction is needed to exclude these other, non NSZD-related sources.	Prescreen the background fossil-based gas flux outside the LNAPL footprint. Consider performing ¹⁴ C analysis in background areas to quantify the fossil-based fraction of CO ₂ derived from underlying petroleum reservoirs and using it as a basis for correction.
Large depth to LNAPL (e.g. >100-feet below ground surface)	Soil vapour mixing in the large vadose zone above the hydrocarbon impacted soil may obscure/dilute the ground surface efflux of CO ₂ and cause inaccuracies in these methods.	Use non-ground surface-based NSZD monitoring methods such as the gradient method (see section 4.3) or the biogenic heat method (see section 5).
Cold climate (i.e. ambient temperatures sustained below freezing for long durations)	Cold/frozen subsurface conditions may stall biodegradation, limit vapour transport, and reduce NSZD rates at sites with shallow LNAPL impacts (Sihota <i>et al</i> 2016).	Monitor seasonal changes to determine the effect of sub-freezing ambient temperatures on subgrade NSZD rates.
Saturated silt/clay geology or perched water bearing zone overlying petroleum hydrocarbon-impacted soils	Low-permeability, saturated soils and perched water may restrict soil gas movement. Note that this is a similar effect as imposed by ground cover such as asphalt or compacted soil.	Verify the soil gas concentration profile to demonstrate that ample O ₂ is penetrating the subsurface through diffusion gradients. If elevated CH ₄ is present in shallow soils above the hydrocarbon impacts, then include CH ₄ flux monitoring and add stoichiometric conversions of both CO ₂ and CH ₄ flux to estimate the total NSZD rate (see section 4.1).
Natural CO ₂ generation from calcareous sands or dissolution of carbonate rock	CO ₂ flux from background sources can also include soil/rock with carbonates. Modified correction is needed to exclude these other, non-soil respiration-related, sources of CO ₂ .	Characterise the background CO ₂ flux using isotopic methods such as ¹⁴ C, which will exclude CO ₂ from carbonate-containing geologic materials.

2. Measurement preparation

2.1 Establishing data use objectives and measurement scope

Like any environmental monitoring program, it is important to establish data use objectives prior to performing NSZD measurements. These will help define why the NSZD measurements are being collected. Use of NSZD monitoring is appropriate at sites that have a need for theoretical, qualitative, or quantitative understanding of NSZD processes. The scope and duration of the field effort will vary depending on the ultimate data use.

Table 3 reproduces information from API (2017) and presents the spectrum of data use objectives from simple desktop assessment to a more complex long-term evaluation. It highlights the basic monitoring program parameters and how each data use objective can impact the scope and duration of the effort.

Except for the LNAPL compositional change method, all methods provide NSZD rate results that are bulk petroleum hydrocarbon measurements (e.g. total petroleum hydrocarbon mass loss over time). This is acceptable for many data uses. However, if a chemical(s) of concern (COC)-specific NSZD rate measurement is needed to, for example, estimate the depletion of a benzene risk driver, then the practitioner is advised to consider the value of measurement and carefully select an appropriate method, consistent with the needed data use, prior to proceeding.

Figure 3 presents a decision logic flowchart to aid practitioners in selecting an appropriate data quality level for NSZD monitoring (see yellow-highlighted boxes). The selection of a screening-level, evaluation, or long-term monitoring data quality level depends upon project stage and data objectives. A screening-level NSZD assessment may simply involve use of existing data and a theoretical calculation as described in section 2.6. A one-time NSZD evaluation would involve field data collection using one the methods described in sections 3 through 6. The methodology for long-term NSZD monitoring is highly site-specific and may involve theoretical or field techniques and periodic or continuous measurements.

Table 3. Typical NSZD monitoring data use objectives and scopes of work. *Reproduced with permission from table 3-2 of API (2017).*

Data use objective	Scope	Onsite monitoring duration
Screening-level qualitative assessment of NSZD	Desktop, theoretical analysis using pre-existing data as described in section 3.1.4.1.	No onsite monitoring
NSZD spot check or affirmation of occurrence	One event, single hydrocarbon-impacted location, during warmer time of year.	~1 week
NSZD snap shot in time	One event, multiple locations, during time of year with mean ambient temperature (e.g. late fall or early winter for temperate climate (Sihota <i>et al</i> 2016).	~1 month
Assessment of range in NSZD rates	Two events, multiple locations, to coincide with extremes in seasonal changes in temperature and/or water table elevation (Sihota <i>et al</i> 2016).	~6–8 months
Annual NSZD estimate	Two or more events, multiple locations, to monitor seasonal high and low and intermediate times with conditions closer to annual mean value temperature and water table elevation. Fewer events needed for monotonic climates than for temperate climates.	~1 year
Long-term NSZD monitoring	Variable scope options dependent on pre-existing understanding of NSZD rates and actual rate of NSZD, ranges from annual monitoring to 5–10 year intervals. For example, if the initial evaluation adequately characterised the statewide NSZD rate, then long-term monitoring may only be needed at one or two key locations.	Long-term for the duration of an NSZD remedy

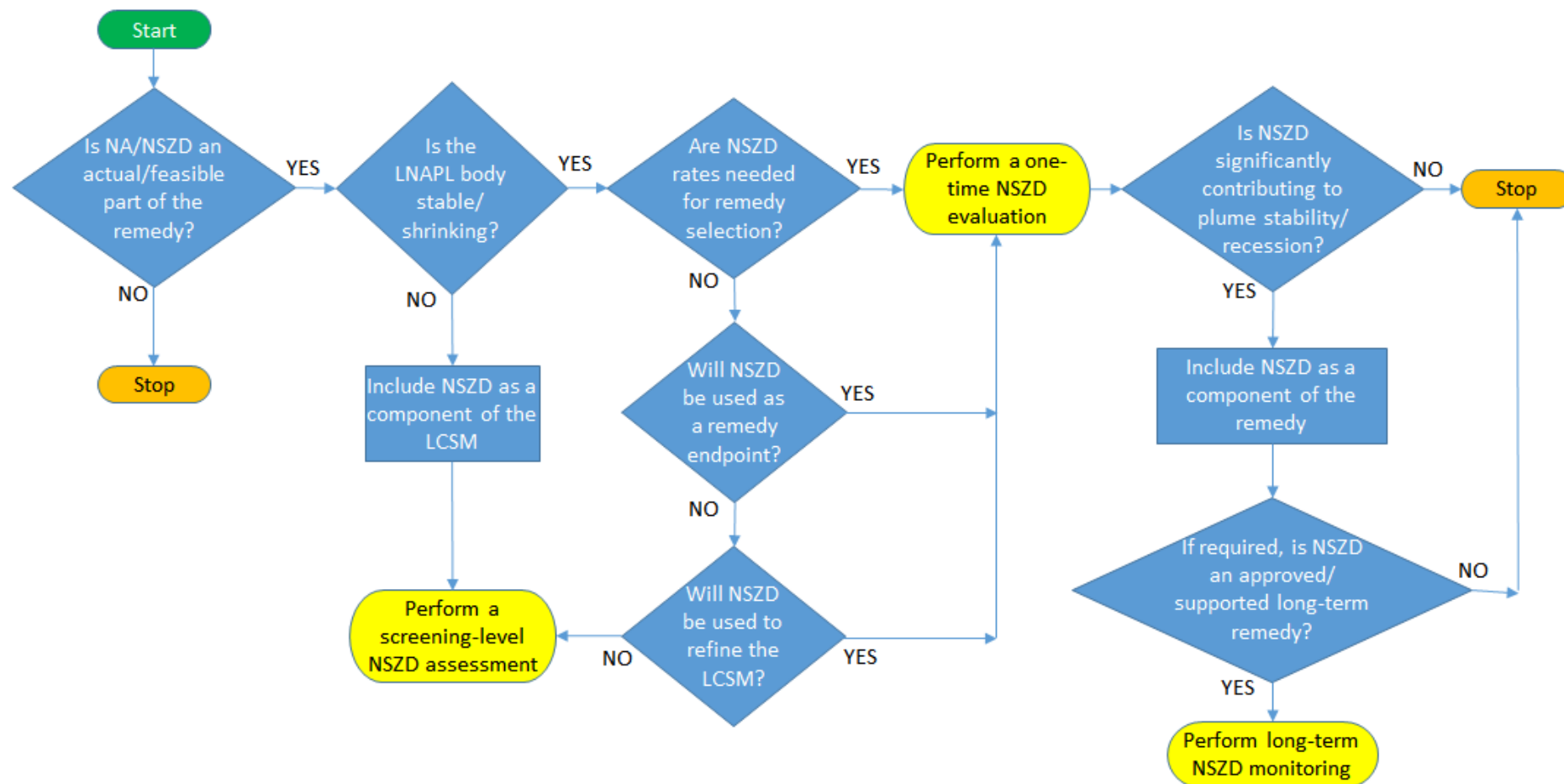


Figure 3. Decision logic flowchart for selection of NSZD measurement data quality levels (screening-level, evaluation, or long-term monitoring).

At the start of the process and following each key decision point, consult the auditor and/or regulator to discuss and agree upon a scope for the NSZD measurements. This decision logic provides a framework for discussion of the NSZD monitoring work; site-specific adaptations/deviations are expected. For example, a project team may decide to implement long-term NSZD monitoring prior to receiving auditor support if it aids cost-effective decision making.

2.2 Review of the LNAPL conceptual site model (LCSM)

Selection of an NSZD measurement scope and method also depends on the LCSM. Preparation of an LCSM is described in detail in *CRC CARE Technical Report 34* (2015). Table 4 reproduces information from API (2017) and lists the key elements of the LCSM important to NSZD monitoring and how they may impact NSZD rates. Assess these elements as part of the NSZD monitoring scoping effort.

Table 4. Key elements of the LCSM and how they relate to NSZD measurement. *Reproduced with permission from table 3-1 of API, (2017).*

Element of LCSM	Relation to NSZD monitoring design
Lateral extent of LNAPL	Forms the area of the NSZD survey – monitoring outside the LNAPL footprint can generally be considered background if there are data to document no hydrocarbon impacts at depth. Multiple releases/separate LNAPL bodies on the same facility or deep LNAPL occurrence with tortuous soil gas transport pathways, for example, require adaptation of the NSZD monitoring program.
Vertical extent of LNAPL	NSZD occurs only in petroleum hydrocarbon-impacted areas. The rate may vary based on the amount of LNAPL present and where it occurs in the subsurface, although these effects remain a subject of study.
Type of LNAPL and fluid density	Conversion of biodegradation byproduct vapour flux to an NSZD rate requires a stoichiometric conversion using a hydrocarbon representative of the LNAPL mixture. Conversion to a volumetric-based NSZD rate requires the LNAPL density.
Depth to groundwater and water table fluctuation	NSZD monitoring using these vapour phase-related methods can only be performed in the unsaturated zone above the hydrocarbon impacted soil. The effects of LNAPL submergence on NSZD rates is uncertain. Consider timing NSZD measurements at extremes of seasonal high and low water table for site-specific assessment of this potential effect.
Ambient temperature climate	At sites with shallow petroleum hydrocarbon source zones (e.g. <6 m (Sweeney & Ririe, 2014)) or significant changes in groundwater temperatures, NSZD rates may vary with seasonal change in soil temperatures. At these types of sites, ambient temperature changes affect soil temperature. Effects of root zone activity on shallow soil gas profiles and flux is highest during the warmer, vegetation growing season. Competent ground ice may limit shallow soil vapour flux. Ground frost is often permeable and does not necessarily restrict soil gas exchange with the atmosphere. Consider the temperature and water table elevation effects in parallel as there can often be optimum times to measure when water tables are lowest and soil temperatures highest.
Depth to top of hydrocarbon impacts in soil	The top of the hydrocarbon impacts will drive soil gas concentration profiles and determine where gradient method monitoring should be located. Layers of shallow zones of petroleum in soil, separated by “clean” soil, above the bulk of the hydrocarbon mass in the LNAPL smear zone, for example, may confound data interpretation from the gradient method.
Soil type and moisture content	Movement of gases (i.e. VOCs, O ₂ , CO ₂ , and CH ₄) is more limited in finer-grained formations and soils with a higher moisture content. Limitation of O ₂ influx will limit NSZD rates. Bedrock presence does not preclude NSZD monitoring, but effects method selection.
CH ₄ concentration in shallow soil gas	Presence of elevated CH ₄ at or near ground surface indicates soil gas exchange is limited, CH ₄ oxidation is incomplete. CH ₄ will drive method selection to potentially include measurement of CH ₄ flux.
LNAPL distribution and hydrostratigraphy	LNAPL can occur in the subsurface under unconfined, confined, or perched conditions. Each of these conditions could affect the NSZD rates.

2.3 Measurement locations and relationship to LNAPL distribution

Understanding the hydrogeological environment is a key starting point for scoping the locations of NSZD measurements. The location of NSZD monitoring depends significantly on the LNAPL distribution. Figures 4 through 9 present six of the most common hydrogeological environments encountered at LNAPL remediation sites in Australia. As defined by CL:AIRE (2014), the environments include LNAPL releases into clean (e.g., beach) sands, fill, granite or igneous rock, interbedded sand and silt/clay, marine clays, and limestone.

On figures 4 through 9, the yellow-shaded areas show where the subsurface NSZD measurement method installations should be located (i.e. for the gradient and biogenic heat methods). The purple-shaded areas show where the surface NSZD measurement method installations should be located (i.e. for the passive flux trap and DCC methods). In all cases, measurements are made above the LNAPL footprint, but the depth and width varies depending upon the LNAPL and vapour distribution. In this case, the vapour distribution signifies VOCs or biogases (e.g. CH₄ or CO₂) within which the hydrocarbon oxidation zone lies. A zone number on figures 4–9 implies a uniquely different subsurface condition (i.e. LNAPL distribution or geology) that will affect gas flux. If more than one zone number is shown, then separate profiling and/or background corrections must be made for each.

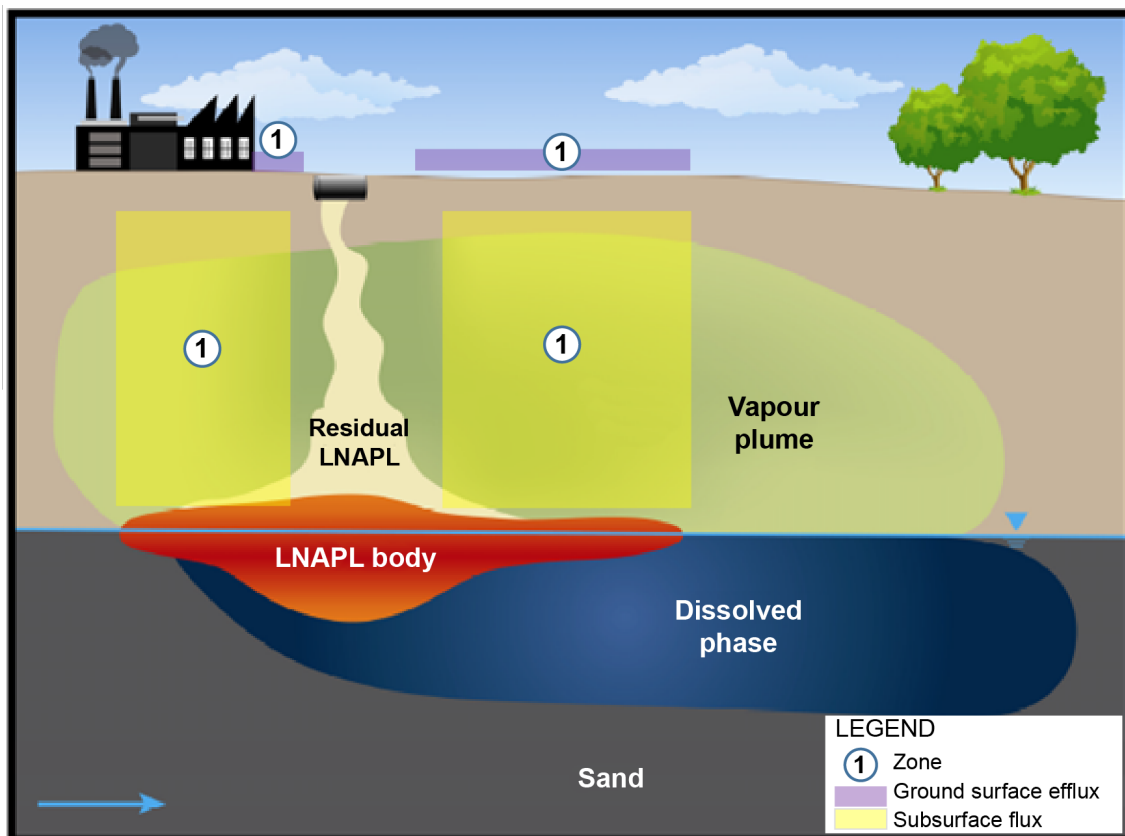


Figure 4. NSZD monitoring locations at a site with LNAPL release into clean (e.g. beach) sands. Modified with permission from CL:AIRE (2014). The homogeneity of the sands allows for a simple NSZD measurement approach with only one zone where flux could be expected to be reasonably uniform. Subsurface flux techniques (gradient, biogenic) may be used in the yellow areas and/or surface techniques (passive flux trap, DCC) may be employed in the purple areas.

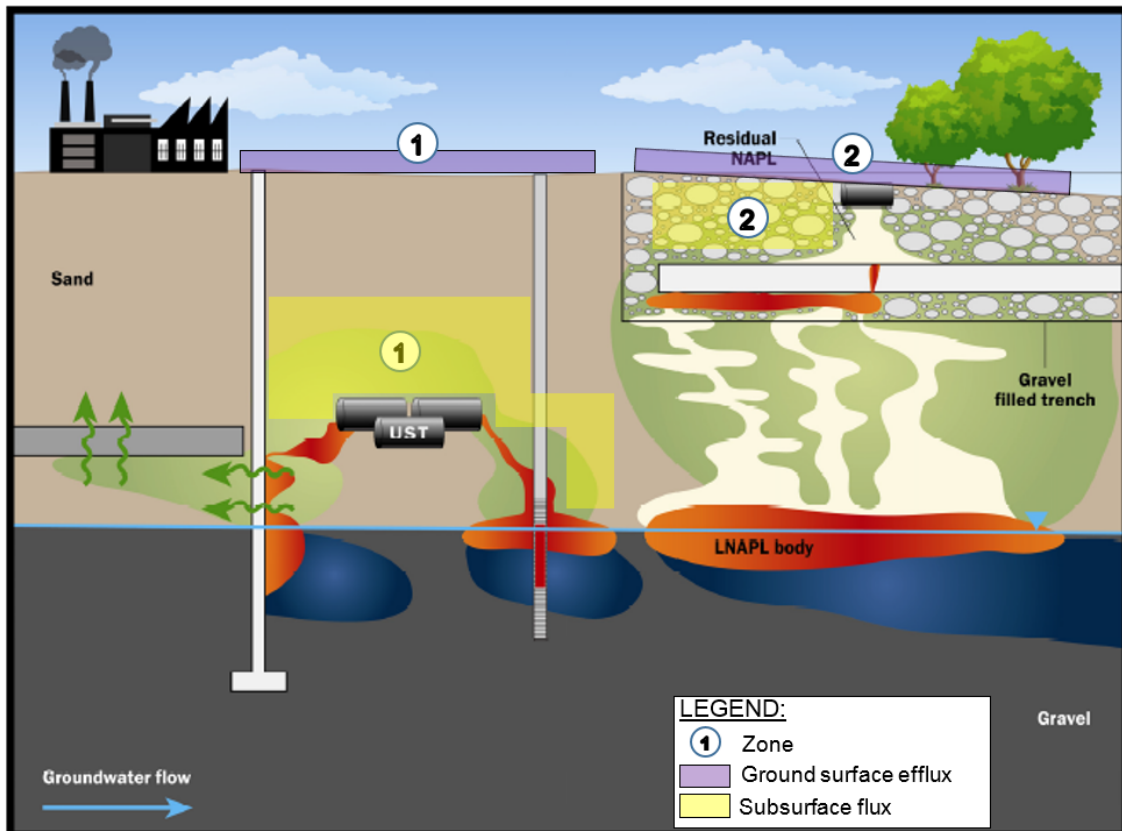


Figure 5. NSZD monitoring locations at a site with LNAPL release into fill. Modified with permission from CL:AIRE (2014). At this multiple release site, there are two different zones where flux could be measured, within either a sand formation or gravel trench. Key aspects of NSZD monitoring within this type of LCSM are to perform measurements above the LNAPL impacts in soil (e.g. shallower in the case of zone 2 where LNAPL followed a preferential flow path in a utility corridor). Measurements in zone 1 are like those in figure 4. Due to the shallower and coarser nature of the soils in zone 2, the available vertical space is limited and ground surface NSZD methodologies may be preferred.

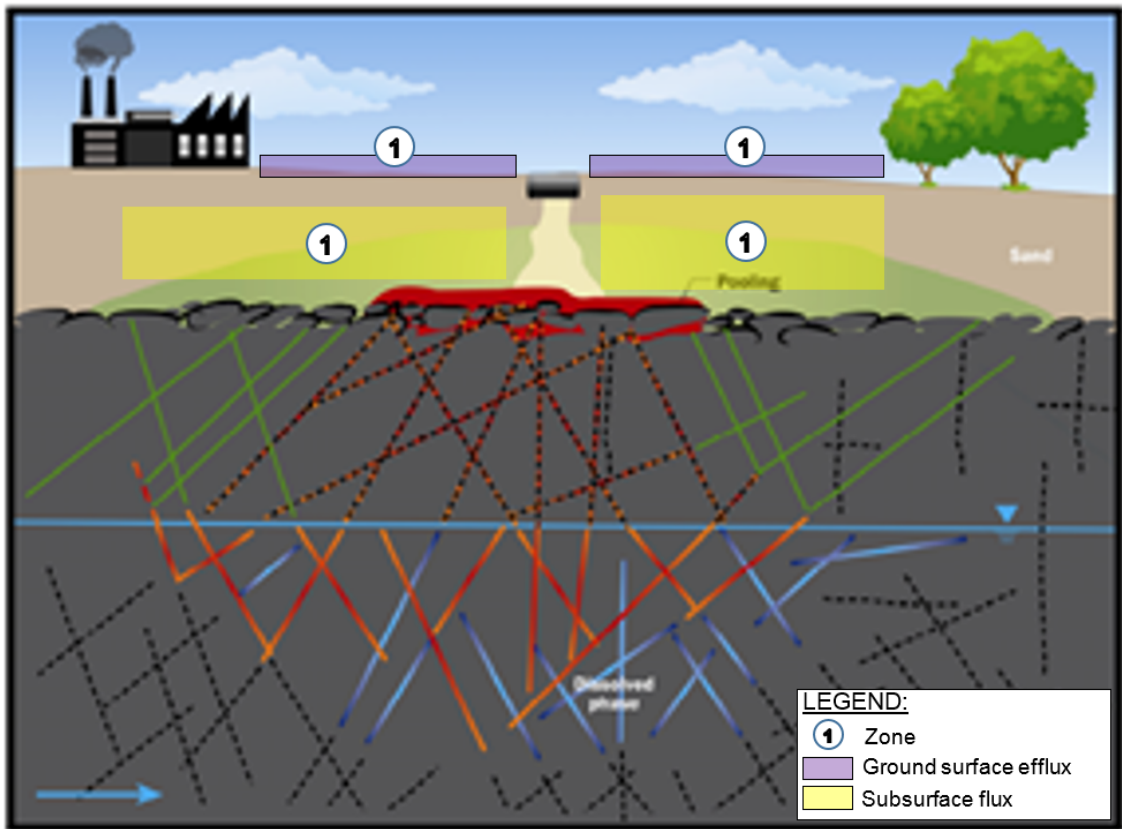


Figure 6. NSZD monitoring locations at a site with LNAPL release into granite or igneous rock. Modified with permission from CL:AIRE (2014). NSZD measurement options in a bedrock setting are limited and highly variable. This LCSM scenario suggests that it be performed in the unconsolidated overburden above the bedrock where gas flux patterns will be more uniform. LNAPL distribution in the underlying interconnected fractures and the associated biodegradation gas flux will determine the lateral extent of the measurements and may extend beyond the extent of the LNAPL at the top of the bedrock interface. Like the scenario in figure 4, within the overburden, NSZD can be measured using both surface (purple zone 1) and subsurface (yellow zone 1) technologies.

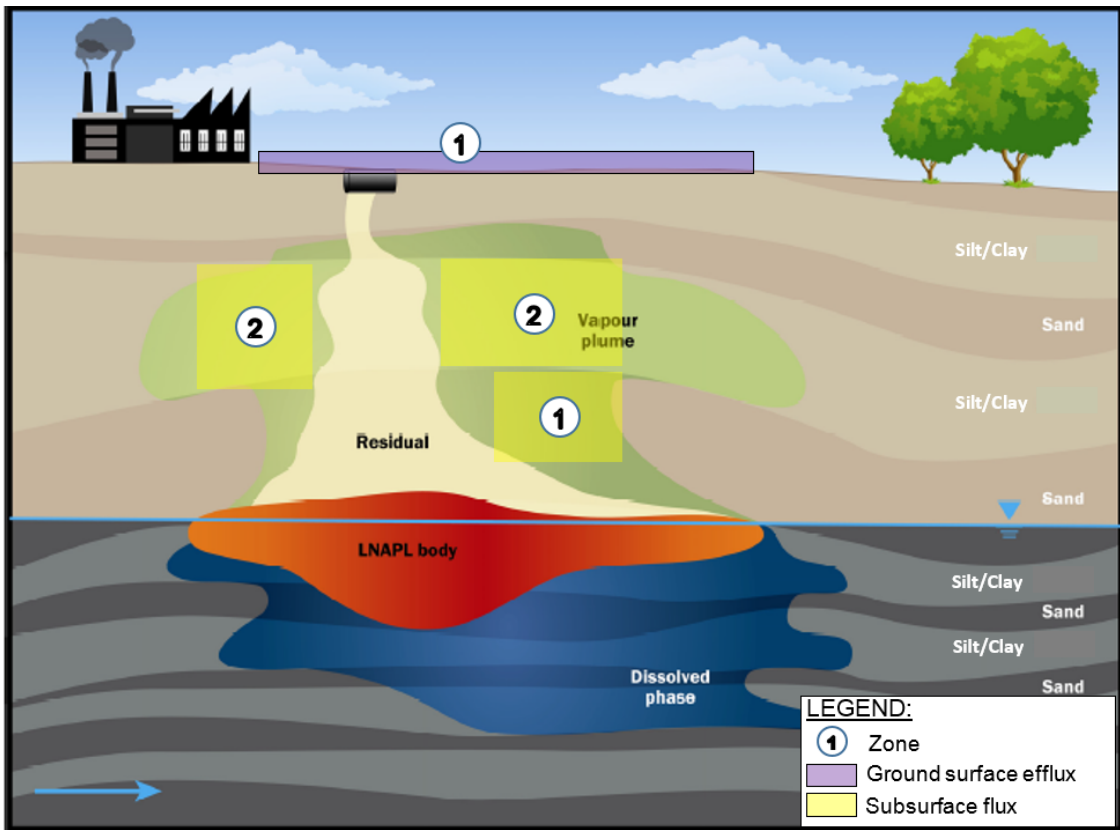


Figure 7. NSZD monitoring locations at a site with LNAPL release into interbedded sand and silt/clay. Modified with permission from CL:AIRE (2014). Due to the heterogeneity of the interbedded layers above the LNAPL footprint, profiles of overlying soil gases associated with NSZD are expected to be stratified. The simplest method would be use of surface methods of NSZD measurement applied atop the LNAPL footprint in zone 1 (purple). If a subsurface method is used, then care must be taken to account for the unique properties of the sand and/or silt/clay lenses. If diffusion coefficients or thermal properties are used, they should be estimated for the particular zone (1 or 2) where measurements are made. In the extreme case where a partially saturated, fine-grained lithology or perched water bearing zone is dominant (zone 2) significantly limits or restricts gas exchange, then subsurface NSZD techniques should be employed beneath these layers (zone 1 yellow).

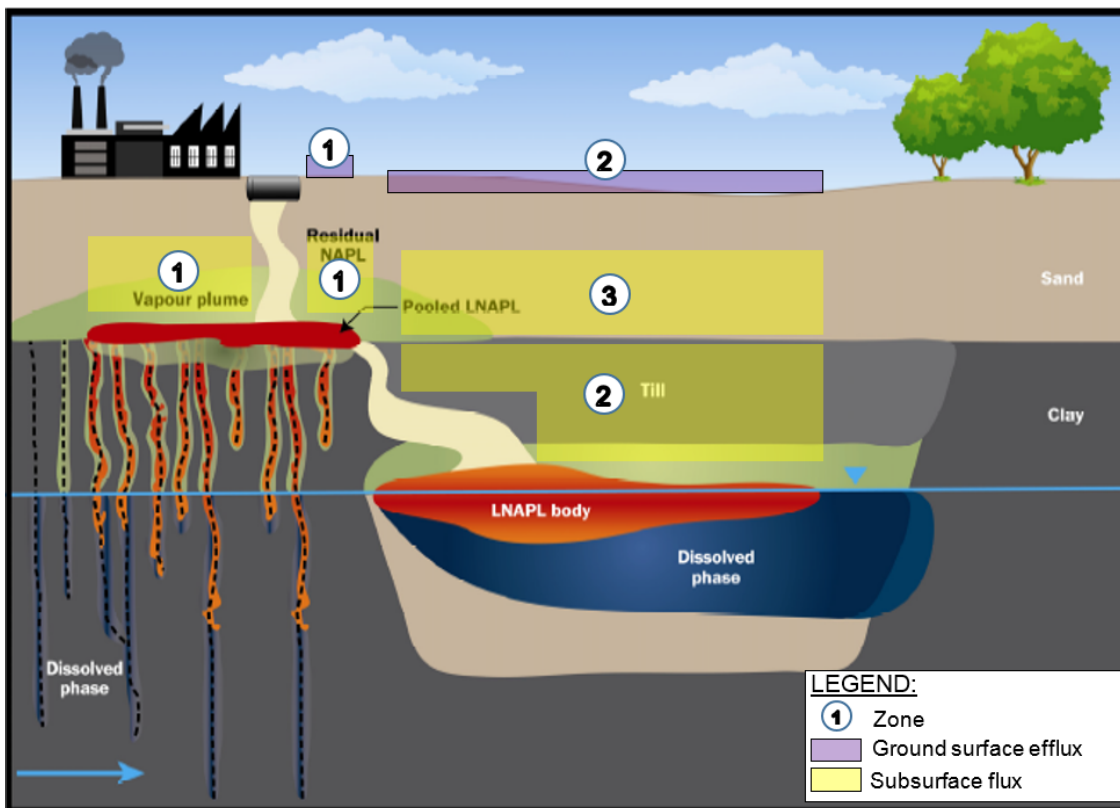


Figure 8. NSZD monitoring locations at a site with LNAPL release into marine clays. Modified with permission from CL:AIRE (2014). This complex LCSM resulted from a single LNAPL release and the stratigraphy of the marine clays containing vertical fractures with an adjacent pocket of till resulted in a complex LNAPL distribution. Ground surface-based NSZD measurements could be performed in one of two zones (purple zone 1 and 2) and will likely exhibit different results due to the unique nature of the underlying LNAPL and geology. As in the other LCSMs, the presence of the building poses a limitation to where ground surface methods can be deployed. Efflux results immediately adjacent to the building may be elevated due to surficial gas efflux restrictions posed by the building which cause higher efflux around the perimeter of the building. For subsurface NSZD measurements, there are three zones differentiated both by LNAPL distribution and geology (till or sand). No measurements are recommended in the clay. In this case, it may be easiest to measure NSZD within the overlying sand (yellow zones 1 and 3), but additional measurements within the deeper till may be valuable to assess soil gas quality (e.g. CH₄ concentrations) closer to the LNAPL source.

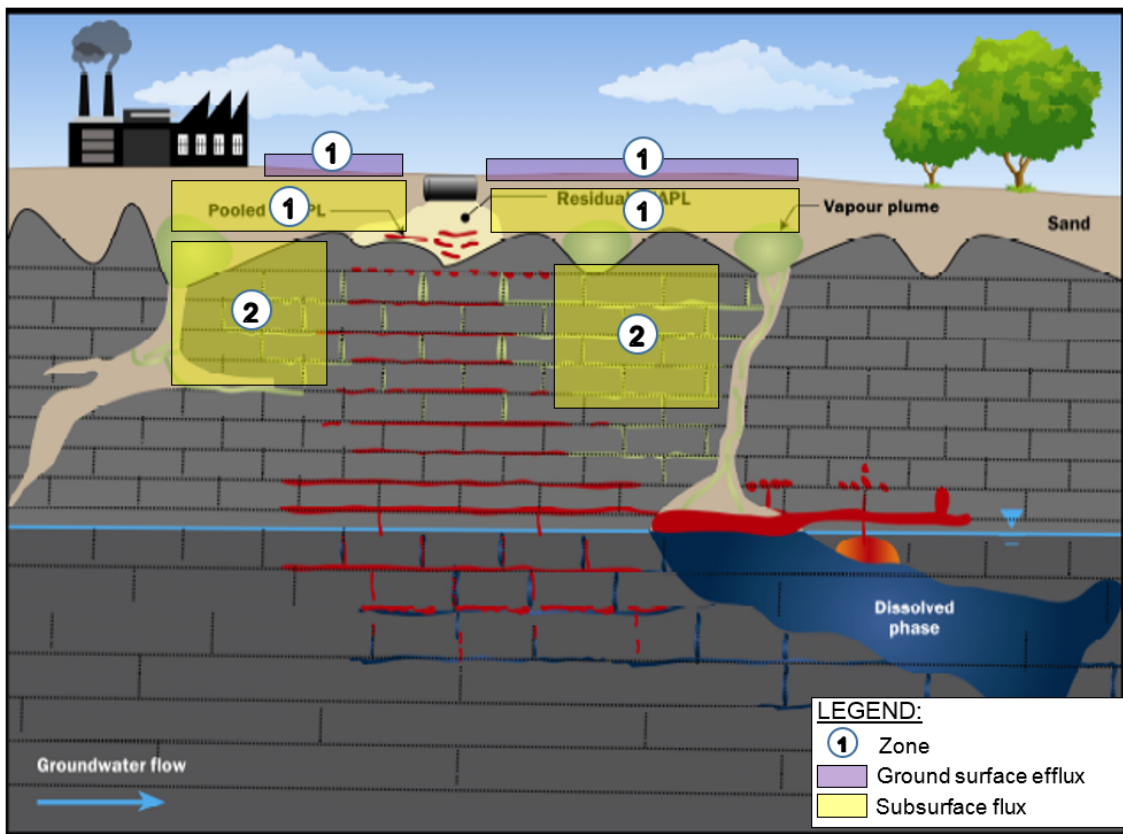


Figure 9. NSZD monitoring locations at a site with LNAPL release into limestone. Modified with permission from CL:AIRE (2014). A thin sand overlying a limestone formation poses a significant challenge for NSZD measurements. The simplest approach is to monitor gas flux in the overburden, identified as zone 1, using both surface (purple area) and subsurface (yellow area) techniques. In some situations, it may be useful to measure NSZD from the limestone, using existing monitoring wells screened in the vadose zone. However, due to low permeability and the irregularity of limestone fractures, use of subsurface methodologies should be carefully considered prior to use.

2.4 Effects of LCSM on NSZD rates

As discussed previously, soil gas profiles, fluxes of O_2 , CO_2 , and CH_4 , and the associated NSZD rates will vary with differences in the LNAPL distribution and location at the site. Figure 10 shows hypothetical soil gas concentration profiles for background (no NSZD), low-moderate NSZD, and high NSZD rate locations. A background location (far right-hand side of figure) typically shows very little O_2 consumption within the vadose zone and an associated flat rate of change in concentration over depth. On the contrary, locations with high rates of NSZD will show significant O_2 consumption within a short distance of ground surface. The high rates of gas flux, whether it be O_2 consumption or CO_2 production, is typified by the steep change in concentration over depth. Additional discussion of soil gas concentration profiles and how they are used to estimate rates of NSZD is provided in section 4.3.

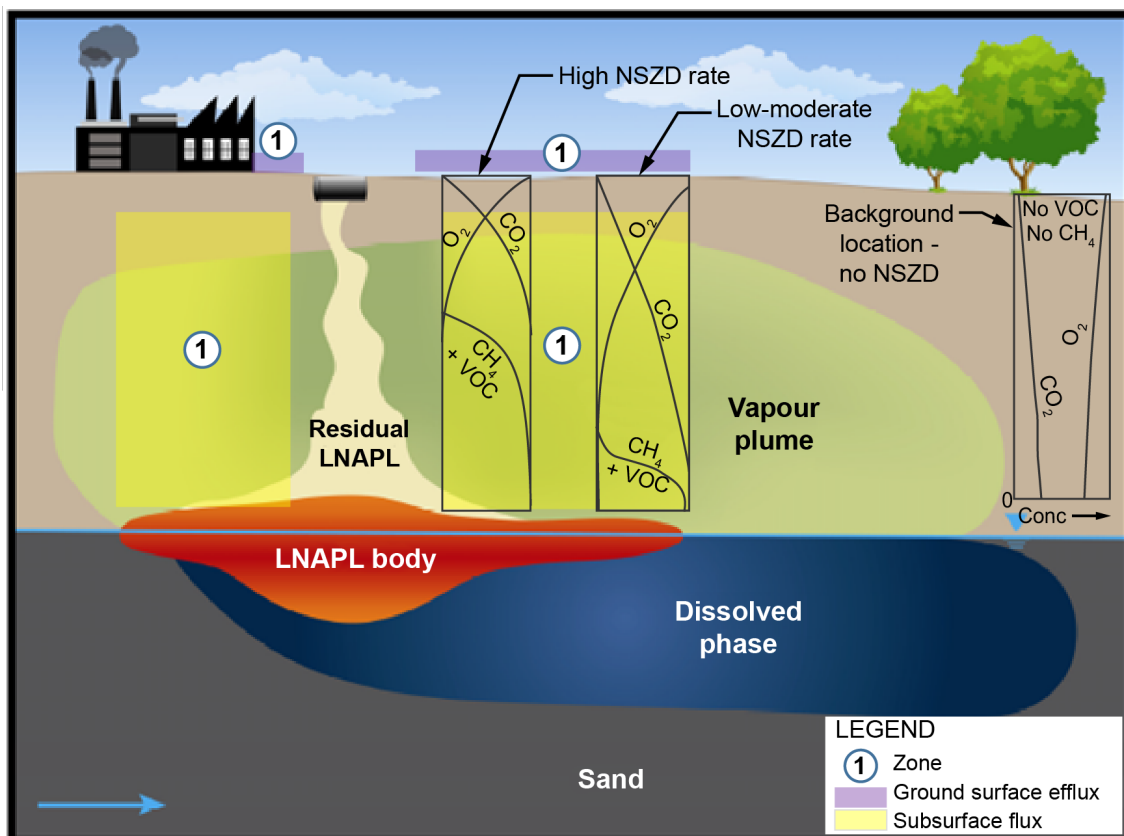


Figure 10. Hypothetical soil gas concentration profiles for background, low-moderate, and high NSZD rates. Modified with permission from CL:AIRE (2014).

2.5 Characterisation for LCSM validation

If existing information is insufficient to ascertain the hydrogeologic environment and/or verify baseline assumptions for the NSZD monitoring program, the following additional characterisation may be valuable prior to the NSZD evaluation.

2.5.1 Soil Gas Survey

Collection of shallow and/or deep soil gas samples may help verify concentration profiles and appropriate depths for the subsurface monitoring methods (i.e. gradient and biogenic heat). The samples are collected above the LNAPL-impacted soils to verify the shallow absence of CH_4 and maximum depth of O_2 ingress. They can be collected from existing monitoring wells (Sweeney & Ririe 2017) or existing or new vapour monitoring probes (CRC CARE 2013). Appendix D.4 contains example procedures for collecting these samples.

Soil gas sampling can also be used to verify the predominance of diffusion for the purposes of affirming use of the gradient method. As discussed in appendix A, advection is not typically significant away from the LNAPL within a zone containing O_2 ; however, the literature is thin on this subject, and the gradient method measurement accuracy depends upon data collection outside the influence of advection. Therefore, analysis of nitrogen (N_2) at the proposed concentration gradient profiling depth may be helpful, as used in Molins *et al* (2010), to verify that concentrations are near ambient and advective influence small or negligible within the depth interval used for the data analysis and NSZD rate calculation.

2.5.2 Subsurface temperature

Another preliminary characterisation option is measurement of subsurface temperature. As discussed in appendix A, NSZD processes create a thermal signature above the LNAPL footprint. Knowledge of the depth of peak temperature and magnitude as compared to background can be informative when planning to use one of the subsurface methods (i.e. gradient or biogenic heat) for an NSZD monitoring program. The depth of peak soil temperature can inform the depth interval of the hydrocarbon oxidation zone (aerobic) within and immediately above which subsurface NSZD monitoring is ideally performed. Additionally, it can be helpful to inform all vapour phase-related NSZD monitoring methods as higher soil temperatures within the source zone is an indicator of NSZD and ample supply of O₂ and conversion of CH₄ to CO₂.

There are various ways to collect screening-level temperature data to suit these purposes, including the following:

- Measurement of in-situ groundwater temperature within LNAPL-impacted areas. As discussed further in section 5, groundwater can be warmed by an overlying hydrocarbon oxidation zone. Therefore, elevated groundwater temperatures are also indicative of NSZD processes. Assuming the heat losses to groundwater are minor compared to atmosphere, in-situ groundwater temperature monitoring was suggested as one way in which to estimate NSZD rates (Warren & Bekins 2015).
- Measurement of the thermal profile within an existing, atmospherically sealed monitoring well or borehole installed within the LNAPL source zone. Sweeney & Ririe (2014) proposed two methods; cable-and-reel and sensor string. The cable-and-reel approach uses a thermistor probe and collects real-time data by a manual incremental lowering and measurement process. The temperature sensor string can be left in place to data log long-term temperatures at pre-established depth intervals.

Further detail on these temperature screening methods is provided in section 5 and appendix G.

2.5.3 Chemical composition of LNAPL

Sampling and laboratory analysis of the LNAPL itself can also be an informative measurement of NSZD processes. Forming the basis of the LNAPL compositional change method prescribed in section 6, the chemical content of the LNAPL, albeit variable across the source zone, is a direct measurement of the LNAPL losses. Where the other NSZD measurement methods are bulk measures, the LNAPL compositional-change method can also provide a chemical-specific NSZD rate.

LNAPL samples can be collected from in-well or extracted from subsurface soil samples. The samples are analysed in the laboratory using an appropriate analytical protocol. Table 5 lists some of the available analytical options that can be used to inform the calculation of a chemical-specific NSZD rate using the LNAPL compositional change method. Of key importance is selection of the appropriate COC for analysis. This is a site-specific decision based on various factors including risk assessment and regulatory requirements.

Table 5. Laboratory analytical options for whole-oil and forensic evaluation of LNAPL mass losses.

Method no.	Title and description	Data use
SW8015	GC-FID for relevant hydrocarbon fractions	Quantitation of the defined hydrocarbon fractions based on specified carbon ranges. Visual evaluation of chromatograms for product type(s) (e.g. petrol, diesel, motor oil, kerosene, jet fuel) identification and estimate of product weathering.
SW8260/8270	GC/MS for VOCs and SVOCs	Identification of individual constituents present in the samples. VOC target compounds typically included BTEX and SVOC target compounds typically include parent PAHs. TICs may also be identified based on the use of mass spectrometry for identification.
ASTM D2887	Simulated distillation	Measures individual alkanes C6-40 to develop a fingerprint of the distribution constituents making up the LNAPL based on the boiling range of the constituents.
ASTM D5739	Biomarkers – pristane/phytane ratio	Identification of biomarkers and associated compounds assists with the identification of petroleum hydrocarbon impacts and degradation rates.
8270SIM	16-18 parent PAHs by GC/MS-SIM	The identification and quantitation of the US EPA priority PAHs. These PAHs may be primary drivers in risk assessment for petroleum products.
8270SIM	Parent and alkyl (approx. 30) PAHs by GC/MS-SIM	Identification and quantitation of the parent and alkylated PAHs. The patterns of the parent and alkylated PAHs may be used for source identification (anthropogenic versus pyrogenic), as well as fingerprinting of possible sources.
TPHCWG direct method, NWTPH VPH/EPH, MADEP VPH/EPH	VPH/EPH	Fractionation and quantitation of hydrocarbons based on aliphatic and aromatic hydrocarbons, as well as hydrocarbon ranges that are appropriate for risk determination.
ASTM D5739	Oil spill identification, ideally incorporates analysis of a fresh (unweathered) LNAPL sample	Through the full analysis of oil constituents and detection by mass spectrometer this method reports 14 groups of EICs that may be used for identification of fuel type, comparison to potential sources of LNAPL, and assessment of weathering that is impacting the released product.
SW8260 Modified	PIANO	Identification of PIANO present in the LNAPL. The make-up and ration of these PIANO constituent groups may be used to identify LNAPL sources.
SW8260 Modified	Fuel Oxygenates	Identification and quantitation of fuel oxygenates typically added to petrol. Typical oxygenates include MtBE, ethanol, DIPE, TAME, ETBE, and TBA. The presence of individual oxygenates may indicate the age of the petrol and assist with the identification of source.
SW8080 Modified	Alkyl Leads, EDB, MMT	Identification and quantitation of leaded petrol additives (TML, TML, DMDEL, MTEL, TEL), MMT, and EDB that may have been added to petrol depending on the age of the potential release.

It is important to have a point of reference for comparison of the laboratory results. Therefore, either a fresh LNAPL analysis, analysis of a biomarker (i.e., a compound resistant to biotic and abiotic degradation), and/or a time-series of analytical results is recommended to assess chemical-specific or bulk LNAPL loss rates using LNAPL analysis. More details on the use of LNAPL analytical results and their relationship to NSZD rates are presented in section 6.

2.6 Theoretical assessment

Theoretical assessment of NSZD may be valuable to help establish expectations for field measurements of NSZD. An analytical calculation based on the gradient method and type curve approach is discussed below to support this assessment.

Currently available commercial models are inadequate to represent NSZD. New models that can reasonably represent key NSZD processes such as direct-contact oil biodegradation and outgassing are currently in development (Wilson *et al* 2016; Garg *et al* 2017).

2.6.1 Analytical calculations and preparing a type curve

API (2017) presents an approach to create a site-specific type curve to estimate the range of potential NSZD rates at a site. It couples basic existing data (e.g. no tracer testing required), analytical and empirical equations, and reasonable parameter assumptions to predict NSZD rates. Inherent to theoretical analysis, the approach makes simplifying assumptions and is therefore considered of screening-level data quality.

Box 2.1 presents an example of how a type curve is constructed and used to assess the range of potential NSZD rates at a site. The calculations for this type curve approach is largely based on Fick's law and the gradient method. For additional explanation of the parameters, see section 4.3 and appendix D.5 for example calculations.

It should be noted that these type curves were developed based on the same equations used for the gradient method, assuming the gradient can be estimated from the O₂ concentration difference between atmospheric at ground surface and the zero depth. However, this is only appropriate for screening purposes and should not be used a substitute for the gradient method itself (see section 4.3).

2.7 Overview of methods and guidance for method selection

Six NSZD measurement methods are currently available. Selection of a method or methods is a site-specific judgment based on data objectives and site conditions. To support selection, table 6 summarises key attributes of each method. Review their attributes, compare them to basic site conditions such as remoteness of location, bedrock geology, and depth to LNAPL, and evaluate which best suits the project goals.

Note that the stated attributes on table 6 apply to the original proposed methods largely consisting of dedicated equipment installations. Various adaptations have been made and continue to be made to the methods to reduce the associated burden (e.g. use of existing monitoring wells to measure soil gas and soil temperature). As a result, table 6 may not accurately reflect the attributes of the method with adaptation. As discussed in the detailed method descriptions in sections 3 through 6, review the options and consider adapting the method to optimize the monitoring program.

2.8 Quality assurance/quality control documentation

QA/QC checklists were prepared to summarise the minimum requirements for implementation of the NSZD measurement methods described herein. The checklists are included in appendix B. They are designed as tools for practitioners, auditors, and regulators alike. They are intended for use before, during, and after a measurement program to ensure that the NSZD evaluation is properly vetted and has gone through the appropriate design, implementation, and evaluation procedures. With most items performed/checked off, they will support data quality such that results can be relied upon for decision making purposes. The checklists essentially condense the content of sections 3 through 6 into a series of questions that walk the reviewer through the key elements and findings such as proper background correction, geospatial data density, and reconciliation of variability in results.

Box 2.1 Type curve construction for NSZD rate assessment

Objective: Calculate the theoretical range of plausible, diffusive-driven NSZD rates using O_2 gradients and existing soil properties.

For more information: Appendix D.5

Principle: Fick's first law of diffusion

$$J_{O_2} = D_{O_2}^{eff} \left(\frac{dO_2}{dz} \right)$$

Millington and Quirk (1961)

$$D_{O_2}^{eff} = D_{O_2}^{air} * \frac{\theta_v^{3.33}}{\theta_v^2}$$

Key assumptions:

- Steady-state snap shot in time
- Diffusion-controlled gas flux
- Representative $D_{O_2}^{eff}$, based on assumed total and air-filled porosity
- O_2 consumption is from NSZD processes (no background correction)

Key calculation parameters:

- Effective vapour diffusion coefficient
- Concentration gradient

Parameter assumptions:

- Total porosity, $\theta_T = 0.178$ (tuffaceous sandstone, volcanic reservoirs (Zou, 2013))
- Prior vapour extraction tests affirmed literature value permeability of $0.014 \mu m^2$
- Range of air-filled porosity, $\theta_v = 0.089$ – 0.134 (50–75% of total porosity)
- $D_{O_2}^{air} = 2.1 \times 10^{-5} m^2/s$ (API 2017)
- Water table depth = 30 mbg
- Upper control point = 17.1% by vol O_2 at 0.2 mbg (actual soil gas measurement)
- LNAPL density = $8 \times 10^3 g/m^3$

Estimated range of effective diffusivity:

$$D_{O_2}^{eff} = 2.1 \times 10^{-7} - 8.0 \times 10^{-7} m^2/s$$

NSZD rate calculation:

$$R_{NSZD} = J_{O_2} * \frac{mol_{C_8H_{18}} + MW_{C_8H_{18}}}{mol_{O_2} + MW_{O_2}}$$

Example calculation (octane, C_8H_{18}):

$\theta_v = 0.089$, 10 mbg depth, 0% by vol O_2

$$D_{O_2}^{eff} = 2.1 \times 10^{-5} * \frac{0.089^{3.33}}{0.178^2} = 2.1 \times 10^{-7} m^2/s$$

$$J_{O_2} = 2.1 \times 10^{-7} * \frac{(0.21 - 0) * 32}{(10 - 0.2)} = 4.9 \times 10^{-6} g/m^2/s$$

$$R_{NSZD} = 4.9 \times 10^{-6} * \frac{(2 * 114)}{(25 * 32)} = 1.4 \times 10^{-6} g/m^2/s = 550 L/ha/yr$$

Type curve calculation tabulation

Depth to Zero O_2 (mbg)	$\theta_v = 0.089$	$\theta_v = 0.111$	$\theta_v = 0.134$
0.3	49,619	103,539	193,837
1.5	3,927	8,195	15,342
3.0	1,826	3,810	7,132
4.6	1,189	2,482	4,646
6.1	882	1,840	3,445
7.6	701	1,462	2,738
9.1	581	1,213	2,271
10.7	497	1,036	1,940
12.2	434	905	1,694
13.7	385	803	1,503
15.2	346	721	1,351
16.8	314	655	1,226
18.3	287	600	1,123
19.8	265	553	1,036
21.3	246	513	961
22.9	229	479	896
24.4	215	449	840
25.9	202	422	790
27.4	191	398	746
29.0	181	377	706
30.5	172	358	671

Range of potential NSZD rates at, 10 mbg depth to zero O_2 :

500–2,000 L/ha/yr of LNAPL

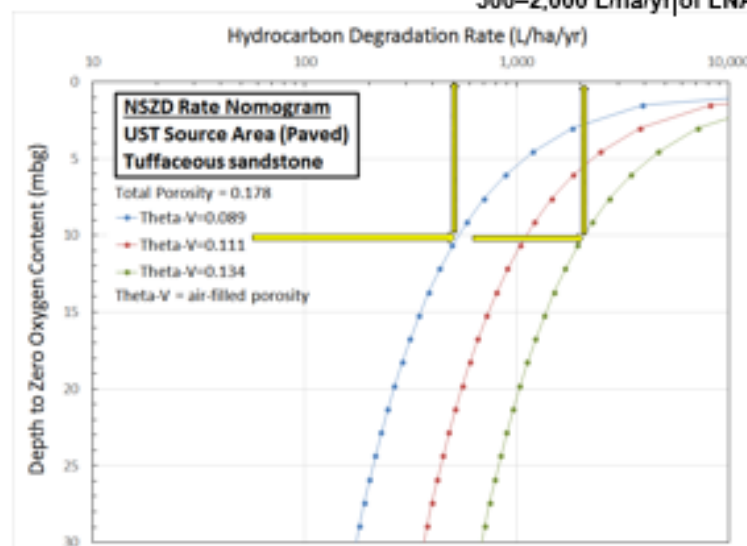


Table 6. Summary of key attributes of NSZD measurement methods. Adapted with permission from table 3-3 of API (2017).

Attribute	Aqueous	Gradient	Passive flux trap	Dynamic closed chamber	Biogenic heat	LNAPL composition
Media	Groundwater samples	Soil gas samples	Soil gas efflux	Soil gas efflux	Soil temperature	LNAPL/oil
Best for sites with:	Solely interested in aqueous portion of NSZD (accounts for <10% of total)	Vadose zones >1.5 metres (below root zone) with pre-existing vapour sampling probes	Variable effects of natural soil respiration on O ₂ and CO ₂ flux	Uniform background gas flux	Long-term NSZD monitoring requirement	Chemical (COC)-specific NSZD rate data needs
Intrusiveness	Low, use existing monitoring wells	High, new probe installations (Low if using existing sample probes)	Low, shallow installation	Low, shallow installation	Low, using existing in-well measurement. Moderate, for new probe installations. No mobilisation needed for long-term measures.	Low, use existing monitoring wells (Moderate if soil borings needed)
Transport processes quantified	Groundwater advection	Gaseous diffusion	Gaseous diffusion and advection ^a	Gaseous diffusion and advection ^a	Gaseous diffusion and advection ^a	Not applicable
Instantaneous or time-averaged measurement?	Instantaneous	Instantaneous	Time-averaged	Instantaneous or time-averaged	Instantaneous, but continuous measurements can be time-averaged	Instantaneous
Method of background (i.e. non-NSZD related processes) correction	Background monitoring of electron acceptors and biodegradation byproducts	Background O ₂ and/or CO ₂ flux monitoring ^c	¹⁴ C	Background CO ₂ efflux monitoring ^c	Background temperature profiling	Fresh oil/LNAPL or biomarker analysis
Spatial coverage/data density	Low	Low	Moderate	High	Low	Low
Real-time data	No	Yes, using field gas analyser	No	Yes	Yes	No

Laboratory analysis	Yes	Optional	Yes	No	No	Yes
Field labor intensity	High	High	Low	Moderate	High initial, low routine	Low
Relative one-time implementation cost ^b	\$\$\$	\$\$\$ (\$-\$\$ if using existing sample probes and field gas analyser)	\$\$	\$	\$\$ (\$ if considered over long-term)	\$\$\$ (\$-\$\$ if using existing monitoring wells)

^a Methods quantify the combined effects of diffusion and advection. The method does not allow for the quantification of the individual contributions from each gas transport process, however.

^b Reported cost ranges include an accounting of the labor, materials, and analytical expenses required to perform a one-time round of NSZD measurements. For the gradient method, it is inclusive of costs for soil gas sampling probe installation, D^{eff}_v tests, and field measurement of soil gas profiles using nested vapour probes. For the passive flux trap method, it is inclusive of trap supply, lab analysis of CO₂ and ¹⁴C, and field installation and retrieval. For the DCC method, it is inclusive of DCC unit rental, collar installation and retrieval, and one round of field measurements.

^c New methods of using ¹⁴C correction on soil vapour samples are emerging.

3. Rate measurement using aqueous data

Information provided by the analysis of groundwater samples can be used to estimate the portion of the NSZD rate as manifested as changes in groundwater. Note that the aqueous manifestation of NSZD is traditionally called natural attenuation (NA), and the methods described in this section align with the methods typically used for monitored natural attenuation (MNA). In the context of NA, the dissolved phase is the primary petroleum hydrocarbon phase considered; the LNAPL and sorbed phases generally represent sources of dissolved-phase contamination.

The evaluation of the distribution of various dissolved constituent changes within the aquifer, such as concentrations of terminal electron acceptors (TEAs) and biodegradation by-products, can provide an indication of the aqueous portion of NSZD (appendix A.1). NSZD within the context of this document is considered to represent the sum of all natural processes that act to deplete the LNAPL source zone. These processes occur within both the unsaturated and saturated zones and result in gaseous and dissolved-phase changes (aqueous), respectively. This section of the document addresses measurement of the aqueous changes and demonstrates how those changes can be stoichiometrically converted to an NSZD rate, or the equivalent portion of petroleum hydrocarbon that is degraded.

Appendix C presents a field procedure for groundwater sampling, the process of data analysis, and example calculations of rate measurement using aqueous data.

3.1 Use of dissolved contaminant concentration trends

NSZD, as expressed by changes in the aqueous phase, can be estimated using groundwater samples and laboratory analytical data of COC concentrations. This generates a chemical (COC)-specific NSZD rate that can be compared to the NSZD rate measured using LNAPL compositional change data (see section 6). The NSZD rate as expressed by changes in the aqueous phase is a fraction of the total NSZD rate estimated using LNAPL compositional change method. If this comparison is to be performed, then it is important to ensure that both methods use the same COC and analytical basis. Note that NSZD results using dissolved- and LNAPL-phase analysis focus solely on one or a small class of chemicals. For this reason, the chemical-specific NSZD rate is typically significantly smaller than the bulk hydrocarbon NSZD rate estimated using the other methods described herein.

COCs are typically selected as part of a risk/exposure assessment. As described in *CRC CARE Technical Report 15* (Beck & Mann 2010), the chemical properties of consideration are solubility, sorption, volatility, biodegradability, chemical stability, density of LNAPL, and toxicity. In general, it is the more soluble benzene, toluene, ethylbenzene, and xylenes (BTEX) and other light fraction (C₆–C₁₂) hydrocarbons which form dissolved-phase petroleum hydrocarbon plumes, which are typically the main targets for NSZD rate measurement. For example, in petrol-derived plumes the COCs typically include BTEX constituents. For a diesel-derived plume, the COCs may include naphthalene and mid-fraction hydrocarbons.

CRC CARE (Beck & Mann 2010) and US EPA (Newell *et al* 2002) explain how to perform first-order attenuation rate constant calculations for COCs. As summarised in

table 7, there are different types of first-order rate constants used to represent different attenuation processes; the documents provide examples of how the three types of rate constants are calculated and applied.

Table 7. Summary of first-order rate constants for natural attenuation studies. *Reproduced with permission from Newell et al (2002).*

Rate constant	Method of analysis	Significance	Use of rate constant
Point attenuation rate (k_{point})	Concentration vs. time plot	Reduction in contaminant concentration over time at a single point	Used for estimating how quickly remediation goals will be met at a well.
Bulk attenuation rate (k)	Concentration vs. distance plot	Reduction in dissolved contaminant concentration with distance from source.	Used for estimating if a plume is expanding, showing relatively little change, or shrinking due to the combined effects of dispersion, biodegradation, and other attenuation processes.
Biodegradation rate (λ)	Model calibration, tracer studies, calculations	Biodegradation rate for dissolved contaminants after leaving source, exclusive of advection, dispersion, etc.	Used in solute transport models to characterise the effect of biodegradation on contaminant migration. These constants are usually applied over both time and space, but only apply to one attenuation mechanism.

As it relates to NSZD measurement in this guidance, the rate constants are solely used to estimate COC degradation rates and are not intended for use in remedial timeframe calculations. The point attenuation rate (k_{point}) is useful to assess geospatial or temporal trends across the plume. The bulk attenuation rate (k) is a more useful calculation when assessing sitewide NSZD rate trends. This document focuses on k_{point} because time-series data sets are common, the procedures are relatively straight-forward, and the results are useful, especially when integrated across multiple locations around the site.

There are a number of things to keep in mind when calculating k_{point} . First, an adequate record of long-term monitoring data must be available to make a statistically valid projection of the rate of aqueous NSZD. As a practical matter, it is difficult to extract rate constants that are statistically significant with fewer than six sampling dates, or with a sampling interval of less than three years. Second, it is unrealistic to expect a few years of monitoring data can accurately predict plume behaviour that often requires one or more decades to achieve remedial goals. Third, it is important to realise that these are merely estimates, and the true NSZD rate may change over time (Newell *et al* 2002).

US EPA (2011) presents a statistical approach to measure k_{point} from the data collected during site characterisation and long-term monitoring. The statistical methods include application of linear regression to estimate decay rate constants using a spreadsheet that also documents the level of confidence. Additionally, the US Interstate Technology & Regulatory Council (ITRC) provides an online guidance document to help environmental professionals better apply statistical methods for evaluation of groundwater data (ITRC 2013).

The point attenuation rate constant (k_{point} , $\text{g}/\text{m}^3/\text{yr}$) is estimated using equation 3 and is often calculated using a spreadsheet tool (e.g. US EPA 2011).

$$\text{Equation 3: } k_{point} = \left(\frac{\ln(C) - \ln(C_0)}{t - t_0} \right)$$

where C and C₀ are the current and initial COC concentrations (g_{COC}/m³), respectively, and t and t₀ are the current and initial time (yr), respectively.

Figure 11 illustrates a result of application of the US EPA (2011) statistical method for trending dissolved benzene degradation rates. k_{point} is shown in the linear regressions solution and is the slope of the line, 0.076 g/m³/yr. See appendix C.2 for the complete example calculation.

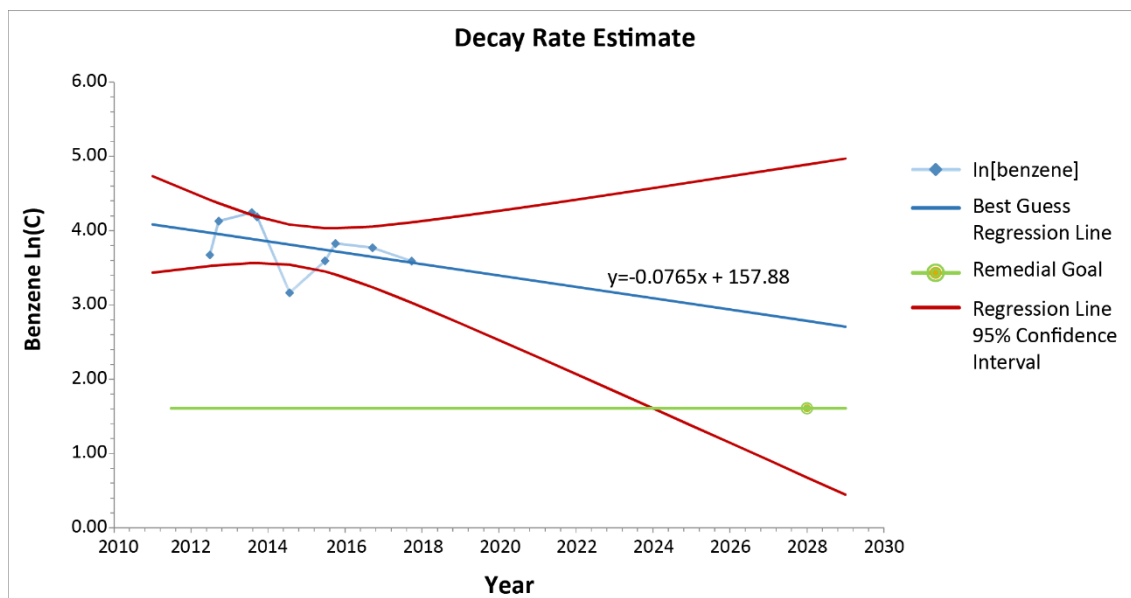


Figure 11. Decay rate estimate using dissolved contaminant concentrations (benzene) and the regression function

Once the rate constant is estimated, it can then be used to calculate the COC-specific NSZD rate as shown on equation 4.

$$\text{Equation 4: } R_{COC-aq} = -k_{point} * \theta_w * h_{gw}$$

where R_{COC-aq} is the chemical-specific NSZD rate (g_{COC}/m²/yr), θ_w is water-filled porosity (m³/m³), and h_{gw} is the saturated thickness of the plume (m³/m²).

3.2 Use of geochemical indicators of NSZD in groundwater

A variety of groundwater reactions transform contaminants; they are called biogeochemical. All are chemical (prefix *chem*) and occur in a geological setting (prefix *geo*), but some are catalysed by microorganisms (prefix *bio*) using various TEA reactions. Some biogeochemical reactions transform a contaminant into a benign form or immobilise it permanently so that it no longer contributes to groundwater pollution (NRC 2000). In-situ biodegradation is the most important attenuation mechanism as it results in mineralisation of contaminant mass, and not just mass transfer (as occurs with non-destructive mechanisms such as advection and dispersion). CRC CARE (Beck & Mann 2010) outline how hydrogeological and geochemical data can be used to indirectly demonstrate the type(s) of aqueous NSZD processes active at the site, and the rate at which such processes will mineralise petroleum hydrocarbons in

groundwater. This method is based on the concentrations of available electron acceptors and biodegradation by-products in the aquifer. Quantification of their changes within the plume provides an indication of which reactions are occurring and what the aqueous NSZD capacity of the system may be. CRC CARE (Beck & Mann 2010) presents example methods for assessing the geochemical indicators of NA. They are described in detail below.

3.2.1 Natural attenuation indicating parameters (NAIPs)

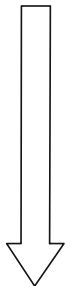
Biodegradation may be defined as microbially mediated chemical transformation of organic compounds to new daughter compounds (by-products). Microbes obtain energy by reduction and oxidation (redox) reactions with organic compounds, hydrogen (H_2), or reduced inorganic forms of iron (Fe), manganese (Mn), N_2 , sulphur, and/or phosphorus. TEAs are necessary for these microbially mediated redox reactions to occur. Under aerobic conditions, dissolved O_2 is the TEA, whereas under progressively more anaerobic conditions, nitrate (NO_3^-), sulphate (SO_4^{2-}), ferric iron (Fe^{3+}), Mn^{4+} , and eventually CO_2 may act as TEAs. Thus, biodegradation may be described as either aerobic and/or anaerobic with variable redox state, depending on the degree of aquifer oxygenation, the bacterial species, and the type of electron acceptors present. The end results of aerobic biodegradation of petroleum hydrocarbons are CO_2 , water (H_2O), and cell mass. The end products of anaerobic biodegradation include simple organic acids, CO_2 , H_2O , CH_4 , hydrogen sulphide (H_2S), N_2 , soluble ferrous iron (Fe^{2+}) and Mn^{2+} , and cell mass.

Table 8, also in *CRC CARE Technical Report 15* (Beck & Mann 2010), summarises the NAIPs and associated TEA and by-product concentration trends typically observed from NSZD reactions. They are listed (top to bottom) from aerobic, most thermodynamically favourable, to anaerobic methanogenic, which are least preferred. Thermodynamics drive microbial use of the TEAs that generate more energy, starting with oxygen (Bethke *et al* 2011). The sequence of reactions is complex with multiple overlapping TEA processes, but is generally determined by how much energy is derived from each of these processes. Methanogenesis is at the bottom of the list since it generates relatively little energy compared to reactions driven by other TEAs. This does not necessarily mean that the rate of methanogenesis will be slow nor that it rarely occurs. To the contrary, methanogenic zones are common in LNAPL source zones, methanogenesis is increasingly acknowledged as a dominant NSZD process and the fate of biogas that it generates is a significant aspect of NSZD assessment (Garg *et al* 2017; ITRC 2018).

There are various graphical methods for assessing the relationships between petroleum hydrocarbons and geochemical indicators, including X-Y (scatter) plots, plume centreline (line) plots, hydrochemical plots (e.g. Radial or Stiff diagrams), and contour (or isopleth) plans. Use of these methods are described in detail in *CRC CARE Technical Report 15* (Beck & Mann 2010). Figure 12, reproduced from *CRC CARE Technical Report 15* (Beck & Mann 2010), shows examples of how scatter plots can be used to plot NAIP data and assess the redox state and effectiveness of aqueous NSZD.

Table 8. Evaluation of geochemical indicators (NAIPs) and preferable biodegradation reactions.

Adapted from Washington State Department of Ecology 2005.

Type of microbial respiration	Electron acceptor	Metabolic by-product	Geochemical indicator response		Redox potential, E _H ⁰ (mV @ pH 7, 25°C) *	
Aerobic (Oxidation)	Oxygen	CO ₂	O ₂ ↓	CO ₂ ↑	+820	Most preferred
Anaerobic (Reduction)	Nitrate (NO ₃ ⁻)	N ₂	NO ₃ ⁻ ↓	CO ₂ ↑	+720	
	Manganese (Mn ⁴⁺)	Mn ²⁺	Mn ²⁺ ↑	CO ₂ ↑	+520	
	Ferric iron (Fe ³⁺)	Ferrous iron (Fe ²⁺)	Fe ²⁺ ↑	CO ₂ ↑	-50	
	Sulphate (SO ₄ ²⁻)	H ₂ S	SO ₄ ²⁻ ↓	CO ₂ ↑	-220	
	Carbon dioxide (CO ₂)	Methane (CH ₄)	CH ₄ ↑	CO ₂ ↑	-240	

* Bacteria associated with these TEA processes are active under a wide range of redox conditions and this table of E_H⁰ values is not intended to be absolute. The field observed E_H for a given redox state may differ from the stated E_H⁰ values. For example, nitrate reduction is commonly observed at a field measured E_H of approximately +200 mV. A resource to assess the plausible range of field measured E_H for the various TEA process is Figure 8 of CRC CARE Technical Report 15 (Beck & Mann 2010).

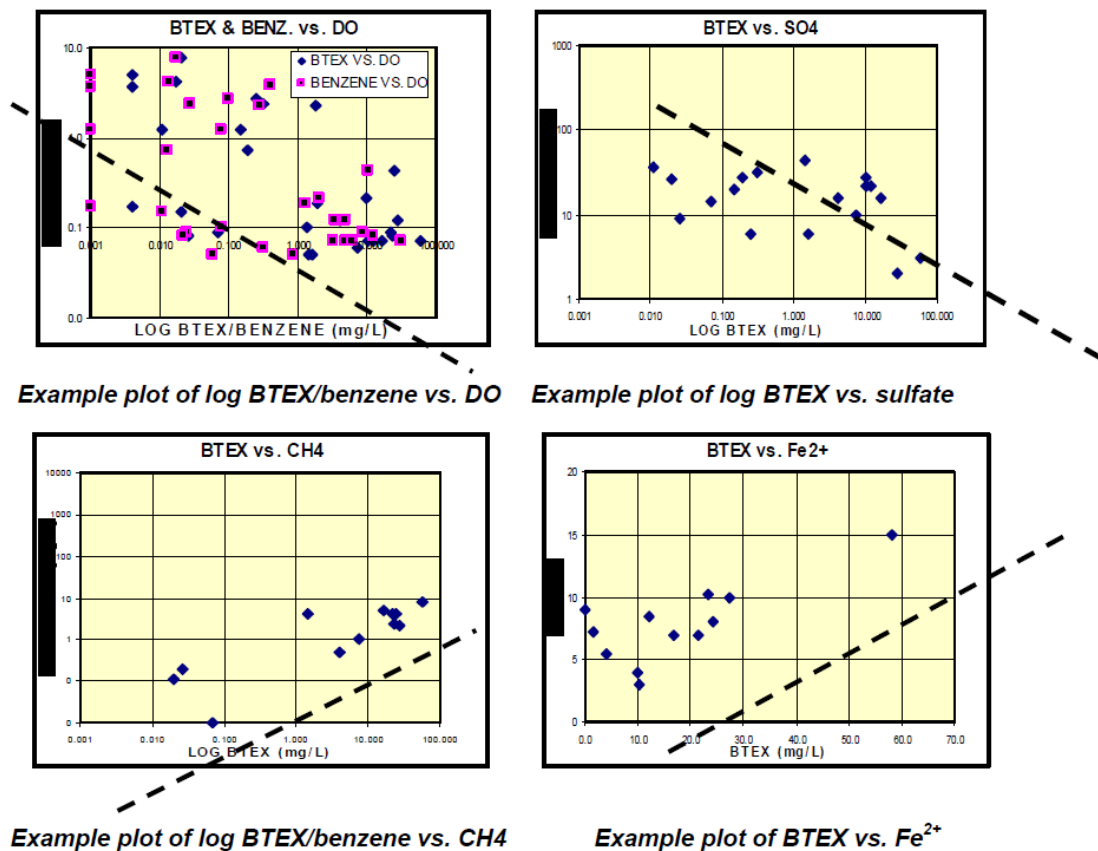


Figure 12. Example X-Y scatter plots of geochemical indicators (NAIPs) of biodegradation. Excerpt from CRC CARE Technical Report 15 (Beck & Mann 2010).

Field-measured parameters such as electrical conductivity (EC) are useful when interpreted together with dissolved O₂, oxidation reduction potential (ORP), and pH for identification of groundwater recharge zones. Localised recharge processes may confound the typical assessment of NAIPs based on spatial correlations between the contaminant and TEA and by-product concentrations. For example, a localised recharge zone characterised by low SO₄²⁻ concentrations may be interpreted as being a zone of active biodegradation, whereas the low SO₄²⁻ (in reality) is reflecting infiltration and the mixing of low-salinity rainwater with regional groundwater. In this case, it may be useful to plot EC versus SO₄²⁻ concentrations. If a mixing line is apparent, then sulphate may not be able to be used for assessing aqueous NSZD processes (Beck & Mann 2010).

Temperature can also influence biodegradation rates. Optimum temperatures are between 20 °C and 40 °C (Atlas 1981). Higher temperatures may also increase contaminant solubility; however, this would generally be negligible due to the buffering effect of the vadose zone, resulting in relatively stable groundwater temperatures (Beck & Mann 2010).

3.2.2 Mass budgeting

It is possible to estimate the ongoing in-situ biodegradation of petroleum hydrocarbons using the change in electron acceptor/metabolic by-product concentrations between background and plume areas and the stoichiometry of the petroleum hydrocarbon biodegradation reactions.

Mass budgeting uses the NAIP data to calculate the rate at which TEAs are consumed and by-products are produced and stoichiometrically equates it to the aqueous NSZD rate. The relative rates of each TEA reaction reveal which processes are important and which are not. Appendix C presents an example of how mass budgeting can provide evidence that biodegradation is causing the loss of contaminants.

The fundamental equation for mass budgeting is stated in equation 5.

$$\text{Equation 5: } R_{aq} = V_D(AC)(YZ)$$

where R_{aq} is the aqueous reaction rate (g/d), V_D is the Darcy velocity of groundwater flow (m/d, also known as the specific discharge), AC is assimilative capacity of all TEA biotransformation processes combined (g/m³), and YZ = the area perpendicular to groundwater flow (m²).

The reaction rates of all NAIPs (i.e. TEAs and biodegradation by-products) are calculated, stoichiometrically converted to hydrocarbon degradation equivalents, and summed to arrive at an NSZD rate as manifested in aqueous changes.

One common problem in applying a straightforward mass budget analysis is that advection may not dominate the inputs and outputs of all the footprint materials. Phase transfers can supply or remove materials independently of water flow. When sufficient measures are available, the unknown phase transfers can be computed from the budget analysis.

There are two more NAIPs that can be used to demonstrate that biodegradation is causing the loss of contaminants and contributing to aqueous NSZD: inorganic carbon (CO₂) and alkalinity. The aerobic biodegradation of petroleum hydrocarbons consumes O₂ and produces CO₂ in stoichiometric ratios. Estimating the O₂ supply rate and

correlating it with increases in CO₂ can yield a quantitative estimate of the rate of hydrocarbon biodegradation. The biodegradation of organic contaminants, including hydrocarbons, under denitrifying or SO₄²⁻-reducing conditions consumes NO₃⁻ or SO₄²⁻ and produces CO₂ and alkalinity. Estimating the supply rates of SO₄²⁻ or NO₃⁻ and correlating them with changes in inorganic carbon concentration and alkalinity can provide evidence for these anaerobic biodegradation reactions (NRC 2000).

Consistency among these three types of evidence (electron acceptor, CO₂, and alkalinity) can be used to demonstrate that other loss mechanisms or confounding factors are unlikely. As shown in the example presented in appendix C.3, using several types of information allows for identification of important mechanisms that are not detected through sampling and COC analysis of the groundwater.

Box 3.1 summarises the process of mass budget analysis for NSZD rate calculation and the use of changes in CO₂ and alkalinity concentrations as a quality control tool. Appendix C.3 presents a more detailed numerical example for the application of mass budget analysis for NSZD rate calculation.

3.3 Aqueous-based NSZD measurement quality assurance/quality control

Appropriate QA/QC measures are essential to assess the accuracy and precision of the data collected. Use proper, manufacturer-recommended calibration procedures for all field instruments. A minimum two-point calibration is typically prudent with a span calibrated to the range of expected concentrations. Ensure that field and laboratory samples comply with project-specific duplicate sample collection, as well as field equipment blanks.

As mentioned above, a useful QA/QC step that can be used to help ascertain the results of mass budgeting analysis includes comparing measured and computed changes in total inorganic carbon (dissolved CO₂) and total alkalinity. Stoichiometric amounts of both dissolved CO₂ and alkalinity are produced as a by-product of biodegradation (NRC 2000). Comparison of the measured and computed values allows further assessment of the results. For example, if the measured increase is greater than the computed, then the NSZD calculation could be considered low biased. Because reactions of both dissolved CO₂ and alkalinity are complex (i.e. associated with the dynamics of the earth's carbon cycle) and involve geochemical processes other than NSZD, this comparison is considered qualitative in nature. It is performed for the purposes of assessing the potential accuracy of the calculations (e.g. is the actual NSZD rate closer to the upper or lower end of the range of estimates) and simple validation that aqueous-based NSZD biodegradation is responsible for the loss of petroleum hydrocarbons.

Box 3.1 Measurement of the aqueous portion of NSZD

Objective: Mass budgeting analysis to estimate the aqueous NSZD rate using TEAs and biodegradation by-product concentrations and groundwater properties.

For more information: Appendix C.3

Principle: Mass budgeting and total assimilative capacity (NRC 2000)

$$R_{aq} = V_D(AC)(YZ)$$

Key assumptions:

- Steady-state, lateral advection
- All changes in NAIPs are attributable to hydrocarbon biodegradation (aq NSZD)

Key calculation parameters:

- NAIP concentrations in background locations and within source/plumes areas
- Stoichiometric ratios
- Darcy velocity

Example monitoring plan:



Summary of implementation procedure:

- Groundwater sampling and analysis
- Calculate the changes in NAIPs
- Perform stoichiometric conversions and AC calculations
- Calculate the NSZD rate

Nov 2015 field monitoring results:

Plume Region Location	DO (mg/L)	Methane (µg/L)	Ferrous iron (mg/L)	Carbon Dioxide (mg/L)	Nitrate (mg/L)	Sulphate (mg/L)	BTEX (µg/L)	Alkalinity (CaCO ₃) (mg/L)
Background	5.6	0.01	0.33	80	0.60	120	1.0	583
Source	5.8	4.34	3.2	159	0.25	2.9	200	710
Plume Edge	7.2	2.48	0.40	131	0.25	5.2	2.0	703

Average changes in NAIPs

Constituent	Background	Average AC	Change Average
O ₂	mg/L 5.6	6.5	0.87
NO ₃	mg/L 0.60	0.25	-0.35
SO ₄	mg/L 120	4.1	-116
Fe ²⁺	mg/L 0.33	1.8	1.5
Methane (CH ₄)	µg/L 0.01	3.4	3.4
Alkalinity (CaCO ₃)	mg/L 583	707	123
Total CO ₂ (C)	mg/L 80	145	65

Stoichiometric ratios (for octane, C₈H₁₈):

Reaction	Octane g C ₈ H ₁₈ /g Acc-BP
Aerobic (O ₂)	0.29 g C ₈ H ₁₈ /g O ₂
Denitrification (NO ₃ ⁻ as N)	0.18 g C ₈ H ₁₈ /g NO ₃ ⁻
Sulphate reduction (SO ₄ ²⁻ as S)	0.19 g C ₈ H ₁₈ /g SO ₄ ²⁻
Iron Reduction (Fe ²⁺ generated)	-0.04 g C ₈ H ₁₈ /g Fe ²⁺
Methanogenesis (CH ₄ generated)	-1.14 g C ₈ H ₁₈ /g CH ₄

Stoichiometry and AC calculation:

Multiply observed changes by the stoichiometric ratios to estimate AC for upper-, mean, and lower-end ranges of NAIP values.

Mean AC value scenario

Reaction	Computed Change Octane (mg C ₈ H ₁₈ / L)
Aerobic Respiration (O ₂)	0
Denitrification (NO ₃ ⁻)	-0.06
Sulphate Reduction (SO ₄ ²⁻)	-22
Iron Reduction (Fe ²⁺ generated)	-0.060
Methanogenesis (CH ₄ generated)	-3.9
Total	-26

Note: Computed change in octane for aerobic respiration is zero due to observed increase in DO in source and plume edge areas.

Aqueous NSZD rate calculation:

Darcy velocity = 0.0016 m/d

Average LNAPL width = 127 m

Average LNAPL smear thickness = 3 m

$$R_{aq} = 0.0016 \frac{m}{d} * 26 \frac{g}{m^3} * (127 * 3 m^2) = 15 \frac{g C_8H_{18}}{d}$$

Estimated range aqueous NSZD:

14–16 g/d of LNAPL

6–7 L/yr of LNAPL (SG=0.81)

3.4 Aqueous-based NSZD measurement considerations

Sources of measurement uncertainty and variability, how they affect NSZD rate measurement using aqueous method calculations, and potential mitigation means are presented in table 9.

Table 9. Aqueous method uncertainty and variability considerations.

Factor	Effect	Mitigation
First-order, dissolved-COC degradation rate constants	NSZD rates, as measured in bulk, have been observed as zero-order as discussed further in section 4.1. This is contrary to traditional practice in groundwater areas absent of LNAPL, where first-order kinetics are assumed.	Carefully screen for LNAPL presence within the vicinity of the monitoring well(s). Where present, LNAPL will affect rates. Use of the rate constants for purposes of remedial timeframe is limited to areas outside the LNAPL footprint.
LNAPL bias	When groundwater samples are collected from monitoring wells screened within zones containing LNAPL (mobile or residual), there is a potential for small LNAPL droplets to enter the sample train and bias laboratory analytical results. Evidence of LNAPL bias includes COC concentrations above predicted solubility limits.	Use of techniques such as polyethylene microfiber filtration, laboratory settling, or passive diffusion bag samplers can eliminate LNAPL bias and protect sample integrity.
Seasonal variability	Large seasonal changes in groundwater hydraulic and/or geochemical conditions may result in significant changes in NSZD rates.	Assess seasonal changes in groundwater table and quality water to determine if multiple rounds of NAIP monitoring are useful to assess seasonal variability.
Monitoring well screen	Monitoring wells screened over large intervals or multiple stratigraphic units will provide water from the most hydraulically conductive zone and may not be solely representative of the LNAPL smear zone interval.	To avoid analytical bias, utilise monitoring wells that are screened solely across the stratigraphy where the LNAPL smear zone exists, or are demonstrated to provide representative water quality.
Groundwater advection	Advection may not dominate the inputs and outputs of the NAIPs. Rather, phase transfers may contribute more significantly. This will impact the analysis as it is a primary assumption of the mass budgeting analysis.	Assess the hydrogeochemistry, and determine the primary mass transfer processes. Perform sufficient measures to estimate the phase transfers (i.e. non-advection contributions).

As discussed in section 1.5, the portion of NSZD as measured using aqueous data must be added to the NSZD accounted using gaseous or biogenic heat data. However, the aqueous portion of the NSZD rate is typically very small (e.g. less than 1% of the total NSZD rate). If confirmed insignificant and there are no data use drivers, then measurement of the aqueous portion of NSZD may be omitted from a monitoring program.

4. Rate measurement using soil gas flux data

In addition to the aqueous changes discussed in section 3, NSZD also manifests itself as changes in the vadose-zone gases. CH₄ is created by methanogenesis and, to a lesser extent CO₂, from the multitude of TEA biotransformation processes within the LNAPL smear zone. In overlying aerobic soils, the CH₄ is oxidised to CO₂, and the CO₂ vents at ground surface. Gases are transported through the vadose zone via diffusion and, to a lesser extent, advection. The flux of the gases (i.e. mass flow per unit area per unit time) can be measured and used to estimate the NSZD rate.

The content of this section starts with a general discussion of the soil gas flux calculation basis and a description of implementation elements that are common to all methods of measurement. Following, is a presentation of three methods that can be used to measure the soil gas flux: gradient, passive flux trap, and dynamic closed chamber (DCC). Table 6 summarises the key attributes of each and where best to use them. Appendices D, E, and F contain detailed procedures that can be used to implement the gradient, passive flux trap, and DCC methods, respectively.

4.1 Stoichiometric calculation of NSZD rates using gas flux measurements

Each of the primary gases associated with NSZD is consumed (O₂) or created (CH₄ and CO₂) in stoichiometric quantities. Therefore, LNAPL degradation rates occurring via NSZD can be determined by stoichiometrically converting the measured gas flux (Davidson *et al* 2002; Molins *et al* 2010; Sihota *et al* 2011, 2013).

This is done by first assuming a representative hydrocarbon based on site-specific information. Table 10 presents a range of hydrocarbons that could be used, their associated balanced equations, and stoichiometric ratios to CO₂ (API 2017). Table 11 presents the various units of measure used in the NSZD calculations.

For demonstration purposes in this document, octane (C₈H₁₈) is consistently assumed the representative hydrocarbon for an LNAPL composition that is dominated by the C₈ carbon fraction. Equations 6 and 2, restated below, are the microbially mediated reactions that can be used as the basis for stoichiometric calculation of NSZD.

Equation 1: Methanogenesis – $C_8H_{18} + 3.5 H_2O \rightarrow 1.75 CO_2 (g) + 6.25 CH_4 (g)$

Equation 2: Methane oxidation – $CH_4 + 2 O_2 \rightarrow CO_2 (g) + 2 H_2O$

Equations 1 and 2 are typically combined into a single summary reaction for stoichiometric calculation purposes as shown in equation 6.

Equation 6: $C_8H_{18} + 12.5 O_2 \rightarrow 8 CO_2 (g) + 9 H_2O$

Table 10. Example representative hydrocarbons and CO₂ stoichiometric conversion factors. *Reproduced with permission from API (2017).*

Representative hydrocarbon (HC)	Chemical formula	Stoichiometric equation	Molecular weight of HC	Stoichiometric ratio HC:CO ₂	CO ₂ flux multiplier
Benzene	C ₆ H ₆	2 C ₆ H ₆ + 15 O ₂ → 12 CO ₂ + 6 H ₂ O	78.1	0.16	13.0
Heptane	C ₇ H ₁₆	C ₇ H ₁₆ + 11 O ₂ → 7 CO ₂ + 8 H ₂ O	100.2	0.14	14.3
Octane	C ₈ H ₁₈	2 C ₈ H ₁₈ + 25 O ₂ → 16 CO ₂ + 18 H ₂ O	114.2	0.125	14.3
Decane	C ₁₀ H ₂₂	2 C ₁₀ H ₂₂ + 33 O ₂ → 20 CO ₂ + 22 H ₂ O	142.3	0.10	14.2
Dodecane	C ₁₂ H ₂₆	2 C ₁₂ H ₂₆ + 37 O ₂ → 24 CO ₂ + 26 H ₂ O	170.3	0.083	14.2
Tetradecane	C ₁₄ H ₃₀	2 C ₁₄ H ₃₀ + 43 O ₂ → 28 CO ₂ + 30 H ₂ O	198.4	0.071	14.2

Table 11. Parameter units involved in estimating NSZD rates from gas flux measurements. *Reproduced with permission from API (2017).*

Parameter	International system (SI) units	
	Unit	Abbreviation
Gradient method	milligrams/square metre/hour, or grams/square metre/second	mg/m ² /hr, or g/m ² /s
Gas flux	micromoles/square metre/second	µmol/m ² /s
Mass-based NSZD rate	grams/square metre/day kilograms/square metre/year	g/m ² /d kg/m ² /yr
Volumetric NSZD rate	litres/square metre/day cubic metres/square metre/year	L/m ² /d m ³ /m ² /yr
Statewide mass-based NSZD rate	kilograms/day kilograms/year	kg/d kg/yr
Statewide volumetric NSZD rate	litres/day cubic metres/year	L/d m ³ /yr

The rate of NSZD is assumed to be equivalent to the rate of consumption of C₈H₁₈ as determined stoichiometrically from either consumption of O₂ or production of CO₂. At many sites with ample atmospheric exchange and measurements taken from the soil overlying the LNAPL footprint and hydrocarbon oxidation zone, equation 1 can be ignored. In this case, it is assumed that all CH₄ is converted into CO₂. At some sites, where ample O₂ exchange with atmosphere does not occur, it may be useful to also measure CH₄ flux and make a second stoichiometric calculation. In this case, the NSZD rate equals the summation of the stoichiometric petroleum hydrocarbon (e.g. C₈H₁₈) contributions from both anaerobic (equation 1) and aerobic (equation 6) processes.

Equation 7 shows how to estimate the NSZD rate at individual locations using a gas flux measurement.

$$\text{Equation 7: } R_{NSZD} = \left[\frac{J_{NSZD} m_r MW}{10^6} \right] \times \frac{86400s}{d}$$

where R_{NSZD} is the total hydrocarbon degraded or NSZD rate (g/m²/d), J_{NSZD} is the background corrected soil gas flux measurement (micromoles per square metre per second (μmol/m²/s)), m_r is the stoichiometric molar ratio of hydrocarbon degraded in equation 6 (unitless), and MW is the molecular weight of the representative hydrocarbon (g/mol) from table 10.

Once the NSZD rates are calculated for each measurement location, the results can be mapped to visualise gas flux patterns across the site and assess alignment with the known extent of subsurface LNAPL.

If the data objective drives a need (see section 2.1) and enough representative measurements are made across the LNAPL footprint, then the NSZD rates can be integrated across the site to estimate a site-wide NSZD rate (in units of L/d).

Similarly, if the data objective drives a need and enough rounds of measurements are performed to account for seasonal variability, then the NSZD rates can be integrated over time to estimate a monthly or annual NSZD rate (kg/m²/yr or L/yr).

4.2 Common procedures using soil gas data

Some design, implementation, and data analysis elements are common to the three soil gas flux methods. This section describes these common procedures that are useful to improve data quality from an NSZD measurement program.

4.2.1 Background correction

Use of vadose-zone gas flux to estimate NSZD rates is confounded by the presence of reactions associated with plant and organic matter (Rochette *et al* 1999). These natural soil respiration (NSR) reactions are considered background and must be quantified in order to isolate the gas flux associated with NSZD alone. In simple terms, the NSZD-related gas flux (J_{NSZD}) rate is equal to the total flux (J_{Total}), minus the flux associated with NSR processes ($J_{Background}$) as stated in equation 8.

$$\text{Equation 8: } J_{NSZD} = J_{Total} - J_{Background}$$

Background correction is required for all three soil gas flux methods, but the exact field implementation and analytical approach used to correct the gas flux is specific to each

of the measurement methods. The background correction approaches for the gradient, passive flux trap, and DCC methods are presented in sections 4.3.2, 4.4.2, and 4.5.2, respectively.

4.2.2 Monitoring frequency

The number and frequency of gas flux measurements at a site depends upon the data objectives (see section 2.1). Use of table 3 is helpful to frame the scope of the NSZD measurement program. Additionally, review of table 4 is useful to flag certain site conditions such as ambient temperature climate and fluctuations in soil moisture that may lead to more or less variability in NSZD rates (Sihota *et al* 2016). If site conditions are identified that would result in variable NSZD rates, then multiple rounds of measurements are useful to estimate long-term (e.g. annual) NSZD rates.

4.2.3 Ambient monitoring

Gas flux can be affected by conditions above and below the vadose zone, including atmospheric and groundwater. To support data evaluation efforts after the field measurement program, it is typically prudent to synoptically monitor and record atmospheric conditions such as temperature, barometric pressure, wind speed, and precipitation. This can often be done remotely using data from a local meteorological data station that posts their data on a publicly available website or onsite using a weather monitor. Likewise, synoptic measurements of the groundwater level and temperature can also help inform data evaluation efforts.

4.2.4 Quality control and quality assurance

QA/QC is of utmost importance to the quality of the NSZD measurements. As with all other environmental monitoring activities, extra measurements are implemented to ensure consistent and quality data collection. For the gas flux methods, the following QA/QC measurements are typically collected:

- Field blank – relevant to the DCC method, the chamber is placed on an air-tight collar and allowed to collect a series of blank measurements. This is discussed in more detail in section 4.5.3.
- Trip blank – relevant to the passive flux trap method, a laboratory-sealed trip blank trap accompanies the shipment from point of origin through field deployment and back to laboratory. Results are used to measure the incidental amount of CO₂ sorbed by the trap during manufacturing and transport. This is discussed in more detail in section 4.4.3.
- Duplicate – relevant to all gas flux methods, used to assess reproducibility of measurements in side-by-side installations (passive flux trap and DCC methods) and/or sample points (gradient method).

The results of the QA/QC measurements can be used to perform data validation, similar to that done for groundwater analytical chemistry. Detection limits can be assigned, results adjusted for cross contamination, and data can be qualified due to poor duplicate correlation in the field. Additional details on the QA/QC measurements are discussed in the subsections for each gas flux method below.

4.3 Gradient method

As discussed in section 1.5, NSZD manifests itself as changes in O₂ and CO₂ concentrations above the hydrocarbon-impacted soil. After correction for non-petroleum-related effects, the concentration gradients, or the change in concentration with depth at a monitoring location, can be used to estimate the gas flux (Johnson *et al* 2006; Lundegard & Johnson 2006). As detailed in section 4.1, the gas flux can then be stoichiometrically converted to an NSZD rate.

Historical studies demonstrated that the gradient method is a suitable tool for both short- and long-term measurement of gas flux (API 2017). The gradient method uses soil gas measurements taken at discrete depths to estimate the diffusive flux through the vadose zone. Because NSZD directly impacts both O₂ and CO₂, either the diffusive flux of O₂ (consumption) or CO₂ (production) can be stoichiometrically equated to an NSZD rate. Thus, the calculated O₂ influx can serve as a check on the calculated CO₂ efflux, or vice versa.

The gradient method is based on Fick's first law of diffusion as shown in equation 9.

$$\text{Equation 9: } J = D_v^{\text{eff}} \left(\frac{dC}{dz} \right)$$

where J is the steady-state diffusive flux (g/m²-soil/s), dC/dz is the soil gas concentration gradient (g/m³-m) or change in gas concentration (C, g/m³) over change in depth (z, m), and D_v^{eff} is the effective vapour diffusion coefficient (m²/s), also known as the effective diffusivity, that is specific to the soil and gas being measured. It is typically annotated with a subscript that specifies the gas (e.g. D_{O₂}^{eff} is the effective diffusion coefficient for oxygen). Typically, the gas flux is reported in molar-based units of mass per area per time (e.g. μmol/m²/s). Figure 13 illustrates typical soil gas concentration profiles that exist above LNAPL-impacted soil and in background areas.

4.3.1 Gradient method key assumptions

Application of the gradient method is founded on two key assumptions: diffusion is the dominant mechanism for gas flux, and vadose zone soil is homogeneous and isotropic and can be represented by a single representative D_v^{eff}. Vadose-zone N₂ concentrations were used to assess the assumption of diffusion controlled flux at the Bemidji crude oil release site (Molins *et al* 2010; Sihota & Mayer 2012; Sihota *et al* 2013). The findings indicated that advective flux was only present adjacent to the LNAPL source zones where CH₄ generation was sufficiently high to create pressure gradients. However, in overlying aerobic zones, where CH₄ is absent and gradient method measurements are typically collected, diffusion remains the dominant transport mechanism. Therefore, the gradient method is applicable provided that soil gas measurements for the gradient method are taken from the aerobic zone above the hydrocarbon-impacted soil.

With respect to the assumption of the representativeness of D_v^{eff}, in practice, subsurface soil is rarely homogeneous and isotropic. While it may contribute uncertainty, it does not preclude use of the gradient method. Take care to review the geology/stratigraphy within the aerobic zone and measure D_v^{eff} from the different lithology within the measured depth intervals. Methods are available to estimate weighted average diffusivity values (Pingingtha *et al* 2010) within the depths of interest. It is important to note that measurements of D_v^{eff} are not needed throughout the

unsaturated zone, rather only in the depth interval where soil gas measurements are used to estimate dC/dz in equation 9.

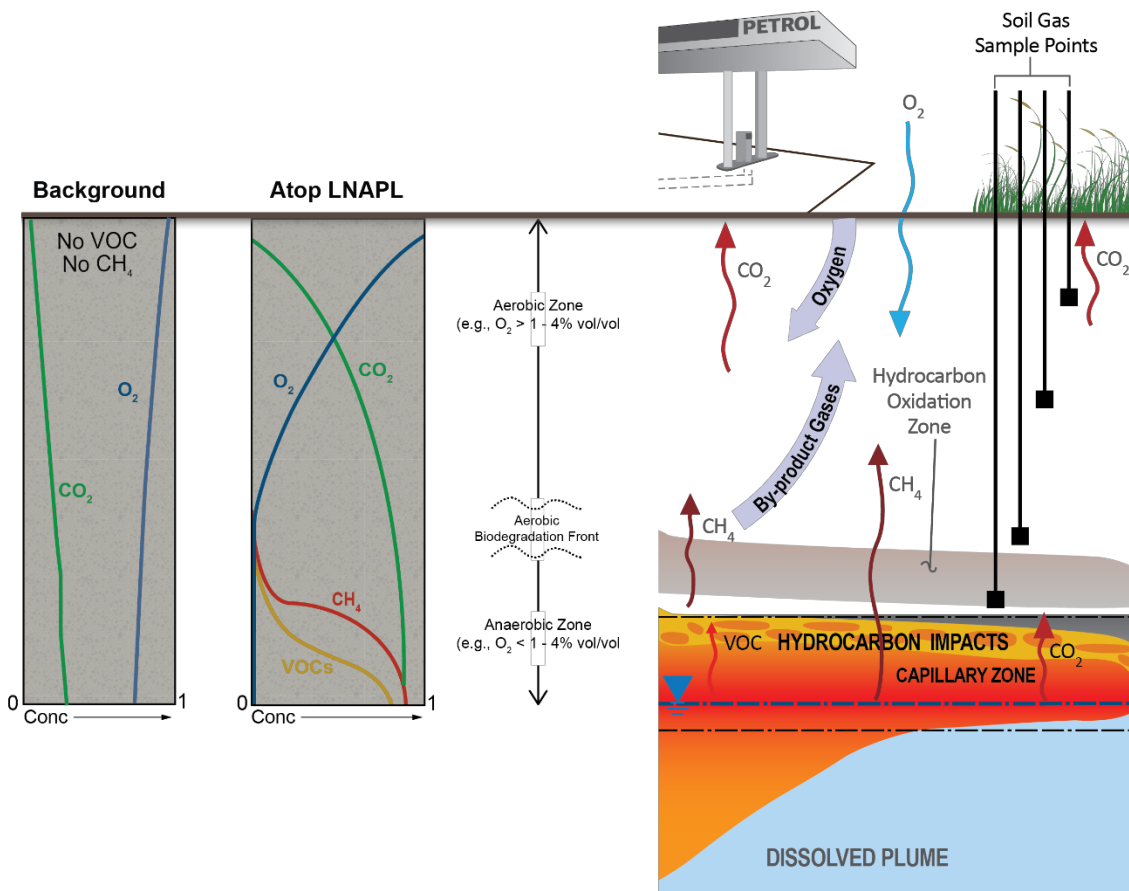


Figure 13. Schematic of gradient method soil gas monitoring setup.

Appendix D presents field procedures for soil gas D_v^{eff} measurement and gas profile measurements, the process for background correction and data analysis, and example calculations of rate measurement using soil gas data.

4.3.2 Gradient method process

Box 4.1 illustrates application of the gradient method at a single location with background correction. It comprises the following general steps:

1. Install new multi-level vapour sampling probes or establish alternative means for vapour sampling as discussed in appendix D.4.
2. Perform the following during a concurrent field effort:
 - a) Soil vapour sampling from the monitoring probes to measure O_2 , CO_2 , CH_4 , and VOC concentrations, and
 - b) In-situ tracer tests to estimate a representative range of soil vapour diffusion coefficients
3. Plot the data and estimate the concentration gradient(s)
4. Assess the background O_2 consumption and CO_2 production and compensate for background flux, and
5. Calculate the NSZD rate.

Box 4.1 Gradient Method of NSZD Rate Calculation

Principle: Fick's first law of diffusion

$$J = D_v^{eff} \left(\frac{dC}{dz} \right)$$

For more information: Appendix D.5

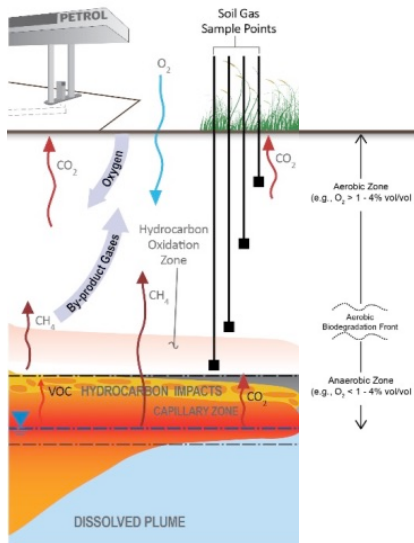
Key Assumptions:

- Steady-state "snap shot" in time
- Diffusion-controlled gas flux
- Representative D_v^{eff}

Key Calculation Parameters:

- Effective vapour diffusion coefficient
- Concentration gradient

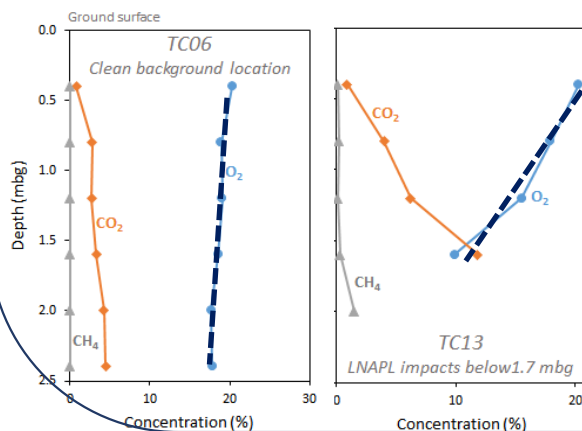
Visual Conceptualization:



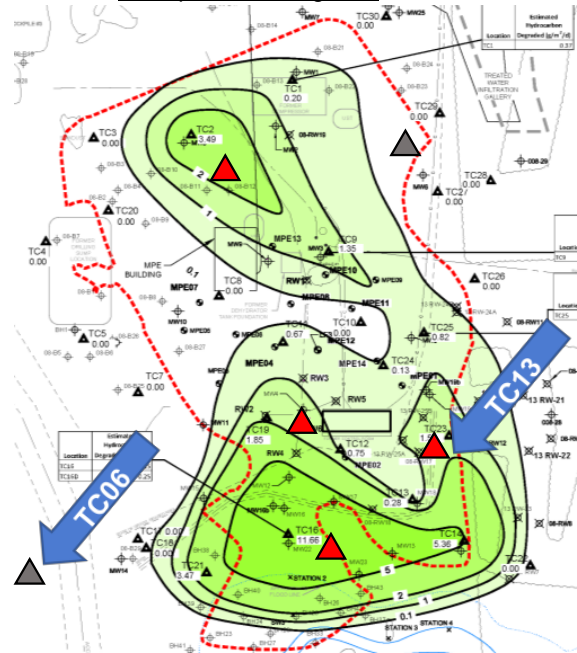
Summary of Implementation Procedure:

1. Install vapour monitoring probes
2. Vapour sampling
3. Tracer testing
4. Gradient estimation
5. Calculate the NSZD rate

Oct 2015 Field Monitoring Results:



Example Monitoring Plan:



Legend

- ▲ Background nested vapour probe
- ▲ Nested vapour probe
- NSZD rate (0.1 g/m²/d)
- NSZD rate (5 g/m²/d)
- Extent of LNAPL in soil

Monitoring Location Selection Criteria:

- Gravel pad northern half, incl. background
- Vegetated southern half, incl. background

Helium Tracer Test-based Diffusivity:

Range of D_v^{eff} 0.0013 – 0.0038 cm²/s

Gradient Estimates – vegetated areas:

$$\text{Background TC06 } \frac{dC}{dz} = \frac{(20-18)}{(2.4-0.4)} = 14 \text{ g/m}^4$$

$$\text{Impacted TC13 } \frac{dC}{dz} = \frac{(20-11)}{(1.6-0.4)} = 102 \text{ g/m}^4$$

$$\text{Background corrected } \frac{dC}{dz} = 88 \text{ g/m}^4$$

NSZD Rate Calculation:

$$\text{O}_2 \text{ flux, } J \text{ (g/m}^2\text{/d)} = D_v^{eff} * \frac{dC}{dz}$$

High-end O₂ flux, J = 3 g/m²/d

Low-end O₂ flux, J = 1 g/m²/d

Stoichiometric conversion: 0.3 g C₈H₁₈/g O₂

Range of estimated NSZD at TC13:

0.3-0.8 g/m²/d of LNAPL

3-10 L/ha/d of LNAPL

The following sections provide an overview of the key steps. Appendix D provides detailed analytical and field procedures. Ensure probe installations and soil gas monitoring conform to well-established, standard practice (CRC CARE 2013) or other locally required procedures.

Measuring the soil vapour diffusion coefficient

The effective vapour diffusion coefficient D_v^{eff} can be estimated using two different means; site-specific measurements and empirical. Spatial and temporal variability in moisture content in the unsaturated zone (e.g. perched water) can have multiple orders-of-magnitude impact to the value of D_v^{eff} (Tillman & Smith 2005; Wealthall *et al* 2010). In a lithologically layered vadose zone, vapour diffusion from depth will be limited by the wettest and/or least porous soil layer (Davis *et al* 2005). This may be near-surface soils periodically inundated by rainfall or a deeper fine-grained layer that perches water, for example. Therefore, it is incumbent on the practitioner to review the geology and moisture content when applying the gradient method so that a representative value, or more appropriately a range of values, of D_v^{eff} are used. For this reason, site-specific measurements are the preferred means to estimate vapour diffusivity.

Empirical estimates of D_v^{eff} using Millington & Quirk (1961), for example, are only recommended for qualitative or screening-level assessment of NSZD using the gradient method. For quantitative NSZD evaluations, site-specific measurements at each multilevel soil gas sample port are recommended to be completed at the same time of soil gas concentration profile measurement to reduce uncertainty about scale effects and soil sample representativeness. Tracer test procedures are described in appendix D.2.

Measuring the concentration gradient (dC/dz) using nested soil vapour monitoring probes or alternate methods

This is the traditional means to monitor soil gas concentration profiles and estimate dC/dz for use in the gradient method. Soil gas concentration profiles are measured above the LNAPL footprint and used as a basis to estimate the NSZD rate using the gradient method. Appendix D.3 describes the probe installation and sampling procedures.

Optional means have been investigated to more efficiently measure dC/dz . These include the use of existing monitoring wells and manually installed shallow vapour probes. They are described in detail in appendix D.4. However, before these methods are used, scrutinise their validity through close inspection of the vadose-zone properties (e.g. boring logs, soil samples) and preferably confirmed with at least one nested vapour monitoring probe installation.

Estimating the concentration gradient

Estimation of the gradient requires careful assignment of upper and lower boundary control points. As described in detail in API (2017) and appendix D.1, carefully select these locations above the hydrocarbon oxidation zone and based on geologic and gas profile shape considerations. The difference in concentration between the upper and lower boundary control points of measurement, divided by the vertical distance between the control points, gives an estimate of the vertical concentration gradient, dC/dz in equation 9.

Assessing and compensating for background using the gradient method

As discussed in section 4.2.1, NSR within organic matter throughout the vadose zone profile can also consume O₂ and create CO₂. It must be accounted and subtracted from the total flux to isolate the gas flux attributed only to NSZD as shown in equation 8. If not accounted, the NSZD rate may be over-estimated. This background correction can be done by simply measuring the gas flux using the same procedures described in this subsection in a background location outside the LNAPL footprint with similar subsurface properties as the other measurement locations. If the subsurface has multiple distinctly different features across the LNAPL footprint, then multiple background locations may be necessary to account for non-petroleum effects within each distinctly different feature. Figures 4 to 9 illustrate this with different zone numbers for each unique setting.

Calculating the NSZD rate

Section 4.1 describes how to estimate an NSZD rate using the CO₂ efflux and O₂ influx results alike. To adapt the calculation for O₂, multiply the O₂ gas influx by the stoichiometric ratio with the hydrocarbon to obtain the NSZD rate. Table 10 presents example representative hydrocarbons and CO₂ flux stoichiometric conversion factors that can be used in the calculations.

4.3.3 Gradient method quality assurance/quality control

Appropriate QA/QC measures are essential to assess the accuracy and precision of the data collected. Use proper, manufacturer-recommended calibration procedures for all field instruments. A minimum two-point calibration is typically prudent with a span gas calibrated to the range of expected concentrations. Ensure field and laboratory samples comply with project-specific duplicate sample collection as well as ambient field blanks, if samples are to be sent to a laboratory.

4.3.4 Gradient method considerations

Sources of measurement uncertainty and variability, how they affect gradient method calculations, and potential mitigation means are presented in table 12.

Table 12. Gradient method uncertainty and variability considerations. *Reproduced with permission from API (2017).*

Factor	Effect	Mitigation
Effective diffusion coefficient, D_v^{eff}	Gas diffusion varies significantly with soil moisture after rain events and seasonally	Schedule monitoring during dry weather. Perform diffusivity tests during the same field event with gas concentration measurements.
Geologic conditions across the LNAPL footprint	Variable geology will result in variable diffusion rates	Measure D_v^{eff} and soil gas concentration profiles within each unique geologic area at the site.
Short measurement period	The gradient method provides only a “snap shot” in time of flux that can be dynamic	Perform additional measurements at different times of the year to ascertain the variability.
Advective flux	Analytical calculations assume only diffusion, pressure gradients are neglected	Verify that advection is negligible through either pressure or N ₂ measurements.

Interpretation of results from the gradient method, alike the other NSZD monitoring methods, can be challenging. Some items to consider when interpreting the data include:

- changes (geospatial and/or temporal) in soil moisture can significantly affect the measured soil gas profiles
- a non-uniform vadose zone, for example containing thin, low-permeability layers, may significantly affect the shape of the soil gas concentration profiles
- the gradient method measurement is considered a snap shot in time, and
- gradient method results are sensitive to selection of the lower boundary control point.

Any of the above factors can influence the NSZD rate calculation. If data interpretation challenges arise, then review the LCSM and site-specific assumptions that went into the NSZD monitoring program (API 2017). In most situations, data inconsistencies can be resolved.

4.4 Passive flux trap method

The passive flux method was adapted from the static chamber design. Passive flux traps historically were composed of a chemical trap to collect and measure CO₂ gas moving from the subsurface to the atmosphere (Humfeld 1930; Edwards 1982; Rochette & Huchinson 2005). Through research conducted at Colorado State University, the passive flux trap method was modified for NSZD monitoring (McCoy *et al* 2014). The company E-Flux, LLC (Fort Collins, Colorado, USA) commercialised the method and further refined it.

The traps collect CO₂ gases moving from the subsurface to the atmosphere using a caustic sorbent material. Collection of the gas is conducted over a multi-day time period that is generally around two weeks. They are composed of a receiver pipe, the main trap body containing the caustic sorbent material, and a rain cover. A schematic showing a cross-section of a passive CO₂ trap side-by-side with an installed trap is presented in figure 14. The receiver pipe is installed into the ground and provides an anchor point for the CO₂ trap body and prevents atmospheric CO₂ from entering the bottom of the trap. The trap body attaches to the receiver pipe via a rubber sleeve, which also prevents lateral gas movement. A rain cover is placed on the top of the CO₂ trap body to prevent precipitation interfering with the sorbent.

The main CO₂ trap body is constructed with two separate layers of the caustic sorbent material (an upper and bottom layer). The bottom layer is open to the subsurface and is used to collect the CO₂ leaving the subsurface into the atmosphere. The upper layer is open to the atmosphere and used to collect any CO₂ moving from the atmosphere into the subsurface during flow reversal caused by changes in barometric pressure. Thus, preventing atmospheric CO₂ biasing the efflux gas measurement.

Box 4.2 Passive flux trap method of NSZD rate calculation

Principle: Flux, $J = \left(\frac{M}{A \cdot t}\right)$, with CO₂ mass sorbed on trap (M, g), trap cross-sectional area (A, m²), and deployment time (t, d)

For more information: Appendix E.3

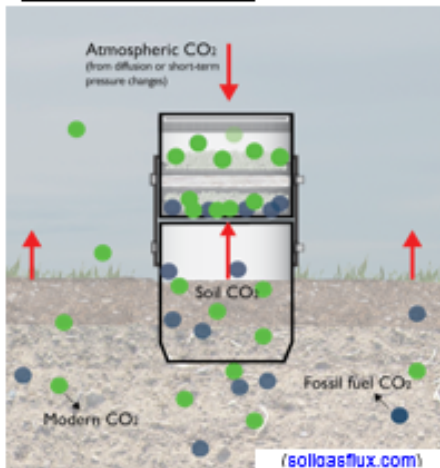
Key assumptions:

- Time-integrated trap results (e.g. 2 weeks)
- Vertical migration of CO₂ into receiver pipe and sorption onto media in trap
- Representative Hydrocarbon = hexadecane (C₁₆H₃₄)
- Hydrocarbon density = 0.92 g/mL

Key laboratory analyses:

- Mass of CO₂ sorbed
- Radiocarbon ¹⁴C and fossil fuel fraction

Visual conceptualisation:



Summary of implementation procedure:

1. Deploy and retrieve the passive flux traps
2. Perform carbon and ¹⁴C lab analysis
3. Assess the modern (background) and fossil fuel (NSZD) fractions of carbon
4. Calculate the NSZD rate

NSZD measurements:

(lab report provided by trap supplier)

Sample ID	Deployment Dates			Raw Results (not blank corrected)				Blank Corrected Results ^a and ¹⁴ C Analysis (Fossil Fuel)									
	Deployed	Retrieved	Days	Moisture	Dry Sorbent Mass (g)	Num. of Traps, ^b	Avg CO ₂ ^c	CV CO ₂ ^c	Carbon Content ^d		CO ₂ Flux ^e (microM ² /sec)	Modern Carbon, As Reported ^f	Std. Dev. Modern	Modern CO ₂ Flux (microM ² /sec)	Adjusted Fossil Fuel Carbon ^g	Grams Of Fossil Fuel CO ₂ (g)	Fossil Fuel CO ₂ Flux (microM ² /sec)
									%	(g)							
PJUEPMR1-CO2-TB	NA	NA	0.00	17.8%	42.777	2	1.31%	1.01%	0.0%	-	77.2%	0.27%	-	26.5%	-	-	
PJUEPMR1-CO2-01	8/18/14 16:33	10/14 11:35	18.75	13.5%	57.267	2	19.5%	3.26%	35.4%	11.03	22.4%	0.23%	8.3	64.6%	8.87	35	
PJUEPMR1-CO2-02	8/18/14 16:33	10/14 11:35	18.75	18.1%	55.207	2	21.8%	3.05%	44.2%	13.35	43.4%	0.43%	3.1	64.6%	8.87	35	
PJUEPMR1-CO2-03	8/18/14 16:33	10/14 11:35	18.80	20.8%	48.498	2	20.8%	1.82%	42.2%	18.35	55.1%	0.28%	8.1	64.6%	8.87	35	

a.

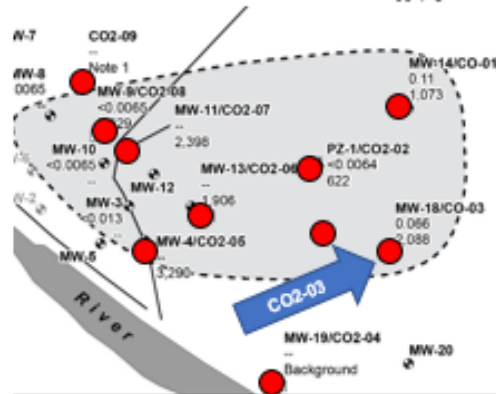
b.

c.

d.

Example monitoring plan:

$$J = \left(\frac{M}{A \cdot t}\right)$$



Legend

- Passive CO₂ flux trap
- Extent of LNAPL in soil

CO₂ efflux laboratory analytical results:
(see callout letters on lab report below)

Box a. Trip blank (TB) CO₂ content = 1.31% by wt

Box b. TB-corrected CO₂ at CO2-03 = 19.5% by wt

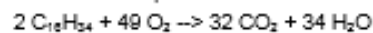
Box c. Fossil fuel carbon-fraction (NSZD-related) at location CO2-03 = 52.3

Box d. TB- and background-corrected CO₂

efflux at CO2-03 = 8.8 μmol/m²/s

NSZD rate calculation:

Assign hexadecane as representative hydrocarbon and balance equation:



MW C₁₆H₃₄ = 226.45 g/mol

Molar conversion of C₁₆H₃₄:CO₂:

0.0825 mol C₁₆H₃₄/mol CO₂

NSZD rate at CO2-03 = 10.6 g/m²/d

(115.2 L/ha/d) of LNAPL (SG=0.92)

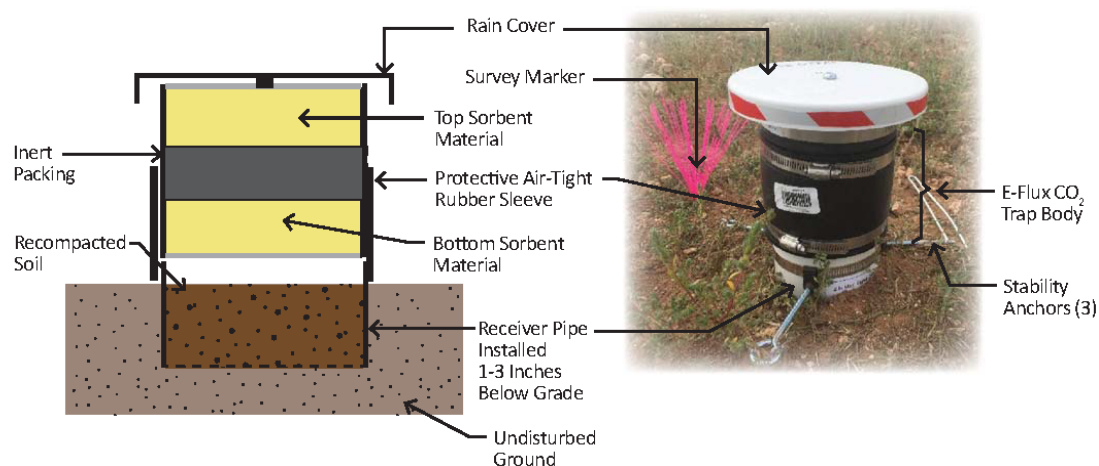


Figure 14. Schematic and actual trap side-by-side comparison. *Reproduced with permission from API (2017).*

4.4.1 Passive flux trap key assumptions

The key assumption in use of the passive flux trap method is that gas flux is vertical and the results can be attributed to directly underlying NSZD processes. This is a direct measurement method and involves few analytical calculations. Therefore, it is not susceptible to significant underlying analytical assumptions. Unlike the gradient method, the passive flux trap method can be used at sites where CO₂ is migrating via diffusion and advection.

Carbon 14 (¹⁴C) is an unstable carbon isotope and can be used for background correction using a similar technique as is used for radiocarbon dating. ¹⁴C is generated by cosmic rays in the atmosphere and is present in all living things. ¹⁴C is absent from petroleum due to the fact that it decays over time (with a 5,600 year half-life) and petroleum is multiple millions of years in age. Thus, CO₂ derived from background, non-NSZD-related sources such as NSR, are rich in ¹⁴C while CO₂ from NSZD is essentially depleted. Researchers developed a method whereby atomic mass spectrometry (AMS) is used to measure the ¹⁴C content of the carbon in the CO₂ and use the results in a two source mass balance to estimate the mass fraction of the carbon related to NSZD (also known as the fossil-fuel fraction).

The ¹⁴C background correction method, inclusive with the lab analysis that comes with the E-Flux, LLC passive CO₂ flux traps, for example, requires the assumption that all fossil fuel carbon is derived from the subject LNAPL release. It should be noted that if the soil contains fossil fuel derived solids (e.g. kerogen in sedimentary rock), then the reported LNAPL loss rate will be over-estimated.

4.4.2 Passive flux trap method measurement process

Box 4.2 illustrates application of the passive flux trap method at a single location with background correction. It comprises the following general steps:

1. install/deploy the passive flux traps
2. retrieve the traps, pack, and return ship them to a specialty laboratory
3. perform laboratory analysis of carbon on the sorbent and ¹⁴C radiocarbon in the carbon

4. assess the modern (background) and fossil fuel (NSZD) carbon fractions to compensate for background flux, and
5. calculate the NSZD rate.

The following sections provide an overview of the key steps. Appendix E provides a detailed analytical and field procedures. Ensure flux trap deployment and analysis conform to well-established, standard practice (CRC CARE 2013) or other locally required procedures.

Trap deployment and retrieval

After measurement locations have been determined, vegetation and large pieces of gravel or cobble at each location are removed. The receiver pipe is then installed into the ground surface approximately three to eight centimetres (cm), enough to provide a good seal and prevent lateral short-circuiting of atmospheric gases into the pipe. All gases migrating upwards through the vadose zone should enter the CO₂ trap and be captured by the sorbent material. Ensure that the installation depth is consistent across the site to produce comparable results. Installing the receiver pipes at too deep might cause some compacted ground surface layers to be penetrated and create chimney effects as also discussed in section 4.5.2.

The receiver pipe is installed by directly pushing by hand in soft soil or the use of a rubber mallet in hard soil. In some cases, the soil is more compacted and requires a circular score with a hand tool around the diameter of the receiver pipe. If this is necessary, care needs to be taken to have the least disturbance to the ground surface to prevent impacting the efflux conditions prior to installation of the receiver pipe. Prop the receiver pipe as close to upright as possible, to prevent the trap body from leaning and the sorbent material moving resulting in a thicker layer of material towards one side and a thinner layer at the other. If this occurs, the potential for the sorbent material becoming saturated over longer deployment times in the thinner layer is increased, and results may underestimate the true conditions.

Once the receiver pipe is installed, secure it using stakes and stabilisers as needed. After the addition of stakes and/or stabilisers, restore pre-existing ground conditions. This can be accomplished with a standard-compaction slide hammer.

After installation of the receiver pipe is completed, the CO₂ trap body is attached. This involves removal of the shipping caps, slipping the exposed lower end within the rubber sleeve on the receiver pipe and securing the sleeve with a hose clamp. When the trap body has been attached to the receiver pipe, a vented rain cover is added to the top of the trap. Appendix E presents a more detailed installation procedure.

The period a trap is deployed should allow for enough time to collect CO₂ in which the quantity of CO₂ efflux exceeds the limit of detection (discussed in section 4.4.3), but does not allow enough time for saturation of the sorbent material (e.g. estimated approximately 30% by weight of the sorbent material).

Laboratory analysis

The flux traps are analysed at a laboratory for both ASTM D4373-02 (*Rapid determination for carbonate content in soils*) and ASTM D6686-12 (*Determining the biobased content in solids, liquids, and gases using radiocarbon analysis*). The carbon content in both the top and bottom traps is analysed. If the carbon content in the top trap is less than sorption limit, the bottom trap result can be used to quantify the NSZD

rate. If the top trap is saturated, then the bottom trap is considered compromised, and the NSZD rate result must be qualified accordingly.

Background correction using ^{14}C

Background correction is needed to remove modern carbon contributions from NSR associated with plants/vegetation and other natural organic matter in the ecosystem from the NSZD of LNAPL, which is the source of older, fossil-fuel-derived carbon at a site. The quantitation of unstable carbon isotope composition is an established quantitative basis (ASTM International Method D6866-16) that is used to differentiate old sources of fossil-based carbon from modern sources. The ^{14}C background correction process is described in more detail in appendix E. The use of ^{14}C obviates the need to monitor CO_2 efflux in areas outside of the LNAPL footprint.

Calculating the NSZD rate

Section 4.1 describes how to estimate an NSZD rate using the CO_2 efflux results. Table 10 presents example representative hydrocarbons and CO_2 flux stoichiometric conversion factors. Provided the laboratory is given the proper hydrocarbon and LNAPL density, the laboratory may do the calculations and directly report total CO_2 efflux, fossil fuel-derived CO_2 efflux, and NSZD rates for each trap result.

4.4.3 Passive flux trap quality assurance/quality control

QA/QC procedures are important in evaluating the accuracy and precision of the data collected. One duplicate trap location every 10 locations is recommended to evaluate consistency between installation procedures and replication of results. Place the duplicate trap approximately 0.3 metres from the parent location and installed in an area of similar ground cover. Statistics such as the calculation of a relative percent difference (RPD) from the parent and duplicate sample data can be performed to assess data quality. An elevated RPD of greater than 30% is typically used as a criterion to re-evaluate the soil receiver pipe installation procedures to ensure a good seal with the subsurface was attained. However, heterogeneities in the subsurface impact the ability to achieve an RPD of less than 30% at many sites, therefore the 30% criterion may not be achieved in all cases.

In addition to the simple statistics, a trip blank is provided by the passive flux trap laboratory and analysed along with the samples for each field event. The trip blank accounts for CO_2 not associated with flux from the subsurface that either came from manufacturing or sorbed from atmosphere (through the caps) during the shipment.

Detection limit

The detection limit of a passive CO_2 trap is dictated by the detection limit of the analytical method. The detection limit of the analytical method is found by multiplying a typical coefficient of variation (cv) of 3% on trap CO_2 analyses, and a typical blank trap CO_2 content of 1% by weight by five (i.e. 3% cv * 1% CO_2 by weight * 5). The detection limit of the analytical method of CO_2 trap is approximately 0.15% CO_2 by weight of the sorbent (API 2017). Then using deployment time, the area exposed to efflux, and the quantity of sorbent material the detection limit of the CO_2 trap can be determined. The detection limit is typically 0.1 $\mu\text{mol}/\text{m}^2/\text{s}$ for a 15-day deployment time, a cross-sectional diameter of 10.16 centimetres of the Schedule 40 polyvinyl chloride (PVC) receiver pipe, and 40 grams of sorbent material. A decrease in deployment time of 4 days would result in approximately a 5-fold increase in the detection limit (0.5 $\mu\text{mol}/\text{m}^2/\text{s}$). Note that

if laboratory results are less than the analytical detection limit, the resulting detection limit of the CO₂ traps are considered non-detect.

4.4.4 Passive flux trap method considerations

Sources of measurement uncertainty and variability, how they affect passive flux trap method calculations, and potential mitigation means are presented in table 13.

Table 13. Passive flux trap method uncertainty and variability considerations. *Reproduced with permission from API (2017).*

Factor	Effect	Mitigation
Impervious ground cover or highly compacted, confining soil layers	Soil gas can migrate laterally in the vadose zone and is effected by various manmade and geologic materials.	Avoid impervious areas or areas with highly compacted, low-permeability surface soil. Consider use of a new trap design that utilizes a gas tight top cap with pressure equilibration to minimise short-circuit effects.
Wind effects	Wind can cause the passive flux trap method to over-estimate the actual efflux (Tracy 2015).	Use latest trap design, adjusted to provide most accurate results. At sites with excessive winds, monitor wind speeds and consider correcting for wind effects (Tracy 2015; E-Flux 2015)
Precipitation during deployment	The rain cover on the trap assembly may prevent wetting of immediately underlying soil, causing a rain shadow in which preferential flow can develop. Research is ongoing to determine effects of precipitation on trap measurements.	Minimise deployment duration and schedule time of year to avoid heavy rainfall events. Turn off irrigation systems during deployment. Schedule monitoring during dry weather, preferably a week or more after heavy rainfall.

Interpretation of results from the passive flux trap method, like the other NSZD monitoring methods, can be challenging. Consider the following items when interpreting the data:

- Soil moisture changes can be more dynamic in shallow soil and may impact ground surface methods more than methods implemented deeper in the subsurface such as the gradient method.
- The passive flux trap method represents a time-integrated efflux value whereas other methods are considered snapshots which may be higher or lower depending on weather conditions during deployment.
- The use of ¹⁴C is arguably the best, most quantitative means for background correction; consider it of utmost reliability.

Any of the above factors can influence the NSZD rate calculation. If data interpretation challenges arise, then review the LCSM and site-specific assumptions that went into the NSZD monitoring program (API 2017). In most situations, data inconsistencies can be resolved.

4.5 Dynamic closed chamber method

The DCC method directly measures soil gas efflux at the ground surface. It employs an active approach in which gas emitted from the ground surface is circulated in a closed loop between a chamber and a field gas analyser that measures changes in the concentration of CO₂ over time. The timed rate of change in concentration is used to

calculate the soil gas efflux. Chamber methods (including open/closed and static/dynamic methodologies) have been used to estimate shallow soil respiration for more than 80 years and are the most commonly used approaches in agriculture (Rochette & Hutchinson 2005). Over that time-frame, the DCC method has been shown to be a reliable efflux measurement method and used as a reference for comparison of other methods (Norman *et al* 1997). Recently it has been applied for NSZD monitoring (Sihota *et al* 2011).

The DCC system is frequently composed of a ground-mounted chamber, into which soil gas flows, connected to a portable pump and a soil gas analyser. As an example, the LI-8100A (LI-COR Biosciences, Inc., Lincoln, Nebraska) is a DCC system that employs a domed chamber connected to a vapour pump, a temperature/moisture analyser, a portable infrared gas analyser (IRGA), and a control assembly. The chamber contains an engineered, top-mounted vent to maintain a quasi-equilibrium between the chamber and atmosphere during the short measurement period. The chamber closes onto the soil collar and measurement of CO₂ concentrations by the IRGA begins. The basic set-up of a DCC system is presented in figure 15.

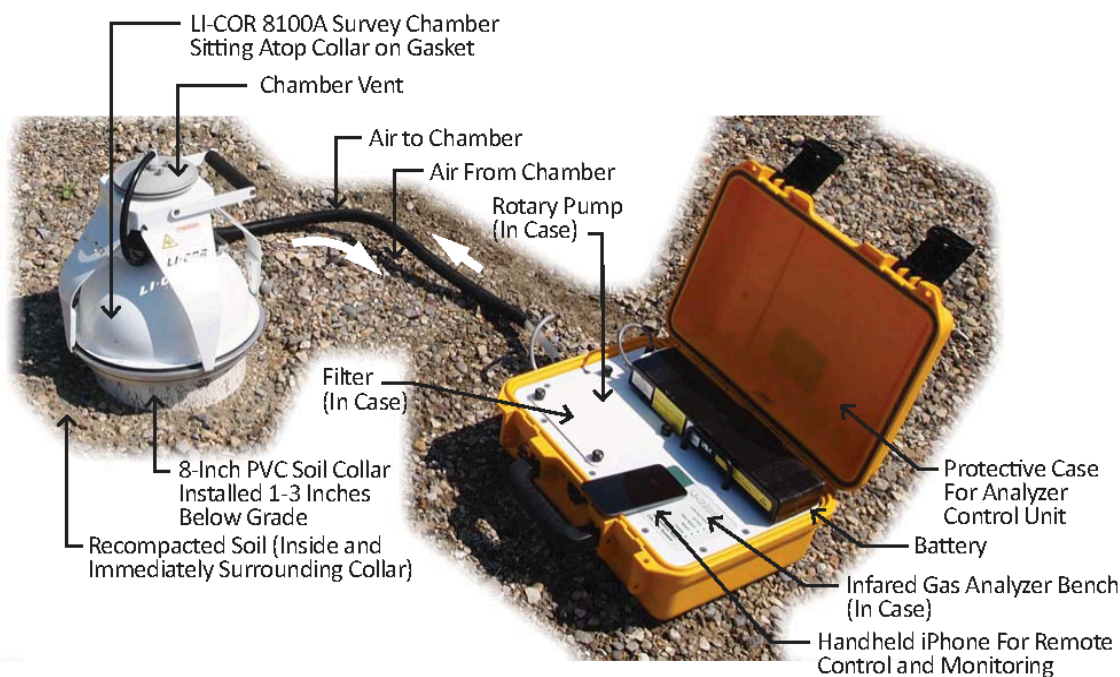


Figure 15. LI-COR 8100A dynamic closed chamber (DCC) soil gas flux system. *Reproduced with permission from API (2017).*

4.5.1 Dynamic closed chamber method key assumptions

The key assumption in use of the DCC method is that gas flux is vertical and the results can be attributed to directly underlying NSZD processes. This is a direct measurement method and involves few analytical calculations. Therefore, it is not susceptible to significant underlying analytical assumptions. Unlike the gradient method, the DCC method can be used at sites where CO₂ is migrating via diffusion and advection.

The DCC measurements are a snapshot in time; literally each flux measurement is approximately 90 seconds long. Therefore, use measurement units of per second or per day at the longest in duration, assuming multiple measurements were collected

from each location in a day in the span of multiple days. If DCC measurements are to be used for estimating annual NSZD rates, then multiple measurements are required to assess the seasonal variability and derive a time-weighted average rate.

4.5.2 DCC method measurement process

Box 4.3 illustrates application of the DCC method at a single location with background correction. It comprises the following general steps:

1. install collars and allow re-equilibration
2. perform gas efflux survey using DCC soil gas flux system
3. perform data validation and visualisation
4. assess the background and NSZD fractions of CO₂ efflux, and
5. calculate the NSZD rate

The following sections provide an overview of the key steps. Appendix F provides detailed analytical and field procedures. Ensure DCC soil gas flux measurements conform to well-established, standard practice (CRC CARE 2013) or other locally required procedures.

Install the DCC collars

After measurement locations have been determined, vegetation and large pieces of gravel or cobble at each location are removed. The collar is then installed into the ground surface approximately three to eight cm, enough to provide a good seal and prevent lateral short-circuiting of atmospheric gases into the collar. Ensure consistent installation depth across the site to produce comparable results. Installing the collars too deep might cause compacted ground surface layers to be penetrated and create soil gas chimney effects.

The collar is installed by directly pushing by hand in soft soil or the use of a rubber mallet in hard soil. In some cases, the soil is more compacted and requires a manual tool to score around the diameter of the receiver pipe to properly and firmly seat the collar into the ground surface. If this is necessary, care needs to be taken to have the least disturbance to the ground surface as possible to prevent impacting the natural efflux. Prop the collar as close to upright as possible, to prevent the collar from leaning and the chamber from going off-centre and seating incorrectly when closing.

Once the collar is installed, secure it by backfilling around the edges to existing grade and re-compacted to pre-existing conditions using a standard compaction slide hammer.

Perform the DCC soil gas efflux survey

Efflux measurements are made by placing the chamber onto the soil collar and using the DCC soil flux system control software to initiate the measurement cycle. The pneumatically actuated bellows closes the chamber and starts the IRGA measurements of CO₂ concentration, temperature, and relative humidity. Following the end of the measurement period (e.g. 90 seconds), the bellows opens the chamber, and a purge cycle ensues to clear the system. After the purge, the system continues to close the chamber and perform routine measurements until the user-set number of measurements are taken. The unit then opens and goes idle until the unit is picked up and moved to the next measurement location.

Box 4.3 Dynamic closed chamber method of NSZD rate calculation

Principle: Flux, $J = \left(\frac{dC}{dt} * \frac{V_c}{A_c}\right)$, with change in CO₂ over time (t) in a chamber of volume (V_c) and cross-sectional area (A_c)

For more information: Appendix F.2

Key assumptions:

- Steady-state snap shot in time
- Vertical migration of CO₂ into chamber
- Vented chamber, short measurement (e.g. 30–120 seconds) to minimise accumulation effects in chamber

Key field measurements:

- Rate of increase of CO₂ in DCC
- CO₂ efflux at background and impacted locations (0.5 μmol/m²/s)

Visual conceptualisation:

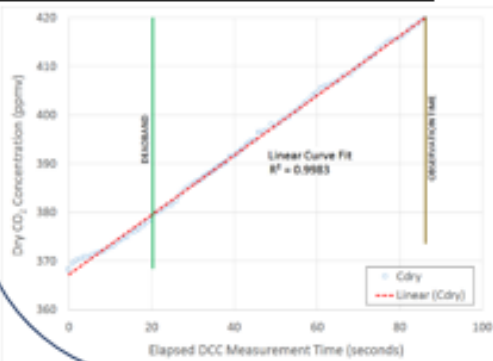


Figure 6-1 U-COR 8300A DCC Apparatus and Setup

Summary of implementation procedure:

1. Install collars and allow re-equilibration
2. Perform gas efflux survey using DCC soil gas flux system
3. Perform data validation and visualisation
4. Assess the background and NSZD fractions of CO₂ efflux
5. Calculate the NSZD rate

Apr 2016 field monitoring results (SC-9):



Measured total CO₂ efflux = 4.66 μmol/m²/s
Background-corrected = 4.17 μmol/m²/s

Example monitoring plan:



Legend

- DCC CO₂ efflux survey location
- NSZD rate (0.1–0.5 g/m²/d)
- NSZD rate (4–5 g/m²/d)

Data validation – field blank results:

Method detection limit = 0.06 μmol/m²/s

Background CO₂ efflux assessment (Apr 16):

One ground cover type = little/no vegetation
Avg. background total CO₂ efflux in little/no vegetation zone = 0.5 μmol/m²/s

Background-corrected Results:

Range of measured CO₂ efflux =
Total = 0.2 - 4.7 μmol/m²/s
Corrected = 0–4.2 μmol/m²/s

NSZD rate calculation:

Assign octane representative hydrocarbon:
2 C8H18 + 25 O2 -> 16 CO2 + 18 H2O
Molar conversion: 0.125 mol C₈H₁₈/mol CO₂

Sitewide range of NSZD rates =
0–5.1 g/m²/d or 0–63 L/ha/d of LNAPL
(SG = 0.81)

After the preset number of measurements is collected, the user assesses the data to determine whether additional measurements are needed or whether measurements are complete at that location. If no additional measurements are needed at that location, the DCC system is moved to the next sample location, and the process is repeated until the survey is completed.

The measurements obtained using the DCC method is of a very short duration. A minimum of three sequential total CO₂ efflux measurements are made at each location encompassing a period of approximately five minutes. Additional measurements are often made to obtain three sequential readings within 10% of each other. For planning purposes, a network of 30 collars typically can be measured in a single-day field effort.

Perform data validation and visualisation

The process of validating the DCC field measurement data is as follows:

1. Tabulate the data from the CO₂ efflux field survey
2. Calculate the limit of detection for each individual field event using the field blank results
3. Optimise the CO₂ concentration curve, and
4. Eliminate data that are outliers, poor curve fit correlations, results from poor field procedures, or outside the manufacturer's recommended operating limits (i.e. IRGA bench temperature of 50 °C and minimum of 90 recorded data points).

The DCC software system calculates and plots the dry CO₂ concentration, which is the CO₂ mole fraction corrected for water vapour dilution, over time (figure 16).

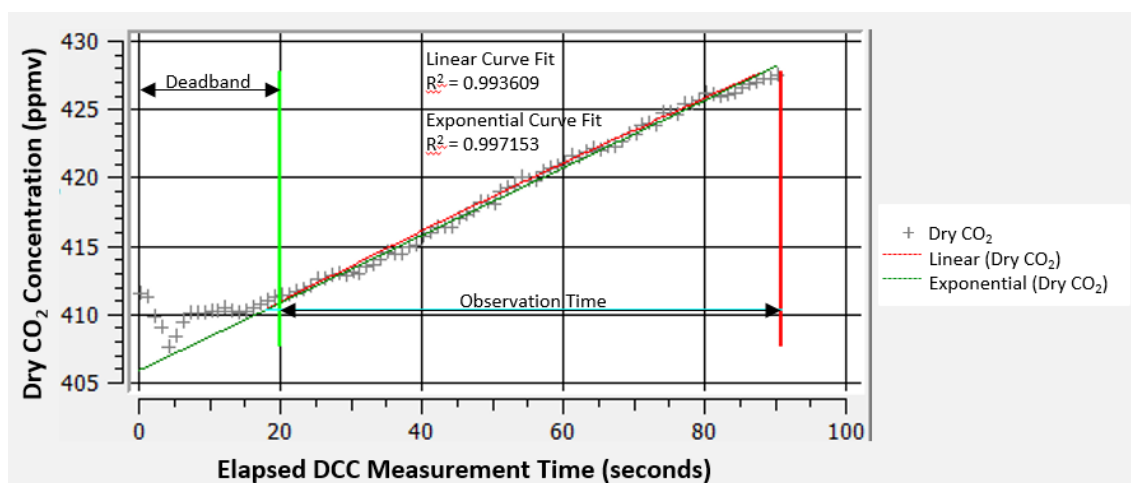


Figure 16. Example output from a CO₂ efflux measurement using a DCC soil flux system.

With the software supplied by LI-COR, Inc. (SoilFluxPro version 4.1 in 2017), the rate of change in the CO₂ concentration is fit using either a linear or exponential regression. The CO₂ flux is then calculated and logged using the slope of the curve fit and various other parameters such as the volume of the gas in the chamber, pressure, temperature, and collar surface area.

A geospatial mapping of the CO₂ efflux survey results can be informative to correlate with the LNAPL footprint and can be used as a basis to estimate the site-wide

degradation/loss of LNAPL. This can be done by visually mapping the calculated rates of NSZD at individual locations across the site, then linear interpolating or kriging to develop an isocontours. The areas of each contour interval can then be used to estimate the NSZD occurring across the site.

Assess the background and NSZD fractions of CO₂ efflux

Background correction is important and is needed to determine the NSZD-derived CO₂. The background correction is a subtraction of natural soil CO₂ (modern CO₂) efflux from the measured total CO₂ efflux. At a minimum one background location outside the LNAPL footprint is needed per vegetative ground cover. An arithmetic average of the CO₂ background locations is calculated if more than one background location is used for a particular ground cover. The background CO₂ efflux for each vegetative ground cover is subtracted from each survey location of that vegetative ground cover collected over or immediately adjacent to the LNAPL footprint. The background CO₂ efflux is only representative of a particular field event as CO₂ efflux changes over time due to changes in sources such as vegetation growth.

Calculate the NSZD rate

Section 4.1 describes how to estimate an NSZD rate using the CO₂ efflux results. Table 10 presents example representative hydrocarbons and CO₂ flux stoichiometric conversion factors.

4.5.3 DCC quality assurance/quality control

QA/QC measures are critical in evaluating the accuracy and precision of the efflux measurements obtained using DCC methodology. Manufacturers of the DCC systems commonly periodically perform a thorough and intensive calibration under controlled conditions in laboratory settings. In addition, calibration of the instrument in the field using a span gas is recommended to set the instrument to atmospheric conditions encountered in the field. This field calibration involves calibration to a 0 parts per million by volume (ppmv) CO₂ standard (zero gas) and a span gas cylinder with a 500-ppmv CO₂ concentration.

It is recommended that a duplicate collar be installed and efflux measurement be made at a frequency of one for every 10 locations. Collect the duplicate location measurement during the same time of day as the normal (parent) sample location. Locate the normal and the duplicate locations less than 0.3 m apart and within the same ground cover. General statistics such as RPD between normal and duplicate sample locations are performed to assess data quality and identify potential differences in soil collar installation, ensure a good seal with the subsurface was attained, and evaluate any heterogeneities in the subsurface. Generally, an RPD greater than 30% indicates that the practitioner should evaluate installation procedures and influences of soil heterogeneities. The 30% RPD is a target only and may not be achievable at many sites due to soil heterogeneities.

Variability in sequential measurements may be observed greater than 10% of each other. If this situation arises, it is recommended to perform a second round of measurements at the same location. If efflux measurements are to be repeated at the same collar within an individual day, delay the subsequent measurement by 20 minutes to allow re-equilibration of vapours in the soil.

In addition, a field blank measurement comprised of 60 readings, is collected during each field event. A collar with a sealed bottom cap is used for the field blank. The field blank is used to estimate the detection limit of the DCC system as described below.

Detection limit

The detection limit of the DCC method is dictated by the detection limit of the IRGA. The IRGA of the LI-COR 8100A has an accuracy of 1.5% of the measured CO₂ concentration, with a peak to noise ratio of approximately 2 ppmv. Under a controlled experiment by LI-COR, the limit of detection of the analyser was found to be 0.01 µmol/m²/s (LI-COR 2014).

Atmospheric conditions influence the limit of detection of the LI-COR 8100A analyser. Therefore, atmospheric differences (e.g. changes in barometric pressure) influence the limit of detection. To account for this, collect a CO₂ flux field blank during each individual field event to determine a limit of detection for the particular atmospheric conditions encountered during a particular event. This is performed by performing efflux measurements on a completely sealed collar that is impermeable to gas flow into the chamber (LI-COR 2014). Typically, the detection limit found with a field blank is composed of the average of 60 readings and the addition of three times the standard deviation. Measured efflux values below the field limit of detection are considered non-detect.

4.5.4 DCC method considerations

Sources of measurement uncertainty and variability, how they affect DCC method calculations, and potential mitigation means are presented in table 14.

Interpretation of results from the DCC method, like the other NSZD monitoring methods, can be challenging. Consider the following items when interpreting the data:

- Soil-moisture changes can be more dynamic in shallow soil and may impact ground surface methods more than methods implemented deeper in the subsurface such as the gradient method.
- The DCC measurement is a snapshot in time and dynamic conditions such as diurnal fluctuations in temperature and change in weather conditions especially wind and rainfall events, may affect the DCC results.

Any of the above factors can influence the NSZD rate calculation. If data interpretation challenges arise, then review the LCSM and site-specific assumptions that went into the NSZD monitoring program (API 2017). In most situations, data inconsistencies can be resolved.

Table 14. Dynamic closed chamber method uncertainty and variability considerations. *Reproduced with permission from API (2017).*

Factor	Effect	Mitigation
Irrigation or rainfall events	Changes natural soil respiration rate and inhibits gas transport.	Turn off irrigation system, if possible, or do measurements at the same time of day. Avoid rainfall events and wait until a dry period, preferably a week or more after a heavy rainfall.
Short measurement period and CO ₂ efflux subject to diurnal fluctuations	Only a snapshot in time of the CO ₂ efflux. Different CO ₂ efflux measured depending on time of day.	Assess diurnal variability through multiple measurements at various times of day at the same collar (e.g. morning, midday and evening).
Impervious ground cover or highly compacted, confining soil layers	Soil gas can migrate laterally in the vadose zone and is effected by various manmade and geologic materials.	Avoid impervious areas or areas with highly compacted, low permeability surface soil.
Thick vegetation and elevated background CO ₂ efflux	Highly organic soils can create high CO ₂ efflux value which can mask NSZD-related efflux.	Use ¹⁴ C method of background correction (adapt method developed for passive flux traps, see section 4.4.2) or perform efflux survey during colder, non-growing season.
Wind effects	Wind can cause the DCC method to underestimate the actual efflux.	At sites with excessive winds, monitor wind speeds and consider correcting results for elevated wind speeds (Tracy 2015).

5. Rate measurement using temperature data

5.1 Biogenic heat method

As discussed in section 1.5 and 2.5.2, NSZD manifests itself as changes in soil temperature above the hydrocarbon-impacted soil. The NSZD reactions on the LNAPL are exothermic and the gases created by NSZD are oxidised in a biologically mediated exothermic aerobic reaction in the overlying unsaturated zone soil. By conducting a heat balance in the vadose zone, the heat flux from the exothermic reactions can be thermodynamically equated to an NSZD rate. The thermal gradients, or the change in soil temperature with depth at a monitoring location, can be used to estimate the heat flux. After correction for non-petroleum related effects, the heat flux can then be converted into an NSZD rate by dividing it by the heat of reaction from microbial biodegradation.

As summarised in appendix G, various entities have researched the use of biogenic heat to measure NSZD rates (Sweeney & Ririe 2014; Warren & Bekins 2015, 2018; Sale *et al* 2014; Zimbron *et al* 2017). Multiple studies demonstrated that the biogenic heat method is a suitable tool for quantitative, short- and long-term measurement of heat flux (ITRC 2018). A range of assumptions were made and a range of approaches were taken in the studies. Like the assumptions made for the gas efflux NSZD methods, all approaches assumed one-dimensional vertical heat flux. Both steady-state and transient solutions were used. All studies presented solutions to estimate the NSZD rate from biogenic heat, and two presented screening-level approaches that could be simply used to closely approximate it.

5.1.1 Biogenic heat method key assumptions

After comparing the methods, several common assumptions were found:

- soil is homogeneous and isotropic
- steady-state, constant biogenic heat source
- heat conduction is the dominant mechanism of heat transfer, and
- instantaneous and complete reaction, including methane oxidation.

The assumption of homogeneity and isotropy is necessary for practical application of the method. The challenge lies in assigning values, or better yet, a range of values, that are representative of the formation within which the heat flux is observed. The values required by the method can be obtained using site-specific measurements and/or a range of literature values for soil thermal conductivity, for example.

Application of the biogenic heat method proposed herein assumes that the biomass be at a quasi-steady state and generating a constant heat source. As discussed in the literature, this typically holds true for sites with LNAPL in a middle- to late-stage condition (Tracy 2015).

As discussed in section 4.3.1, diffusion dominates gas transfer in natural soils. Analogously, conduction, or temperature gradient-driven transport, is assumed dominant in heat transfer in soil. In so doing, Fourier's first law of conduction, a diffusion-like process, can be used to estimate the heat flux as shown in equation 10 (Hillel 1982).

Equation 10: $q_H = K_T \left(\frac{\Delta T}{\Delta Z} \right)$

where q_H is the steady-state conductive heat flux (J/m²-soil/s), $\Delta T/\Delta z$ is the temperature gradient (°K/m), and K_T is the thermal conductivity of the soil (J/m/s/°K) that is specific to the soil within the hydrocarbon oxidation zone.

The biogenic heat method relies on the assumption of instantaneous reaction for methane oxidation (Davis *et al* 2009) and complete conversion of all petroleum hydrocarbons to CO₂ and H₂O (Stockwell 2015). The kinetics of biodegradation can be complex with many concurrently occurring processes such as protozoa predation and intermediate acetate build-up (Garg *et al* 2017). However, it is assumed that the net effect of these collective microbiological processes is a zero-order (constant) biodegradation rate.

The biogenic heat method uses soil temperature measurements taken at discrete depths to estimate the heat flux through the vadose zone. Figure 17 illustrates a typical temperature profile that exists above LNAPL-impacted soil. Averaging temperatures and estimating the thermal gradient in section 5.1.2 further explains how the upper and lower temperature gradients are used in the heat flux calculations.

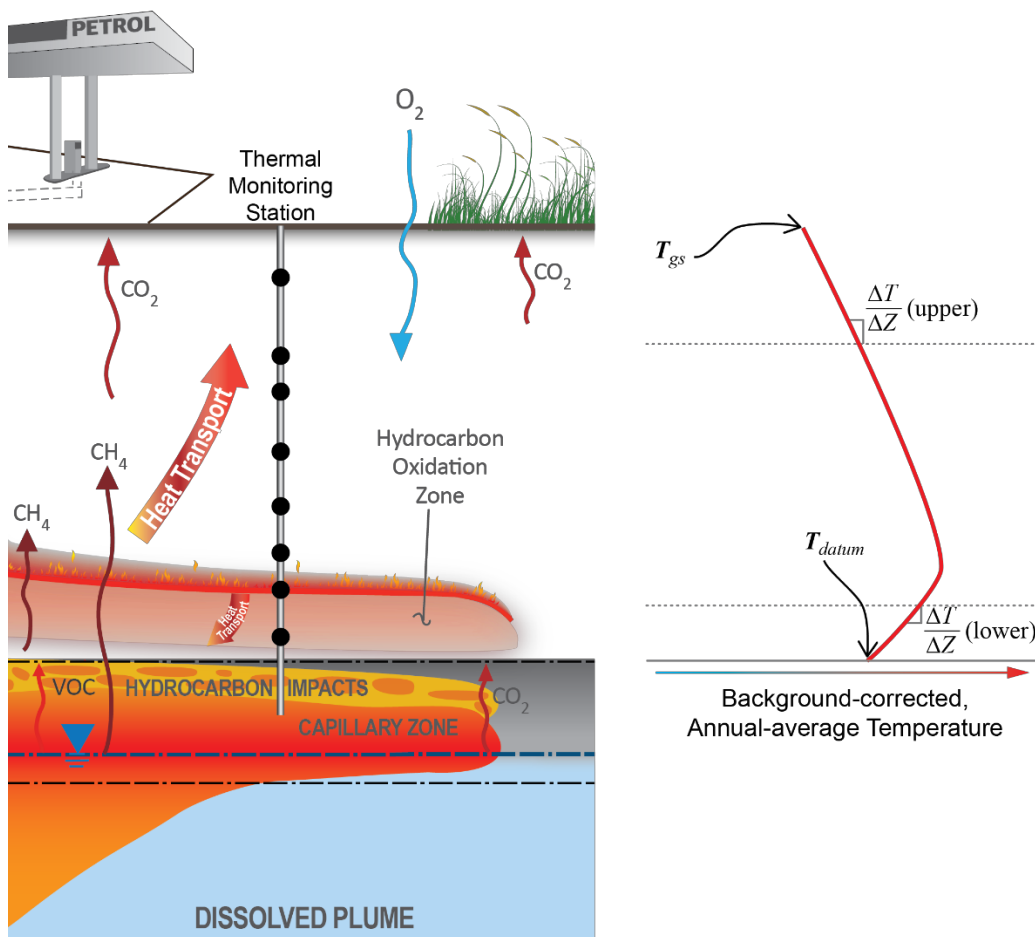


Figure 17. Schematic of a biogenic heat method monitoring setup and a typical background-corrected NSZD temperature profile.

Depending upon the depth to the hydrocarbon oxidation zone and the seasonal changes in the ambient and groundwater temperatures, the temperature profile can

vary with time. Authors that describe biogenic heat methods noted the large variation in subsurface temperatures that are affected by seasonal and climatic effects (e.g., some winters are warmer than the climatology-based average). They also noted that the variability can be numerically managed through averaging of depth temperature profiles to provide a more representative time-integrated thermal gradient. Figure 18 presents data published by Warren & Bekins (2015) from the Bemidji site (Minnesota, USA) that shows the results and the simplification achieved when temperatures are averaged over a year. As shown on the right-hand figure (B), the thermal signature from oxidation of gases generated by underlying NSZD (background corrected) has a peak ΔT of approximately 1.6 °C at a depth equivalent to approximately 0.6 of the vadose zone thickness. This is the data (figure 18 B) that is carried forward into the calculations.

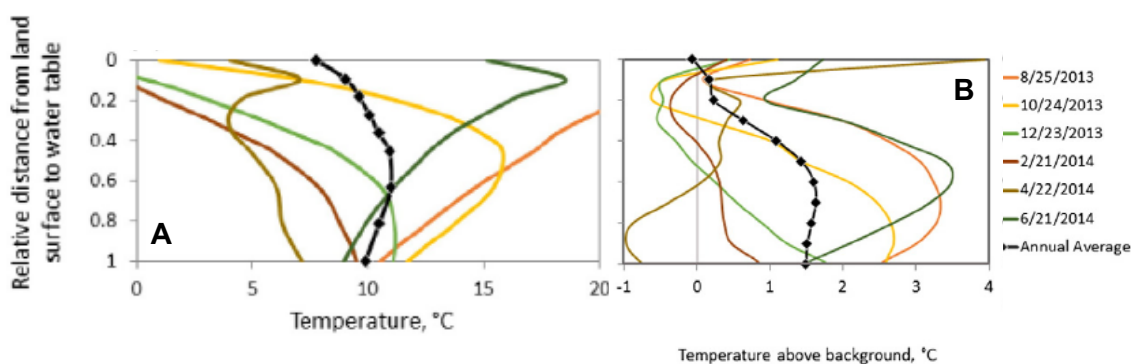


Figure 18. Annual average temperature profiles at a site (A) and background corrected temperature profile (B). Reproduced with permission from Warren & Bekins (2015).

5.1.2 Biogenic heat method process

Box 5.1 illustrates application of the biogenic heat method at a single location with background correction. It comprises the following general steps:

1. Install soil temperature measurement devices or establish alternative means for temperature monitoring as discussed in appendix G.2
2. Log soil temperatures for an extended period of time as discussed below
3. Estimate the soil thermal conductivity
4. Tabulate the data and calculate the average temperatures at all monitoring depths
5. Plot the average data and account for background
6. Estimate the thermal gradient, and
7. Calculate the NSZD rate.

The following sections provide an overview of the key steps. Appendix G provides detailed analytical and field procedures.

Box 5.1 Biogenic Heat Method of NSZD Rate Calculation

Objective: Measure soil temperatures and quantify biogenic heat flux to estimate the NSZD rate.

For more information: Appendix G.3

Principles: Modified Van Wijk and de Vries:

$$T(z,t) = T_o + A_o * [\exp(-z/D) * \sin(w*t - z/D)]$$

Fourier's first law of heat conduction:
 $q_h = -K_T (\Delta T / \Delta z)$

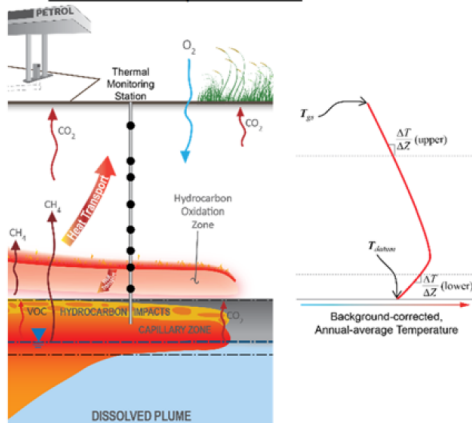
Key Assumptions:

- Constant heat source
- Vertical conduction only (no convection)
- Atmospheric heat loss only
- Groundwater does not impact soil temperature

Key Calculation Parameters:

- Thermal diffusivity, α ; $D = (2 * \alpha / w)^{0.5}$
- Heat flux, q_h
- Thermal conductivity, K_T
- Upward thermal gradient, $\Delta T / \Delta z$

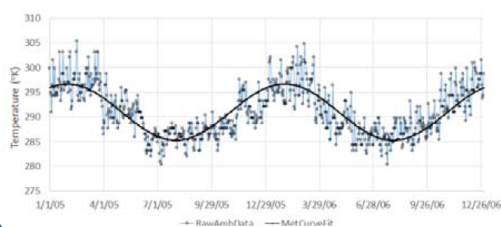
Visual Conceptualisation:



Summary of Implementation Procedure:

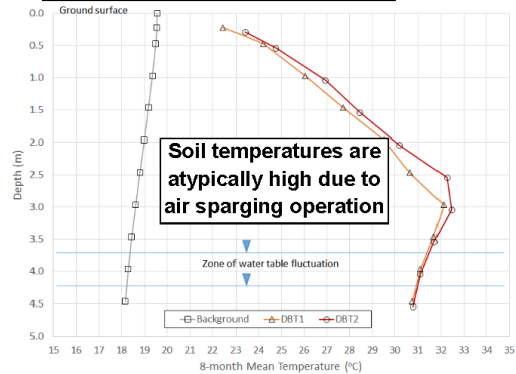
1. Install temperature monitoring probes
2. Ambient and soil temperature monitoring at two locations and annual averaging
3. Estimate soil properties and thermal gradients and do background correction
5. Calculate the NSZD rate

Nov2005 – Jul2006 Meteorological Data:**

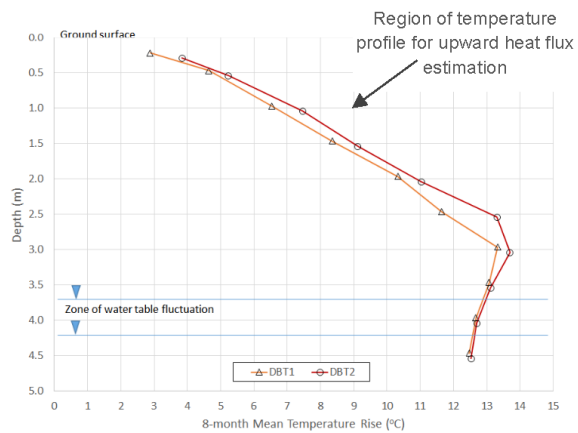


** Modified Van Wijk and de Vries equation used in lieu of background measurements

In-situ Thermal Monitoring Results:



Background Correction Results:



- Thermal diffusivity, $\alpha = 8 \times 10^{-7} \text{ m}^2/\text{s}$
- Thermal conductivity, $K_T = 1.86 \text{ J}/(\text{m}\cdot\text{s}\cdot^\circ\text{K})$
- Heat release, $\Delta H^\circ = 43,900 \text{ J}/\text{g}_{\text{C}_6\text{H}_{14}}$

Calculated Parameters (MP-1):

Max. thermal anomaly, $\Delta T = 13.5 \text{ }^\circ\text{C}$

(above background temperature)

Depth of thermal anomaly, $z = 3 \text{ m}$

$$\text{Heat flux, } q_H = K_T \left(\frac{\Delta T}{\Delta z} \right) = 1.86 * \left(\frac{13.5 - 4}{3 - 0.2} \right) = 6.3 \text{ J}/\text{m}^2/\text{s}$$

NSZD Rate Calculation:

$$R_{NSZD} = q_H / \Delta H^\circ$$

$$R_{NSZD} = \frac{q_H}{\Delta H^\circ} = \frac{6.3}{43,900} * \frac{86,400 \text{ s}}{d}$$

$$= 12 \text{ g}/\text{m}^2/\text{d}$$

$$\text{NSZD rate, } R_{NSZD} = 12 \text{ g}/\text{m}^2/\text{d}$$

$$= 150 \text{ L}/\text{ha}/\text{d} \text{ (SG=0.8)}$$

Installing soil temperature measurement devices and data logging

As shown in figure 17, soil temperature measurements above, within, and below the hydrocarbon oxidation zone are useful to estimating thermal gradients. The depth and intervals of thermal monitoring depend upon fluctuation in the range of hydrocarbon oxidation and the temperature maxima. This range is expected to be larger in climates with wider swings in ambient temperatures and/or groundwater temperatures. At sites with a warm climate (e.g. Perth, Western Australia), the range of change in the depth of the peak temperature may be small as shown on figure 19. The daily mean ambient temperature range at this site ranges from 13.1 to 25.1 °C³, and the depth of the peak temperature vertically changes approximately 0.5 metre. In contrast, figure 20 shows a thermal profile after background correction for a temperate climate (Bemidji, Minnesota, USA) where ambient average temperature ranges more widely from -14.5 to 20 °C⁴. The depth to the temperature maxima (darker colour) varies greatly from water table in the winter months to halfway to the water table (average depth to water is approximately 6 metres below grade (mbg) at the y-axis' relative depth value of 1). The subsurface soil temperatures at this site were impacted both by warm temperatures from summer rains and colder snow melt in spring that infiltrated downward through the unsaturated zone (Warren & Bekins, 2015).

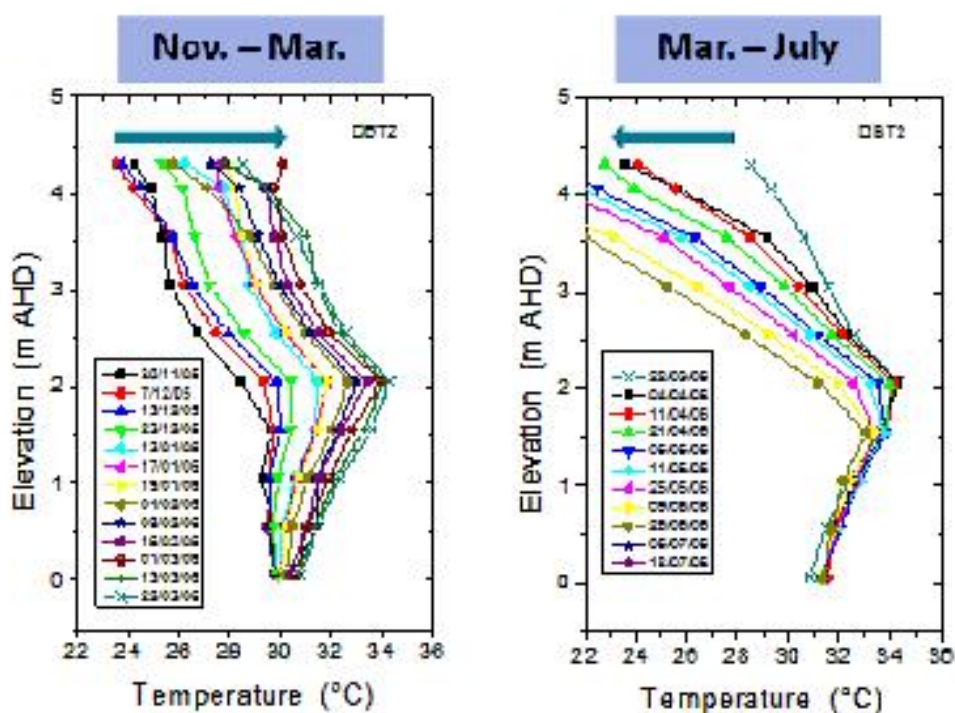


Figure 19. Soil temperature variability at a site with a warm climate. Unpublished data, with permission from C. Johnston, CSIRO.

³ wikipedia.org/wiki/Perth

⁴ wikipedia.org/wiki/Bemidji,_Minnesota

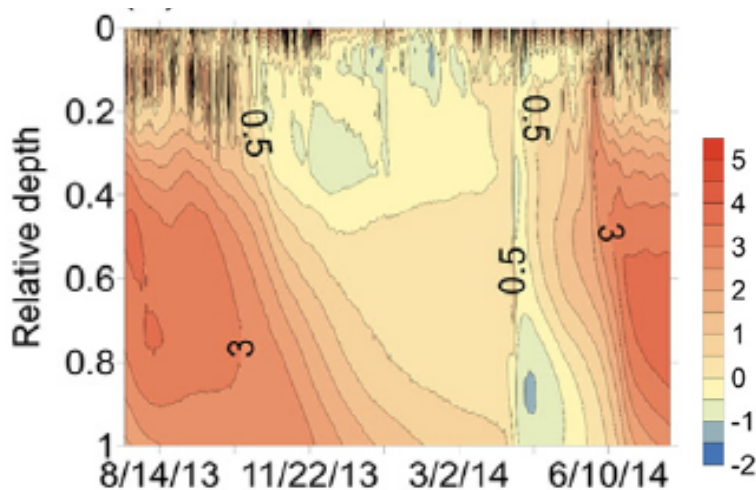


Figure 20. Soil temperature (°C) variability at a site with a temperate climate. Reproduced with permission from Warren & Bekins (2015).

There are several options to monitor soil temperature profiles and estimate $\Delta T/\Delta z$ for use in the biogenic heat method. Temperature profiles are measured above and aside (background) the LNAPL footprint and used as a basis to estimate the NSZD rate using the biogenic heat method using various techniques, including the following:

- dedicated nested string of thermistor or thermocouples
- existing monitoring wells – thermocouple and reel, and
- existing monitoring well – dedicated string of button-type temperature loggers.

Appendix G describes and shows examples of each type of temperature measurement technique. The most direct measurement is dedicated thermistor strings; a solid rod with multiple thermocouples or thermistors attached to it, which is installed and backfilled in soil boreholes. Thermistors are wired to an at-grade datalogger that is set to record temperatures at least twice daily at a daily maximum and daily minimum temperature times of day. The datalogger can be manually downloaded or connected to the internet for remote data access and periodic download. A similar string of thermistors can also be dropped into a small-diameter, solid casing installed using conventional drilling. The string can be left in place if using wired thermistors or temporarily removed and manually downloaded if using wireless button-type temperature data loggers.

Sweeney & Ririe (2014) proposed using existing monitoring wells to measure subsurface temperatures. An existing monitoring well with a sealed wellhead can be used as a screening tool to assess subsurface soil temperatures. As shown in appendix G, this can be performed using either a thermocouple on a reel or a dedicated string of button-type loggers. The reel method requires sequential drop of the thermocouple probe and a wait time of at least three minutes at each stop depth before taking a measurement in the vadose zone and a 1-minute wait time before taking groundwater temperatures. The wireless button-type temperature data logger strings are typically left in place for a year or more and periodically removed and manually downloaded.

Depending upon the latitude of the site and the magnitude of the seasonal ambient temperature swing, a minimum temperature monitoring period between one month and one year is recommended to improve the representativeness of the data. While NSZD

estimates can be made with short-term temperature monitoring data, the quality of the NSZD rate estimates will improve as the duration of monitoring increases. One-time or routine temperature measurements may be collected, but the data quality may be qualified as screening-level if not collected when conditions are near an average condition.

Biogenic heat flux can be affected by conditions above and below the vadose zone, including atmospheric and groundwater. To support data evaluation efforts after the field measurement program, it is typically prudent to synoptically monitor and record atmospheric conditions such as temperature, barometric pressure, wind speed, and precipitation. This can often be done remotely using data from a local meteorological data station that posts their data on a publicly available website or onsite using a weather monitor. Likewise, synoptic measurements of the groundwater level and temperature can also help inform data evaluation efforts.

The installation and temperature measurement procedures are described in detail in appendix G. Before these methods are used, however, scrutinise their validity through close inspection of the vadose-zone properties (e.g. boring logs, soil samples, soil vapour measurements) and preferably confirmed with at least one nested soil temperature measurement probe installation.

Estimating the soil thermal conductivity

Thermal conductivity can be estimated using either laboratory testing, calculations, or literature sources. Use a volume-weighted average value (or geometric mean) that is representative of all different lithologies within the oxidation zone (Warren & Bekins 2018). The thermal conductivity of most earth materials is between 0.1 to 4 joules per metre squared per second per degrees Kelvin ($J/m/s/^\circ K$). Considering this relatively small range, empirical estimates of K_T using literature values based on known soil conditions are feasible without significantly compromising data quality level. Appendix G presents typical thermal conductivity and diffusivity values based on soil type (Sweeney & Ririe 2014).

A laboratory method (USGS 1984) is available to measure the thermal conductivity of soil. A constant current source is applied to the soil sample, and the temperature change is monitored and equated to a material thermal conductivity. This method is commercially available at large geotechnical laboratories.

Averaging temperatures and estimating the thermal gradient

Simple statistics are performed on the database of temperature measurements to calculate average temperatures at all depth intervals that were monitored. This is performed for locations above and aside (background) the LNAPL footprint. The data can be visually presented as shown in black line on figure 18.

As shown on figure 17, there are upper and lower segments of the background-corrected temperature profile, on either side of the temperature maxima, where $\Delta T/\Delta z$ can be measured. Therefore, the total heat flux (or loss of heat from the hydrocarbon oxidation zone) is the summation of the upper (upward) and lower (downward) heat fluxes. In practice, it can be difficult to measure the lower heat flux due to compressed thickness and impracticability of installing high-density temperature monitoring systems. As a result, the lower heat flux term is often omitted from the calculations (Warren & Bekins 2015). For the purposes of this measurement guidance, omission of

the lower heat flux term is optional since its exclusion most often results in a low-biased (or conservative) estimate of the NSZD rate. Under the most common scenarios, groundwater is either at or slightly colder than the overlying hydrocarbon oxidation zone. As a result, if the lower heat flux is accounted, then NSZD rates will increase proportionally. If the lower heat flux is accounted, ensure that a thermal conductivity is used that is representative of that deeper (and often wetter) depth interval.

Estimation of the upward thermal gradient requires careful assignment of upper and lower boundary control points. Analogous to the control point assignment described for the gradient method in section 4.3 and appendix C, carefully select these locations above the hydrocarbon oxidation zone and based on geologic and temperature profile shape considerations. The difference in temperature between the upper and lower boundary control points of measurement, divided by the vertical distance between the control points, gives an estimate of the vertical thermal gradient, $\Delta T/\Delta z$ in equation 10. Appendix G further describes how to estimate the thermal gradient.

Assessing and compensating for background using the biogenic heat method

As discussed in section 5.1.1, there is an ambient variation in soil temperatures due to atmospheric conditions. Additionally, as discussed in sections 1.5.2 and 4, NSR within organic matter throughout the vadose-zone profile can also undergo exothermic oxidation processes and consume O_2 and create CO_2 . It must be accounted and subtracted from the total heat flux to isolate the heat flux attributed only to NSZD. If not accounted, the NSZD rate may be over-estimated. Selection of high quality background monitoring locations is vital to the success of the biogenic heat method.

This background correction can be done by measuring temperature profiles, using the same procedures, in a background location with similar subsurface properties as the LNAPL footprint measurement locations. If the subsurface has multiple distinctly different features across the LNAPL footprint (e.g. topography, vegetation, concrete foundations/pipelines/infrastructure, or lithologic layers as shown on figures 4–9), then multiple background locations may be necessary to account for non-petroleum effects within each distinctly different feature. If additional sources of heat are identified (e.g. subgrade pipelines), then it is important to account for this additional heat source otherwise NSZD rates will be over-estimated (Warren & Bekins 2018). Preference is to monitor biogenic heat distal from any additional sources of heat that may confound the data evaluation.

Additionally, the background correction can be performed using local meteorological data and the Van Wijk and de Vries function as summarised in appendix G. Note that this background correction option neglects the effects that groundwater temperature has on the overlying soil. Therefore, if groundwater temperatures depart from the annual average ambient/atmospheric temperature, then reconsider using this approach.

Applicable to both means of background correction, measurement and mathematical, a careful review of other heat sources in the subsurface thermal monitoring area must be performed (e.g. utilities) to minimise the potential for inaccuracies.

Calculating the NSZD rate

The NSZD rate is calculated from the thermal gradient and heat flux using equation 11.

Equation 11: $R_{NSZD} = \frac{q_H}{\Delta H^\circ}$

where R_{NSZD} is the NSZD rate (g/m²/s), q_H is the steady-state conductive heat flux (J/m²-soil/s), and ΔH° is the heat of reaction or enthalpy (J/mol).

The enthalpy is determined using an accounting of heat released during the hydrocarbon oxidation reaction. The heat released can be estimated using the stoichiometric equation specified in equation 2.

As described in detail in API (2017), enthalpy from oxidation of CH₄ and octane (C₈H₁₈) is similar at 43.9 and 44.8 kJ/g, respectively. As such, the enthalpy of CH₄ can be used as a surrogate to estimate heat released from all hydrocarbon oxidation whether it be CH₄ or other VOCs. The accounting of enthalpy from anaerobic biodegradation was determined to be negligible as it represents only approximately 2% of the enthalpy from aerobic biodegradation (e.g. 0.89 kJ/g for C₈H₁₈). Therefore, for the purposes of approximating biogenic heat mass-based NSZD estimates, sole use of the CH₄ oxidation heat of reaction ($\Delta H^\circ = 43.9$ kJ/g CH₄) is adequate to account for 98% of the mass of all hydrocarbons (e.g. VOCs and CH₄) that are oxidised (API 2017).

5.1.3 Biogenic heat method quality assurance/quality control

Appropriate QA/QC measures are essential to assess the accuracy and precision of the data collected. Use proper, manufacturer-recommended calibration procedures for all field instruments. A minimum two-point calibration is typically prudent with a span temperature calibrated to the range of expected soil temperatures.

5.1.4 Biogenic heat method considerations

Sources of measurement uncertainty and variability, how they affect biogenic heat method calculations, and potential mitigation means are presented in table 15.

Table 15. Biogenic heat method uncertainty and variability considerations.

Factor	Effect	Mitigation
Thermal conductivity (K_T)	Heat conduction varies significantly with soil moisture after rain events and seasonally.	Monitor rainfall along with soil temperatures and assess the impacts of rainfall on NSZD rates. Consider modifying the K_T or range of K_T values to incorporate these intermittent effects, if significant.
Geologic conditions across the LNAPL footprint	Variable geology may result in variable thermal gradients.	Estimate K_T for each unique lithology and use as statistical volumetric-average (e.g. geomean) in the NSZD calculations (Warren & Bekins 2018)
Seasonal or climatic	For sites with LNAPL at less than 10 mbg, a climatic anomaly (e.g. abnormally cold winter) may impact NSZD rates.	Perform longer-term temperature data logging (e.g. 1–2 years) and calculate a periodic rolling average NSZD rate using averaged temperatures to assess the drift in rates.
Other heat sources	As highlighted by Warren & Bekins (2015), other sources of heat in the soil such as pipelines and surface water recharge areas can confound background correction.	Perform temperature monitoring at least 10 m away from other heat sources.

Interpretation of results from the biogenic heat method, like the other NSZD monitoring methods, can be challenging. Consider the following items when interpreting the data:

- Exterior sources of heat (e.g. pipelines, utilities, surface water recharge) can cause thermal anomalies that confound data interpretation
- Changes (geospatial and/or temporal) in soil moisture can significantly affect the measured thermal profiles, and
- A non-uniform vadose zone, for example containing thin, low-permeability layers, may significantly affect the shape of the soil temperature profiles.

Any of the above factors can influence the NSZD rate calculation. If data interpretation challenges arise, then review of the LCSM and site-specific assumptions that went into the NSZD monitoring program design is advised (API 2017). In most situations, data inconsistencies can be resolved.

6. Rate measurement using LNAPL compositional change data

As introduced in section 2.5.3, NSZD results in changes to the chemical composition of the LNAPL. This section discusses the mechanisms, sometimes called weathering, and measurements that can be made to estimate chemical of COC-specific NSZD rates in LNAPL ($R_{\text{COC-LNAPL}}$). These are analogous to and comparable with the COC-specific NSZD rates calculated using the aqueous methods ($R_{\text{COC-aq}}$) described in section 3 and stated in equation 4). As discussed in section 1.2, considering that degradation is occurring both in the aqueous (waterborne) and LNAPL (direct-contact oil biodegradation), it is expected that the $R_{\text{COC-LNAPL}}$ will be larger than $R_{\text{COC-aq}}$ since $R_{\text{COC-LNAPL}}$ is inclusive of COC dissolution to the aqueous phase plume adjacent to the LNAPL body where the waterborne biodegradation occurs. At many sites, $R_{\text{COC-aq}}$ will be indicative of $R_{\text{COC-LNAPL}}$ since the two processes are interrelated.

The results from these measurements may be useful on sites where a more detailed understanding of NSZD is needed as it relates to rates of attenuation of a COC(s) that is driving decision making on the remedial efforts.

6.1 LNAPL weathering mechanisms

Some literature on this subject refers to NSZD processes as LNAPL weathering, and various literature on it can be found in the field of environmental forensics and remediation. The primary processes are not surprisingly the same as those for NSZD, which include dissolution (water washing), volatilisation (evaporation), and biodegradation. More recently, direct-contact oil biodegradation was also identified as a significant COC mass loss mechanism from the LNAPL (Ng *et al* 2014, 2015). Factors that may influence weathering rates, and thus chemical-specific NSZD rates, include the following:

- LNAPL saturation (e.g. residual-disconnected or mobile-connected)
- LNAPL distribution (i.e. submerged or exposed to vadose zone)
- Redox state and microbiology (e.g. ranging from aerobic to methanogenic)
- Hydraulic condition (e.g. low to high groundwater flux), and
- Geology (e.g. fine to coarse grained soils or bedrock).

As a result of the various factors and inherent heterogeneities in the subsurface, LNAPL weathering rates are non-uniform within the LNAPL footprint and, in fact, variable LNAPL chemical composition could be expected to occur at any particular LNAPL smear zone profile location at a site. These effects are illustrated in figure 21, which presents a vertically profiled, laser-induced fluorescence (LIF) log from the subsurface soil source zone of a condensate LNAPL release. At this low organic matter, sand and gravel site, LIF generally indicates the relative composition of PAHs in the LNAPL. Generally, the higher the response (percent reference emitter (%RE)), the larger the PAH content. The datalogging software (Dakota Technologies, Inc., Fargo, North Dakota, USA) uses red, green, blue (RGB) colour mixing calculations to differentiate response to four different wavelengths of light (350, 400, 450, and 500 nanometre (nm)) at each measurement depth. LIF takes measurements at roughly 1-cm depth intervals. As shown on figure 21, the fluorescent response within this

approximately 4-m LNAPL smear zone depth interval impacted by a single release of condensate LNAPL was highly variable. Of note is the variable LNAPL chemical quality as indicated by the LIF response RGB colour scale within the vadose, capillary, and submerged zones.

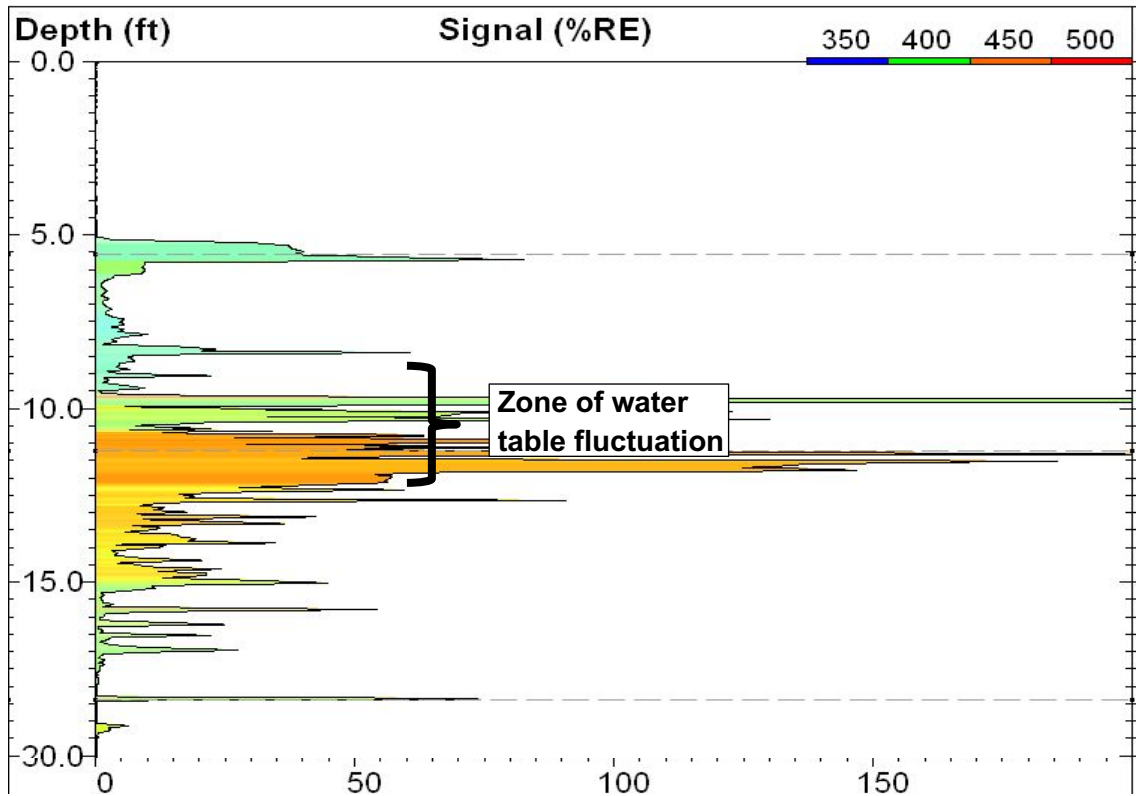


Figure 21. Laser-induced fluorescence log in condensate LNAPL source zone. Courtesy of Dakota Technologies, Inc. at www.dakotatechnologies.com.

While figure 21 is a good visual example of the variability in LNAPL chemical quality at a single location, others have measured the chemical changes in the LNAPL. Kaplan *et al* (1996) performed gas chromatography/mass spectrometry (GC/MS) analysis of gasoline, diesel, and Bunker C oil and constructed a biodegradation hierarchy of the chemical constituents in the oils (figure 22). It shows that n-alkanes are expected to biodegrade first, followed by alkylcyclohexanes, isoprenoids, and PAHs. Others have also reported very similar results (Volkman *et al* 1984; Peters & Moldowan 1993).

The increased susceptibility of n-alkanes to biodegradation relative to isoprenoids, with some completely removed after approximately 20 years (Christensen and Larsen 1993), led to the development of ratios to assess the extent of biodegradation as well as estimate the spill age of petroleum (Christensen & Larsen 1993; Douglas *et al* 1996; Wade 2001).

Extensive research performed at the Bemidji crude oil release site (Minnesota, USA) quantified the losses of alkanes and alkylcyclohexanes from oil samples at four sites around the release area (Warren *et al* 2014). Alkanes were absent from most of the samples, so their research focused on the alkylcyclohexanes instead. Their findings are summarised on figure 23. It shows a more significant depletion in oil at sites 2, 3, and 4 and, at those sites, a greater depletion of compounds in the C-14 to C-17 range,

followed by C-18 to C-24. Compounds below and above these ranges showed lesser depletion. The oil sample from Site 5 was expected to be less weathered as it is located in a less degraded end of the LNAPL body where CO₂ efflux and methanogen concentrations were also both low.

Fuel Type	Level of Biodegradation	Chemical Composition
Bunker C fuel Diesel Gasoline	1	Abundant n-alkanes
	2	Light end n-alkanes removed
	3	Middle range n-alkanes, olefins, benzene & toluene removed
	4	More than 90% of n-alkanes removed
	5	<i>Alkylcyclohexanes & alkylbenzenes removed</i> Isoprenoids & C ₀ -naphthalene reduced
	6	Isoprenoids, C ₁ -naphthalenes, benzothiophene or alkylbenzothiophenes removed C ₂ -naphthalenes selectively reduced
	7	Phenanthrenes, dibenzothiophenes and other polynuclear aromatic hydrocarbons reduced
	8	Tricyclic terpanes enriched Regular steranes selectively removed C ₃₁ to C ₃₅ -homohopanes reduced
	9	Tricyclic terpanes, diasteranes & aromatic steranes abundant
	10	Aromatic steranes & demethylated hopanes* predominant

*Present under certain conditions only.

Figure 22. Change in gasoline, diesel fuel, and Bunker C composition during biodegradation. *Reproduced from Kaplan et al (1996).*

In summary, significant work has been done looking at changes in LNAPL composition over time. Warren *et al* (2014) found that the n-alkylcyclohexane reductions in LNAPL samples correlated well with methanotroph microbiological concentrations and methanogens (mcrA-methanogenic archaea) and suggested use of n-alkylcyclohexane reductions in LNAPL as a proxy for NSZD. In fact, this was shown to be a better NSZD proxy than CO₂ efflux, which correlated slightly worse with CH₄ concentrations and n-alkylcyclohexane losses in LNAPL. The available literature points to the potential use of LNAPL composition as a reliable indicator of NSZD.

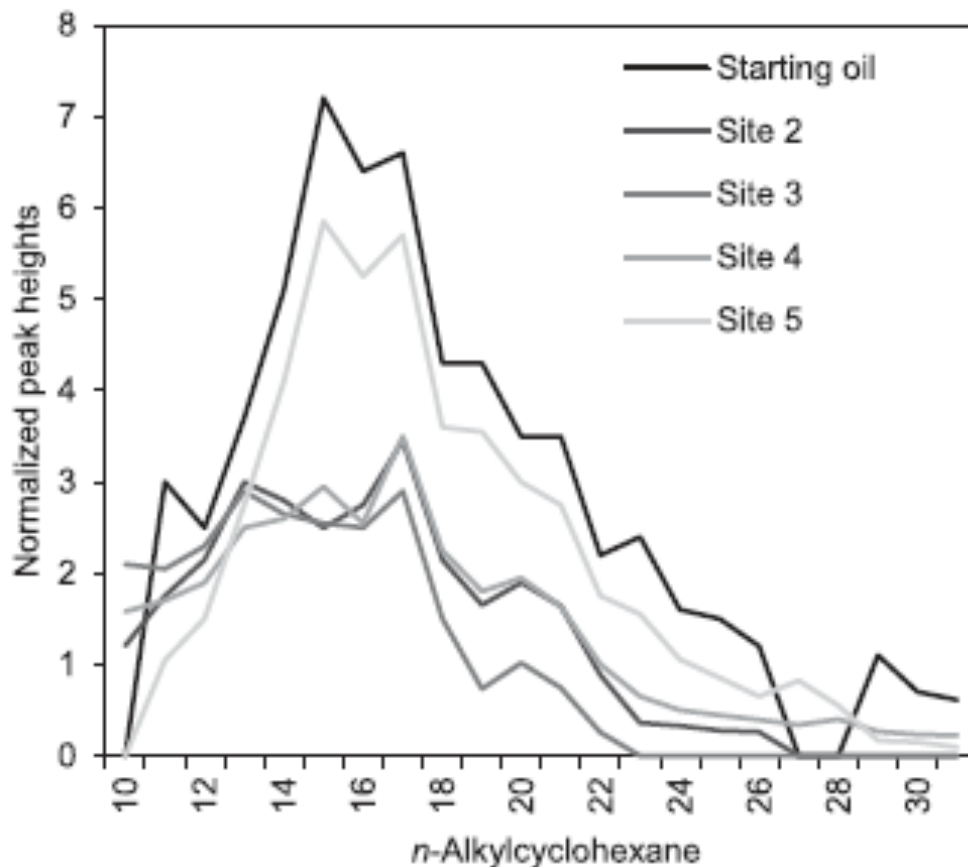


Figure 23. Change in gasoline, diesel fuel, and Bunker C composition during biodegradation. Reproduced with permission from Warren et al (2014).

6.2 LNAPL compositional change method key assumptions

The following are the primary assumptions in using LNAPL compositional change to estimate a COC-specific NSZD rate:

- A time-series regression of the chemical content of the LNAPL, corrected for bulk oil depletion, is representative of the NSZD rate.
- LNAPL samples, collected from either monitoring wells or soil samples, are representative of the entire vertical LNAPL interval in the surrounding formation, and
- $R_{COC-LNAPL}$ is inclusive of losses due to dissolution, volatilisation, waterborne biodegradation, and direct-contact oil biodegradation.

6.3 LNAPL compositional change method process

Box 6.1 illustrates application of the LNAPL compositional change method at a single location. Application of the LNAPL compositional change method is governed by equations 12 and 13.

$$\text{Equation 12: } R_{COC-LNAPL} = \frac{dm_{COC}}{dt} * \rho_{LNAPL} * D_{LNAPL}$$

$$\text{Equation 13: } dm_{\text{COC}} = m_{\text{COC}-0} - m_{\text{COC}-t} * \frac{m_{\text{marker}-0}}{m_{\text{marker}-t}}$$

where $R_{\text{COC-LNAPL}}$ is the COC-specific NSZD rate (grams of COC per square metre per day ($g_{\text{COC}}/m^2/d$)), dm_{COC} is the change in chemical content in the LNAPL normalized for the conservative marker (grams of chemical of concern per grams of LNAPL ($g_{\text{COC}}/g_{\text{LNAPL}}$)), t is time (d), ρ_{LNAPL} is the LNAPL density (g_{LNAPL}/m^3), and D_{LNAPL} is the specific volume of in-situ LNAPL (m^3/m^2).

The change in the chemical (COC) content in the LNAPL (dm_{COC}) is confounded by the concurrent depletion of the bulk LNAPL. The change in mass fraction of a single component over time concurrent with losses of many other components in the LNAPL could cause the mass fraction concentration of the single component to increase if it is not depleted at a faster rate than the bulk of the LNAPL is depleted by weathering. To account for this bulk depletion, the COC mass fraction (m_{COC}) is normalized using the concentration of a conservative marker (Douglas *et al* 1996). The conservative marker is resistant to degradation and therefore its concentration increases over time in the LNAPL. As such, it can be used to correct for the bias imparted on the COC concentration change from bulk LNAPL depletion.

The COC content in the LNAPL is normalized by applying a correction factor or the initial marker mass fraction ($m_{\text{marker}-0}$) divided by the marker mass fraction at time t ($m_{\text{marker}-t}$). The normalization equation 13 uses mass fraction data for both a COC (COC subscript) and the conservative marker (marker subscript) from the current LNAPL sample at time t (t subscript) and either fresh oil data at time zero or at some earlier time (0 subscript).

Prescription of the selection process for identification of the conservative marker is beyond the scope of this document. Example conservative markers include the saturated hydrocarbons hopane, pristane, and phytane. Ample published literature exists on this topic to help guide the effort (for example Douglas *et al* 1996, 2012; Baedecker *et al* 2017). Each situation requires a general assessment of the petroleum type, mixtures present, extent of weathering, and specific compounds present in the right biodegradation window where compounds are currently being altered by biodegradation. There are many compounds to choose from and factors like their relative abundances need to be taken into consideration (e.g. the n-alkylcyclohexanes may not work for some sites since they may be completely removed by biodegradation, unaffected by biodegradation, or too low in their relative abundance in the original petroleum). It is difficult to describe a specific method as the work usually involves more of a decision tree approach as well as a bit of screening and professional judgement to see what compounds/biomarkers are present and useful.

It should be noted that use of the LNAPL compositional change method is feasible without use of the LNAPL specific volume (D_{LNAPL}). This is further discussed in section 6.3.3.

Implementation of the LNAPL compositional change method comprises the following general steps:

1. LNAPL sampling from monitoring wells or subsurface soil
2. Laboratory analysis of LNAPL for COCs, conservative markers, and fluid density
3. Laboratory analysis of intact soil cores for capillarity and pore fluid saturation
4. Regression analysis of COC and marker content in LNAPL

5. Calculation and mapping of LNAPL specific volume, and
6. Geospatial integration of COC content change and specific volume to calculate the NSZD rate.

The following sections provide an overview of the key steps.

6.3.1 LNAPL sampling from in-well or soil samples

An LNAPL sample can be collected directly from a monitoring well or extracted from a soil sample. No extraordinary procedures or QA/QC are required to meet the data objectives of this method. Follow local, regulatory-accepted and best practices for collection of representative groundwater and/or soil samples, paying particular attention to ample purging and collection of an LNAPL samples from the formation (i.e. not a static LNAPL sample from a well casing) and minimising losses of VOCs from the sample. Coordinate closely with the analytical laboratory to determine the quantity of sample required for the specified analyses.

6.3.2 Laboratory analysis of LNAPL and soil

This method relies upon laboratory analysis of LNAPL and soil samples.

Laboratory analysis of LNAPL for COCs, markers, and fluid density

Various laboratory methods are available for LNAPL and table 5 summarises some of the analytical options. It is beyond the scope of this document to describe the theoretical basis and practical application of all the listed analyses; they are listed for information purposes only. Selection of the appropriate method depends upon the COC and data objectives and must be made by a practitioner experienced with the science. For example, if the work plan calls for a qualitative analysis, then use of Method SW8015 GC-FID with chromatogram review is appropriate. If a quantitative goal is intended, then ASTM D2887 simulated distillation is appropriate to measure individual alkanes. If BTEX or PAHs are desired, then methods SW8260 and SW8270 by GC/MS-select ion method (SIM), respectively, are appropriate. Other forensic-type methods, not listed on table 5, are also commercially available for unique COC and/or marker analytical needs, such as metastable reaction ion monitoring commonly used for biomarker analyses.

In some cases, it may be useful to develop a site-specific sampling and analysis plan to meet the data quality objectives. For example, Warren *et al* (2014) describes a method of using dichloromethane (DCM) to extract oil from an intact soil core collected using a freezing drive shoe. Laboratory analysis was by GC/MS either as whole oils dissolved in DCM or after being separated into aliphatic and aromatic fractions by liquid chromatography on a mixed silica–alumina column. Profiles of n-alkylcyclohexanes were extracted from ion chromatograms using mass spectrometry scan range m/z 83. Compounds in the profile were normalised to C23 tricyclic terpane as a conserved internal standard in order to evaluate relative concentration levels between samples of the suite of compounds. They used an archived sample of fresh Bemidji oil as a reference standard.

Box 6.1 LNAPL composition change for COC-specific NSZD rates

Objective: Measurement and analysis of decreasing trends in the COC content in LNAPL to estimate COC-specific NSZD rate

For more information: section 6

Principles: Regression-based estimate

$$R_{COC-LNAPL} = \frac{dm_{COC}}{dt} * \rho_{LNAPL} * D_{LNAPL}$$

where dm_{COC} is normalized using concurrent changes in a conservative marker:

$$dm_{COC} = m_{COC-t} - m_{COC-0} * \frac{m_{marker-t} - m_{marker-0}}{m_{marker-0}}$$

Key assumptions:

- Time series regression of COC-content in LNAPL, corrected for bulk oil loss, represents the NSZD rate
- Samples are representative of the in-situ LNAPL in the formation
- $R_{COC-LNAPL}$ is inclusive of dissolution, volatilisation, and waterborne and direct-contact oil biodegradation

Key laboratory analyses:

- Whole oil analysis of current and fresh LNAPL using GC/MS for COC(s) and marker
- LNAPL fluid density
- Soil core analysis for soil capillarity properties and LNAPL pore fluid saturation

Conceptualisation – LNAPL weathering:



Various weathered LNAPL samples from ten monitoring wells across a single release site.

Summary of implementation procedure:

1. LNAPL sampling from in-well or soil samples
2. Laboratory analysis of LNAPL for COC, conservative marker, and fluid density
3. Laboratory analysis of intact soil cores for capillarity and pore fluid saturation
4. Calculation of COC and marker loss in LNAPL and normalization of COC change in mass fraction over time
5. Estimation of LNAPL specific volume
6. Calculate the NSZD rate

Example analytical results (2010 data in mg/g_{oil}):

Location	BTEX	Pr+Ph*
411	4.4	9.6
421B	7.1	8.5
422	3.1	8.7
301A	5.3	8.3
306	4.8	8.4
315	7.0	7.9
319	7.1	9.3
Average	5.5	8.7
Fresh Oil	13.7	6.5

Notes:

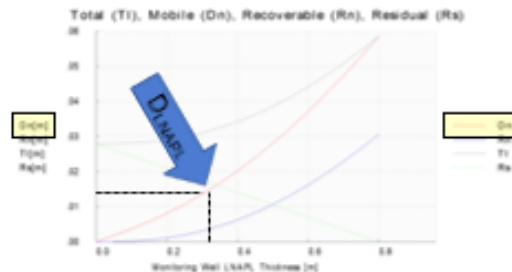
BTEX = benzene, toluene, ethylbenzene, and total xylenes
Pr+Ph = pristane and phytane isoprenoid hydrocarbons
* marker

(Baedecker et al 2017, north oil pool near spill)

- COC = BTEX
- $m_{BTEX-0} = 0.0137$ g/g_{LNAPL}
- $m_{BTEX-t} = 0.0031-0.0071$ (0.0055 average) g/g_{LNAPL}
- Marker = Pr+Ph
- $m_{marker-0} = 0.0065$; $m_{marker-t} = 0.0087$ g/g_{LNAPL}
- $dm_{BTEX} = 0.0084-0.0114$ (0.0096) g/g_{LNAPL}
- Oil age, $dt = 31$ years (release occurred in 1979)
- LNAPL density, $\rho = 8.9 \times 10^5$ g/m³

Specific volume (D_{LNAPL}) estimation:

- LDRM used to estimate D_{LNAPL} (API 2007)
- Soil type = well-graded, fine-coarse sand w/gravel
- $D_{LNAPL} = 0.014$ m³/m² at a location with 0.3 m in situ LNAPL thickness, from LDRM chart below.



(API LNAPL Distribution and Recovery Model result)

** As discussed in section 6.3, use of the method is feasible without estimation of D_{LNAPL} , but it results in a value that is not comparable to the other methods.

Benzene-specific NSZD rate calculation:

$$R_{COC-LNAPL} = \frac{dm_{COC}}{dt} * \rho_{LNAPL} * D_{LNAPL}$$

$$R_{COC-LNAPL(AVG)} = \frac{0.0096}{31} * 8.9 \times 10^5 * 0.014 = 3.9 \text{ g}_{BTEX}/\text{m}^2/\text{yr (average)}$$

$$\text{Range of } R_{COC-LNAPL} = 3.4-4.6 \text{ g}_{BTEX}/\text{m}^2/\text{yr}$$

$$\text{NSZD rate, } R_{BTEX} = 3.4-4.6 \text{ g}_{BTEX}/\text{m}^2/\text{yr} = 39-53 \text{ L}_{BTEX}/\text{ha}/\text{yr}$$

If possible, collect a sample of raw material, fresh LNAPL, and run the same analysis. As shown in box 6.1, this is a useful benchmark for comparison of laboratory results and the assessment of constituent degradation. In lieu of a fresh LNAPL sample, which is often not practically obtained at sites with old, legacy releases, time-series measurements of LNAPL constituent concentrations can be used. However, depending upon the COC depletion rate, the frequency of sampling may range from annual to once every decade.

Include fluid density (ρ_{LNAPL}) with the laboratory analysis of LNAPL. As shown in equation 12, this is used in NSZD rate calculation. Fluid density is a standard analysis that most commercial petrophysical laboratories can perform.

Laboratory analysis of intact soil cores for capillarity and pore fluid saturation

As shown in equation 12, the LNAPL specific volume is useful in order to extrapolate the chemical constituent results to a representative volume of LNAPL within a unit area of the site. LNAPL specific volume, volume of LNAPL (m^3) per unit area (m^2), is a calculated value based on soil properties. It is beyond the scope of this document to describe the laboratory methods used to determine the LNAPL specific volume. The practitioner is referred to API (2007) for information on the required parameters and associated lab methods. Alternatively, soil and LNAPL properties can be selected from a database by closely matching the grain-size distribution from the site to the database. Likewise, LNAPL fluid properties can be picked from the database using known type of fuel.

6.3.3 Regression analysis of chemical content in LNAPL

The laboratory results of the fresh LNAPL (time zero) and samples from monitoring wells or soil samples over time are plotted on a chart to track the reduction in the COC content over time (dm_{COC}/dt in equation 12). Figure 24 shows an example of this procedure performed at a jet fuel site (AFCEE 2003). Note that the results presented in figure 24 assumes no bulk LNAPL depletion during the 8-year period of the study; they were not corrected using a conservative marker.

6.3.4 Calculation and mapping of LNAPL specific volume

It is beyond the scope of this document to describe the procedure to estimate and map the LNAPL specific volume (D_{LNAPL} in equation 11). The practitioner is referred to API (2007) for the LNAPL distribution and recovery model (LDRM) that can be used to estimate it. LDRM requires a host of soil and LNAPL parameters that are used to model the LNAPL pore fluid saturation profile.

As noted at the beginning of this section, use of the LNAPL compositional change method is feasible without estimation of D_{LNAPL} . Estimation of D_{LNAPL} requires a firm understanding of soil and LNAPL properties and screening-level modelling (API 2007). If this information is not available, then equation 11 may be used without the term. The net effect of eliminating this parameter is estimating $R_{COC-LNAPL}$ in the units of $g_{COC}/m^3/d$. This value would no longer be comparable to the NSZD rates from the other methods, but may be adequate to meet the project data objectives.

**ZERO-ORDER BTEX WEATHERING IN JP-4 LNAPL AT 1610-1, 2, AND 3
BUILDING 1610, SHAW AFB, SOUTH CAROLINA
FUEL WEATHERING STUDY**

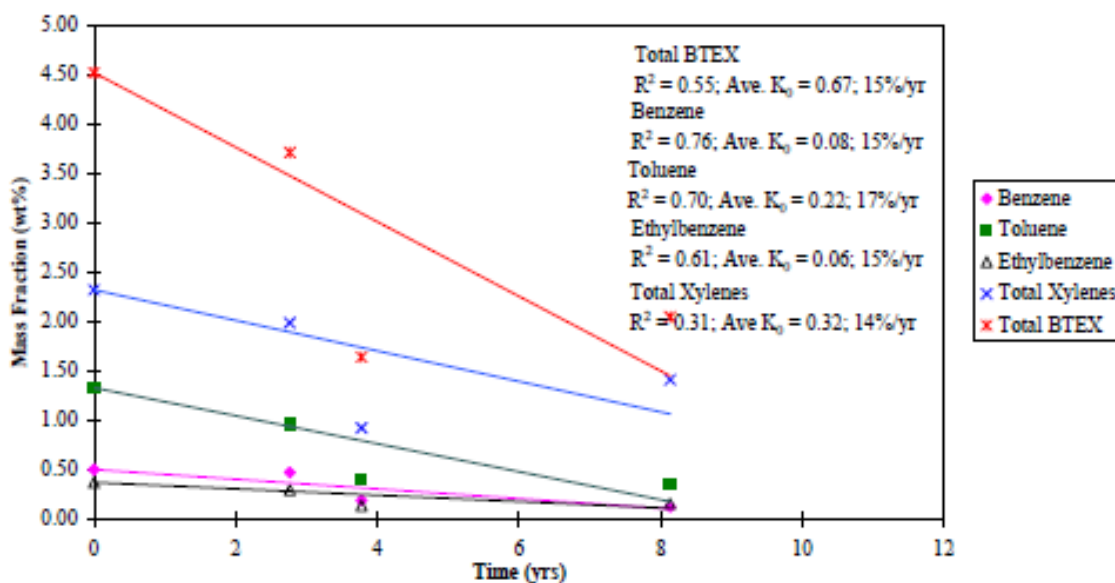


Figure 24. Linear regression analysis on the change in total BTEX content in LNAPL over time. Reproduced from AFCEE (2003).

6.3.5 Calculate the NSZD rate

The COC-specific NSZD rate is estimated using equation 11. Box 6.1 shows a simple example calculation. Because this is a COC-specific NSZD rate, it is expected to be significantly smaller than a bulk NSZD measurement from the gas flux methods, for example. Similar to that done for the other NSZD measurement methods, the COC-specific NSZD rates can be plotted and geospatially integrated to estimate at a site-wide NSZD value.

6.4 NSZD emerging science

The use of LNAPL compositional change measurements for the distinct purpose of estimating a COC-specific NSZD rate is an emerging science. Few publications on this specific topic exist. As a result, a database to assess the relative magnitude of these measurements is not established. Practitioners are urged to carefully evaluate the data within the context of other site monitoring results before bringing the data into a decision-making context. The value of the LNAPL compositional change method will grow as multiple sequential laboratory analyses trend and affirm the COC-specific NSZD rates.

Work is underway, partially using the Bemidji site as a data basis, to create a new analytical model that can more accurately simulate NSZD processes and chemical weathering from the LNAPL. The purpose of the new models is to better project remedial timeframes (Garg *et al* 2017). This is acknowledged as an area of future research, as current models do not reasonably account for the current understanding of the NSZD biodegradation processes (e.g., direct oil contact biodegradation and outgassing). Typically of particular interest, are the timeframes for groundwater to meet COC-specific numeric clean-up criteria within the LNAPL source zone. The use of COC-specific NSZD rates is useful to understand short-term rates of COC depletion

from LNAPL, but their use to support long-term remedial timeframe projections is currently limited without an appropriate model.

6.5 LNAPL compositional change method quality assurance/quality control

Appropriate QA/QC measures are essential to assess the accuracy and precision of the data collected using the LNAPL compositional change method of NSZD estimation. Conform to standard and regulatory-agency required practices related to LNAPL and/or soil sampling, including collection of duplicate samples. Because of the typically high concentration results from LNAPL analysis, field and laboratory blanks are typically unnecessary. However, evaluate laboratory COC- and conservative marker-specific analytical detection limit capabilities in advance of the analyses and ensure they can and do meet the project data quality objectives.

6.6 LNAPL compositional change method considerations

Interpretation of results from the LNAPL compositional change method, like the other NSZD monitoring methods, can be challenging. Consider the following items when interpreting the data:

- The chemical quality of the LNAPL is highly variable in space, and an adequate number of samples is necessary to generate a representative COC-specific NSZD rate.
- The NSZD rate calculation may be sensitive to the conservative marker used to correct for the bulk LNAPL depletion. Calculation of the NSZD rate using multiple markers may be prudent to assess the variability in rate estimates.
- The method is emerging with few, if any, published rates for use as a basis for comparison. Consistent with the use of an emerging method, the onus of proof is on the practitioner, and a more intensive data collection and analysis program may be necessary to validate the results.

Any of the above factors can influence the NSZD rate calculation. If data interpretation challenges arise, then the reader is advised to closely review the LCSM and site-specific assumptions that went into the NSZD monitoring program design. In most situations, data inconsistencies can be resolved.

7. Conclusions

NSZD is a term used to extend the traditional understanding of natural attenuation to the LNAPL source zone and describes the collective, naturally occurring processes of dissolution, volatilisation, and biodegradation that result in mass losses of LNAPL petroleum hydrocarbon constituents from the subsurface. This document provides practical guidance on the measurement of NSZD rates using various available methods, including the following:

- aqueous methods using dissolved contaminant concentration trends and NAIP mass budgeting analysis
- soil gas flux methods using concentration gradients, passive flux traps, and the DCC
- biogenic heat method based on soil temperatures, and
- LNAPL compositional change method based on chemical analysis of the oil.

Significant advances have been made in the methods used to measure NSZD processes using gas flux and biogenic heat. Traditional methods of measuring natural degradation rates using groundwater and LNAPL samples also remain viable. Monitoring the chemical changes in the LNAPL and applying it to NSZD rate estimates is an emerging method. Using the information contained herein, practitioners have what they need to select a method and implement NSZD monitoring at their site.

The main objective of this document is to provide a knowledge base and procedures for consistency in the measurement of NSZD in Australia. It leverages materials previously developed by CRC CARE, as well as work in Australia from CSIRO and North America from ITRC, USGS, API, and various universities. It captures the state of the practice and is useful as a guide to develop site-specific plans.

Like many environmental remediation monitoring methodologies, this is an evolving field, and the practical portions of the document are subject to change as new approaches evolve. Place the information in this document into proper context using a project team that is well-versed in site conditions and project data quality and need objectives.

This guidance is generally applicable to a wide range of environmental remediation sites containing petroleum hydrocarbon impacts in the subsurface. Its use is appropriate at sites that have a need for theoretical, qualitative, or quantitative understanding of NSZD processes.

API (2017) and Garg *et al* (2017) summarise emerging science related to method modifications (e.g. use of ^{14}C for background correction of the gradient and DCC measurements) and future research needs in the NSZD measurement technology. The reader is advised to consult current literature for more recent advances and method improvements.

7.1 Summary of primary NSZD measurement guidance

The following list highlights the key points made in this guidance. At a minimum, the practitioner is advised to review and internalise them as part of their NSZD monitoring planning phase.

- NSZD measurements are useful at many petroleum-impacted sites where risk management and/or remediation is ongoing.
- NSZD is most prominently manifested as changes in gases and soil temperatures above the LNAPL footprint. Calculating the NSZD rate without considering these biodegradation by-products would result in a significant underestimate of the effectiveness of the NSZD remedial technology for source mass loss.
- The total NSZD rate is equal to the summation of the stoichiometric conversions of the aqueous and gaseous (or heat) manifestations. The aqueous portion of NSZD is typically very small as compared to the gaseous portion.
- Establish clear data use and quality objectives prior to performing NSZD monitoring. An NSZD monitoring program take can many forms ranging from a simple spot check at a single location in time to determine the potential of NSZD compared to active remediation, to monitoring multiple locations site-wide over multi-year increments in time to assess the long-term change in NSZD rates.
- Vet the inherent assumptions associated with each monitoring method prior to their use. These include diffusion- or heat conduction-controlled transport (gradient and biogenic heat methods, respectively) and complete CH₄ and VOC hydrocarbon oxidation (passive CO₂ trap and DCC methods).
- Understanding key elements of the LCSM as it relates to NSZD is an important first step as it will highlight site conditions which control NSZD rates. The LCSM is used as a basis for method selection and monitoring design.
- Theoretical evaluation of NSZD with a tool as simple as a type curve, can be useful and serve to establish a basis for expectations and comparison to field measurements.
- Background correction is the largest challenge associated with NSZD monitoring and, therefore, is a key design element for all methodologies that must be tailored to site-specific conditions.
- This document presents five bulk hydrocarbon-based methods to measure NSZD rates (i.e., mass budgeting, gradient, passive flux trap, DCC, and biogenic heat). A reasonable accounting can be performed solely using the gas flux or biogenic heat methods. However, in theory the total NSZD rate also includes an accounting of changes in dissolved chemical constituents using mass budgeting.
- If a COC-specific NSZD rate is needed, two methods are proposed – dissolved contaminant concentration trending and LNAPL compositional change. The results from these measurements may be useful on sites where a more detailed understanding of NSZD is needed as it relates to rates of attenuation of COC(s) that are driving remedial efforts.
- Extrapolation of NSZD rate measurements, typically collected in units of g/m²/d, over large spatial areas and time must be done with careful consideration of the spatial and temporal variability of the data presented using statistical approaches. Extrapolation requires multiple measurement locations and monitoring events, the degree to which depends upon the data use objective.

NSZD rates vary geospatially and temporally and, in addition, each monitoring method has its own inherent simplifying assumptions. The end result of this compounded uncertainty is a value for NSZD that is considered an order-of-magnitude estimate. The practitioner is advised to carefully consider the sources of variability and tailor their NSZD monitoring program objectives and procedures accordingly.

8. References

- American Petroleum Institute (API) 1998, *Recommended practices for core analysis, second edition*, Recommended Practice No. 40.
- API 2007, *LNAPL distribution and recovery model (LDRM) – volume 1: Distribution and recovery of petroleum hydrocarbon liquids in porous Media*, Publication No. 4760.
- API 2017, *Quantification of vapor phase-related natural source zone depletion processes*, Publication No. 4784.
- ASTM International 2002, *Standard test method for rapid determination for carbonate content of soils*, D4373-02.
- ASTM International 2016, *Standard test methods for determining the biobased content of solid, liquid, and gaseous samples using radiocarbon analysis*, D6686-16.
- Amos, RT, Mayer, KU, Bekins, BA, Delin, GN & Williams, RL 2005, 'Use of dissolved and vapor-phase gases to investigate methanogenic degradation of petroleum hydrocarbon contamination in the subsurface', *Water Resources Research*, vol. 41, no. 2, p. W02001.
- Atlas, RM 1981, 'Degradation of petroleum hydrocarbons: an environmental perspective', *Microbiological Reviews*, vol. 45, no. 1, pp. 180–209.
- Baedecker, MJ, Eganhouse, RP, Qi, H, Cozzarelli, IM, Trost, JJ & Bekins, BA 2017, 'Weathering of oil in a surficial aquifer', *Groundwater*, vol. 56, no. 5, pp. 797–809.
- Barcelona, MJ, Holm, TR, Schock, MR & George, GK 1989, 'Spatial and temporal gradients in aquifer oxidation-reduction conditions', *Water Resources Research*, vol. 25, no. 5, pp. 991–1003.
- Beck, P & Mann, B 2010, *A technical guide for demonstrating monitored natural attenuation of petroleum hydrocarbons in groundwater*, CRC CARE Technical Report no. 15. CRC for Contamination Assessment and Remediation of the Environment, Adelaide, Australia.
- Bethke, C, Sandford, R, Kirk, M, Jin, Q & Flynn, T 2011, 'The thermodynamic ladder in geomicrobiology', *American Journal of Science*, vol. 311, no. 3, pp. 183–210.
- Braissant O, Wirz, D, Gopfert, B & Daniels, AU 2010, 'Use of isothermal microcalorimetry to monitor microbial activities', *FEMS Microbiol. Lett.*, vol. 303, pp. 1–8.
- California Environmental Protection Agency (CalEPA). 2012. *Advisory: active soil gas investigations*, Department of Toxic Substances Control, available at <www.dtsc.ca.gov/SiteCleanup/upload/VI_ActiveSoilGasAdvisory_FINAL_043012.pdf>.
- Christensen, LB & Larsen, TE 1993, 'Method for determining the age of diesel oil spills in the soil', *Ground Water Monitoring & Remediation*, vol. 13, pp. 142–149.
- Commonwealth Scientific and Industrial Research Organisation (CSIRO) 2016, *Safe work instruction: in-well soil gas sampling and temperature monitoring*, Issued by CSIRO Land and Water; Pollutant Fate and Remediation Team.

Contaminated Land: Applications in Real Environments (CL:AIRE) 2014, *An illustrated handbook of LNAPL transport and fate in the subsurface*, CL:AIRE, London.

Cooperative Research Centre for Contamination Assessment and Remediation of the Environment (CRC CARE) 2013, *Petroleum hydrocarbon vapour intrusion assessment: Australian guidance*, CRC CARE Technical Report no. 23. CRC for Contamination Assessment and Remediation of the Environment, Adelaide, Australia.

CRC CARE 2015, *A practitioner's guide for the analysis, management and remediation of LNAPL*, CRC CARE Technical Report no. 34. CRC for Contamination Assessment and Remediation of the Environment, Adelaide, Australia.

Chaplin, BP, Delin, GN, Baker, RJ & Lahvis, MA 2002, 'Long-term evolution of biodegradation and volatilization rates in a crude oil-contaminated aquifer', *Bioremediation Journal*, vol. 6, pp. 237–256.

Christensen, LB & Larsen, TE 1993, 'Method for determining the age of diesel oil spills in the soil', *Ground Water Monitoring & Remediation*, vol. 13, pp. 142–149.

Davidson, EA, Savage, K, Verchot, LV & Navarro, R 2002, 'Minimizing artifacts and biases in chamber-based measurements of soil respiration', *Agric. For. Meteorol.*, vol. 113, pp. 21–37.

Davis, GB, Rayner, JL, Trefry, MG, Fisher, SJ & Patterson, BM 2005 'Measurement and modeling of temporal variations in hydrocarbon vapor behavior in a layered soil profile', *Vadose Zone Journal*, vol. 4, pp. 225–239.

Davis, GB, Patterson, BM & Trefry, MG 2009a, *Biodegradation of petroleum hydrocarbon vapours*, CRC CARE Technical Report no. 12. CRC for Contamination Assessment and Remediation of the Environment, Adelaide, Australia.

Davis, GB, Patterson, BM & Trefry, MG 2009b, 'Evidence for instantaneous oxygen-limited biodegradation of petroleum hydrocarbon vapors in the subsurface', *Ground Water Monitoring & Remediation*, vol. 29, no. 1, pp. 126–137.

Douglas, GS, Bence, AE, Prince, RC, McMillen, SJ & Butler, EL 1996, 'Environmental stability of selected petroleum hydrocarbon source and weathering ratios', *Environmental Science & Technology*, vol. 30, no. 7, pp. 2332–2339.

Douglas, GS, Hardenstine, JH, Liu, B & Uhler, AD 2012, 'Laboratory and field verification of a method to estimate the extent of petroleum biodegradation in soil', *Environmental Science & Technology*, vol. 46, no. 15, pp. 8279–8287.

Edwards, NT 1982, 'The use of soda lime for measuring soil respiration rate in terrestrial ecosystems', *Pedobiologia*, vol. 23, pp. 321–330.

E-Flux, LLC 2015, *Technical memo 1504.2: wind effects on soil gas flux measurements at ground level*, Last revision 10 June, 2015.

E-Flux, LLC 2017, *Draft user manual – bio-term, a model for biogenic heat generation and transfer in soils from contaminant natural source zone depletion*. Fort Collins, Colorado, USA.

E-Flux, LLC 2018, *Manufacturer-recommended field procedures*, available at <www.soilgasflux.com/ff2>.

Garg, S, Newell, CJ, Kulkarni, PR, King, DC, Adamson, DT, Irianni Renno, M & Sale, T 2017, 'Overview of natural source zone depletion: processes, controlling factors, and composition change', *Groundwater Monitoring & Remediation*, vol. 37, iss. 3, pp. 62–81.

Gorder, K & Holbert, C 2010, '*Thiessen area and mass calculator for assessment of plume dynamics*', Poster presentation at the Seventh Annual Conference on the Remediation of Chlorinated and Recalcitrant Compounds, Monterey, California, USA, May 24–27.

Hers, I, Atwater, J, Li, L & Zapf-Gilje, R 2000, 'Evaluation of vadose zone BTX biodegradation vapours', *Journal of Contaminant Hydrology*, vol. 46, pp. 233–264.

Hillel, D 1982, *Introduction to soil physics*, Academic Press, Inc., San Diego, CA.

Hua, Q, Barbetti, M & Rakowski, AZ 2013, 'Atmospheric radiocarbon for the Perdio 1950-201', *Radiocarbon*, vol. 55, no. 4, pp. 2059–2072.

Humfeld, H 1930, 'A method for measuring carbon dioxide evolution from soil', *Soil Science*, vol. 30, iss. 1, pp: 1–12.

Interstate Technology & Regulatory Council (ITRC) 2009, *Evaluating natural source zone depletion at sites with LNAPL*, LNAPL-1, Interstate Technology & Regulatory Council, LNAPLs Team, Washington, USA.

ITRC 2013, *Groundwater statistics and monitoring compliance, statistical tools for the project life cycle*, GSMC-1, Interstate Technology & Regulatory Council, Groundwater Statistics and Monitoring Compliance Team, Washington, USA.

ITRC 2018, *Light non-aqueous phase liquids (LNAPL) document update*, LNAPL-3, Interstate Technology & Regulatory Council, LNAPL Update Team, Washington, USA.

Irianni-Renno, M 2013, *Biogeochemical characterization of a LNAPL body in support of STELA*, thesis in partial fulfillment of the requirements for the Degree of Master of Science. Civil and Environmental Engineering, Colorado State University. Fort Collins, Colorado.

Jassal, RS, Black, TA, Nestic, Z & Gaumont-Guay, D 2012, 'Using automated non-steady-state chamber systems for making continuous long-term measurements of soil CO₂ efflux in forest ecosystems', *Agricultural and Forest Meteorology*, vol. 161, pp. 57–65.

Johnson, P, Lundegard, P & Liu, Z 2006, 'Source zone natural attenuation at petroleum hydrocarbon spill sites – I: site-specific assessment approach', *Groundwater Monitoring & Remediation*, vol. 26, iss. 4, pp. 82–92.

Johnston, CD, Robertson, BS & Bastow, TP 2007, 'Evidence for the success of biosparging LNAPL diesel in the water table zone of a shallow sand aquifer', in *Proceedings of the 6th International Groundwater Quality Conference*, Fremantle, Western Australia, 2–7 December.

Johnston, CD 2010, *Selecting and assessing strategies for remediating LNAPL in soil and aquifers*, CRC CARE Technical report no. 18. CRC for Contamination Assessment and Remediation of the Environment, Adelaide, Australia.

Kaplan, IR, Galperin, Y, Alimi, H, Lee, RP & Lu, ST 1996, 'Patterns of chemical changes during environmental alteration of hydrocarbon fuels', *Groundwater Monitoring & Remediation*, vol. 16, iss. 4, pp. 113–124.

Kostecki, PT & Calabrese, EJ 1989, *Petroleum contaminated soils, volumes 1 through 3*. Lewis Publishers, Inc., Chelsea, MI, USA.

LI-COR Biosciences Inc. 2014, *Testing the limits with the LI-8100A*, available at <www.licor.com/env/newsline/2014/07/testing-the-limits-with-the-li-8100a/>.

LI-COR Biosciences Inc. 2015, *Using the LI-8100A soil gas flux system & the LI-8150 multiplexer*.

Lundegard PD & Johnson, PC 2006, 'Source zone natural attenuation at petroleum hydrocarbon spill sites – II: application to a former oil field', *Groundwater Monitoring & Remediation*, vol. 26, iss. 4, pp. 93–106.

McCoy, K, Zimbron, J, Sale, T & Lyverse, M 2014, 'Measurement of natural losses of LNAPL using CO₂ traps', *Groundwater*, vol. 53, iss. 4, pp. 658–667.

McLaughlan, RG, Merrick, NP & Davis, GB 2006, *Natural attenuation: a scoping review*, CRC CARE Technical Report no. 3. CRC for Contamination Assessment and Remediation of the Environment, Adelaide, Australia.

Millington, RJ & Quirk, JM 1961, 'Permeability of porous solids', *Transaction of the Faraday Society*, vol. 57, pp. 1200–1207.

Molins, S, Mayer, KU, Amos, RT & Bekins, BA 2010, 'Vadose zone attenuation of organic compounds at a crude oil spill site-interactions between biogeochemical reactions and multicomponent gas transport', *Journal of Contaminant Hydrology*, vol. 112, pp. 15–29.

National Research Council (NRC) 1993, *In situ bioremediation – when does it work?* Committee on In Situ Bioremediation, Water Science and Technology Board, Commission on Engineering and Technical Systems, National Academy Press, Washington, USA.

NRC 2000, *Natural attenuation for groundwater remediation*, Committee on Intrinsic Remediation, Water Science and Technology Board, Board on Radioactive Waste Management, Commission on Geosciences, Environment, and Resources, National Academy Press, Washington, USA.

Newell, CJ, Rifai, HS, Wilson, JT, Connor, JA, Aziz, JA & Suarez, MP 2002, *Calculation and use of first-order rate constants for monitored natural attenuation studies*, EPA/540/S-02/500, US Environmental Protection Agency National Risk Management Research Laboratory, Cincinnati, OH, USA.

Ng, GHC, Bekins, BA, Cozzarelli, IM, Baedecker, MF, Bennett, PC & Amos, RT 2014, 'A mass balance approach to investigating geochemical controls on secondary water quality impacts at a crude oil spill site near Bemidji, MN', *Journal of Contaminant Hydrology*, vol. 164, pp. 1–15.

Ng, GHC, Bekins, BA, Cozzarelli, IM, Baedecker, MF, Bennett, PC, Amos, RT & Herkelrath, WN 2015, 'Reactive transport modeling of geochemical controls on secondary water quality impacts at a crude oil spill site near Bemidji, MN', *Water Resour. Res.*, vol. 51, pp. 4156–4183.

Norman, JM, Kucharik, CJ, Gower, ST, Baldocchi, DD, Crill, PM, Rayment, M, Savage, K & Striegl, RG 1997, 'A comparison of six methods for measuring soil-surface carbon dioxide fluxes', *Journal of Geophysical Research*, vol. 102, no. D24, pp. 28, 771–28, 777.

Palala, T 2016, 'Natural source zone depletion rate assessment', *Applied NAPL Science*, review 6.

Peters, KE & Moldowan, JM 1993, *The biomarker guide. Interpreting molecular fossils in petroleum and ancient sediment*, Prentice-Hall Inc., Englewood Cliff, New Jersey.

Pingintha, N, Leclerc, MY, Beasley J PJr, Zhang, G & Senthong, C 2010, 'Assessment of the soil CO₂ gradient method for soil CO₂ efflux measurements: comparison of six models in the calculation of the relative gas diffusion coefficient', *Tellus*, vol. 62B, pp. 47–58.

Revesz, K, Coplen, TB, Baedecker, MJ, Glynn, PD & Hult, M 1995, 'Methane production and consumption monitored by stable h and c isotope ratios at a crude oil spill site, Bemidji, Minnesota', *Applied Geochemistry*, vol. 10, pp. 505–516.

Rochette, P & Angers, DA 1999, 'Soil-surface CO₂ fluxes induced by spring, summer and fall moldboard plowing in a sandy loam', *Journal of Soil Science Society of America*, vol. 63, pp. 621–628.

Rochette, P & Hutchinson, GL 2005, *Measurement of soil respiration in situ: chamber techniques*, Publications from USDA-ARS/UNL Faculty, Paper 1379.

Sale, T, Stockwell, E, Newell, C & Kulkarni, P 2014, *Devices and methods for measuring thermal flux and estimating rate of change of reactive material within a subsurface formation*, US Patent Application 2015/0233773, provisional application no. 61/941,194 filed on February 18, 2014.

Sass, JH, Kennelly, J PJr, Smith, EP & Wendt, WE 1984, *Laboratory line-source methods for the measurement of thermal conductivity of rocks near room temperature*, US Department of the Interior Geological Survey, Open-File Report 84-91.

Sihota, NJ, Singurindy, O & Mayer, KU 2011, 'CO₂-efflux measurements for evaluation source zone natural attenuation rates in a petroleum hydrocarbon aquifer', *Environment, Science and Technology*, vol. 45, pp. 482–488.

Sihota, NJ & Mayer, KU 2012, 'Characterizing vadose zone hydrocarbon biodegradation using carbon dioxide effluxes, isotopes and reactive transport modeling', *Vadose Zone Journal*, vol. 11, no. 4.

Sihota, NJ, Mayer, KU, Toso, MA & Atwater, JF 2013, 'Methane emissions and contaminant degradation rates at sites affected by accidental releases of denatured fuel-grade ethanol', *Journal of Contaminant Hydrology*, vol. 151, pp. 1–15.

Sihota, NJ, Trost, JJ, Bekins, BA, Berg, A, Delind, GN, Mason, B, Warren, E & Mayer, KU 2016, 'Seasonal variability in vadose zone biodegradation at a crude oil pipeline rupture site', *Vadose Zone Journal*, vol. 15, no. 5.

Stockwell, EB 2015, *Continuous NAPL loss rates using subsurface temperatures*, Thesis, Colorado State University, Fort Collins, Colorado.

- Stout, SA & Lundegard, P 1998, 'Intrinsic biodegradation of diesel fuel in an interval of separate phase hydrocarbons', *Applied Geochemistry*, vol. 13, pp. 851–859.
- Stuiver, M & Polach, HA 1977, 'Discussion – reporting of ¹⁴C data', *Radiocarbon*, vol. 19, no. 3, pp. 355–363.
- Sweeney, RE & Ririe, GT 2014, 'Temperature as a tool to evaluate aerobic biodegradation in hydrocarbon contaminated soil', *Groundwater Monitoring & Remediation*, vol. 34, no. 3, pp. 41–50.
- Sweeney, RE & Ririe, GT 2017, 'Small purge method to sample vapor from groundwater monitoring wells screened across the water table', *Groundwater Monitoring & Remediation*, vol. 37, iss. 4.
- Tillman, FD & Smith, JA 2005, *Vapor Transport in the Unsaturated Zone*, John Wiley & Sons, Inc.
- Tracy, MK 2015, *Method comparison for analysis of Inapl natural source zone depletion using CO₂ fluxes*, Thesis in partial fulfillment of the requirements for the Degree of Master of Science, Colorado State University, Fort Collins, Colorado.
- U.S. Air Force Center for Environmental Excellence (AFCEE) 2003, *Final light nonaqueous-phase liquid weathering at various fuel release sites – 2003 update*. Science and Engineering Division, Brooks City-Base, San Antonio, Texas, USA.
- U.S. Environmental Protection Agency (US EPA) 2011, *An approach for evaluating the progress of natural attenuation in groundwater*, Office of Research and Development. Wilson, John T. EPA 600/R-11/204.
- US EPA 2015, *OSWER technical guide for assessing and mitigating the vapor intrusion pathway from subsurface vapor sources to indoor air*, OSWER Publication 9200.2-154. Office of Solid Waste and Emergency Response.
- Van Wijk, WR & de Vries, DA 1963, 'Periodic temperature variations in a homogeneous soil', in Van Wijk WR (ed) *Physics of Plant Environment*.
- Volkman, JK, Alexander, R, Kagi, RI, Rowland, SJ & Sheppard, PN 1984, 'Biodegradation of aromatic hydrocarbons in crude oils from the Barrow Sub-basin of Western Australia', *Organic Geochemistry*, vol. 6, pp. 619–632.
- Wade, MJ 2001, 'Age-dating diesel fuel spills: using the european empirical time-based model in the USA', *Environmental Forensics*, vol. 2, iss. 4, pp. 347–358.
- Warren, E, Sihota, NJ, Hostettler, FD & Bekins, BA 2014, 'Comparison of surficial CO₂ efflux to other measures of subsurface crude oil degradation', *Journal of Contaminant Hydrology*, vol. 164, pp. 275–284.
- Warren, E & Bekins, BA 2015, 'Relating subsurface temperature changes to microbial activity at a crude oil-contaminated site', *Journal of Contaminant Hydrology*, vol. 182, pp. 183–193.
- Warren, E & Bekins, BA 2018, 'Relative contributions of microbial and infrastructure heat to a crude oil-contaminated site', *Journal of Contaminant Hydrology*, vol. 211, pp. 94–103.
- Washington State Department of Ecology 2005, *Guidance on remediation of petroleum-contaminated ground water by natural attenuation*, Publication no. 05-09-091 (version 1.0). Toxics Cleanup Program, Olympia, Washington, USA.

Wealthall, GP, Rivett, MO & Dearden, RA 2010, *Transport and attenuation of dissolved-phase volatile organic compounds (VOCs) in the unsaturated zone*. British Geological Survey Commissioned Report, OR/10/061, Natural Environment Research Council.

Wiedemeier, TH, Rifai, HS, Newell, CJ & Wilson, JT 1999, *Natural attenuation of fuels and chlorinated solvents in the subsurface*, John Wiley & Sons, New York, USA.

Wilson, J, Hers, I & Jourabchi, P 2016, *A simple spreadsheet model to simulate the natural attenuation of residual hydrocarbon NAPL*, NGWA Groundwater Summit, Denver, Colorado, USA, April 25.

Zimbron, J 2017, *Establishment of contaminant degradation rates in soils using temperature gradients, associated methods, systems and devices*, Patent Application Publication No. US 2017/0023539 A1.

APPENDIX A.

Overview of NSZD processes

The microbial communities present in soil and groundwater at light non-aqueous phase liquid (LNAPL) release sites adapt and acclimate as the LNAPL degrades over time. For example, as the more volatile hydrocarbon constituents leave the LNAPL during the early stages of a release, volatilisation rates decrease, and the most significant mass loss mechanism transitions to biodegradation (Chaplin *et al* 2002). The bioactivity in the source zone changes to acclimate to sequentially less thermodynamically favourable conditions (i.e. methane (CH₄) producing), and may ultimately result in methanogenic conditions in zones where electron acceptors are depleted. For the purposes of conceptualisation, it is assumed that a microbial population associated with NSZD of an LNAPL body in a middle- to late-stage (i.e. the LNAPL is stable and largely near residual saturation) stabilises and achieves a pseudo-steady state. The subsequent discussion is based upon this assumption.

Emerging research has recently improved the understanding of the gaseous expression of NSZD processes (Davis *et al* 2005; Amos *et al* 2005; Johnson *et al* 2006; Sihota *et al* 2011; McCoy *et al* 2014). A large advance occurred with respect to the quantification of the gases that are produced from petroleum hydrocarbon biodegradation processes, predominantly methanogenesis. At the Bemidji site in the USA¹, the gaseous expression of NSZD has been shown to account for greater than 70% of the hydrocarbon biodegradation that occurs in the subsurface (Molins *et al* 2010). Within the highly reduced saturated zone and overlying capillary fringe, methanogenesis occurs and generates CH₄. Degassing of excess CH₄ occurs along with the outgassing effects of direct-contact oil biodegradation because of the relatively low solubility of CH₄ (Garg *et al* 2017), CH₄ is subsequently transported up into the vadose zone along with smaller amounts of carbon dioxide (CO₂) and volatile organic compounds (VOCs). Within the vadose zone where they meet atmospherically supplied oxygen (O₂), the CH₄ and VOCs are oxidised to form CO₂ and heat. A new conceptualisation of these vapour transport-related NSZD processes that are occurring at petroleum release sites is shown in figure A-1.

The signatures of NSZD can be exploited to quantify petroleum hydrocarbon mass loss rates. The methods are aligned with the following three ways in which NSZD manifests itself:

- aqueous (dissolved by-product-related)
- gaseous (vapour by-product-related), and
- heat (vapour by-product-related).

¹ Several research sites have been critical to the understanding of NSZD and facilitated application to other petroleum hydrocarbon-impacted sites. Since 1983, significant research has taken place at the USGS Bemidji Crude-Oil Research Project site, near Bemidji, Minnesota, USA (mn.water.usgs.gov/projects/bemidji/index.html). Research concerning NSZD processes began in the early 2000s. At 47°28'25" north latitude (Melbourne is 37°48'49" south latitude), it is situated in a temperate/subarctic climate zone with short warm summers, long cold winters, an annual average daily high temperature of 10 degree Celsius (°C), and an average annual precipitation of 68 cm (en.wikipedia.org/wiki/Bemidji,_Minnesota). The 1,700 m³ crude oil pipeline release occurred in glacial outwash soils consisting of sand and gravel with thin fine sand and silt interbeds.

The total NSZD rate is a summation of the reaction by-products that include both dissolved and vapour changes. The aqueous methods account for the dissolved by-products. The vapour by-products can be accounted using either the gaseous method or the heat method.

It is important to note that NSZD rates are expected to decline as LNAPL source mass is depleted over the multiple decades of time that it will persist in the subsurface (Revesz et al 1995). Biodegradation results in significant changes to the composition of petroleum after its release with the compound types altered in an apparent stepwise depletion of compounds in a specific order, based on their susceptibilities to biodegradation (Volkman et al 1984; Kaplan et al 1996), possibly due to the compounds undergoing biodegradation at different rates. However, there is no published data on the change in NSZD rates at sites over a period greater than 30 years. Recent publications, with data records less than 30 years, suggest that NSZD rates could be zero order (i.e. the same rate year over year) (Garg et al 2017). The practitioner is advised to keep abreast of current research on this.

A.1 – Aqueous manifestations of NSZD

The aqueous manifestations of petroleum hydrocarbon NSZD are well-described in the existing literature (NRC 2000; ITRC 2009; Beck & Mann 2010). Soluble hydrocarbon constituents from the LNAPL dissolve into the groundwater. Upon partitioning into the aqueous phase, the chemical constituents become available for biodegradation. Microbial biodegradation of dissolved petroleum hydrocarbon plumes in groundwater is well-documented (NRC 1993). It can occur through various terminal electron acceptor (TEA) reactions. Decreases in dissolved O_2 , nitrate (NO_3^-), and sulphate (SO_4^{2-}), as well as increases in dissolved iron (Fe^{2+}), manganese (Mn^{2+}), CO_2 , and CH_4 in groundwater downgradient of the source zone, provide evidence of saturated zone biodegradation (NRC 2000). Naturally occurring groundwater hydrogeology and geochemistry often control the electron acceptor supply and the dominant TEA processes. The microbes preferentially use O_2 as an electron acceptor. As O_2 is depleted, the other electron acceptors are used and, when they are consumed, the saturated zone generally proceeds to a methanogenic state in LNAPL source zones.

Figure A-2 presents a general illustration of the aqueous manifestations of NSZD as shown by changes in dissolved TEA and biodegradation by-product concentrations. Groundwater monitoring is used to quantify the changes.

It is important to note that a mixed redox state often exists in the subsurface and saturated zones typically consist of hydraulically mobile and immobile domains (Barcelona *et al* 1989; ITRC 2018). For example, where LNAPL is present in an immobile domain, the redox state will often be methanogenic due to a limited supply of electron acceptors restricted by low groundwater flux. These immobile domains can be bounded by hydraulically mobile domains where electron acceptor supply is ample. In this way, methanogenic and lesser reducing redox zones can be adjacent to each other. Groundwater samples collected from monitoring wells screened across both these zones will often represent a mixed redox state. Therefore, while the presence of dissolved CH_4 concentrations near solubility are a good indicator of

methanogenesis, the presence of lower concentrations does not necessarily mean it is an insignificant biodegradation process.

The aqueous manifestations of NSZD are quantified using traditionally accepted methods for an MNA remedy. When mass budgeting is used (as described in section 3.2.2), this portion of the NSZD measurement is a stoichiometric conversion of the summed total of select TEA consumption and biodegradation by-product formation. This accounts for one part of the total NSZD rate, the dissolved by-products. Section 3 provides more details on these processes, the measurement methods, and the NSZD rate calculation.

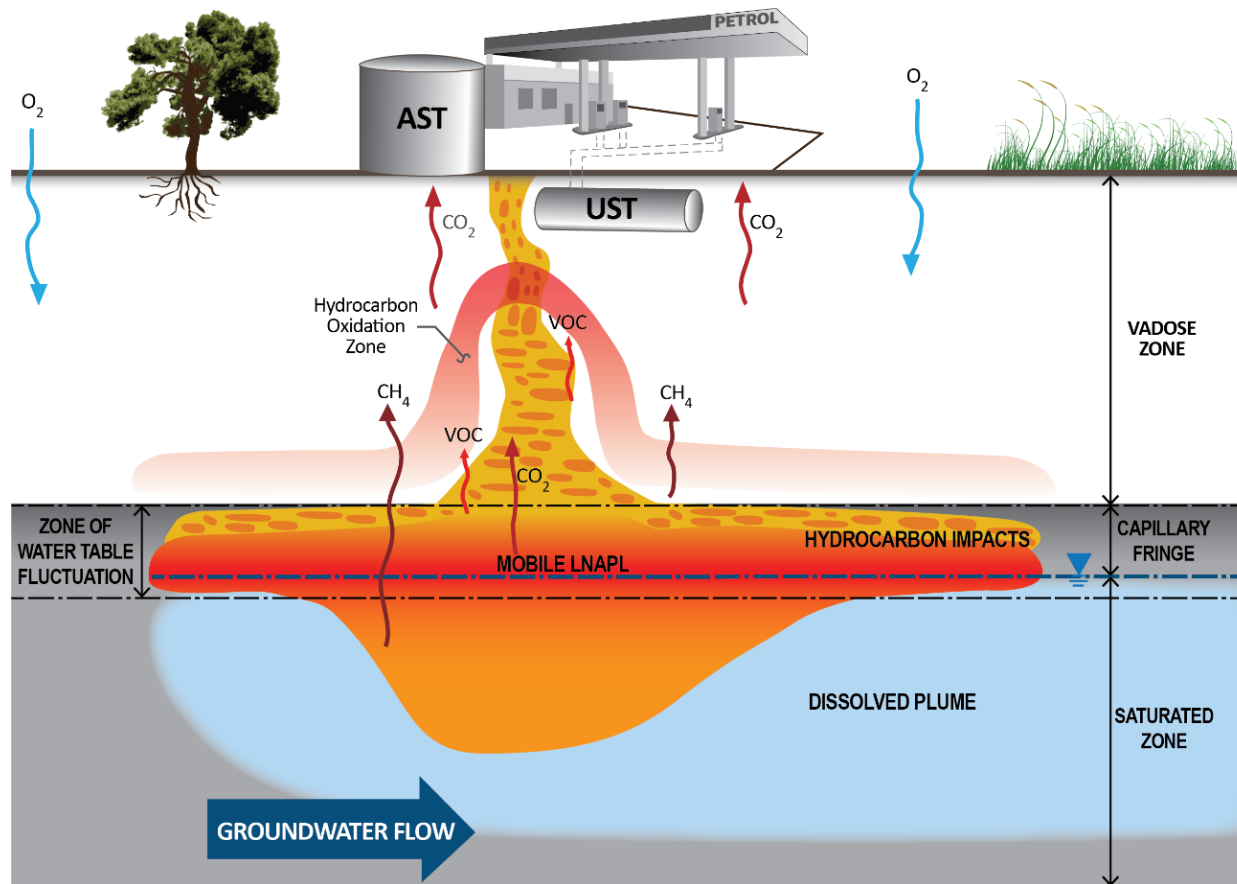
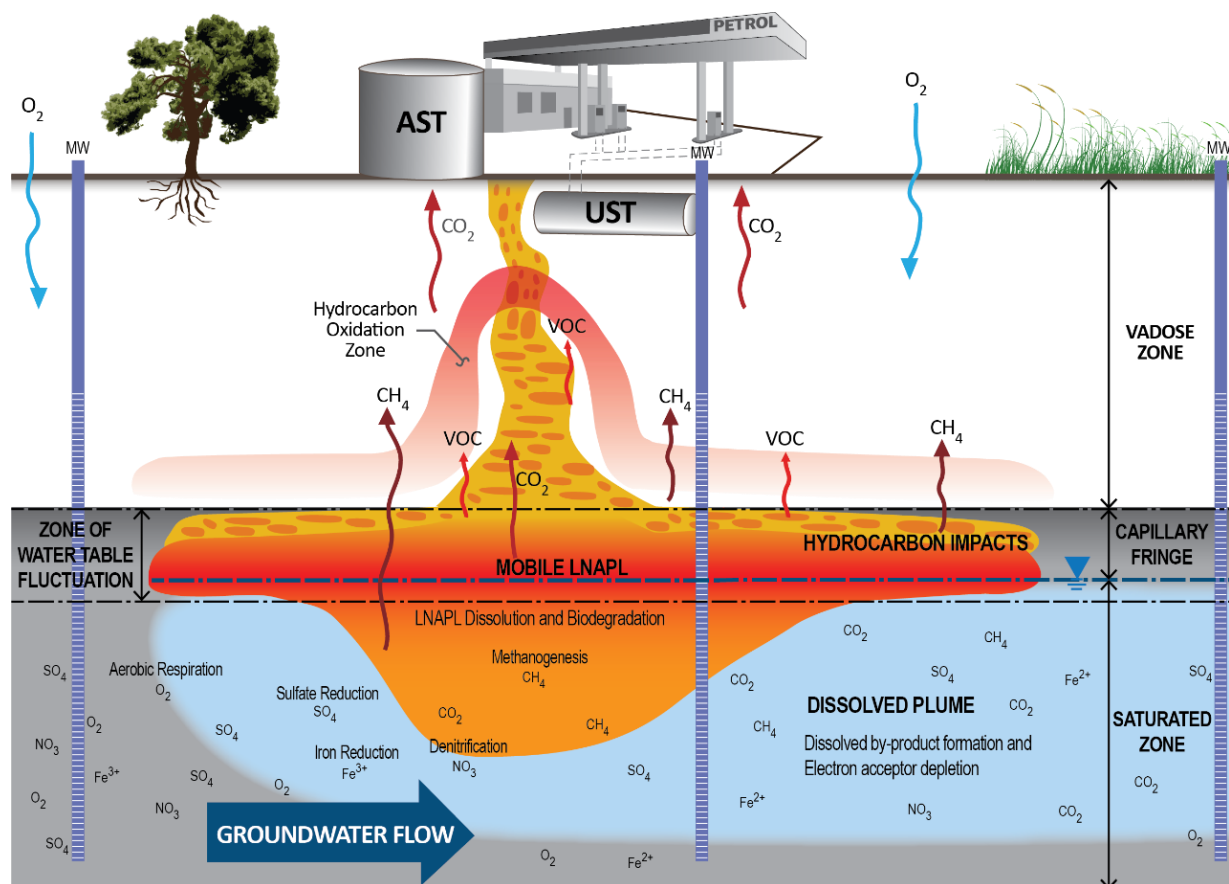


Figure A-1. Comprehensive conceptualisation of petroleum hydrocarbon NSZD processes.²

² This figure represents a typical petroleum hydrocarbon release scenario where LNAPL enters the subsurface from a tank and infiltrates downward until it encounters the water table. The LNAPL expands laterally until the LNAPL can't penetrate the pore entry pressure either vertically or laterally. Over time, NSZD degrades the LNAPL and the resultant LNAPL body includes zones of higher, potentially mobile, LNAPL saturation (red) within the capillary fringe and residual LNAPL (orange). Hydrocarbon impacts present within the vadose zone and top of the capillary fringe are residual and often disconnected (orange with darker orange blebs). Within the saturated zone, both elevated and residual LNAPL is present. A dissolved plume (light blue) forms where chemical constituents leach/solubilise and migrate downgradient with groundwater flow.



NOTE:
This is a conceptual depiction of a typical setting and thereby idealizes conditions. No indication of process magnitude or location are implied.

Figure A-2. Conceptualisation of aqueous manifestations of NSZD.

A.2 – Gaseous manifestations of NSZD

Within the LNAPL-impacted soil, biodegradation occurs and creates gases. Two different types of biodegradation occur, including waterborne and direct-contact. Waterborne biodegradation is dependent upon partitioning of LNAPL constituents into the aqueous phase (i.e. dissolution) where microorganisms degrade them. The by-product gases CH_4 and CO_2 , first enter the aqueous phase, and upon accumulation beyond the solubility limit, degas into gas bubbles that vent into the vadose zone through ebullition. Direct-contact biodegradation occurs in the immediate proximity to the LNAPL, within pores with oil where air-phase porosity is present (e.g. top of LNAPL body). Less is known about this biodegradation process, except that by-product gases are directly outgassed to the vadose zone and do not enter the bulk groundwater. At the U.S. Geological Survey Bemidji Crude Oil Research Site, near Bemidji, Minnesota, USA greater than 80 per cent of the observed carbon efflux may be attributed to direct-contact biodegradation and outgassing (Ng *et al* 2014, 2015).

Figure A-3 presents a conceptualisation of the gaseous manifestations of NSZD, including changes in soil gas concentrations and heat production that occur above and within the hydrocarbon oxidation zone.

Gases are produced in both the saturated and vadose zones where LNAPL biodegradation is occurring. Under anaerobic conditions, methanogenic organisms consume hydrocarbons (e.g. octane, C₈H₁₈) to create CO₂ and CH₄ gases as demonstrated by the summary reaction in equation A.1.



At the Bemidji crude oil research site, a mass balance modelling simulation estimated that approximately 98% of the carbon generated from biodegradation is released as a gas (i.e. CO₂) across the ground surface, while the remaining carbon enters the groundwater (Molins et al 2010). Similarly, at the former Guadalupe oil field in California, USA³, LNAPL mass losses associated with vapour-phase by-products of source zone biodegradation were approximately two orders of magnitude higher than losses associated with dissolved by-products in groundwater (Lundegard & Johnson 2006).

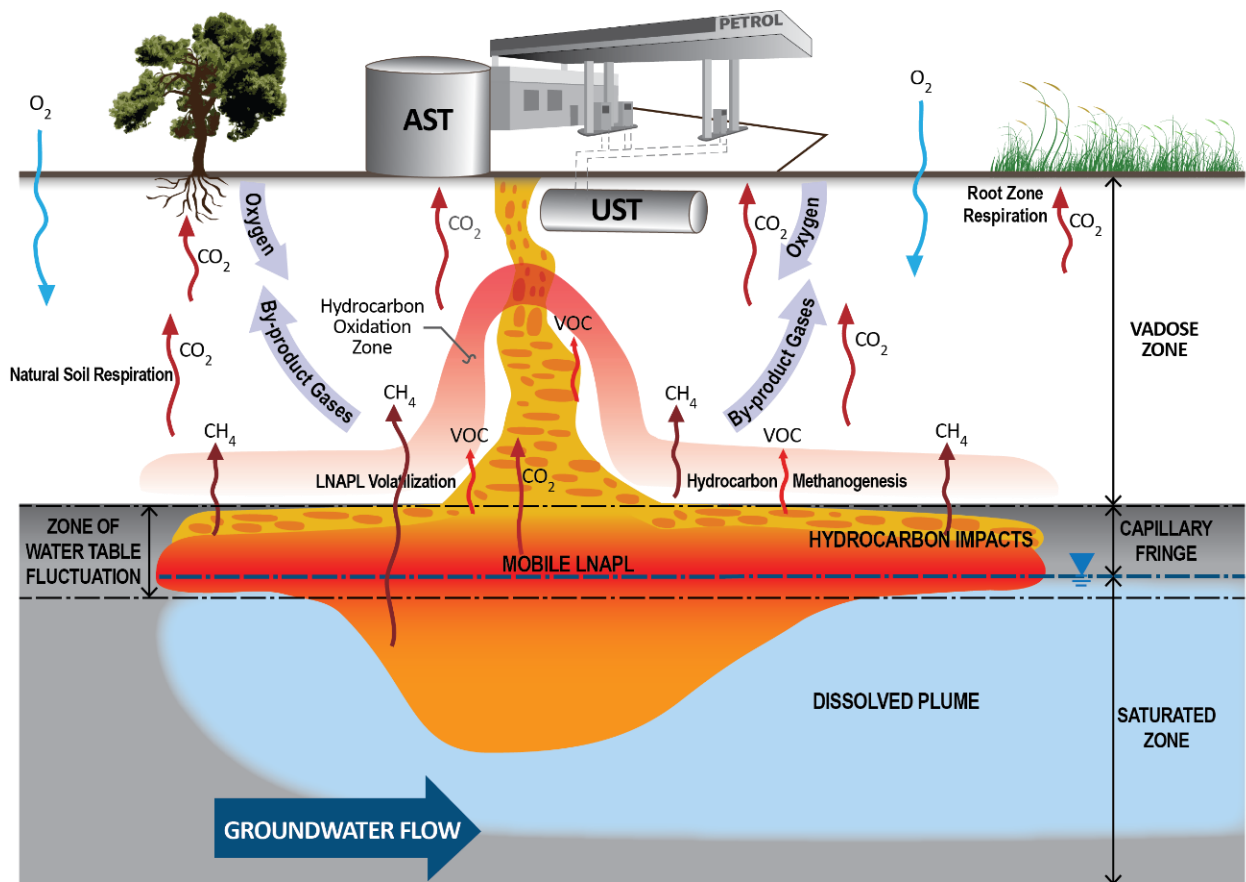
As shown on figure A-3, the key vapour-phase-related petroleum hydrocarbon NSZD processes include the following (API 2017):

- volatilisation of LNAPL and sorbed hydrocarbon constituents
- shallow aerobic biodegradation of volatilised hydrocarbons partitioned into soil moisture
 - production of gaseous CO₂ from hydrocarbon oxidation
- aerobic oxidation of CH₄ derived from saturated, partially saturated, and vadose zone processes
 - production of gaseous CO₂ from CH₄ oxidation

Other non-NSZD sources of CO₂ production and O₂ consumption that need to be accounted for include the following:

- production of CO₂ from respiration of natural organic matter such as peat and humic matter, and
- production of CO₂ from root-zone respiration in shallow soil.

³ Several research sites have been critical to the understanding of NSZD and facilitated application to other petroleum hydrocarbon-impacted sites. Since the 1990s, research on NSZD has been conducted at the Guadalupe Oil Field in California, USA (www.wildlife.ca.gov/OSPR/NRDA/Guadalupe-Oil-Field). At roughly 34°57'56" north latitude (Melbourne is 37°48'49" south latitude), it is situated on the Pacific ocean coast in a warm dry climate zone with warm (not hot) summers, an annual average daily high temperature of 20 °C, and an average annual precipitation of 35 cm (en.wikipedia.org/wiki/Santa_Maria,_California). A reported 45,000 m³ of diluent releases occurred between 1955 to 1990 from the distribution system and impacted the sand dunes. Depths to water range from less than 1 m to approximately 45 m below grade.

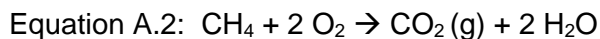


NOTE:
This is a conceptual depiction of a typical setting and thereby idealizes conditions. No indication of process magnitude or location are implied.

Figure A-3. Conceptualisation of gaseous manifestations of NSZD.

The gases generated by NSZD, vented into the vadose zone through ebullition and/or direct outgassing, will be transported upward in the vadose zone by advection and diffusion. Driven by pressure gradients, advection is known to predominate wherever CH₄ generation from anaerobic biodegradation is sufficiently high (US EPA 2015). This condition was verified occurring at the Bemidji crude oil research site at the base of the vadose zone (Amos *et al* 2005). Driven by concentration gradients and limited by the soil air-filled porosity and the gas's effective diffusion coefficient, diffusion will typically result in vertical transport toward the ground surface. Subject to geologic anisotropy, diffusion is the dominant transport mechanism contributing to vertical gas flux; advection found to be predominantly lateral across the oil body (Molins *et al* 2010).

Counter-current to the upward transport of CH₄ and VOCs is the downward transport of O₂ from atmosphere. Where the CH₄ and VOCs meet in the vadose zone, a relatively thin hydrocarbon oxidation zone exists where CO₂ is generated according to equation A.2.



The depth of the oxidation zone is controlled by the magnitude of CH₄ production and limitations of O₂ ingress through the ground surface and shallow soil and the top elevation of the

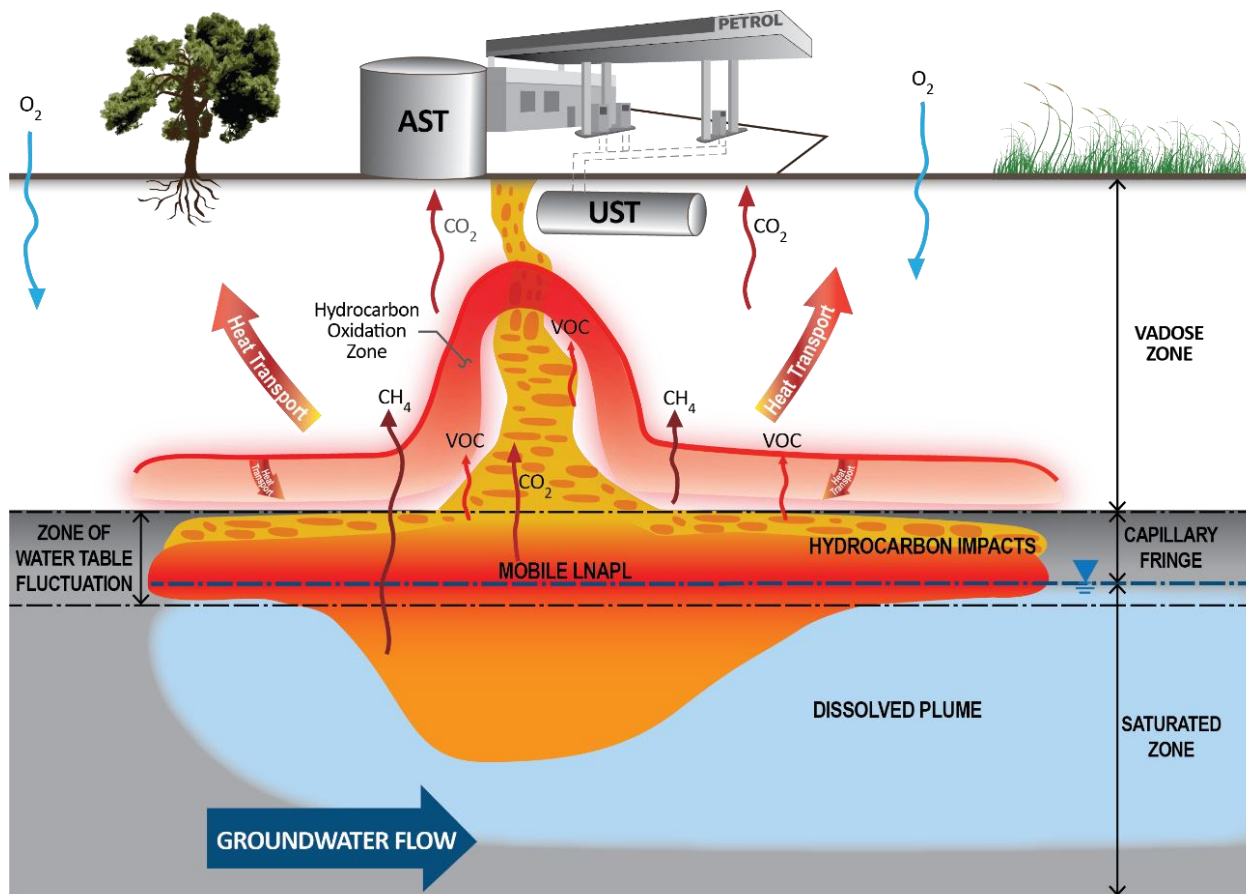
underlying hydrocarbon-impacted soil. Additionally, the depth may fluctuate seasonally due to gas flux variations (Davis *et al* 2005; Irianni-Renno 2013). As shown at the Perth, Western Australia site⁴, the O₂ penetration from the atmosphere into a sandy soil profile above a gasoline body was greatly enhanced in summer (Davis *et al* 2005). As demonstrated in the petroleum vapour intrusion literature (CRC CARE 2013), ground surface efflux is dominated by CO₂ with VOC and CH₄ emissions generally insignificant providing ample O₂ ingress occurs (Sihota *et al* 2016). Section 4 details methods to measure soil gas concentrations and gas flux and calculate NSZD rates.

A.3 – Thermal manifestations of NSZD

Hydrocarbon biodegradation and oxidation reactions are exothermic – they produce energy. Most of this energy is used by microbes to grow and to fuel their metabolism, but some is given off as heat. Under a pseudo-steady-state, microbial growth rates are relatively small, and most of the energy produced is given off as heat to the surrounding soil, as typically observed in a compost pile. The resultant temperature increase in soil is proportional to the NSZD rate, as the heat of these reactions is stoichiometrically related to the extent of biodegradation and subsequent oxidation reactions. Previous laboratory research using calorimeters confirmed that biodegradation reactions generate a stoichiometric amount of heat (for example Braissant *et al* 2010). Figure A-4 presents a conceptualisation of the biogenic heat signature observed at sites where NSZD is occurring.

The interaction of surrounding ambient temperatures, heat released from biodegradation and oxidation, and the heat transfer processes will determine local soil temperatures. The maximum amount of heat generated from biodegradation and oxidation will occur where O₂ is being depleted from the soil gas (i.e. where aerobic reactions are occurring and depleting O₂). This occurs within the hydrocarbon oxidation zone and results primarily (with often smaller contributions from VOC oxidation) from the reaction shown in equation A.2.

⁴ Several research sites have been critical to the understanding of NSZD and facilitated application to other petroleum hydrocarbon-impacted sites. Since the 1990s, research on NSZD has been conducted at a major industrial site in the Perth coastal plain in Western Australia. At roughly 32.15° south latitude (Melbourne is 37°48'49" south latitude), it is situated near the Indian ocean coast in a warm climate zone with hot summers and mild wet winters, an annual average daily high temperature of 25 °C, and an average annual precipitation of 77 cm (en.wikipedia.org/wiki/Perth). Gasoline and diesel releases impacted the calcareous dune sands with occasional limestone nodules and cemented layers. Depths to water range from 3 to 5 m below grade across the site.



NOTE:
This is a conceptual depiction of a typical setting and thereby idealizes conditions. No indication of process magnitude or location are implied.

Figure A-4. Conceptualisation of thermal manifestations of NSZD from biogenic heat.

Less heat will be released if the rate of microbial biodegradation is low (i.e. limited by temperature, nutrients, or other environmental factors). Warren & Bekins (2015) investigated biogenic heat released from NSZD at the Bemidji crude oil research site and found that temperatures above the crude oil body in the unsaturated zone were up to 2.7 degree Celsius (°C) higher than temperatures outside of the LNAPL footprint. Enthalpy calculations and observations demonstrated that the temperature increases primarily resulted from aerobic CH₄ oxidation in the unsaturated zone above the oil. CH₄ oxidation rates at the site independently estimated from ground surface CO₂ efflux data were comparable to rates estimated from the observed temperature increases. Section 5 details methods to measure soil temperatures and calculate NSZD rates.

APPENDIX B.

NSZD rate measurement checklists

This appendix contains checklists useful for practitioners to reference when planning and implementing an NSZD measurement program and useful for auditors and regulators to assess the results and ensure proper measurement and data analysis quality assurance/quality control (QA/QC).

Acknowledging that NSZD measurement programs vary significantly, the checklists specify minimum (“required”) and “optional” requirements for each method discussed within this guidance. It is the responsibility of the user to select and apply the checklists most appropriate to the proposed monitoring program. At the start of the process and following each key decision point, the practitioner is advised to consult the auditor and/or regulator to discuss and agree upon a scope for the NSZD measurements.

The checklists contain a list of minimum planning, field implementation, and data analysis requirements. They include items specifically called out in the guidance text including establishing data objectives, performing field sampling and analysis, and data evaluation including estimating gradients, performing background correction, and QA/QC procedures.

The checklists allow for alternate approaches and provide space for explanations where practitioners either omit or deviate from any of the required steps. Explanations should discuss implications for data use.

The following checklists are included (guidance text section number in parenthesis):

- B.1 – Mass budgeting analysis-based NSZD measurement checklist (section 3.2)
- B.2 – Gradient-based NSZD rate measurement checklist (section 4.3)
- B.3 – Passive flux trap-based NSZD rate measurement checklist (section 4.4)
- B.4 – Dynamic closed chamber-based NSZD rate measurement checklist (section 4.5)
- B.5 – Biogenic heat-based NSZD rate measurement checklist (section 5)
- B.6 – LNAPL compositional change-based NSZD rate measurement checklist (section 6)

B.1 – Mass budgeting analysis-based NSZD measurement checklist

The following is a checklist useful to plan, review, and assess NSZD (NSZD) rate measurements made using the mass budgeting analysis method as described in section 3.2 and appendix C. Acknowledging that NSZD measurement programs vary significantly, the checklists specify minimum (required) and optional requirements. It is the responsibility of the user to consult with the auditor/regulator and select the applicable elements to meet the data use and quality objectives. The checklists allow for alternate approaches and provide space for explanations where practitioners either omit or deviate from any of the required steps. Present explanations to discuss implications or limitations, if any, on data use.

Data quality objectives

Required Optional

- | | | |
|--------------------------|--------------------------|--|
| <input type="checkbox"/> | <input type="checkbox"/> | 1. Have data use and quality objectives been established to properly bound the NSZD monitoring effort and data evaluation? |
| <input type="checkbox"/> | <input type="checkbox"/> | 2. Is the scope of the NSZD monitoring effort consistent with the data objectives? |
| <input type="checkbox"/> | <input type="checkbox"/> | 3. Have the data objectives been achieved? |

Note: The applicability of the following items is contingent upon the scope of the NSZD effort. Items may not be applicable if the scope of the NSZD evaluation is screening-level, for example.

Groundwater sampling and analysis, natural attenuation indicator parameters (NAIP) changes calculation, stoichiometric conversions and NSZD rate calculation

Required Optional

- | | | |
|--------------------------|--------------------------|---|
| <input type="checkbox"/> | <input type="checkbox"/> | 4. Has an appropriate number of monitoring locations been selected for groundwater sampling, adequate to meet the data objectives and represent the potential range of NSZD rates at the site? |
| <input type="checkbox"/> | <input type="checkbox"/> | 5. Has existent information such as the light non-aqueous phase liquid (LNAPL) distribution, local site geology, and hydraulic gradient obtained from site investigations been used to aid in the selection of measurement locations? |
| <input type="checkbox"/> | <input type="checkbox"/> | 6. Do monitoring locations include a minimum of one well in upgradient (background, clean) source and dissolved-phase impacted downgradient areas? |
| <input type="checkbox"/> | <input type="checkbox"/> | 7. Have standard practices been followed for groundwater sampling? |
| <input type="checkbox"/> | <input type="checkbox"/> | 8. Have monitoring wells screened solely across the stratigraphy where the LNAPL smear zone exists, or are demonstrated to provide representative water quality, been utilised to avoid analytical bias? |
| <input type="checkbox"/> | <input type="checkbox"/> | 9. Have seasonal changes in groundwater table and quality water been assessed to determine if multiple rounds of NAIP monitoring are useful to assess seasonal variability? |

- | | | |
|--------------------------|--------------------------|--|
| <input type="checkbox"/> | <input type="checkbox"/> | 10. Have techniques such as polyethylene microfiber filtration, laboratory settling, or passive diffusion bag samplers been used during groundwater sampling to eliminate LNAPL bias and protect sample integrity? |
| <input type="checkbox"/> | <input type="checkbox"/> | 11. Have the recommended NAIPs been analysed following the recommended analytical methods presented in Appendix B? |
| <input type="checkbox"/> | <input type="checkbox"/> | 12. Has the hydrogeochemistry been assessed and the primary mass transfer processes been determined? Have sufficient measures been performed to estimate the phase transfers (i.e. non-advection contributions)? |
| <input type="checkbox"/> | <input type="checkbox"/> | 13. Has the change in concentrations up-gradient and down-gradient for each NAIPs been calculated and a field measurement table been populated? |
| <input type="checkbox"/> | <input type="checkbox"/> | 14. Have the stoichiometric ratios for the chemical of concern (COC) been calculated using the molecular weights of the electron acceptors and by-products and the chemical representation of each transformation process? |
| <input type="checkbox"/> | <input type="checkbox"/> | 15. Has the fundamental equation for mass budgeting presented in Section 3 been used to calculate the NSZD rate? |
| <input type="checkbox"/> | <input type="checkbox"/> | 16. Has the portion of NSZD as measured using aqueous data been added to the NSZD accounted using gaseous or biogenic heat data? |
| <input type="checkbox"/> | <input type="checkbox"/> | 17. Has the standard operating procedure (SOP) presented in Appendix B been followed for mass budgeting analysis? |

Quality assurance/quality control

Required Optional

- | | | |
|--------------------------|--------------------------|--|
| <input type="checkbox"/> | <input type="checkbox"/> | 18. Have measured and computed changes in total inorganic carbon and total alkalinity been compared in order to assess the accuracy of the calculations and validate that aqueous-based NSZD biodegradation is responsible for the loss of petroleum hydrocarbons? |
| <input type="checkbox"/> | <input type="checkbox"/> | 19. Do field and laboratory samples (if applicable) comply with project-specific duplicate sample collection as well as ambient field blanks and equipment blanks? |
| <input type="checkbox"/> | <input type="checkbox"/> | 20. Have all field instruments been calibrated using proper, manufacturer-recommended calibration procedures? |
| <input type="checkbox"/> | <input type="checkbox"/> | 21. Have all field activities been recorded in a field logbook? |

Data evaluation

Required Optional

- | | | |
|--------------------------|--------------------------|--|
| <input type="checkbox"/> | <input type="checkbox"/> | 22. Have an adequate number of monitoring events been performed to meet the data objectives and/or adequately characterise the temporal variability? |
| <input type="checkbox"/> | <input type="checkbox"/> | 23. Has representative stoichiometry been used to calculate a site-specific NSZD rate? |

- 24. Has a sitewide geospatially-averaged NSZD rate been presented?
- 25. Has spatial and/or temporal variability been adequately explained?
- 26. Are the magnitude of the results intuitive and consistent with expectations, published literature, and/or known site conditions?

Explanation of deviations and/or alternative approaches

B.2 – NSZD rate measurement using gradient method checklist

The following is a checklist useful to plan, review, and assess NSZD rate measurements made using the gradient method as described in section 4.3 and appendix D. Acknowledging that NSZD measurement programs vary significantly, the checklists specify minimum (required) and optional requirements. It is the responsibility of the user to consult with the auditor/regulator and select the applicable elements to meet the data use and quality objectives. The checklists allow for alternate approaches and provide space for explanations where practitioners either omit or deviate from any of the required steps. Present explanations to discuss implications or limitations, if any, on data use.

Data quality objectives

Required Optional

- | | | |
|--------------------------|--------------------------|--|
| <input type="checkbox"/> | <input type="checkbox"/> | 1. Have data use and quality objectives been established to properly bound the NSZD monitoring effort and data evaluation? |
| <input type="checkbox"/> | <input type="checkbox"/> | 2. Is the scope of the NSZD monitoring effort consistent with the data objectives? |
| <input type="checkbox"/> | <input type="checkbox"/> | 3. Have the data objectives been achieved? |

Note: The applicability of the following items is contingent upon the scope of the NSZD effort. Items may not be applicable if the scope of the NSZD evaluation is screening-level, for example.

Measuring the soil vapour diffusion coefficient (D_v^{eff}) and the concentration gradient (dC/dz) using nested soil vapour monitoring probes (VMPs)

Required Optional

- | | | |
|--------------------------|--------------------------|---|
| <input type="checkbox"/> | <input type="checkbox"/> | 4. Has an appropriate number of monitoring locations been selected for soil gas concentration profiling, adequate to meet the data objectives and represent the potential range of NSZD rates at the site?? |
| <input type="checkbox"/> | <input type="checkbox"/> | 5. Have soil gas measurements for D_v^{eff} and dC/dz been taken/derived from the aerobic zone above the hydrocarbon-impacted soil? |
| <input type="checkbox"/> | <input type="checkbox"/> | 6. Has the site geology been reviewed to identify the different lithology/unique geologic areas within the aerobic zone? |
| <input type="checkbox"/> | <input type="checkbox"/> | 7. If different lithology within the aerobic zone was identified, has the D_v^{eff} been measured from the different lithology/unique geologic areas within the aerobic zone? |
| <input type="checkbox"/> | <input type="checkbox"/> | 8. Have changes in soil moisture content and weather conditions been considered when scheduling D_v^{eff} measurements? |
| <input type="checkbox"/> | <input type="checkbox"/> | 9. Have site-specific measurements of D_v^{eff} at each multilevel soil gas sample port been completed at the same time of soil gas concentration profile measurement? |
| <input type="checkbox"/> | <input type="checkbox"/> | 10. Has the standard practice CRC CARE 2013 been followed during probe installations and soil gas monitoring? |

11. Has advective flux been verified to be negligible through either pressure or nitrogen (N₂) measurements?

Measuring the concentration gradient using alternate methods: monitoring wells and shallow soil gas sampling

If alternate method/s was/were used to measure the soil gas concentration profile:

Required Optional

12. Has the validity of the/these method/s been previously scrutinised through close inspection of the vadose zone properties (e.g. boring logs, soil samples)?
13. Has the validity of the/these method/s been confirmed with at least one nested vapour monitoring probe installation?

Estimating the concentration gradient

Required Optional

14. Have the upper and lower boundary control points been carefully selected above the hydrocarbon oxidation zone?
15. Have geologic and gas profile shape considerations been taken into account in the selection of the upper and lower boundary control points?

Background correction

Required Optional

16. Have non-petroleum related effects been accounted for by measuring the gas flux in background location/s?
17. Does/do the background location/s have similar subsurface properties as the measurement locations above the light non-aqueous phase liquid (LNAPL) footprint?
18. If multiple distinctly different features were identified in the subsurface across the LNAPL footprint, has the gas flux been measured in multiple background locations to account for non-petroleum effects within each distinctly different feature?
19. Have the non-petroleum related effects been subtracted from the total flux to isolate the gas flux attributed only to NSZD/avoid NSZD rate over-estimation?

Quality assurance/quality control

Required Optional

- | | | | |
|--------------------------|--------------------------|-----|--|
| <input type="checkbox"/> | <input type="checkbox"/> | 20. | Have all field instruments been calibrated using proper, manufacturer-recommended calibration procedures? |
| <input type="checkbox"/> | <input type="checkbox"/> | 21. | Do field and laboratory samples (if applicable) comply with project-specific duplicate sample collection as well as ambient field blanks and equipment blanks? |
| <input type="checkbox"/> | <input type="checkbox"/> | 22. | Have empirical means (e.g. Millington and Quirk (1961) equation) been used to estimate vapour diffusivity for screening-level assessment of NSZD for data quality check? |
| <input type="checkbox"/> | <input type="checkbox"/> | 23. | Have leak detection tests of the soil gas sampling train and sample probes been conducted? |
| <input type="checkbox"/> | <input type="checkbox"/> | 24. | Have all field activities (installation, leak tests, purging, sampling, etc.) been recorded in a field logbook? |

Data evaluation

Required Optional

- | | | | |
|--------------------------|--------------------------|-----|---|
| <input type="checkbox"/> | <input type="checkbox"/> | 25. | Have an adequate number of monitoring events been performed to meet the data objectives and/or adequately characterise the temporal variability? |
| <input type="checkbox"/> | <input type="checkbox"/> | 26. | Do independent estimates of gas flux from O ₂ and CO ₂ soil gas profiles generally confirm each other? If not, has a rational explanation been posed? |
| <input type="checkbox"/> | <input type="checkbox"/> | 27. | Has representative stoichiometry been used to convert the gas flux to a site-specific NSZD rate? |
| <input type="checkbox"/> | <input type="checkbox"/> | 28. | Has a sitewide geospatially-averaged NSZD rate been presented? |
| <input type="checkbox"/> | <input type="checkbox"/> | 29. | Has spatial and/or temporal variability been adequately explained? |
| <input type="checkbox"/> | <input type="checkbox"/> | 30. | Is the magnitude of the results intuitive and consistent with expectations, published literature, and/or known site conditions? |

Explanation of deviations and/or alternative approaches

B.3 – NSZD rate measurement using passive flux trap method checklist

The following is a checklist useful to plan, review, and assess NSZD rate measurements made using the passive flux trap method as described in section 4.4 and appendix E. Acknowledging that NSZD measurement programs vary significantly, the checklists specify minimum (required) and optional requirements. It is the responsibility of the user to consult with the auditor/regulator and select the applicable elements to meet the data use and quality objectives. The checklists allow for alternate approaches and provide space for explanations where practitioners either omit or deviate from any of the required steps. Present explanations to discuss implications or limitations, if any, on data use.

Data quality objectives

Required Optional

- | | | |
|--------------------------|--------------------------|--|
| <input type="checkbox"/> | <input type="checkbox"/> | 1. Have data use and quality objectives been established to properly bound the NSZD monitoring effort and data evaluation? |
| <input type="checkbox"/> | <input type="checkbox"/> | 2. Is the scope of the NSZD monitoring effort consistent with the data objectives? |
| <input type="checkbox"/> | <input type="checkbox"/> | 3. Have the data objectives been achieved? |

Note: The applicability of the following items is contingent upon the scope of the NSZD effort. Items may not be applicable if the scope of the NSZD evaluation is screening-level, for example.

Passive flux traps deployment and retrieval, and laboratory analysis

Required Optional

- | | | |
|--------------------------|--------------------------|---|
| <input type="checkbox"/> | <input type="checkbox"/> | 4. Has an appropriate number of monitoring locations been selected for passive flux analysis, adequate to meet the data objectives and represent the potential range of NSZD rates at the site? |
| <input type="checkbox"/> | <input type="checkbox"/> | 5. Has existent information such as the light non-aqueous phase liquid (LNAPL) distribution, local site geology, and hydraulic gradient obtained from site investigations been used to aid in the selection of measurement locations? |
| <input type="checkbox"/> | <input type="checkbox"/> | 6. Have passive flux traps been located near groundwater monitoring well or soil borings (if available)? |
| <input type="checkbox"/> | <input type="checkbox"/> | 7. Have individual carbon dioxide (CO ₂) traps been assigned to all distinct areas of LNAPL consistency, geologic, and hydraulic characteristics? |
| <input type="checkbox"/> | <input type="checkbox"/> | 8. Have the standard practices E-Flux 2017 been followed during passive flux traps installation/deployment and retrieval? |
| <input type="checkbox"/> | <input type="checkbox"/> | 9. Have impervious areas or areas with highly compacted, low permeability surface soil been avoided (if possible)? |
| <input type="checkbox"/> | <input type="checkbox"/> | 10. Have weather conditions been considered when scheduling flux traps deployment to avoid heavy rainfall events? |
| <input type="checkbox"/> | <input type="checkbox"/> | 11. Have the monitoring locations been cleared from vegetation and large pieces of gravel or cobble before traps installation? |

- | | | |
|--------------------------|--------------------------|--|
| <input type="checkbox"/> | <input type="checkbox"/> | 12. Were installation depths consistent across the site? |
| <input type="checkbox"/> | <input type="checkbox"/> | 13. Has disturbance to the ground surface been avoided or minimised to prevent impacting the efflux conditions prior to installation of the receiver pipe? |
| <input type="checkbox"/> | <input type="checkbox"/> | 14. Has the receiver pipe been installed as close to upright as possible? |
| <input type="checkbox"/> | <input type="checkbox"/> | 15. Have photographs been taken to document the conditions and surrounding environment after completing traps installation? |
| <input type="checkbox"/> | <input type="checkbox"/> | 16. Has deployment period been determined to allow sufficient time, based on the anticipated CO ₂ efflux, to allow for collection of enough CO ₂ to avoid non-detectable measurements? |
| <input type="checkbox"/> | <input type="checkbox"/> | 17. Has deployment period been determined to avoid oversaturation of the sorbent material? |
| <input type="checkbox"/> | <input type="checkbox"/> | 18. If snowfall or vegetation occurred after a receiver pipe was installed, has as much snow/vegetation as possible been removed prior to the data collection? |
| <input type="checkbox"/> | <input type="checkbox"/> | 19. Have the standard practices ASTM D4373-02 and ASTM D6686-12 been followed for flux traps analysis? |

Background correction

Required Optional

- | | | |
|--------------------------|--------------------------|--|
| <input type="checkbox"/> | <input type="checkbox"/> | 20. Have modern carbon contributions been accounted by measuring the unstable carbon isotope composition carbon 14 (¹⁴ C)? |
| <input type="checkbox"/> | <input type="checkbox"/> | 21. Has the standard practice ASTM D6866-16 been followed during ¹⁴ C measurement? |
| <input type="checkbox"/> | <input type="checkbox"/> | 22. Have modern carbon contributions effects been subtracted from the total flux to avoid NSZD rate over-estimation? |
| <input type="checkbox"/> | <input type="checkbox"/> | 23. Have wind speeds been monitored and efflux been corrected for wind effects at sites with excessive winds? |

Quality assurance/quality control

Required Optional

- | | | |
|--------------------------|--------------------------|---|
| <input type="checkbox"/> | <input type="checkbox"/> | 24. Has at least one duplicate trap location per every 10 locations been installed and analysed to evaluate consistency between installation procedures and replication of results? |
| <input type="checkbox"/> | <input type="checkbox"/> | 25. Has/have the duplicate trap/s been placed approximately 0.7 m (metres) from the parent/s location and installed in area/s of similar ground cover? |
| <input type="checkbox"/> | <input type="checkbox"/> | 26. Have statistics, such as the calculation of a relative percent difference (RPD) from the parent and duplicate sample data, been performed to assess data quality? |
| <input type="checkbox"/> | <input type="checkbox"/> | 27. Has a trip blank been provided by the laboratory and analysed along with all the samples for each field event? |

- 28. Have all field instruments been calibrated using proper, manufacturer-recommended calibration procedures?
- 29. Have all field activities been recorded in a field logbook?

Data evaluation

Required Optional

- 30. Have an adequate number of monitoring events been performed to meet the data objectives and/or adequately characterise the temporal variability?
- 31. Has representative stoichiometry been used to convert the gas flux to a site-specific NSZD rate?
- 32. Has a sitewide geospatially-averaged NSZD rate been presented?
- 33. Has spatial and/or temporal variability been adequately explained?
- 34. Are the magnitude of the results intuitive and consistent with expectations, published literature, and/or known site conditions?

Explanation of deviations and/or alternative approaches

B.4 – Dynamic closed chamber-based NSZD rate measurement checklist

The following is a checklist useful to plan, review, and assess NSZD rate measurements made using the dynamic closed chamber (DCC) method as described in section 4.5 and appendix F. Acknowledging that NSZD measurement programs vary significantly, the checklists specify minimum (required) and optional requirements. It is the responsibility of the user to consult with the auditor/regulator and select the applicable elements to meet the data use and quality objectives. The checklists allow for alternate approaches and provide space for explanations where practitioners either omit or deviate from any of the required steps. Present explanations to discuss implications or limitations, if any, on data use.

Data Quality Objectives

Required Optional

- | | | |
|--------------------------|--------------------------|--|
| <input type="checkbox"/> | <input type="checkbox"/> | 1. Have data use and quality objectives been established to properly bound the NSZD monitoring effort and data evaluation? |
| <input type="checkbox"/> | <input type="checkbox"/> | 2. Is the scope of the NSZD monitoring effort consistent with the data objectives? |
| <input type="checkbox"/> | <input type="checkbox"/> | 3. Have the data objectives been achieved? |

Note: The applicability of the following items is contingent upon the scope of the NSZD effort. Items may not be applicable if the scope of the NSZD evaluation is screening-level, for example.

DCC collar installation, soil gas efflux survey and data validation

Required Optional

- | | | |
|--------------------------|--------------------------|---|
| <input type="checkbox"/> | <input type="checkbox"/> | 4. Has an appropriate number of monitoring locations been selected, adequate to meet the data objectives and represent the potential range of NSZD rates at the site? |
| <input type="checkbox"/> | <input type="checkbox"/> | 5. Has existent information such as the light non-aqueous phase liquid (LNAPL) distribution, local site geology, and hydraulic gradient obtained from site investigations been used to aid in the selection of measurement locations? |
| <input type="checkbox"/> | <input type="checkbox"/> | 6. Have DCC collars been located near groundwater monitoring well or soil borings (if available)? |
| <input type="checkbox"/> | <input type="checkbox"/> | 7. Have individual DCC collars been assigned to all distinct areas of LNAPL consistency, geologic, and hydraulic characteristics? |
| <input type="checkbox"/> | <input type="checkbox"/> | 8. Have impervious areas or areas with highly compacted, low permeability surface soil been avoided (if possible)? |
| <input type="checkbox"/> | <input type="checkbox"/> | 9. Have weather conditions been considered when scheduling DCC collars deployment to avoid heavy rainfall events? |
| <input type="checkbox"/> | <input type="checkbox"/> | 10. Have the monitoring locations been cleared from vegetation and large pieces of gravel or cobble before DCC collars installation? |

- | | | |
|--------------------------|--------------------------|--|
| <input type="checkbox"/> | <input type="checkbox"/> | 11. Were DCC collars installation depths consistent across the site? |
| <input type="checkbox"/> | <input type="checkbox"/> | 12. Has disturbance to the ground surface been avoided or minimised to prevent impacting the efflux conditions prior to installation of the DCC collars? |
| <input type="checkbox"/> | <input type="checkbox"/> | 13. Has the DCC collar been installed as close to upright as possible? |
| <input type="checkbox"/> | <input type="checkbox"/> | 14. Has the collar been secured by backfilling around the edges to existing grade and re-compacted to pre-existing conditions using a standard compaction slide hammer? |
| <input type="checkbox"/> | <input type="checkbox"/> | 15. Have photographs been taken to document the conditions and surrounding environment after completing DCC collars installation? |
| <input type="checkbox"/> | <input type="checkbox"/> | 16. Have measurement period and number of measurements been determined to allow for collection of representative soil gas samples? |
| <input type="checkbox"/> | <input type="checkbox"/> | 17. Have a minimum of three sequential total carbon dioxide (CO ₂) efflux measurements been conducted at each location, encompassing a period of approximately five minutes? |
| <input type="checkbox"/> | <input type="checkbox"/> | 18. Has the standard practice CRC CARE 2013 been followed during soil gas monitoring? |
| <input type="checkbox"/> | <input type="checkbox"/> | 19. Have site conditions, including atmospheric and groundwater, that may lead to more or less variability in NSZD rates been assessed and considered? |
| <input type="checkbox"/> | <input type="checkbox"/> | 20. Has the DCC field measurement data been validated following the process in Appendix E? |
| <input type="checkbox"/> | <input type="checkbox"/> | 21. Has diurnal variability been assessed through multiple measurements at various times of day at the same collar (e.g. morning, midday, and evening)? |
| <input type="checkbox"/> | <input type="checkbox"/> | 22. Has the procedure in Appendix E been followed during DCC collars installation, soil gas efflux survey and data validation? |

Background correction

Required Optional

- | | | |
|--------------------------|--------------------------|--|
| <input type="checkbox"/> | <input type="checkbox"/> | 23. Has at least one background location per vegetative ground cover been installed? |
| <input type="checkbox"/> | <input type="checkbox"/> | 24. Has natural soil CO ₂ (modern CO ₂) efflux been accounted and subtracted from the measured total CO ₂ efflux to avoid NSZD rate over-estimation? |
| <input type="checkbox"/> | <input type="checkbox"/> | 25. Have wind speeds been monitored and efflux been corrected for wind effects at sites with excessive winds? |

Quality assurance/quality control

Required Optional

- | | | |
|--------------------------|--------------------------|---|
| <input type="checkbox"/> | <input type="checkbox"/> | 26. Has at least one duplicate collar location per every 10 locations been installed and analysed to evaluate consistency between installation procedures and replication of results? |
|--------------------------|--------------------------|---|

- | | | |
|--------------------------|--------------------------|---|
| <input type="checkbox"/> | <input type="checkbox"/> | 27. Has/have the duplicate location/s been placed approximately 0.3 metres (m) apart from the parent/s location and installed in area/s of similar ground cover? |
| <input type="checkbox"/> | <input type="checkbox"/> | 28. Has/have the duplicate location/s been sampled during the same time of day as the parent/s sample/s location? |
| <input type="checkbox"/> | <input type="checkbox"/> | 29. Have statistics, such as the calculation of a relative percent difference (RPD) from the parent and duplicate sample data, been performed to assess data quality? |
| <input type="checkbox"/> | <input type="checkbox"/> | 30. Has a field blank measurement comprised of 60 readings been collected during each field event? |
| <input type="checkbox"/> | <input type="checkbox"/> | 31. Have all field instruments been calibrated using proper, manufacturer-recommended calibration procedures? |
| <input type="checkbox"/> | <input type="checkbox"/> | 32. Has field calibration of the instrument been conducted to set the instrument to atmospheric conditions encountered in the field? |
| <input type="checkbox"/> | <input type="checkbox"/> | 33. Have all field activities been recorded in a field logbook? |

Data evaluation

Required Optional

- | | | |
|--------------------------|--------------------------|--|
| <input type="checkbox"/> | <input type="checkbox"/> | 34. Have an adequate number of monitoring events been performed to meet the data objectives and/or adequately characterise the temporal variability? |
| <input type="checkbox"/> | <input type="checkbox"/> | 35. Has representative stoichiometry been used to convert the gas flux to a site-specific NSZD rate? |
| <input type="checkbox"/> | <input type="checkbox"/> | 36. Has a sitewide geospatially-averaged NSZD rate been presented? |
| <input type="checkbox"/> | <input type="checkbox"/> | 37. Has spatial and/or temporal variability been adequately explained? |
| <input type="checkbox"/> | <input type="checkbox"/> | 38. Are the magnitude of the results intuitive and consistent with expectations, published literature, and/or known site conditions? |

Explanation of deviations and/or alternative approaches

B.5 – Biogenic heat-based NSZD rate measurement checklist

The following is a checklist useful to plan, review, and assess NSZD rate measurements made using the biogenic heat method as described in section 5 and appendix G. Acknowledging that NSZD measurement programs vary significantly, the checklists specify minimum (required) and optional requirements. It is the responsibility of the user to consult the auditor/regulator and select the applicable elements to meet the data use and quality objectives. The checklists allow for alternate approaches and provide space for explanations where practitioners either omit or deviate from any of the required steps. Present explanations to discuss implications or limitations, if any, on data use.

Data quality objectives

Required Optional

- | | | |
|--------------------------|--------------------------|--|
| <input type="checkbox"/> | <input type="checkbox"/> | 1. Have data use and quality objectives been established to properly bound the NSZD monitoring effort and data evaluation? |
| <input type="checkbox"/> | <input type="checkbox"/> | 2. Is the scope of the NSZD monitoring effort consistent with the data objectives? |
| <input type="checkbox"/> | <input type="checkbox"/> | 3. Have the data objectives been achieved? |

Note: The applicability of the following items is contingent upon the scope of the NSZD effort. Items may not be applicable if the scope of the NSZD evaluation is screening-level, for example.

Soil temperature measurement devices installation, data logging, thermal gradient estimation and NSZD rate calculation

Required Optional

- | | | |
|--------------------------|--------------------------|---|
| <input type="checkbox"/> | <input type="checkbox"/> | 4. Has an appropriate number of monitoring locations been selected, adequate to meet the data objectives and represent the potential range of NSZD rates at the site? |
| <input type="checkbox"/> | <input type="checkbox"/> | 5. Have the vadose-zone properties been inspected and/or a nested soil temperature measurement probe been installed to scrutinise the biogenic heat method validity? |
| <input type="checkbox"/> | <input type="checkbox"/> | 6. Has existent information such as the light non-aqueous phase liquid (LNAPL) distribution, local site geology, and hydraulic gradient obtained from site investigations been used to aid in the selection of measurement locations? |
| <input type="checkbox"/> | <input type="checkbox"/> | 7. Have the site climatology and groundwater temperatures been reviewed to assess the ideal measurement depths? |
| <input type="checkbox"/> | <input type="checkbox"/> | 8. Have the upper and lower boundary control points been carefully selected above the hydrocarbon oxidation zone and based on geologic and temperature profile shape considerations? |
| <input type="checkbox"/> | <input type="checkbox"/> | 9. Has temperature monitoring been performed at least 10 metres (m) away from other heat sources? |
| <input type="checkbox"/> | <input type="checkbox"/> | 10. Have weather conditions been considered when scheduling temperature monitoring to avoid heavy rainfall events/changes in soil moisture? |

- | | | |
|--------------------------|--------------------------|--|
| <input type="checkbox"/> | <input type="checkbox"/> | 11. Have temperature profiles been measured within, above and below the hydrocarbon oxidation zone? |
| <input type="checkbox"/> | <input type="checkbox"/> | 12. Has a volume-weighted average value of thermal conductivity that is representative of all different lithologies within the oxidation zone been used? |
| <input type="checkbox"/> | <input type="checkbox"/> | 13. Has a long-term temperature data logging (e.g. 1-2 years) been performed and a periodic rolling average NSZD rate been calculated using averaged temperatures to assess the drift in rates? |
| <input type="checkbox"/> | <input type="checkbox"/> | 14. Have the procedures in Appendix F been followed for soil temperature measurement devices installation, data logging, soil thermal conductivity measurement, thermal gradient estimation and NSZD rate calculation? |

Background correction

Required Optional

- | | | |
|--------------------------|--------------------------|--|
| <input type="checkbox"/> | <input type="checkbox"/> | 15. Have non-petroleum related effects been accounted by monitoring the temperature profile in background location(s)? |
| <input type="checkbox"/> | <input type="checkbox"/> | 16. Does/do the background location/s have similar subsurface properties as the measurement locations above the LNAPL footprint? |
| <input type="checkbox"/> | <input type="checkbox"/> | 17. If using the mathematical means of background correction, has a careful review of other heat sources in the subsurface thermal monitoring area been performed (e.g. utilities) to minimise the potential for inaccuracies? |
| <input type="checkbox"/> | <input type="checkbox"/> | 18. Have the non-petroleum related effects been accounted and subtracted from the total heat flux to isolate the heat flux attributed only to NSZD and avoid NSZD rate over-estimation? |

Quality assurance/quality control

Required Optional

- | | | |
|--------------------------|--------------------------|---|
| <input type="checkbox"/> | <input type="checkbox"/> | 19. Have all field instruments been calibrated using proper, manufacturer-recommended calibration procedures? |
| <input type="checkbox"/> | <input type="checkbox"/> | 20. Have all field activities been recorded in a field logbook? |

Data evaluation

Required Optional

- | | | |
|--------------------------|--------------------------|--|
| <input type="checkbox"/> | <input type="checkbox"/> | 21. Have an adequate number of monitoring events been performed to meet the data objectives and/or adequately characterise the temporal variability? |
| <input type="checkbox"/> | <input type="checkbox"/> | 22. Has representative stoichiometry been used to estimate the NSZD rate? |
| <input type="checkbox"/> | <input type="checkbox"/> | 23. Has a sitewide geospatially-averaged NSZD rate been presented? |
| <input type="checkbox"/> | <input type="checkbox"/> | 24. Has the biogenic heat method been used at a site with LNAPL in a middle- to late-stage condition? |

- 25. Has spatial and/or temporal variability been adequately explained?
- 26. Are the magnitude of the results intuitive and consistent with expectations, published literature, and/or known site conditions?

Explanation of deviations and/or alternative approaches

B.6 – LNAPL compositional change-based NSZD rate measurement checklist

The following is a checklist useful to plan, review, and assess NSZD rate measurements made using the light non-aqueous phase liquid (LNAPL) compositional change method as described in section 6. Acknowledging that NSZD measurement programs vary significantly, the checklists specify minimum (required) and optional requirements. It is the responsibility of the user to consult with the auditor/regulator and select the applicable elements to meet the data use and quality objectives. The checklists allow for alternate approaches and provide space for explanations where practitioners either omit or deviate from any of the required steps. Present explanations to discuss implications or limitations, if any, on data use.

Data quality objectives

Required Optional

- | | | |
|--------------------------|--------------------------|--|
| <input type="checkbox"/> | <input type="checkbox"/> | 1. Have data use and quality objectives been established to properly bound the NSZD monitoring effort and data evaluation? |
| <input type="checkbox"/> | <input type="checkbox"/> | 2. Is the scope of the NSZD monitoring effort consistent with the data objectives? |
| <input type="checkbox"/> | <input type="checkbox"/> | 3. Have the data objectives been achieved? |

Note: The applicability of the following items is contingent upon the scope of the NSZD effort. Items may not be applicable if the scope of the NSZD evaluation is screening-level, for example.

LNAPL sampling from in-well or soil samples, laboratory analysis, NSZD rate calculation

Required Optional

- | | | |
|--------------------------|--------------------------|--|
| <input type="checkbox"/> | <input type="checkbox"/> | 4. Has an appropriate number of monitoring locations been selected, adequate to meet the data objectives and represent the potential range of NSZD rates at the site? |
| <input type="checkbox"/> | <input type="checkbox"/> | 5. Has existent information such as the LNAPL distribution, local site geology, and hydraulic gradient obtained from site investigations been used to aid in the selection of measurement locations? |
| <input type="checkbox"/> | <input type="checkbox"/> | 6. Have local, regulatory-accepted practices for collection of representative LNAPL and/or soil samples been followed? |
| <input type="checkbox"/> | <input type="checkbox"/> | 7. Has the quantity of sample required for the specified analysis been coordinated with the analytical laboratory, considering the most appropriate analytical method? |
| <input type="checkbox"/> | <input type="checkbox"/> | 8. Has fluid density (ρ_{LNAPL}) and conservative marker been included with the laboratory analysis of the LNAPL? |
| <input type="checkbox"/> | <input type="checkbox"/> | 9. Have the procedures in section 6 been followed for the estimation of NSZD rate using the LNAPL compositional change method? |

Quality assurance/quality control

Required Optional

- | | | |
|--------------------------|--------------------------|--|
| <input type="checkbox"/> | <input type="checkbox"/> | 10. Has a sample of raw material, fresh LNAPL, been collected and analysed to be used as a benchmark for comparison of laboratory results and assessment of constituent degradation? |
| <input type="checkbox"/> | <input type="checkbox"/> | 11. Have duplicate LNAPL and/or soil samples been collected and analysed? |
| <input type="checkbox"/> | <input type="checkbox"/> | 12. Has a trip blank been provided by the laboratory and analysed along with all the samples for each field event? |
| <input type="checkbox"/> | <input type="checkbox"/> | 13. Do laboratory chemical of concern (COC)-specific and conservative marker analytical detection limits meet the project data quality objectives? |
| <input type="checkbox"/> | <input type="checkbox"/> | 14. Have all field instruments been calibrated using proper, manufacturer-recommended calibration procedures? |
| <input type="checkbox"/> | <input type="checkbox"/> | 15. Have all field activities been recorded in a field logbook? |

Data evaluation

Required Optional

- | | | |
|--------------------------|--------------------------|--|
| <input type="checkbox"/> | <input type="checkbox"/> | 16. Have an adequate number of monitoring events been performed to meet the data objectives and/or adequately characterise the temporal variability? |
| <input type="checkbox"/> | <input type="checkbox"/> | 17. Has representative stoichiometry been used to estimate a site-specific NSZD rate? |
| <input type="checkbox"/> | <input type="checkbox"/> | 18. Has a sitewide geospatially-averaged NSZD rate been presented? |
| <input type="checkbox"/> | <input type="checkbox"/> | 19. Has spatial and/or temporal variability been adequately explained? |
| <input type="checkbox"/> | <input type="checkbox"/> | 20. Are the magnitude of the results intuitive and consistent with expectations, published literature, and/or known site conditions? |

Explanation of deviations and/or alternative approaches

APPENDIX C.

Procedures to measure the aqueous portion of NSZD

This appendix contains procedures useful for practitioners to reference when measuring the aqueous portion of the NSZD. The following procedures are included herein:

C.1 – Field procedure for low-flow groundwater sampling

C.2 – Data evaluation procedure and example of the use of dissolved chemical of concern (COC) concentrations

C.3 – Data evaluation procedure and example of the use of geochemical indicators and mass budgeting analysis

C.1 – Field procedure for low-flow groundwater sampling

The information presented in this section was extracted from Puls, RW & Barcelona, MJ 1996, *Low-flow (minimal drawdown) ground-water sampling procedure*, EPA/540/S-95/504. United States Environmental Protection Agency, Office of Research and Development, Office of Solid Waste and Emergency Response.

Purpose and scope

This field procedure presents general guidelines for the collection of groundwater samples from monitoring wells using a low-flow purging and sampling procedure. This method allows for the collection of representative groundwater samples from monitoring wells that can be used to estimate aqueous NSZD (NZSD) rates, while minimising the amount of purge water generated.

Consult operation manuals for specific calibration and operating procedures of individual low-flow sampling equipment.

Equipment and materials

The following materials are required to undertake this procedure:

- Personal protective equipment (PPE)
- Adjustable-rate, positive-displacement pump, submersible, or peristaltic pump
- Water-quality meter able to measure the following parameters:
 - pH, dissolved oxygen (DO), specific conductance (SC) (if SC is not available measure electrical conductivity (EC)), temperature, and oxidation reduction potential (ORP)
- Flow-through cell with watertight ports for each probe, and inlet/outlet port sized to match pump tubing diameter
- Oil water interface probe and fluid level meter
- Carbon dioxide (CO₂) compressed gas cylinders (preferred) or high-pressure air compressor to drive sample pump
- Connection cable for power source generated from car battery
- Generator (if no onsite power supply available)
- Disposable polyethylene tubing of a diameter to match the port on the pump and the inlet/outlet ports of the flow-through cell
- Disposable inline 0.45-micron (µm) filters (preferred, for collection of dissolved analytes) or disposable stericup 0.45-µm filters vacuum hand pump
- Paper towels
- Well construction information
- Bucket or other container with volume measurements and watch with second hand to determine flow rate
- Calculator

- Sample containers
- Shipping supplies (labels, esky, ice)
- Tablet or field data sheets for:
 - Groundwater sampling purge sheet
 - Equipment calibration sheet
 - Daily investigation diary
 - Chain of custody
 - Sample collection form

Decontaminate the groundwater sampling equipment and reusable materials between sampling locations.

Procedures and guidelines

General

For each well to be sampled, record information obtained on well location, well number, site, date, condition, diameter(s), depth, screened interval(s), and the method for disposal of purged water on the groundwater sampling purge sheet and the daily investigation diary.

Begin sampling at the well that is least impacted, based on previous information (if available) or well location, and proceed systematically to wells that are most impacted.

Calibrate instruments according to manufacturer's instructions. For rented equipment, calibration certificates are to be provided by the equipment supplier for each item of equipment. Record the calibration information on the groundwater equipment calibration sheet.

Clean and decontaminate all sampling equipment and any other equipment to be placed in the well before sampling.

Setup and purging

Inspect the well gatic or monument, lock, and locking cap for evidence of tampering or damage. Record these observations in the daily investigation diary.

Standing up-wind of the well, unlock the cap and carefully open the well. Monitor the well headspace for the presence of volatile compounds using a photoionisation detector (PID) and record the readings on the groundwater sampling purge sheet. If the organic vapour concentration is equal or greater than that noted in the site specific Environmental Health and Safety Plan, immediately recap the well and inform the Field Team Leader or Project Manager. Note additional PPE is required for sampling high organic vapour concentration wells.

Check for the presence of light non-aqueous phase liquids (LNAPL) with the interface probe.

Measure the standing water and LNAPL level and record in the groundwater sampling purge sheet.

Measure the total depth of the bore and record in the groundwater sampling purge sheet. The well may have filled with fine materials (e.g. silt or sand). Therefore, it is important to confirm that the well does not require re-development and if sampling can proceed.

The volume of water in the well bore is calculated as follows:

Bore Volume = casing volume + filterpack volume

$$\text{Bore Volume} = \frac{\pi h_1 d_2^2}{4} + n \left(\frac{\pi h_1 d_1^2}{4} - \frac{\pi h_2 d_2^2}{4} \right)$$

where π is a constant (3.14159), n is the porosity (0.3 for most filter pack material), h_1 is the height of water column from base of well (m), d_1 is diameter of annulus (m), h_2 is the length of filter pack (m), and d_2 is the diameter of casing (m).

Set up pump control unit, pump, tubing, flow cell, pump drive (CO₂ gas cylinder kit, compressor, or battery), and water quality meter in accordance with the manufacturer's instructions.

Attach and secure the polyethylene tubing and stainless steel line to the low-flow pump and slowly lower the pump into the well to the desired depth. Sit the pump inlet near the middle of the well screen unless a specific screen interval depth is desired, this will be site specific⁵. At a minimum, position the pump intake at least 0.5 m above the bottom of the well to avoid mobilisation of any sediment present. Record the depth to the pump intake from ground level and top of casing in the groundwater sampling purge sheet.

If there is less than 200 millimetres (mm) of available water, completely purge the groundwater well and sample it using a peristaltic pump or a bottom loading bailer.

Measure the water level in the well after pump insertion. Leave the water level probe in the well to facilitate continued water level monitoring during purging activities.

Insert the water quality probes into the flow-through cell. Attach the tubing from the pump to the flow-through cell inlet. Attach the discharge tubing to discharge part of the flow-through cell. The purged groundwater is directed through the cell, allowing measurements to be collected before the water contacts the atmosphere.

If using a generator, locate it 10 m downwind from the well to avoid exhaust fumes contaminating the samples.

Start purging the well at a low flow rate at approximately 0.2 litres (L) per minute (L/min), avoid surging. The initial field parameters of pH, SC/EC, DO, ORP, turbidity, and temperature of water are measured and recorded in the groundwater sampling purge sheet.

⁵ Review each well log to evaluate for potential groundwater bearing horizons present within a section of the screen interval, and subsequently locate the low-flow pump inlet accordingly. In this way, pumping will capture water from the more transmissive groundwater bearing horizons within the well screen, helping to minimise the potential for mixing.

Monitor the water level during purging, and, ideally, balance the purge rate and the well recharge rate so that there is little or no drawdown in the well. The goal for water level drawdown is:

- Where the static water level is higher than the screened area of the well - less than 0.3 m, up to a maximum of 5% of the static water column. The water level should stabilise for the specific purge rate.
- Where the static water level is within the screened area of the well - less than 0.1 m (in accordance with recommendations outlined by Puls & Barcelona 1996).

Record adjustments in the purge rate and changes in depth to water in the groundwater sampling purge sheet. Decrease the purge rates, if needed, to the minimum capabilities of the pump to avoid exceeding the maximum water level drawdown. Consider de-watering the well and sampling after the well has recovered when purging rate is less than 0.1 L/min.

Note any odours, chemical sheens, colour, bubbles, turbidity etc. in the comments column.

During purging, measure the field parameters frequently (every 3 to 5 minutes or every 0.5 to 1.0 L purged) until the parameters have stabilised. Base the time interval for the readings on the volume and purge rate. Field parameters are considered stabilised when three consecutive measurements meet the following criteria:

- DO: within 10%
- pH: within 0.05 pH units
- SC / EC: within 3%
- ORP: within 10 millivolts (mV)
- Temperature: 0.2 degrees Celsius (oC)
- Turbidity: <10 nephelometric turbidity units (NTU) or within 10%

Sampling

Once purging is completed, the well is ready to be sampled. Minimise the elapsed time between the completion of purging and the collection of the groundwater sample from the well. Typically, the sample is collected immediately after the well is purged; however, this may also be dependent on well recovery.

After disconnection from the flow-through cell, collect samples directly from the discharge tubing into the appropriate sample bottles. During sample collection, reduce the pump discharge flow rate to create a laminar flow (to minimise loss of volatile organic compounds (VOCs)). Collect samples for VOC analysis first followed by semi volatile organic compound (SVOCs), inorganics and finally physical parameters. Fill VOC sample bottles to the top leaving no headspace. After capping the VOC sample bottle, invert the bottle to check for visible air bubbles. If air bubbles are present, either add additional groundwater sample to the sample or collect another sample. Samples for dissolved analyte analysis (e.g. metals) may be filtered in the field using inline disposable in-line filters (0.45 µm filter), connected to the end of the sample tubing. If a bailer is used, filtration may be completed using a polyethylene syringe connected to an inline filter or stericup.

Record the following information, at a minimum, in a Chain of Custody Form or sample collection form prior to sample collection: site name, location, project number; sample ID/number; depth, sample type/matrix; time/date; analyses and sampler's identity.

Groundwater sampling purge sheet

Client: _____ Project number: _____ Date: _____
 Location: _____ Well ID: _____
 Field Team: _____ PID: _____
 Field equipment calibrated: _____
 SWL measuring point (please circle): TOC / NS TOC – top of casing, NS – natural surface

Purging information

Start Ttime: _____ End time: _____
 Start SWL (mbtoc): _____ In-well LNAPL?: _____ Thickness: _____
 Depth of well (mbtoc): _____ **NB: Do not sample if in-well LNAPL is present**
 Depth to pump intake (mbtoc): _____ (set to approx. middle of well screen or middle of water column if well screen is not fully saturated)
 Pump model: _____
 Approx. purging rate (L/min): _____ SWL stabilised before commence pumping? Yes / No

Bore volume calculation:	Top of filter pack (mbtoc):	Drilling diameter (m):
	Bore casing diameter (m):	Bore volume (L):

Please enter correct units for ORP/Eh, EC and DO from water quality meter

Time	SWL (mbtoc)	Drawdown (m)	Cumulative volume purged (L)	Pump rate (L/min)	Temp (°C)	pH (units)	ORP / Eh _____	SC/EC _____	DO _____	Comments (colour, sheen, odour, turbidity etc.)
Stabilised parameters? Yes/No					± 0.2	± 0.05	± 10 mV	± 3%	± 10%	

Continue purging until a minimum of three stabilised measurements are achieved

Sampling information

Start time: _____

Sample no. _____

End time: _____

No. sample bottles: _____

SWL at completion of sampling (mbtoc): _____

QA/QC sample taken? Y / N Sample ID: _____

Please enter correct units for ORP/Eh, EC and DO from water quality meter

Time	SWL (mbtoc)	Drawdown (m)	Volume purged (L)	Pump Rate (L/min)	Temp (°C)	pH (units)	ORP / Eh	EC	DO	Comments (colour, odour, turbidity etc)

Sample filtered: Yes / No

Filter Size: 0.45 µm / 0.1 µm

Weather conditions: _____

Location of purged water: _____

Final SWL (mbtoc): _____

Purged by: _____

Signature: _____

Date: _____

Sampled by: _____

Signature: _____

Date: _____

Checked by: _____

Signature: _____

Date: _____

C.2 – Data evaluation procedure and example of the use of dissolved COC concentrations

Purpose and scope

This data evaluation procedure presents general guidelines for the chemical-specific aqueous NSZD rate measurement using dissolved COC concentration measurements over time as described in section 3.1 of the main body of the guidance text. Data provided by samples collected from monitoring wells using the low flow sampling method can be used to estimate the chemical-specific, aqueous-phase decay rate by trending COC concentrations over time and conducting subsequent statistical analysis.

Prerequisites

It is assumed that the following prerequisites have been met prior to use of this procedure:

- An appropriate number of monitoring locations was selected for groundwater sampling, adequate to meet the data objectives and represent the potential range of NSZD rates at the site.
- Data from at least six monitoring events over a period of at least three years is needed to calculate a rate constant that is statistically significant.

Procedures and guidelines

Use of the dissolved COC concentrations to estimate the rate of NSZD involves the following steps:

1. Groundwater sampling and analysis
2. Data analysis
 - a) Express the sample dates as decimal years
 - b) Calculate natural logarithms
 - c) Run the regression
 - d) Examine the results
3. Calculate the chemical-specific, aqueous NSZD rate

The following sections detail how to accomplish each step.

Groundwater sampling and analysis

Select the COC(s) based on a review of the light non-aqueous phase liquid (LNAPL) conceptual site model (LCSM) and data objectives. Conduct groundwater sampling following the procedures in appendix C.1. Populate a table with data collected from a single well: sample dates and concentrations of the key COC measured.

Data analysis

Perform the following calculations to prepare the data for the NSZD rate estimate.

Express the sample dates as decimal years

Enter the raw data into an Excel spreadsheet. Insert the sampling dates in a column (e.g. column A). Be sure that the cells are formatted as a date. Copy the dates column (column A) to a new column (e.g. column B). Format this new column to express dates as whole numbers. Use the data in this new column (column B) to create a third column (e.g. column C), which will contain the dates expressed as decimal years. Data in column C is calculated as =1900+X/365.25, where 'X' is the date expressed as number in column B. The value of 1900 is used in this equation because Excel considers January 1 1900 as day one in their whole number format.

Calculate natural logarithms

Enter the reported values for the concentrations of the COC in a consistent unit of measure (e.g. micrograms per litre). Format the cells as a number. In a new column insert a formula =LN(Y) to calculate the natural logarithm of the value in the adjacent cell. Y is the value in the cell that contains the concentration value.

Run the regression

To run the regression function, it is necessary to have the Analysis ToolPak-VBA loaded into Excel. In the spreadsheet, go to 'File' in the upper left corner, select 'Options' and go to 'Add-ins'. If the Analysis Toolpak-VBA is not already listed as an Active Application, then click the Manage drop down menu and select 'Excel add-ins' and click Go. Check the box for Analysis ToolPak-VBA, and click OK. Once the Analysis ToolPak-VBA is loaded, go to 'Data', click on 'Data analysis' in the upper right, and then select the option 'Regression'.

Insert natural logarithm of concentration values in field 'Input Y range' and the decimal years in field 'Input X range'. Input the desired confidence interval (CI), select all the 'Residuals' and 'Normal probability' boxes, enter a filename for the new worksheet, and then click OK. The spreadsheet calculates the regression and presents output in a new tab in the spreadsheet.

Examine the results

The point decay rate (k_{point} , g/m³/yr) is the negative of the slope or gradient of the regression equation, called out as the X Variable 1 Coefficient in the Excel Data Analysis output (presented in the new tab as described above). This equation is shown in the text, section 3.1, equation 3 and is restated here:

$$\text{Equation 3: } k_{point} = \left(\frac{\ln(C) - \ln(C_0)}{t - t_0} \right)$$

where C and C₀ are the current and initial COC concentrations (g_{COC}/m³), respectively, and t and t₀ are the current and initial time (yr), respectively.

The regression function also provides the upper and lower decay rates for the chosen CI probability and the Upper 95% and Lower 95% decay rate (default).

Estimate the NSZD rate

Once the decay rate is estimated, the COC-specific, aqueous NSZD rate can be estimated using equation 4, section 3.1 in the text and restated here:

$$\text{Equatio 4: } R_{COC-aq} = -k_{point} * \theta_w * h_{gw}$$

where $R_{\text{COC-aq}}$ is the chemical-specific NSZD rate ($\text{g}_{\text{COC}}/\text{m}^2/\text{yr}$), Θ_w is water-filled porosity (m^3/m^3), and h_{gw} is the saturated thickness of the plume (m^3/m^2).

Example calculations

A case study with example calculations is presented in this section to illustrate how this guidance can be used to estimate COC-specific, aqueous NSZD rates using dissolved COC concentrations. It is based on a real setting where NSZD monitoring was performed. This section contains brief site background information, the raw groundwater monitoring data and a walk-through of the calculations.

Site background

Groundwater monitoring for benzene was performed immediately downgradient of a residual LNAPL (gasoline/diesel mix) body in monitoring well MW-08C at a shallow water table site comprised of sands and gravels. Natural attenuation was selected as the preferred remedy for the residual LNAPL that could not be excavated. The regulatory agency required semi-annual and, more recently, annual monitoring to track the rate of benzene degradation.

Calculations

1. Groundwater sampling was conducted following the procedures in appendix C.1. The low-flow groundwater sampling and laboratory analysis was comprised of nine groundwater monitoring events between June 2012 and September 2017 (see table C.2-1). Groundwater samples were analysed for benzene. An Excel data table was prepared containing the sample dates and benzene concentrations.

Table C.2-1. MW-08C monitoring dates, benzene concentrations and natural logarithms

Date	Date number	Date decimal Year	Benzene $\mu\text{g}/\text{L}$	Natural logarithm benzene
26/6/2012	41086	2012.6	39.4	3.67
18/9/2012	41170	2012.8	62.2	4.13
29/7/2013	41484	2013.7	69.6	4.24
16/9/2013	41533	2013.8	65.8	4.19
24/7/2014	41844	2014.6	23.7	3.17
24/6/2015	42179	2015.6	36.4	3.60
30/9/2015	42277	2015.8	46.0	3.83
15/9/2016	42628	2016.8	43.4	3.77
23/9/2017	43001	2017.8	36.3	3.59

2. Sample dates were then expressed as decimal years using the formula $1900+X/365.25$, where 'X' is the date expressed as number. These were the values for X in the Excel data analysis add-in tool (Analysis ToolPak-VBA).
3. Natural logarithms (LN) of the benzene concentrations were then calculated. These were the values used for Y in the Excel data analysis add-in tool.

4. An Excel spreadsheet was used to run the Regression function in the Data Analysis add-in. The values of the natural logarithms were used for 'Input Y Range' and the decimal years for 'Input X Range'. The CI selected was 95% (default).
5. The estimated point decay rate was -0.076 /year. The Upper 95% decay rate was 0.081/year and the Lower 95% decay rate was -0.23 /year.
6. Equation 3.2 was used to estimate the 95% CI range of aqueous benzene NSZD rates assuming Θ_w is 0.35 and h_{gw} is 2.78 m.

$$R_{COC-aq} = k_{point} * \theta_w * h_{gw}$$

Upper 95%: R_{COC-aq} = positive rate, increasing trend in benzene, NSZD assumed zero

Mean: $R_{COC-aq} = -(-0.076) * 0.35 * 2.78 = 0.074 \text{ g/m}^2/\text{yr}$

Lower 95%: $R_{COC-aq} = -(-0.23) * 0.35 * 2.78 = 0.22 \text{ g/m}^2/\text{yr}$

The range of estimated aqueous benzene NSZD rates at monitoring well MW-08C is between zero and 0.22 g/m²/yr, with a mean estimate of 0.074 g/m²/yr. In a typical scenario, benzene NSZD rates at various monitoring well locations across the site would be statistically evaluated to estimate a sitewide average for groundwater.

Quality assurance/quality control

Appropriate QA/QC measures are essential to assess the accuracy and precision of the data collected. Use proper, manufacturer-recommended calibration procedures for all field instruments. A minimum two-point calibration is typically prudent with a span calibrated to the range of expected concentrations. Field and laboratory samples should comply with project-specific duplicate sample collection, as well as field equipment blanks.

C.3 – Data evaluation procedure and example of the use of geochemical indicators and mass budgeting analysis

Purpose and scope

This data evaluation procedure presents general guidelines for aqueous NSZD rate measurement using geochemical indicators and a mass budgeting analysis method as described in section 3.2 of this guidance text.

Prerequisites

It is assumed that the following prerequisites have been met prior to use of this procedure:

- An appropriate number of monitoring locations was selected for groundwater sampling, adequate to meet the data objectives and represent the potential range of NSZD rates at the site.
- Ensure monitoring locations include a minimum of one well in background (can be upgradient or sidegradient), source, and dissolved-phase chemical of concern (COC) impacted downgradient areas.
- The recommended natural attenuation indicator parameters (NAIPs) and laboratory analyses are presented in table C.3-1, together with the recommended analytical method. Field methods (e.g. Hach & Chemetrics) are available may be substituted for select parameters.

Table C.1-1. Example of natural attenuation indicator parameter analytical plan

Analyte	Laboratory method reference
Dissolved ferrous iron (Fe^{2+})	APHA 3500
Alkalinity, total (as CaCO_3)	APHA 2320
Dissolved methane (CH_4)	RSK 175
Dissolved carbon dioxide (CO_2)	APHA 4500
Nitrate/nitrite (NO_3^- as N)	APHA 4500
Sulphate (SO_4^{2-})/sulphide (S^{2-})	APHA 4500

Procedures and guidelines

Use of geochemical indicators and mass budgeting analysis to estimate the rate of NSZD involves the following steps:

1. Conduct groundwater sampling and analysis
2. Calculate the changes in NAIPs
3. Perform stoichiometric conversions and calculate the assimilative capacity (AC)
4. Calculate the NSZD rate

The following sections detail how to accomplish each step.

Conduct groundwater sampling and analysis

Conduct groundwater sampling from monitoring wells located in background, source, and dissolved-phase COC impacted downgradient areas following the procedure presented in appendix C.1.

Constituents to be measured include COC and NAIPs, including CO₂ and alkalinity (as calcium carbonate (CaCO₃)). The recommended NAIPs to be sampled and analysed, and the corresponding analytical methods are listed in table C.3-1.

Calculate the changes in NAIPs

Calculate the change in NAIP concentrations from up-gradient locations to source and/or impacted down-gradient locations for each constituent and prepare a field and analytical measurements table. See tables C.3-2 through C.3-4.

Perform stoichiometric conversions and calculate the assimilative capacity

Select an appropriate representative hydrocarbon (or COC) remaining in the LNAPL (e.g. octane or decane). Using the molecular formula for it, calculate the stoichiometric ratios using the molecular weights of the electron acceptors and by-products and the chemical representation of each transformation process. See tables C.3-5 through C.3-9 that use octane (C₈H₁₈) as the representative petroleum hydrocarbon.

Multiply stoichiometric ratios with the observed changes in the electron acceptors and by-products to compute the AC and the total inorganic carbon (CO₂) and alkalinity production. See tables C.3-10 through C.3-12.

Calculate the NSZD rate

Use the fundamental equation for mass budgeting (equation 5) to calculate the NSZD rate:

$$\text{Equation 5: } R_{aq} = V_D(AC)(YZ)$$

where R_{aq} is the aqueous COC NSZD rate (grams per day (g/d)), V_D is the Darcy velocity of groundwater flow (metre per day (m/d), also known as the specific discharge), AC is the assimilative capacity of the all biotransformation processes combined (g/m³), and YZ is the area perpendicular to groundwater flow (m²).

Calculate the specific discharge (or seepage velocity) V_D using Darcy's Law simplified equation divided by the effective porosity:

$$V_D = \frac{K \times i}{n}$$

where K is the average hydraulic conductivity of the plume (m/d), i is the hydraulic gradient (m/m), n is the effective porosity (unitless), and YZ is the area perpendicular to groundwater flow (m²)

The aqueous NSZD rate (g/d) can be divided by the density of the LNAPL (g/L) to express the NSZD rate in volume per time (L/d).

Compare the computed changes in total inorganic carbon (CO₂) and total alkalinity with the changes observed in field measurements to confirm the assumption made that biodegradation is primarily responsible for the loss of the COC.

Example calculations

A case study with example calculations is presented in this section to illustrate how to apply this guidance for NSZD rate measurement using the geochemical indicators and mass budgeting analysis method. It is based on a real setting where NSZD monitoring was performed. This section contains brief site background information, the raw groundwater monitoring data and a walk-through of the calculations.

Site background

Groundwater monitoring for NAIPs was performed within the vicinity of a residual LNAPL (gasoline/diesel/jet fuel mix) body at an unconfined water table aquifer site comprised of sandy silts and silty sands. An evaluation was performed to screen natural attenuation as a potential component of the remedy for site. NAIPs were monitored in groundwater and a mass budgeting analysis was performed to support the evaluation.

Groundwater sampling and analysis

Eleven groundwater monitoring wells were sampled and analysed (see figure C.3-1). Three background monitoring wells were located upgradient/sidegradient, five wells were located within the COC plume (inclusive of the LNAPL source footprint) and three monitoring wells were located on the downgradient edge of the plume (outside the LNAPL footprint). The average concentrations of each of the NAIPs analysed in the background, in the source zone and in the downgradient edge are presented in table C.3-2.

Changes in NAIPs calculations

The average concentrations found at source and downgradient plume edge wells were used for the evaluation of three different scenarios to estimate a plausible range of aqueous NSZD rates:

- A. Values that give the maximum AC (upper-end AC values). These are the minimum concentrations of the NAIPs that are consumed when biodegradation occurs (including dissolved oxygen (DO), NO_3^- , SO_4^{2-}) and the maximum concentration of the NAIPs that are produced when biodegradation occurs (CH_4 , Fe^{2+} , CO_2 and alkalinity) in either the source or downgradient plume edge locations.
- B. Values that give a mean AC (mean AC values). These are the average concentrations of each NAIP at the source and downgradient plume edge locations.
- C. Values that give the minimum AC (lower-end AC values). These are the maximum concentrations of the NAIPs that are consumed when biodegradation occurs (DO, NO_3^- , SO_4^{2-}) and the minimum concentration of the NAIPs that are produced when biodegradation occurs (CH_4 , Fe^{2+} , CO_2 and alkalinity) in either the source or downgradient plume edge locations.

The upper-end, mean and lower-end AC values are presented in table C.3-3.

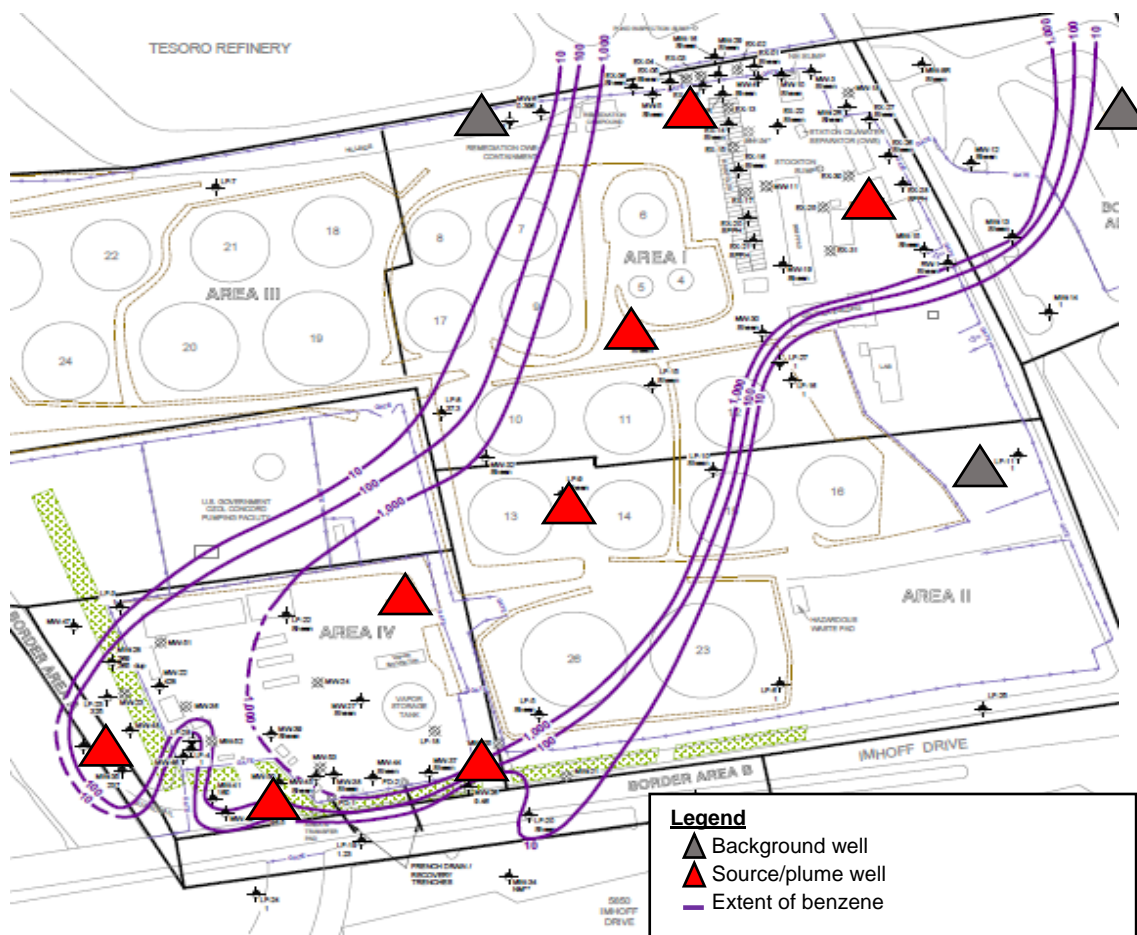


Figure C.3-1 NAIP monitoring well locations.

The changes in NAIPs from background were calculated for each NAIP and for each of the scenarios described above, as shown in grey cells in table C.3-4.

Stoichiometric conversions and assimilative capacity calculation

Octane (C_8H_{18}) was used as the representative petroleum hydrocarbon in the biodegradation reactions. The stoichiometric ratios for octane were calculated using the molecular weights of the electron acceptors and by-products (Acc-BP) and the balanced chemical equation representation of each biotransformation process as shown in tables C.3.5 and C.3.6.

The stoichiometry of the biotransformation processes and the molecular weights of the NAIPs were used to calculate the stoichiometric ratios for octane degradation and CO_2 and alkalinity production, as presented in table C.3-7 through C.3-9.

The stoichiometric ratios summarised in table C.3-9 were multiplied by the observed changes in electron acceptors to predict changes in C_8H_{18} , CO_2 and alkalinity for the three scenarios (upper-end, mean and lower-end aqueous NSZD) as shown in table C.3-10 through C.3-12.

NSZD rate calculation

To calculate the NSZD rate, the fundamental equation for mass budgeting was applied (equation 5):

Equation 5: $R_{aq} = V_D(AC)(YZ)$

where R_{aq} is the aqueous reaction rate (g/d), V_D is the Darcy velocity of groundwater flow (m/d, also known as the specific discharge), AC is the assimilative capacity of all biotransformation processes combined (g/m³), and YZ is the area perpendicular to groundwater flow (m²).

The specific discharge (or seepage velocity) V_D was calculated using Darcy's Law simplified equation divided by the effective porosity:

$$V_D = \frac{K \times i}{n}$$

where K is the hydraulic conductivity (m/s), i is the hydraulic gradient (dimensionless) and n is the effective porosity (dimensionless).

- The average hydraulic conductivity, K , of the plume was determined to be 1.2×10^{-6} m/s.
- The hydraulic gradient, i , was determined to be 0.003.
- The effective porosity, n , was determined to be 0.2.

$$V_D = \frac{1.2 \times 10^{-6} \frac{m}{s} \times 0.003}{0.2} = 1.8 \times 10^{-8} \frac{m}{s}$$

$$V_D = 1.8 \times 10^{-8} \frac{m}{s} * 86,400 \frac{s}{d} = 0.0016 \frac{m}{d}$$

Table C.3-2. Average field and laboratory NAIP analytical results

Location	Date	DO (mg/L)	CH ₄ (µg/L)	Fe ²⁺ (mg/L)	CO ₂ (mg/L)	NO ₃ ⁻ (mg/L)	SO ₄ ²⁻ (mg/L)	BTEX (µg/L)	Alkalinity (as CaCO ₃) (mg/L)
Background	November-15	5.6	0.01	0.33	80	0.60	120	1.0	583
Source	November-15	5.8	4.34	3.2	159	0.25	2.9	200	710
Downgradient	November-15	7.2	2.48	0.40	131	0.25	5.2	2.0	703

Table C.3-3. Upper-end, mean, and lower-end NAIP values

	DO (mg/L)	CH ₄ (µg/L)	Fe ²⁺ (mg/L)	CO ₂ (mg/L)	NO ₃ ⁻ (mg/L)	SO ₄ ²⁻ (mg/L)	BTEX (µg/L)	Alkalinity (as CaCO ₃) (mg/L)
Upper-end AC values ¹	5.8	4.3	3.2	159	0.25	2.9	2.0	710
Mean AC values ²	6.5	3.4	1.8	145	0.25	4.1	101	707
Lower-end AC values ³	7.2	2.5	0.4	131	0.25	5.2	200	703

1 – Upper-end AC values use the most favorable NAIP value from either the average source zone or downgradient plume edge location. This would include the lowest DO, NO₃⁻ and SO₄²⁻ concentrations and the highest concentration of Fe²⁺, CH₄, alkalinity and CO₂; 2 – Mean AC values use the average of the source zone and downgradient plume edge locations; 3 – Lower-end AC values use the least favorable NAIP value from either the average source zone or downgradient plume edge location. This would include the higher DO, NO₃⁻ and SO₄²⁻ concentration and the lowest concentration of Fe²⁺, CH₄, alkalinity and CO₂.

Table C.3-4. Observed NAIPs, changes on upper-end, mean and lower-end AC values

Constituent		Background	Mean AC values	Change from background - mean values	Indication of AC process *	Upper-end AC values	Change from background - upper-end AC values	Lower-end AC values	Change from Background - Lower-end AC Values
Dissolved O ₂	mg/L	5.6	6.5	0.87	No	5.8	0.21	7.2	1.5
NO ₃ ⁻	mg/L	0.60	0.25	-0.35	Yes	0.25	-0.35	0.25	-0.35
SO ₄ ²⁻	mg/L	120	4.1	-116	Yes	2.9	-117	5.2	-115
Fe ²⁺	mg/L	0.33	1.8	1.5	Yes	3.2	2.8	0.4	0.076
CH ₄	µg/L	0.01	3.4	3.4	Yes	4.3	4.3	2.5	2.5
Alkalinity (CaCO ₃)	mg/L	583	707	123	Yes	710	127	703	120
Total CO ₂	mg/L	80	145	65	Yes	159	78	131	51

* Column entitled Indication of AC Process signifies whether the change in the NAIP (either increase or decrease) is consistent with the expected change in the electron acceptor or biodegradation by-product. As compared to background locations, DO, NO₃⁻ and SO₄²⁻ concentrations should decrease in source/plume areas. On the contrary, concentrations of Fe²⁺, CH₄, alkalinity and CO₂ should increase in source/plume areas. For this example calculation, the DO values in both the source and downgradient plume edge zones were higher than background, presumably non-representative. Therefore, the contribution of aerobic respiration to the aqueous NSZD was zero for all scenarios; Grey highlighted cells are used for aqueous NSZD calculations; Blue highlighted cells are used the QA/QC purposes.

Table C.3-5. Balanced chemical equation representation of biotransformation processes for octane (C₈H₁₈)

Biotransformation process	Acc-BP	Balanced chemical equation
Aerobic	O ₂	$2 \text{C}_8\text{H}_{18} + 25 \text{O}_2 \rightarrow 16 \text{CO}_2 + 18 \text{H}_2\text{O}$
Denitrification	NO ₃ ⁻	$\text{C}_8\text{H}_{18} + 10 \text{NO}_3^- + 10 \text{H}^+ \rightarrow 8 \text{CO}_2 + 5 \text{N}_2 (\text{g}) + 14 \text{H}_2\text{O}$
Sulphate reduction	SO ₄ ²⁻	$4 \text{C}_8\text{H}_{18} + 25 \text{SO}_4^{2-} + 50 \text{H}^+ \rightarrow 32 \text{CO}_2 + 25 \text{H}_2\text{S} + 36 \text{H}_2\text{O}$
Iron reduction	Fe(OH) ₃ (s)	$\text{C}_8\text{H}_{18} + 50 \text{Fe(OH)}_3(\text{s}) + 100 \text{H}^+ \rightarrow 8 \text{CO}_2 + 50 \text{Fe}^{2+} + 134 \text{H}_2\text{O}$
Methanogenesis	Fermentation to CH ₄ and CO ₂	$4 \text{C}_8\text{H}_{18} + 14 \text{H}_2\text{O} \rightarrow 7 \text{CO}_2 + 25 \text{CH}_4$

Table C.3-6. Molecular weight of NAIPs and other dissolved constituents

NAIP/dissolved constituent	Molecular weight (g/mol)
O ₂	32.00
NO ₃ ⁻	62.01
SO ₄ ²⁻	96.06
Fe ²⁺	55.84
CH ₄	16.05
CO ₂	44.01
CaCO ₃	100.09
C ₈ H ₁₈	114.23

Table C.3-7. Stoichiometric ratio calculations for octane degradation (C₈H₁₈)

Biotransformation Process	Acc-BP	moles C ₈ H ₁₈	g C ₈ H ₁₈	moles Acc-BP	g Acc-BP	g C ₈ H ₁₈ /g Acc-BP
Aerobic	O ₂	2	228.46	25	800	0.29
Denitrification	NO ₃ ⁻	1	114.23	10	620.1	0.18
Sulphate reduction	SO ₄ ²⁻	4	456.92	25	2401.5	0.19
Iron reduction	Fe(OH) ₃ (s)	1	114.23	50	2792	0.04
Methanogenesis	Fermentation to CH ₄ and CO ₂	4	456.92	25	401.25	1.1

Table C.3-8 Stoichiometric ratio calculations for CO₂ and alkalinity production

Biotransformation Process	Acc-BP	moles CO ₂	g CO ₂	g CO ₂ /g Acc-BP	moles CaCO ₃	g CaCO ₃ -C	g CaCO ₃ /g Acc-BP ⁱⁱⁱ
Aerobic	O ₂	16	704.16	0.88	0 ⁱ	0	0
Denitrification	NO ₃ ⁻	8	352.08	0.57	8	800.72	1.3
Sulphate reduction	SO ₄ ²⁻	32	1408.32	0.59	32	3202.88	1.3
Iron reduction	Fe(OH) ₃ (s)	8	352.08	0.13	8	800.72	0.29
Methanogenesis	Fermentation to CH ₄ and CO ₂	7	308.07	0.77	0 ⁱⁱ	0	0

ⁱ No alkalinity change with aerobic respiration; ⁱⁱ No alkalinity change with methanogenesis (NRC 2000).

Table C.3-9 Summary of stoichiometric ratios for octane (C₈H₁₈) degradation and CO₂ and alkalinity production from biotransformation processes

Biotransformation process	Octane g C ₈ H ₁₈ /g Acc-BP	Carbon Dioxide g CO ₂ /g Acc-BP	Alkalinity CaCO ₃ /g Acc-BP
Aerobic (O ₂ consumed)	0.29 g C ₈ H ₁₈ /g O ₂	-0.88 g CO ₂ /g O ₂	0 g CaCO ₃ /g O ₂
Denitrification (NO ₃ ⁻ consumed)	0.18 g C ₈ H ₁₈ /g NO ₃ ⁻	-0.57 g CO ₂ /g NO ₃ ⁻	-1.3 g CaCO ₃ /g NO ₃ ⁻
Sulphate reduction (SO ₄ ²⁻ consumed)	0.19 g C ₈ H ₁₈ /g SO ₄ ²⁻	-0.59 g CO ₂ /g SO ₄ ²⁻	-1.3 g CaCO ₃ /g SO ₄ ²⁻
Iron Reduction (Fe ²⁺ produced)	0.04 g C ₈ H ₁₈ /g Fe ²⁺	0.13 g CO ₂ /g Fe ²⁺	0.29 g CaCO ₃ /g Fe ²⁺
Methanogenesis (CH ₄ produced)	-1.1 g C ₈ H ₁₈ /g CH ₄	0.77 g CO ₂ /g CH ₄	0 g CaCO ₃ /g CH ₄

The values of Fe²⁺ and CH₄ stoichiometric ratios for octane are negative because both are produced in the process of degrading octane (C₈H₁₈). All values of octane degradation must be negative to indicate a loss of the compound. On the contrary, all values of CO₂ and alkalinity production must be positive; thus, the ratio is negative for biotransformation processes and NAIPs that are consumed or negative values.

Table C.3-10. Computed changes in octane (C₈H₁₈), CO₂ and alkalinity for upper-end AC values

Biotransformation process	Observed change in NAIP (mg/L)	Computed changes		
		CO ₂ (mg/L)	Alkalinity (mg as CaCO ₃ /L)	Octane (mg C ₈ H ₁₈ /L)
Aerobic (O ₂)	0.21	0	0	0
Denitrification (NO ₃)	-0.35	0	0	0
Sulphate reduction (SO ₄ ²⁻)	-117	68	156	-22
Iron Reduction (Fe ²⁺ generated)	2.8	0.36	0.82	-0.12
Methanogenesis (CH ₄ generated)	4.3	3.3	0	-4.9
Total		72	157	-27

Table C.3-11. Computed changes in octane (C₈H₁₈), CO₂ and alkalinity for mean AC values

Reaction	Observed change in acceptor concentration (mg/L)	Computed changes		
		CO ₂ (mg/L)	Alkalinity (mg as CaCO ₃ /L)	Octane (mg C ₈ H ₁₈ /L)
Aerobic (O ₂)	0.87	0	0	0
Denitrification (NO ₃)	-0.35	0	0	-0.06
Sulphate reduction (SO ₄ ²⁻)	-116	68	154	-22
Iron Reduction (Fe ²⁺ generated)	1.5	0.18	0.42	-0.060
Methanogenesis (CH ₄ generated)	3.4	2.6	0	-3.9
Total		71	155	-26

Table C.3-12. Computed changes in octane (C₈H₁₈), CO₂ and alkalinity for lower-end AC values

Reaction	Observed change in acceptor concentration (mg/L)	Computed changes		
		CO ₂ (mg/L)	Alkalinity (mg as CaCO ₃ /L)	Octane (mg C ₈ H ₁₈ /L)
Aerobic (O ₂)	1.5	0	0	0
Denitrification (NO ₃ ⁻)	-0.35	0	0	0
Sulphate reduction (SO ₄ ²⁻)	-115	67	153	-22
Iron Reduction (Fe ²⁺ generated)	0.076	0.010	0.022	-0.003
Methanogenesis (CH ₄ generated)	2.5	1.9	0	-2.8
Total		69	153	-25

1. The area perpendicular to groundwater flow, YZ, was calculated based on the following information:
 - a) Average width of LNAPL footprint (Y) = 127 m
 - b) Average thickness of LNAPL smear zone (Z) = 3 m

$$YZ = 127 \text{ m} \times 3 \text{ m} = 381 \text{ m}^2$$

2. The AC was calculated for the three different scenarios, as shown in table C.3-10 through C.3-12 and summarised below:

- a) Upper-end AC value, where the total stoichiometric degradation was:

$$AC_{\text{upper-end}} = 27 \frac{\text{mg C}_8\text{H}_{18}}{\text{L}} = 27 \frac{\text{mg C}_8\text{H}_{18}}{\text{L}}$$

- b) Mean AC value, where the total stoichiometric degradation was:

$$AC_{\text{mean}} = 26 \frac{\text{mg C}_8\text{H}_{18}}{\text{L}} = 26 \frac{\text{mg C}_8\text{H}_{18}}{\text{L}}$$

- c) Lower-end AC value, where the total stoichiometric degradation was:

$$AC_{\text{lower-end}} = 25 \frac{\text{mg C}_8\text{H}_{18}}{\text{L}} = 25 \frac{\text{mg C}_8\text{H}_{18}}{\text{L}}$$

Thus, the NSZD rate for each of the three scenarios is:

$$[R_{aq}]_{\text{upper-end}} = 0.0016 \frac{\text{m}}{\text{d}} \times 27 \frac{\text{g C}_8\text{H}_{18}}{\text{m}^3} \times 381 \text{ m}^2 = 16 \frac{\text{g C}_8\text{H}_{18}}{\text{d}}$$

$$[R_{aq}]_{\text{mean}} = 0.0016 \frac{\text{m}}{\text{d}} \times 26 \frac{\text{g C}_8\text{H}_{18}}{\text{m}^3} \times 381 \text{ m}^2 = 15 \frac{\text{g C}_8\text{H}_{18}}{\text{d}}$$

$$[R_{aq}]_{\text{lower-end}} = 0.0016 \frac{\text{m}}{\text{d}} \times 25 \frac{\text{g C}_8\text{H}_{18}}{\text{m}^3} \times 381 \text{ m}^2 = 14 \frac{\text{g C}_8\text{H}_{18}}{\text{d}}$$

The estimated range of aqueous NSZD rates using geochemical indicators and mass budgeting analysis is from approximately 14 to 16 g C₈H₁₈/d.

Assuming an LNAPL density of 0.81 gram hydrocarbon per cubic centimetre (g/cm³), this equates to a volumetric NSZD rate of approximately 6 to 7 litres of LNAPL per year (L/yr).

Quality assurance/quality control

The computed changes in CO₂ and alkalinity, shown in tables C.3-10 through C.3-12, roughly correspond with the changes observed in field measurements, presented in table C.3-4. This supports the assumption made that the observed changes in NAIPs are attributable to hydrocarbon biodegradation (aqueous NSZD) because the stoichiometry results are consistent with the observed NAIP measures.

For example, for the average observed changes in CO₂ between background and source/plume locations were 51 to 78 mg/L (table C.3.4). The theoretically estimated range of change in CO₂ was 69 to 72 mg/L as shown on tables C.3.10 through C.3.12. Since the theoretical estimate falls within the observed range, the AC and NSZD rate calculations are assumed valid.

Similarly, the average observed changes in alkalinity between background and source/plume locations were 120 to 127 mg/L (table C.3.4). The theoretically estimated range of change in alkalinity was 153 to 157 mg/L as shown on tables C.3.10 through C.3.12. Since the theoretical estimate lies above the observed range, the AC and NSZD rate calculations must be qualified as estimates and potentially high-biased since the observed alkalinity is lower than predicted by the AC calculations.

Appropriate QA/QC measures are essential to assess the accuracy and precision of the data collected. Use proper, manufacturer-recommended calibration procedures for all field instruments. A minimum two-point calibration is typically prudent with a span calibrated to the range of expected concentrations. Field and laboratory samples should comply with project-specific duplicate sample collection, as well as field equipment blanks.

As demonstrated, a useful QA/QC step that can be used to help ascertain the results of mass budgeting analysis includes comparing measured and computed changes in total inorganic carbon (dissolved CO₂) and total alkalinity. Stoichiometric amounts of both dissolved CO₂ and alkalinity are produced as a by-product of biodegradation (NRC 2000). Comparison of the measured and computed values allows further assessment of the results. For example, if the measured increase is greater than the computed, then the NSZD calculation could be considered low biased. Because reactions of both dissolved CO₂ and alkalinity are complex (i.e. associated with the dynamics of the earth's carbon cycle) and involve geochemical processes other than NSZD, this comparison is considered qualitative in nature. It is performed for the purposes of assessing the potential accuracy of the calculations (e.g. is the actual NSZD rate closer to the upper or lower end of the range of estimates) and simple validation that aqueous-based NSZD biodegradation is responsible for the loss of petroleum hydrocarbons.

APPENDIX D.

Gradient method-based NSZD evaluation procedures

This appendix contains procedures useful for practitioners to reference when implementing the gradient method for NSZD evaluation. The following procedures are included herein:

- D.1 – Procedure for gradient method data analysis (including background correction)
- D.2 – Field procedure for measuring the effective vapour diffusion coefficient
- D.3 – Field procedure for soil gas profile measurement from nested vapour probes
- D.4 – Field procedure for alternative soil gas measurements (existing monitoring wells and shallow manual probes)
- D.5 – Example gradient method-based NSZD rate calculations

D.1 – Procedure for gradient method data analysis (including background correction)

The information presented in this section was extracted from the following source(s):

- American Petroleum Institute (API) 1998, 'Recommended practices for core analysis', *Recommended Practice No. 40*, Second Edition.
- API 2017, *Quantification of vapor phase-related NSZD processes*, Publication No. 4784.
- Johnson, PC, Bruce, C, Johnson, RL & Kemblowski, MW 1998, 'In situ measurement of effective vapor-phase porous medium diffusion coefficients', *Environmental Science and Technology*, vol. 32, no. 21, pp. 3405–3409.
- Johnson, P, Lundegard, P & Liu, Z 2006, 'Source zone natural attenuation at petroleum hydrocarbon spill sites – I: site-specific assessment approach', *Groundwater Monitoring & Remediation*, vol. 26, iss. 4, pp. 82–92.
- Lundegard, PD & Johnson, PC 2006, 'Source zone natural attenuation at petroleum hydrocarbon spill sites – II: application to a former oil field', *Groundwater Monitoring & Remediation*, vol. 26, iss. 4, pp. 93–106.

Purpose and scope

The purpose of this procedure is to provide practical guidelines for the implementation of the gradient method to estimate the rate of NSZD in the subsurface. As described in detail in section 4.3 of this document, this procedure assumes that diffusion is the dominant vapour transport mechanism in the soil and the practitioner has vetted site conditions and determined the method applicable.

This procedure provides step-by-step instructions, ranging from installation of the soil vapour monitoring probes through to the calculation of the NSZD rate. Appendices D.2 through D.4 provide specific procedures for execution of the field work. Example NSZD rate calculations are included in appendix D.5.

The gradient method is based on Fick's first law of diffusion as shown in equation 9.

$$\text{Equation 9: } J = D_v^{eff} \left(\frac{dC}{dz} \right)$$

where J is the steady-state diffusive flux (g/m²-soil/s), which is proportional to the soil gas concentration gradient, dC/dz (g/m³m). D_v^{eff} is the effective soil vapour diffusion coefficient (m²/s), also known as the effective diffusivity, that is specific to the soil and gas being measured.

D_v^{eff} can be expressed as either D_{O₂}^{eff}, D_{CO₂}^{eff}, or D_{CH₄}^{eff}, depending on the gas (O₂, CO₂, or CH₄) being used for the flux estimate. Typically, the gas flux is reported in molar-based units of mass per area per time (e.g. μmol/m²/s). This equation will be cited throughout this procedure because it's a fundamental basis for the calculations.

Prerequisites

It is assumed that the following prerequisites have been met prior to use of this procedure:

- An appropriate number of monitoring locations was selected for soil gas concentration profiling, adequate to meet the data objectives and represent the potential range of NSZD rates at the site.
- Monitoring locations include areas both above the light nonaqueous phase liquid (LNAPL) footprint and in background (non-impacted) areas.

Procedures and guidelines

Use of the gradient method to estimate the rate of NSZD involves the following steps:

1. Install new multi-level vapour sampling probes or establish alternative means for vapour sampling as discussed in appendix D.4
2. Concurrently perform:
 - a) Soil vapour sampling from the monitoring probes to measure O₂, CO₂, CH₄, and volatile organic compounds (VOCs) concentrations, and
 - b) In-situ tracer tests to estimate a representative range of soil vapour diffusion coefficients
3. Plot the data and estimate the concentration gradient
4. Assess the background O₂ consumption and CO₂ production and compensate for background flux
5. Calculate the NSZD rate

The following sections detail how to accomplish each step.

Install multi-level sampling probes

Probes for NSZD monitoring are typical of those used in routine soil gas monitoring (CRC CARE 2013). Install the probe points with an overlying hydrated bentonite seal to mitigate atmospheric short-circuiting. A typical installation may have less than five multi-level probe locations across the LNAPL footprint. Thus, the careful selection of horizontal and vertical sampling locations is critical to gather a representative data set. Soil gas probes are located over the LNAPL footprint. Use the LNAPL Conceptual Site Model (LCSM) and all available lines of evidence to choose appropriate locations for nested soil gas probes. Position them over the petroleum hydrocarbon-impacted soils, but not near release location.

In choosing depths for soil gas probes, the overall objective is to resolve the concentration gradient in sufficient detail to obtain a representative NSZD rate estimate. Figure D.1-1 depicts example soil gas sample port installations for the gradient method for a typical site condition.

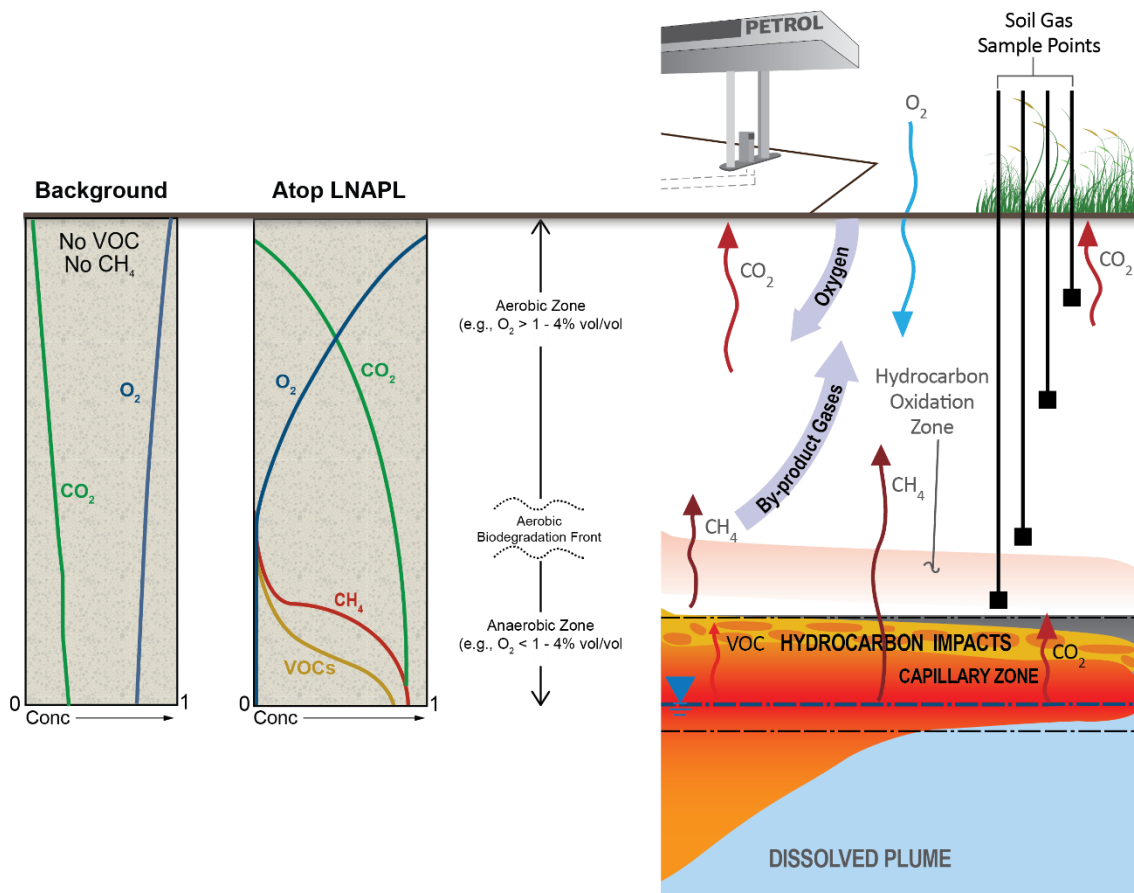


Figure D.1-1. Schematic of gradient method monitoring setup.

Figure D.1-2 depicts potential soil gas concentration profiles for a Scenario A and B. Consider two typical site condition scenarios: (A) petroleum hydrocarbon impacts in the vadose zone soil and no surface vegetation and (B) LNAPL in the capillary fringe and a clean overlying vadose zone (i.e. no hydrocarbon impacted soil) and near surface vegetation and a root zone. The preferred region for locating soil gas probes for concentration gradient estimation, where the gradients and fluxes become less variable. This depth is generally below the vegetative root zone and in the aerobic interval above the hydrocarbon oxidation zone. In this sense, the gradient method may be less susceptible to near-surface influences than the ground surface-based NSZD methods.

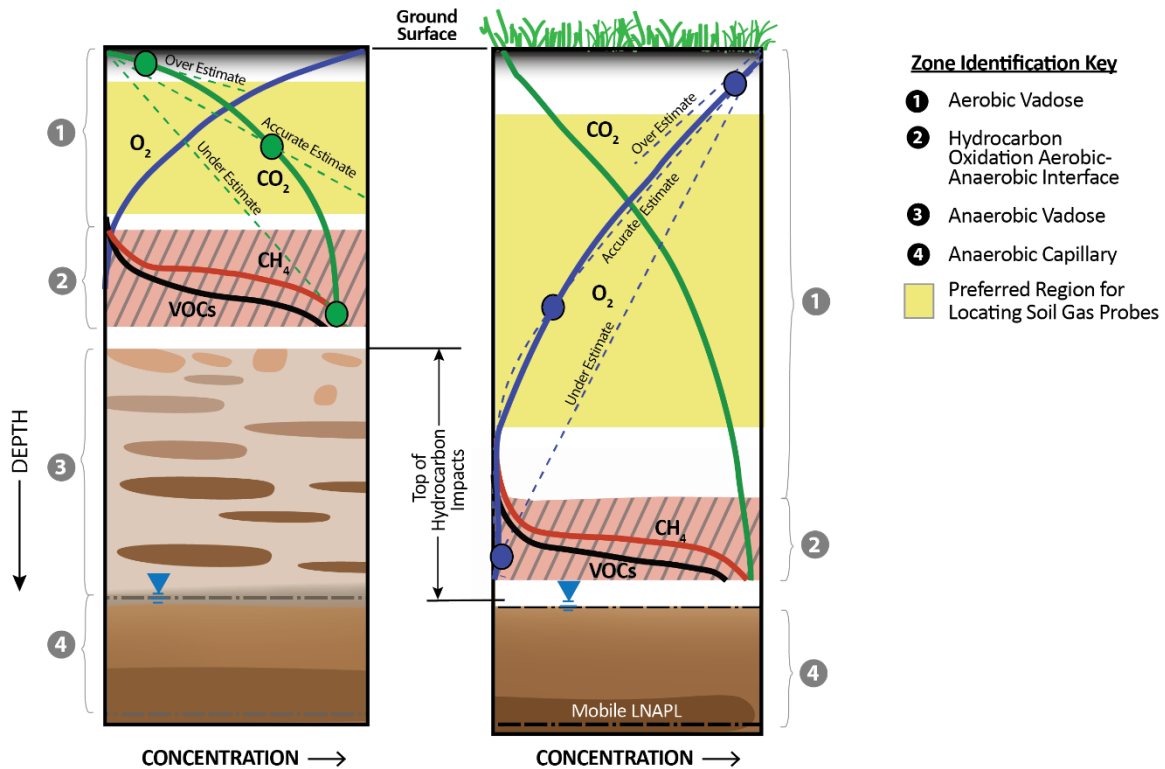


Figure D.1-2. Choice of measurement points and influence on estimated CO₂ gradient (left) and O₂ gradient (right) in soil with (left) and without (right) hydrocarbon impacts in the vadose zone.

Modified with permission from API (2017).

Soil vapour sampling

Sample collection from the probes for soil gas monitoring is typically done using active soil vapour sampling methods and is often subject to site-specific guidelines or procedures. Analytes typically measured by the gradient method include O₂, CO₂, and CH₄ using a calibrated handheld multi-gas meter (e.g. Landtec GEM™5000). Implement precautions to ensure that VOCs are excluded from the CH₄ measurement through use of a granular activated carbon or charcoal filter on the inlet to the meter. VOCs are also typically measured and can be performed in the field using a flame ionisation detector (FID) (e.g. Foxboro TVA1000). Similarly, an additional reading can be taken with carbon or charcoal filter on the inlet to the FID to measure CH₄-related response. Subtraction of the filtered from the unfiltered measurements provides the VOC concentration. Use of a nitrogen (N₂) analyser can serve as a check-sum on the other gas results, because the sum of O₂, CO₂, CH₄, N₂ and VOCs should approach 100%. If CH₄ is elevated at an unexpected location, consider collecting a gas sample for laboratory total petroleum hydrocarbon (TPH) analysis.

Typically, the soil vapour concentration profiles at a single sample probe cluster location can be measured in approximately one hour. A network of up to 10 locations can typically be measured in a one day field effort.

Perform in-situ tracer test

The following subsections describe two means to estimate the soil vapour diffusion coefficient (or soil vapour diffusivity); site-specific measurement and empirical

Site-specific measurement of vapour diffusivity

Site-specific D_v^{eff} can be determined by an in-situ tracer method (Johnson *et al* 1998). A known volume of air spiked with a known concentration of a tracer gas (e.g. helium (He) or sulphur hexafluoride (SF₆)) is injected into the vadose zone at various depths using the same multilevel soil gas probes used to profile soil gas concentrations. After a relatively short duration of time, the same volume of soil gas is extracted from each probe, and the recovered tracer concentration is measured. For a point source, the value of the effective diffusion coefficient for the tracer gas (D_{tracer}^{eff}) is determined using equation D.1.

$$\text{Equation D.1: } D_{tracer}^{eff} = \left[\frac{\Theta_v^{1/3}}{\beta} \right] \left[\frac{1}{4t_s} \right] \left[\frac{3V_s}{4\pi} \right]^{2/3}$$

where Θ_v is the air-filled porosity (cubic metre (m³)-vapour/m³-soil), t_s is the sampling time (s), and V_s is the volume of vapour extracted at the end of the test (m³).

The value of Θ_v can be estimated from literature values (Johnson *et al* 1998) or measured (API 1998). The value of β is determined by iterative approximation or graphical as shown in figure D.1-3, extracted from Johnson *et al* (1998), where η is the fraction of mass recovered, which is calculated as the measured concentration of the recovered gas (g/L) divided by the initial injected concentration of the gas (g/L); V_o is the volume of the injected gas (m³).

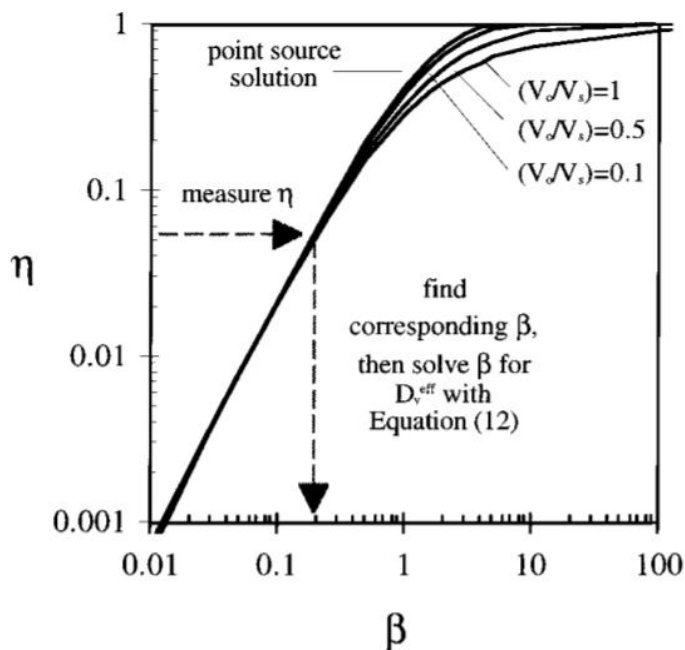


Figure D.1-3. Relationship between β and η , for point-source and finite-size sources. Excerpt from Johnson *et al* (1998).

When O₂ is used as a basis for the gradient method estimate of gas flux, $D_{O_2}^{eff}$ is substituted for D_v^{eff} in equation 9 and is calculated from D_{tracer}^{eff} by correcting for the difference in molecular diffusion coefficients in air, $D_{O_2}^{air}$ and D_{tracer}^{air} (constant values), using equation D.2.

$$\text{Equation D.2: } D_{O_2}^{eff} = D_{tracer}^{eff} \left(\frac{D_{O_2}^{air}}{D_{tracer}^{air}} \right)$$

where $D_{O_2}^{air}$ is a constant, the molecular diffusion coefficient for O_2 (0.21 cm²/s), and D_{tracer}^{air} is also a constant, the molecular diffusion coefficient for the tracer gas in air (He=0.70 cm²/s, SF₆=0.089 cm²/s). If the flux of other gases is of interest (i.e. CO₂ or CH₄), the same substitution for D_v^{eff} in equation 9 can be made using their constant molecular diffusion coefficients in air (CO₂=0.16 cm²/s, CH₄=0.22 cm²/s). Appendix D.2 contains an example field implementation procedure and demonstration of how to measure $D_{O_2}^{eff}$ in situ.

Check the results of the field measured diffusivity against literature values. If the difference is significant, then review the data and soil conditions (i.e. moisture content) at the time of measurement and repeat measurements if necessary to obtain a representative value, or more appropriately, a range of representative values.

Empirical means to estimate vapour diffusivity

As stated above, site-specific measurements are the preferred means to estimate the effective diffusion coefficient. However, it may be necessary or valuable to more quickly estimate them for screening-level data use purposes. The Millington and Quirk (1961) equation can be used to estimate the effective O_2 diffusion coefficient ($D_{O_2}^{eff}$) as shown in equation D.3.

$$\text{Equation D.3: } D_{O_2}^{eff} = D_{O_2}^{air} \times \frac{\Theta_v^{3.3}}{\Theta_T^2}$$

where Θ_T is the total porosity of the vadose zone soil within and above the hydrocarbon oxidation zone (m³-pore/m³-soil). The values of Θ_v and Θ_T can be estimated from literature values (Johnson *et al* 1998) or measured (API 1998).

Estimate the concentration gradient

The difference in concentration between the upper and lower boundary control points of measurement, divided by the vertical distance between the control points, gives an estimate of the vertical concentration gradient as shown in equation D.4.

$$\text{Equation D.4: } \frac{dC}{dz} = \frac{C_2 - C_1}{z_2 - z_1}$$

where C_1 and C_2 are the gas concentrations at depths z_1 and z_2 , respectively.

Soil gas sampling results are summarised in a table along with estimated concentrations of fixed gases at the soil surface (zero depth) that are assumed to be at standard atmospheric conditions.

Results are plot in a graphic form to create a soil gas concentration depth profile for each location.

Soil gas profiles provide evidence of whether NSZD is occurring. For example:

- CH₄ production near the hydrocarbon-impacted soil interface would indicate that anaerobic biodegradation is occurring;
- O₂ depletion and CO₂ production indicate aerobic biodegradation and hydrocarbon oxidation in the overlying formation;
- presence of volatile petroleum hydrocarbons (i.e. gasoline-range organics) in soil gas, concentrations increasing with depth, indicates that volatilisation and degradation of the LNAPL are occurring.

The differences between the concentration of the chosen gas in atmospheric gas and measured concentrations at the chosen gas probe depth is used to determine the gas gradient and, thus, is used as a basis for estimating the NSZD rate.

Compensate for background fluxes

Estimating NSZD-related fluxes is complicated by natural soil respiration (Rochette *et al* 1999). In this document, background is considered O₂ utilisation, CO₂ production, and/or CH₄ production or oxidation that is unrelated to the presence of the petroleum hydrocarbon LNAPL source. This includes contributions from plant roots and microbes present in surficial soils and deeper soils containing natural organic matter such as peat as humic matter. These processes tend to be most significant in the root zone and diminish with increasing depth, but are variable from site to site.

There are numerous challenges with background correction using results from outside the LNAPL footprint, especially at sites with diverse ground cover, very active natural soil processes, or deep LNAPL source zones. More complex site conditions will drive selection of a more complex background correction process.

One strategy to eliminate flux contributions from non-NSZD processes is to install gas flux measurement locations in a nearby uncontaminated setting with similar surface and subsurface conditions. Estimate fluxes for these background locations in the same way as used for the locations overlying the LNAPL footprint. Subtract the background flux from the total flux measured above the source zone to estimate the NSZD rate. The number of background locations will be driven by the variability in the background flux results. If large variability is observed, then a statistical approach may be useful (e.g. based on pre-established confidence limits).

Calculation of CO₂ efflux from petroleum hydrocarbon sources (J_{NSZD}) is given by equation 8, where J_{Total} is the total uncorrected CO₂ efflux from each survey location above the LNAPL footprint and $J_{Background}$ is the average CO₂ efflux measured at the background locations in each different ground cover:

$$\text{Equation 8: } J_{NSZD} = J_{Total} - J_{Background}$$

The use of carbon 14 (¹⁴C) provides an alternative more accurate means to isolate the NSZD-derived CO₂ flux without the need to monitor areas outside of the LNAPL footprint. This can be especially relevant to sites with variable ground cover and soil conditions which affect background CO₂ and O₂ flux. Therefore, it is important to determine which method of background correction will be used as part of the NSZD program design stage because it will affect the number of locations to be measured.

Calculate the NSZD rate

There are different approaches to estimate NSZD rates based on different gradient method calculation bases such as O₂, CO₂ and CH₄. The approach to estimate NSZD rates at a specific site is chosen on a site-specific judgment based on review of the site-specific soil gas profiles.

Gradient method QA/QC

Appropriate QA/QC measures are essential to assess the accuracy and precision of the data collected. Use proper, manufacturer-recommended calibration procedures for

all field instruments. A minimum two-point calibration is typically prudent with a span gas calibrated to the range of expected concentrations. Ensure field and laboratory samples comply with project-specific duplicate sample collection as well as ambient field blanks, if samples are to be sent to a laboratory.

D.2 – Field procedure for measuring the effective vapour diffusion coefficient

This appendix is a modified reproduction of appendix A-1, from API 2017. The information presented in this section was extracted from the following sources:

- American Petroleum Institute (API) 1998, 'Recommended practices for core analysis', *Recommended Practice No. 40*, Second Edition.
- API 2017, *Quantification of vapor phase-related NSZD processes*, Publication No. 4784.
- California Environmental Protection Agency (CalEPA) 2012, *Advisory: active soil gas investigations*, Department of Toxic Substances Control.
- Johnson, PC, Bruce, C, Johnson, RL & Kemblowski, MW 1998, 'In situ measurement of effective vapor-phase porous medium diffusion coefficients', *Environmental Science and Technology*, vol. 32, no. 21, pp. 3405–3409.

Purpose and scope

The purpose is to provide general guidelines for the measurement of vertical soil vapour flux using the gradient method. This procedure assumes that diffusion is the dominant vapour transport mechanism in the soil. Typically, this involves the installation and sampling of multi depth soil vapour monitoring points, in-situ measurement of effective diffusion coefficients, and calculations based on Fick's Law. This procedure assumes the vapour monitoring points were installed previously and describes the sampling procedures.

Equipment and materials

- Personal protective equipment (PPE)
- 1 litre (L) stainless steel syringe
- 10 millilitre (mL) gas tight syringe
- Nonreactive tracer gas (e.g. sulphur hexafluoride (SF₆) or helium (He))
- Gas detection device(s) (e.g. SRI gas chromatograph/electron capture detector (ECD) for SF₆, MGD 2002 multi gas detector for He)
- 1 L Tedlar® bags (12 for each location)
- Field logbook

Procedures and guidelines

Effective soil vapour diffusion coefficient for oxygen

Estimation of subsurface oxygen diffusion coefficients can be accomplished by using the methods and calculations proposed by Johnson *et al* (1998). The field procedure outlined by Johnson *et al* (1998) characterises the effective vapour phase porous medium diffusion coefficient (D_v^{eff}) within a spherical volume of approximately 9 centimetres (cm) in diameter. This corresponds to approximately a 1 L soil gas volume for a vapour filled porosity of 0.30 cm³ vapour/cm³ soil.

The general field procedure as described by Johnson *et al* (1998) is as follows:

1. Prepare a gas mixture containing approximately 10 parts per million by volume (ppm_v) SF₆ (or other conservative tracer gas such as He at detectable concentrations).
2. Inject 5 mL of 1 ppm_v SF₆ into a 1 L Tedlar® bag containing 1 L of SF₆ free air.
3. Measure the resulting concentration in the 1 L Tedlar® bag (target: approximately 5 parts per billion by volume (ppb_v)); record and denote this value as C_{max}.
4. Inject 5 mL of 1 ppm_v SF₆ into the desired location in the vadose zone through small diameter tubing (3 mm stainless steel tubing is preferred). Follow this injection with sufficient SF₆ free air to ensure that the 5 mL of SF₆ has just been flushed from the tubing into the vadose zone (it is desired that the total injected volume be minimised; approximately 3 mL/metre (m) for 304 SS 3 mm OD tubing with 2.1 mm inner diameter (ID)).
5. Immediately withdraw enough soil gas to fill a 1 L Tedlar® bag. Analyse and record the SF₆ concentration in the 1 L Tedlar® bag.
6. Inject 5-10 L of clean air into the vadose zone at this sampling before conducting a longer test.
7. Repeat steps 4, 5, and 6 except wait for periods of 15, 60, and 120 minutes before withdrawing the soil gas sample for analysis.
8. Reduce the data by dividing the measured concentrations by C_{max} (this is equivalent to determining η , the fraction of mass recovered).

Once the field protocol is completed, the theory and equations outlined in Johnson *et al* (1998) can be used to calculate the effective vapour phase porous medium diffusion coefficient. With a relatively simple change in the multiplier, this procedure can be adapted to estimate the diffusion coefficient of any gas of interest for NSZD monitoring including oxygen, carbon dioxide, and methane.

D.3 – Field procedure for soil gas profile measurements from nested vapour monitoring probes

The information presented in this section has been extracted from the following sources:

- CRC CARE 2013, *Petroleum hydrocarbon vapour intrusion assessment*: Australian guidance, CRC CARE Technical Report no. 23. CRC for Contamination Assessment and Remediation of the Environment, Adelaide, Australia.

Purpose and scope

The purpose of this procedure is to provide practical guidelines for soil gas profile measurements using nested vapour monitoring probes. These measurements are used as a basis to estimate the NSZD (NSZD) rate using the gradient method.

Equipment and materials

- Personal protective equipment
- 3 mm outer diameter (OD) or 6 mm OD nylon, Teflon® or stainless steel probe. 3 mm OD tubing is easier to drop down a bore hole than 6 mm OD tubing. Nylon tubing is recommended over Teflon® tubing. Stainless steel probing may be logistically impractical to use due to its inflexibility.
- Stainless steel, ceramic or plastic probe tip.
- Surface termination on tubing: Swagelok fittings or plastic valves (2-way inert plastic valves or stop cocks). An end-cap can also be used. If a valve is used, it is important to secure it tightly to tubing, as the valve is a permanent component of the soil vapour collection system.
- Surface termination on ground: options include flush mounts on floor/surface, below ground level with or without locking cover, variable above ground-level completions.
- Leak check compound and towel, or shroud to cover the entire sampling system and probe.
- Nitrile gloves.
- Pump or syringe equipped with a 3-way valve.
- Vacuum gauge.
- Field gas analyser(s) (photoionisation detector (PID), Foxboro TVA1000, Landtec GEM™ 5000 or Landtech GA-90/GEM-2000, RKI-brand Eagle).
- Temperature meter.
- Sample containers (Tedlar® bags or Summa canisters).
- Field logbook.

The materials used for the vapour probe, tubing and sample train may differ from those presented in this appendix. However, regardless of the materials used, it is important that an equipment blank is conducted to demonstrate that the materials used are clean and suitable for use.

The tubing sizes outlined in this appendix are recommendations only. Different tubing sizes can be utilised provided they can be properly connected. The conduct of leak testing (including the testing of the sample train) is important to demonstrate that all such connections are tight and the installed soil vapour probe and sample train are suitable for the collection of a soil gas sample.

The quality of the installation of the wells is critical to the quality of the results. Hence, it is important that an experienced member of the team oversees the installation of the wells.

Procedures and guidelines

Select the location of the multi-level vapour sampling probes

Site the horizontal and vertical sampling locations to gather a representative data set. A typical installation may have only one to five multi-level probe locations across the light non-aqueous phase liquid (LNAPL) footprint. Use the LNAPL conceptual site model (LCSM) and all available lines of evidence to choose appropriate locations.

Horizontal location

Locate the soil gas probes over the LNAPL footprint. Position them over the petroleum hydrocarbon-impacted soils, but not near release location. If the LNAPL body extends across two different surface soil conditions, locate the probes over the different ground cover types. Locate the background probes outside the LNAPL footprint and over the different ground cover types.

In choosing depths for soil gas probes, the overall objective is to resolve the concentration gradient in sufficient detail to obtain a representative NSZD rate estimate. Consider two typical site condition scenarios: (A) petroleum hydrocarbon impacts in the vadose zone soil and no surface vegetation and (B) LNAPL in the capillary fringe and a clean overlying vadose zone (i.e. no hydrocarbon impacted soil) and near surface vegetation and a root zone. Figure D.3-1 depicts example soil gas sample port installations for the gradient method for both site condition scenarios.

Figure D.3-2 depicts potential soil gas concentration profiles for Scenarios A and B, and the preferred region for locating soil gas probes for concentration gradient estimation, where the gradients and fluxes become less variable. This depth is generally below the vegetative root zone and above the hydrocarbon oxidation zone.

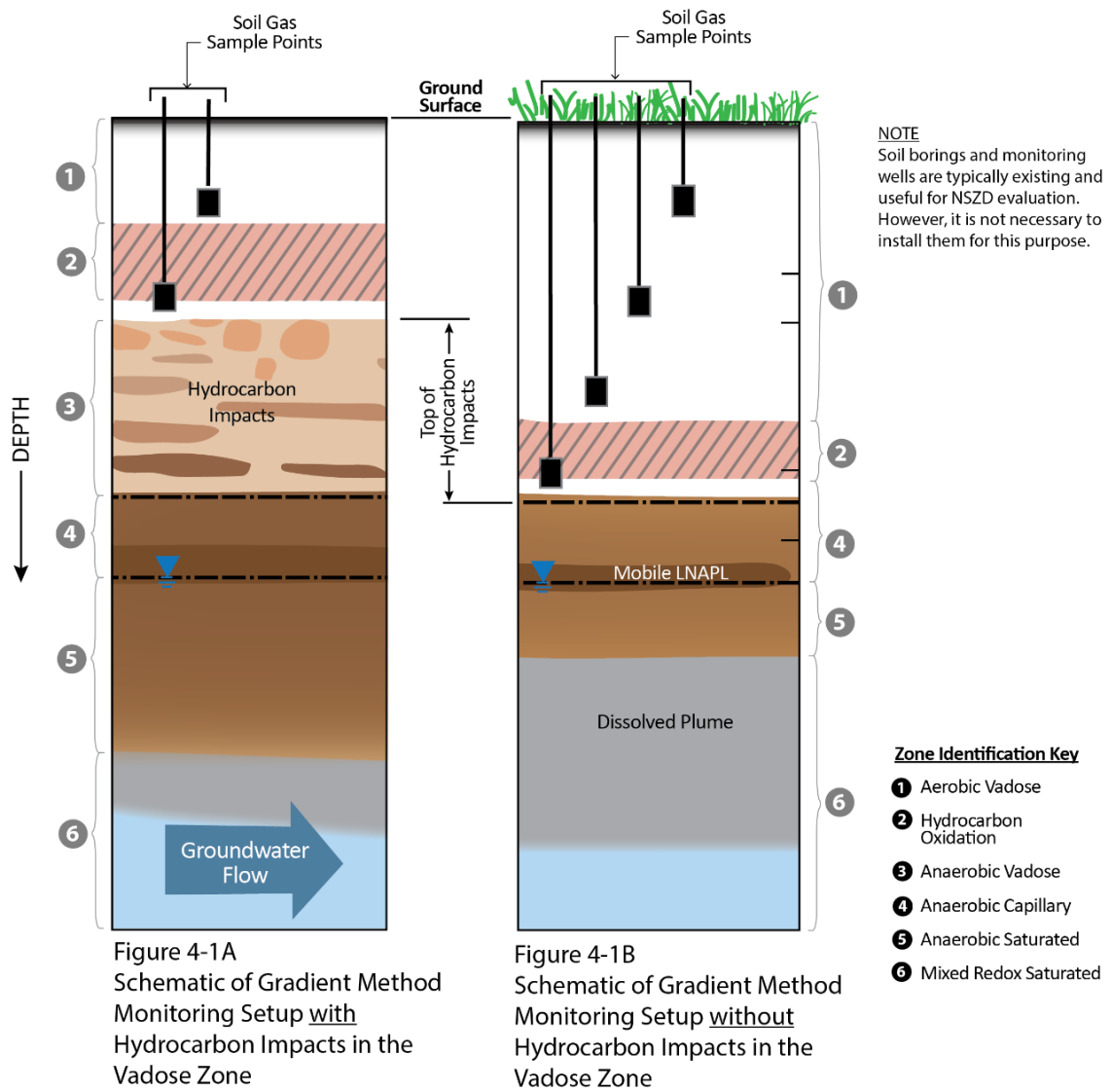


Figure D.3-1. Schematic of gradient method monitoring setup with (A) and without (B) hydrocarbon impacts in the vadose zone. Reproduced with permission from API (2017).

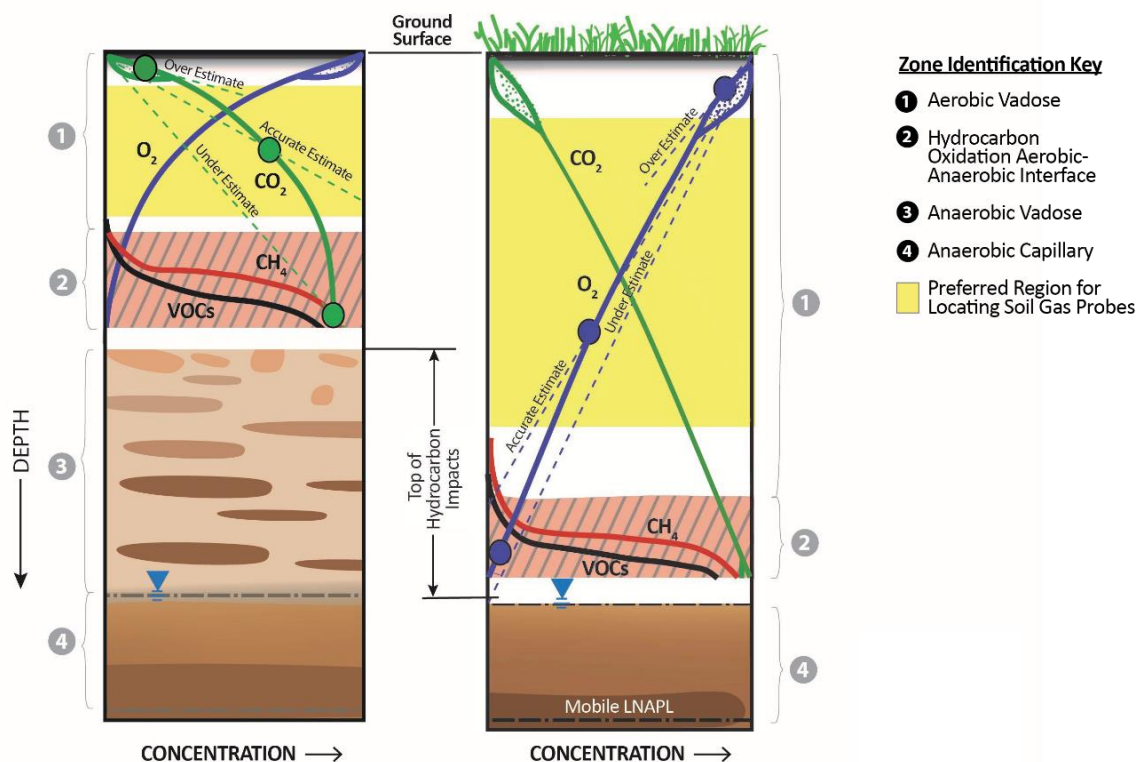


Figure D.3-2. Choice of measurement points and influence on estimated CO₂ gradient (left) and O₂ gradient (right) in soil with (left) and without (right) hydrocarbon impacts in the vadose zone.
 Reproduced with permission from API (2017).

Install the multi-level vapour sampling probes

Soil vapour sampling points can be installed down a variety of boreholes ranging in diameter from 2.5 to 20 cm. Boreholes may be created with hand equipment (hand-auger), by direct-push methods, or rotary drill-rigs. A good understanding of the site geology is useful to ensure the probe is appropriately placed without clogging. Hand-augering will likely be the most common method used to create a borehole if ground disturbance protocols exist or subsurface utilities exist. Installation of nested vapour monitoring probes are easier in boreholes >4 cm inner diameter (ID). It is not recommended to construct nested wells with less than 0.75 m separation between sample ports, to minimise the potential for interconnections (leaks) between sample ports.

In the following procedure, it is assumed that utilities have been cleared and an open borehole exists.

1. Measure depth to the bottom of borehole and cut the probe tubing to appropriate length to have enough for the required type of surface termination (flush, recessed, protruding).
2. Add enough sand to create a 15 cm layer in the bottom of borehole (calculate volume based upon borehole ID).
3. Drop soil vapour point and tubing down borehole. If the hole is deep and borehole narrow, adding a small weight (e.g. nut) can facilitate the probe extending to the bottom of borehole. Cover probe tip with 15 cm of sand. Cover the sand with an 8–10 cm layer of dry bentonite to prevent water seeping into the sand pack from possible over hydrating of bentonite above.

4. Add bentonite grout (hydrating periodically throughout the installation) until reaching 15 cm below the next sample depth. Add 15 cm of sand then insert the next vapour sampling point (be sure to label the tubing at surface before you install in the borehole) and fill with 15 cm of sand, followed by 8–10 cm of dry bentonite then hydrate bentonite until next depth sample is reached. Use this procedure until all sample depths are completed (figure D.3-3).
5. Cut the protruding lengths of tubing at different lengths so that the deepest sample tube is the longest and the others progressively shorter. Having different lengths of tubing is helpful for identification if the labels on each tube are lost or become illegible.
6. Terminate surface ends of tubing with 2-way plastic valves (figure D.3-4), Swagelok nuts & caps or other appropriate end-caps.

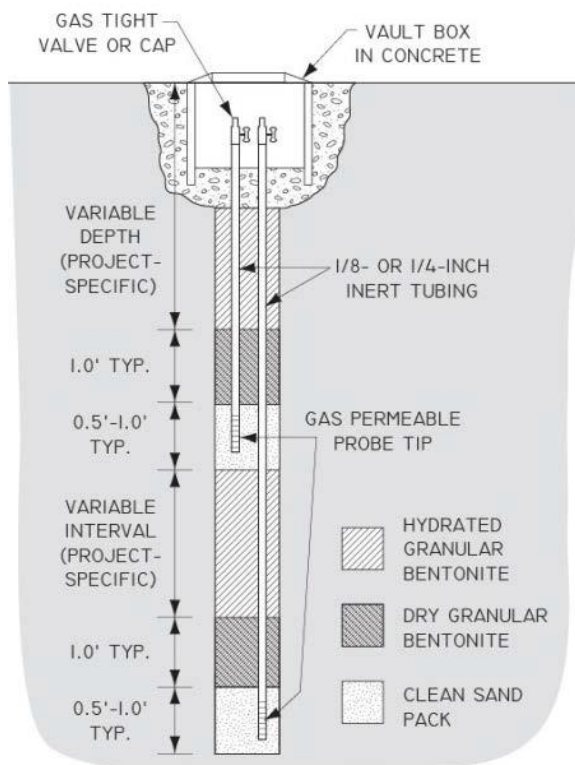


Figure D.3-3. Cross section of nested soil vapour sampling points installed at various depths.

Reproduced from CRC CARE (2013).

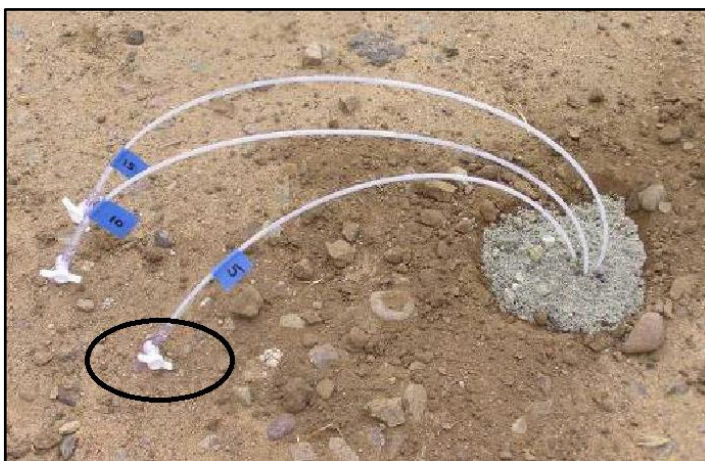


Figure D.3-4. Nested soil gas sample points in a single borehole. *Reproduced from CRC CARE (2013).*

1.1.1 Conduct leak detection test (prior to sampling)

Two methods of leak detection are recommended: (1) Performing a shut-in test of the sampling train and applying a leak detection compound to the vapour probe at the surface or (2) Applying a tracer gas over the probe and over the entire sampling apparatus.

Leak test method 1 – shut-in test and leak detection compound at surface

The shut-in test is performed by sealing the sampling train from the vapour probe tubing termination to the sample container (e.g. canister, Tedlar bag) and applying a vacuum to the sampling train. Hold the applied vacuum steady (not decrease) for at least 30 seconds. If the sampling train does not hold the vacuum, then recheck all connections for the leak and the shut-in test repeated. Record and report the start and end vacuum.

Figure D.3-5 is an example of a simple sampling train arrangement for a shut-in test. The system consists of a 2-way valve at the vapour probe termination, a vacuum gauge, and a 3-way valve on a gas-tight syringe. The 2-way valve is closed. A vacuum is then applied by drawing back the syringe plunger and the 3-way valve turned to shut off the syringe.



Figure D.3-5. Simple sampling train arrangement with vacuum gauge for a shut-in test. *Reproduced from CRC CARE (2013).*

Once the shut-in test has been successfully completed, a leak check compound is applied to the surface completion of the probe. The leak check compound can be

applied by wetting a towel with a liquid compound (e.g. isopropanol), making sure that cross-contamination does not occur, and placing it around the probe tubing at the ground surface, or by placing a small shroud over the surface completion and filling the shroud with a tracer gas (e.g. He).

Leak test method 2 – covering sampling train and probe with gaseous tracer

The second method involves enclosing the entire sampling apparatus, including the sample container, all tubing and connections, and the vapour probe surface completion in a shroud, which is filled with a tracer (figure D.3-6). This method is operationally more cumbersome as it requires a source of the gaseous tracer on site and it is difficult to turn on, turn off, and adjust the collection device once under the shroud but it provides a real time indication of whether there is a leak or not.

Testing the soil vapour sample for leaks

For the two leak test methods described above, it is advantageous to measure both the concentration of tracer compound in the shroud and the concentration of tracer compound in the soil vapour sample in the field using a hand-held field meter.



Figure D.3-6. Covering the entire sampling system & probe with a shroud. *Reproduced from CRC CARE (2013).*

Refer to CRC CARE (2013), appendix F for further details on testing the soil vapour sample for leaks.

Selection of leak detection compound

The selection of leak detection compounds is site and analysis specific. Considerations include whether it is a known or suspected contaminant at the site, or included in the laboratory's list of target analytes for the method being used, and whether it can be monitored with portable measurement devices. Common leak detection compounds are isopropanol and He.

CRC CARE (2013), appendix F presents the advantages and disadvantages of each detection compound.

Purge the probe and sample train

Purge volume

The sample collection equipment used for soil vapour sampling has an internal volume that is filled with air or some other inert gas prior to insertion into the ground. Completely purge this internal volume, often called the dead volume, and fill with soil vapour to ensure that a representative soil vapour sample is collected. If vapour wells (tubing) are installed and sampled the same day as installation (not recommended), include the air volume of the sand pack in the total system volume. Probe purging is typically accomplished using a pump or a syringe equipped with a 3-way valve. Purging may also be conducted using a portable PID or landfill gas meter where the reporting of stabilised parameters can be used to demonstrate that purging is complete and soil gas can be reliably sampled. Take care if the well has the potential to be wet.

At a minimum, withdraw enough vapour prior to sample collection to purge the probe and collection system of all ambient air or purge gas (1 purge volume).

While it is important to collect enough vapour to purge the system, collecting too much vapour can also have drawbacks. Thus, sampling equipment with small internal dead volumes offers advantages over systems with larger dead volumes.

It is recommended that the purge volume is consistent for all samples collected at the same depth from the same site.

Field-screen the soil gas sample

Field-screen the soil gas sample using a calibrated handheld multi-gas meter (e.g. Landtec GEM™5000, Landtech GA-90/GEM-2000, RKI-brand Eagle) to measure concentrations of fixed gases: O₂, CO₂ and CH₄. Implement precautions to ensure that VOCs are excluded from the CH₄ measurement through use of a granular activated carbon or charcoal filter on the inlet to the meter. Volatile organic compounds (VOCs) are also typically measured and can be performed in the field using a flame ionisation detector (FID) (e.g. Foxboro TVA1000). Similarly, an additional reading can be taken with carbon or charcoal filter on the inlet to the FID to measure CH₄-related response. Subtraction of the filtered from the unfiltered measurements provides the VOC concentration. If possible, use a N₂ analyser as a check-sum on the other gas results (the sum of O₂, CO₂, CH₄, N₂ and total VOCs should approach 100%). If CH₄ is elevated at an unexpected location, collect a gas sample for laboratory total petroleum hydrocarbons (TPH) analysis. Chain of custody sheets accompany all samples to the laboratory.

Collect the soil gas samples

Sampling considerations

When probes are installed, the in-situ soil vapour can be displaced and a period of time is required for the soil vapour to re-equilibrate. A United States Environmental Protection Agency (US EPA) study showed the following equilibration times were required to achieve 80% of the final value:

- Sampling through probe rod installed by hand: 15 minutes
- Sampling through probe rod installed with direct push methods: 30 minutes
- For probes where tubing is buried in a sandpack in the ground: 8 hours

This study was done in fine-grained soil. Equilibration times can be expected to be less in coarse grained soils.

It is generally considered to be good practice to only use dedicated connectors and tubing (from the soil gas well to the sampling media) for each location and to order the sampling of soil gas from areas where lower concentrations are expected to areas where higher concentrations are expected (where possible). This minimises the potential for cross-contamination and interference/bias/drift in field instruments that may be used.

Sample flow rate

Studies conducted by the US EPA suggest that flow rate does not appear to be an important variable on soil-vapour concentrations. However, for the purpose of collecting reliable soil gas samples in all soil types in Australia, a flow rate that is <500 mL/min is recommended.

When sampling using canisters of 1–1.5 L, a sampling time of a few minutes to 2 hours is appropriate.

Applied vacuum during sampling

Some guidance documents require applied vacuums at the probe to be less than 25 kiloPascal (kPa). However, for high permeability soils, a qualitative method is typically all that is necessary to estimate if there is little permeability and if too much vacuum is likely to be created during sampling. Connect a 20–50 mL gas-tight, syringe to the probe and pull on the plunger. If the plunger can be pulled easily, there is high permeability and the applied vacuum will likely be small. If the plunger is hard to pull (compared to pulling outside air) or if the plunger retracts towards the probe after being released, then there is likely to be too little permeability to get an uncompromised sample.

For low permeability soils, a quantitative method is preferable using a vacuum gauge placed between the probe and sample container (figure D.3-5). If canisters are being used to collect the soil vapour sample, be aware that a gauge on the Summa canister measures the vacuum in the canister, not the vacuum applied to the soil vapour probe. Place an additional gauge in the sampling train between the flow regulator on the canister and the probe. For gauges located on the flow restrictors, check with the supplying laboratory to determine if they measure the vacuum in the canister or vacuum at the probe tip.

Sample collection into gas-tight (Tedlar®) bags

After purging and application of the leak detection compound over the probe, soil vapour can easily be transferred from the soil vapour probe into a gas-tight bag using a certified clean glass or Teflon® syringe (figure D.3-7A). Other devices such as a vacuum chamber (available from SKC, Inc.) can also be used to fill gas-tight bags (figure D.3-7B), but do not use pumps upstream of the bag as cross-contamination between samples will occur. Fill the bag, while being careful not to over-inflate and potentially compromise the bag seals.

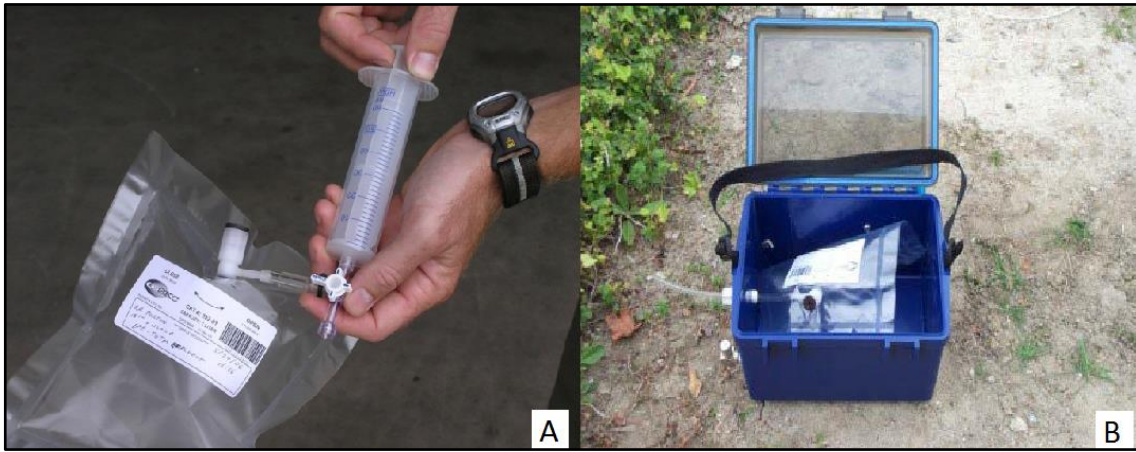


Figure D.3-7. A) Filling a gas-tight bag using a syringe and 3-way valve. Top of the valve is connected to the probe tubing. B) A vacuum chamber (sometimes called a lung-box) to inflate gas-tight bags. Reproduced from CRC CARE 92013).

Using gas-tight bags offers the advantage of testing the actual soil vapour sample that will be later analysed for the VOCs for the leak detection compound (this is not possible with canisters). Connect the portable meter directly to the gas-tight bag and measure the tracer compound (it may also be useful to field-screen fixed gases and VOCs at this time). If it is below acceptable levels, then the soil vapour sample is valid and the remaining amount in the bag can be sent off for analysis. If it is above acceptable levels, the gas-tight bag is easily emptied and can be reused for the same soil vapour sample location once the leak is found and corrected.

Storage time in gas-tight bags for petroleum hydrocarbons is approximately 48 hours, meaning the samples must reach the laboratory and be analysed within 48 hours of sampling. Also, pick a bag that has been shown by the manufacturer or your laboratory to be stable for the compounds of interest. Take care not to puncture or compress the bag during storage. It is best, but not necessary, to store the sample in the dark. Never chill the bags. They can be shipped by air provided they are not completely filled (to allow for pressure changes during the flight). If storage times longer than 48 hours are anticipated, or if a more durable storage container is desired, the sample in the Tedlar® bag can be transferred into a passivated canister. When undertaking such a transfer, take care to ensure the transfer line is leak free and that the potential for cross contamination is minimised. It is also possible that some of the higher boiling point VOCs can adsorb to the internal surface of the bag and be lost to the sample on transfer.

Sample collection into passivated (summa) canisters

For the sampling of soil vapour it is only necessary to collect a small volume of sample. Hence, a 1 to 1.5 L canister is suitable. Sampling of soil vapour is not recommended using large volume canisters (such as 6 L canisters).

Certify passivated canisters clean by the laboratory prior to sampling. This certification can be done either as a batch or on an individual canister basis. Both are suitable for the sampling of soil gas.

Prior to sampling, check the canister to ensure that a vacuum of approximately 88 to 100 kPa is present (note vacuum gauges on canisters typically have an accuracy of +/- 17 kPa although digital gauge can have an accuracy of +/- 0.8 kPa. Connect the

canister to the probe tubing, but do not open, before leak testing has been completed (or a tracer compound is applied) and the well has been purged.

Once the leak detection compound is applied, test an aliquot of the soil vapour for the tracer compound before opening the canister. This is typically done by having a sampling port next to the canister connection (using a Swagelok tee connection or a 3-way plastic valve). If the leak detection compound is below acceptable levels, the well can be purged and canister can then safely be opened. If the leak detection compound is above acceptable levels, then do not sample. Instead, disconnect the canister, and find and correct the source of the leak. By following this procedure, you will avoid filling canisters with soil vapour samples that fail the leak detection test.

If a large volume canister is being used (>1000 mL) or if the sample depth is very close to the surface (e.g. sub-slab samples), retest the soil vapour probe for the leak detection compound after the canister is filled. This is necessary because the canister cannot be tested for the leak detection compound in the field, if the soil vapour is leak-free after the canister is filled, it is reasonable to conclude the sample in the canister is leak free also.

To ensure that a sufficiently low flow rate is achieved, use flow regulators, available from the laboratory. At the completion of sampling, leave a slight negative vacuum in the canister. Do not cool canisters nor leave them in the direct sunlight during storage or transport for analysis.

Log soil gas probe sampling

Record field observations, installation details, leak tests results, purging and sampling measurements in a sampling log.

Record the date, time, sample location name, and the field instrument reading(s) on sample bag label and on data sheets or in logbooks.

Do not label bags directly with a marker or pen (particularly those containing volatile solvents) nor affix adhesive labels directly to the bags. Tie labels to the metal eyelets provided on the bags.

Equipment blanks

Collection of an equipment blank is recommended. Draw clean air or nitrogen through the probe tubing, probe tip, and the sampling train at the start of the field program. Analyse the collected sample for the same compounds as the soil vapour samples.

D.4 – Field procedure for alternative soil gas measurements

The information presented in this section was extracted from the following sources:

- Sweeney, RE & Ririe, GT 2017, 'Small purge method to sample vapor from groundwater monitoring wells screened across the water table', *Groundwater Monitoring & Remediation*, vol. 37, Issue 4, pp. 51–59.
- API 2017, *Quantification of vapor phase-related NSZD processes*, Publication No. 4784.
- Commonwealth Scientific and Industrial Research Organisation (CSIRO) 2016, *Safe work instruction: In-well soil gas sampling and temperature monitoring*, CSIRO Land and Water; Pollutant Fate and Remediation Team.
- CRC CARE 2013, *Petroleum hydrocarbon vapour intrusion assessment: Australian guidance*, CRC CARE Technical Report no. 23. CRC for Contamination Assessment and Remediation of the Environment, Adelaide, Australia.

Purpose and scope

The purpose of this procedure is to provide practical guidelines for alternative soil gas measurements. Soil gas profile measurements are used as a basis to estimate the NSZD rate using the gradient method.

Equipment and materials

- Personal protective equipment
- 3 mm outer diameter (OD) or 6 mm OD nylon, Teflon® or stainless steel probe. 3 mm OD tubing is easier to drop down a bore hole than 6 mm OD tubing. Nylon tubing is recommended over Teflon® tubing. Stainless steel probing may be logistically impractical to use due to its inflexibility.
- Stainless steel, ceramic or plastic probe tip.
- Surface termination on tubing: Swagelok fittings or plastic valves (2-way inert plastic valves or stop cocks). An end-cap can also be used. If a valve is used, it is important to secure it tightly to tubing, as the valve is a permanent component of the soil vapour collection system.
- Well cap with valve that allows tubing from within the well to be connected to a field gas analyser at the surface.
- Leak check compound and towel, or shroud to cover the entire sampling system and probe.
- Nitrile gloves.
- Pump or syringe equipped with a 3-way valve.
- Vacuum gauge.
- Field gas analyser(s) (photo-ionisation detector (PID), Foxboro TVA1000, Landtec GEM™ 5000 or Landtech GA-90/GEM-2000, RKI-brand Eagle).
- Temperature meter.
- Sample containers (Tedlar® bags or Summa canisters).
- Field logbook.

The materials used may differ from those presented in this appendix. However, regardless of the materials used, it is important that an equipment blank is conducted to demonstrate that the materials used are clean and suitable for use.

The tubing sizes outlined in this appendix are recommendations only. Different tubing sizes can be utilised provided they can be properly connected. The conduct of leak testing (including the testing of the sample train) is important to demonstrate that all such connections are tight and the installed soil vapour probe and sample train are suitable for the collection of a soil gas sample.

Procedures and guidelines

Existing monitoring well

Groundwater monitoring wells are present at most hydrocarbon release sites that are being assessed for clean-up. If screened across the vadose zone, these wells provide an opportunity to collect vapour samples that can be used in the evaluation of vapour movement and biodegradation processes occurring at such sites (Sweeney & Ririe 2017). This screening method is adequate for evaluating NSZD potential at light non-aqueous phase liquid (LNAPL) sites using the gradient method. They are considered screening-level primarily because the vapour sample is a composite from the total length of the screen that is open to the unsaturated zone and can't often be associated with a specific depth needed for use in the gradient method.

Sweeney & Ririe (2017) presented a low purge volume method (modified after that developed by the US EPA, large purge method) for sampling vapour from monitoring wells that is easy to implement and can provide an assessment of the soil gas total petroleum hydrocarbon (TPH) and oxygen (O₂) concentrations at the base of the vadose zone. The results of this study show that a low purge volume method is consistent with biodegradation models especially for sampling at sites where low permeability soils exist in and around a LNAPL source zone. The small purge method provides a more rapid and cost-effective approach compared with installation of deep gas sampling probes at a site (Sweeney & Ririe 2017).

Both the large and the small purge methods involve using a cap on the monitoring well with a valve that allows tubing from within the well to be connected to a field gas analyser at the surface. The large purge volume method also includes a pump that removes the gas at 10 L/min. For testing the small purge volume method, use a field instrument to pump the gas at a rate of 1 L/min.

There are three differences between the two methods: (1) pumping rate, (2) purge volume removed, and (3) placement of the tubing in the well, as shown in figure D.4-1 (Sweeney & Ririe 2017).

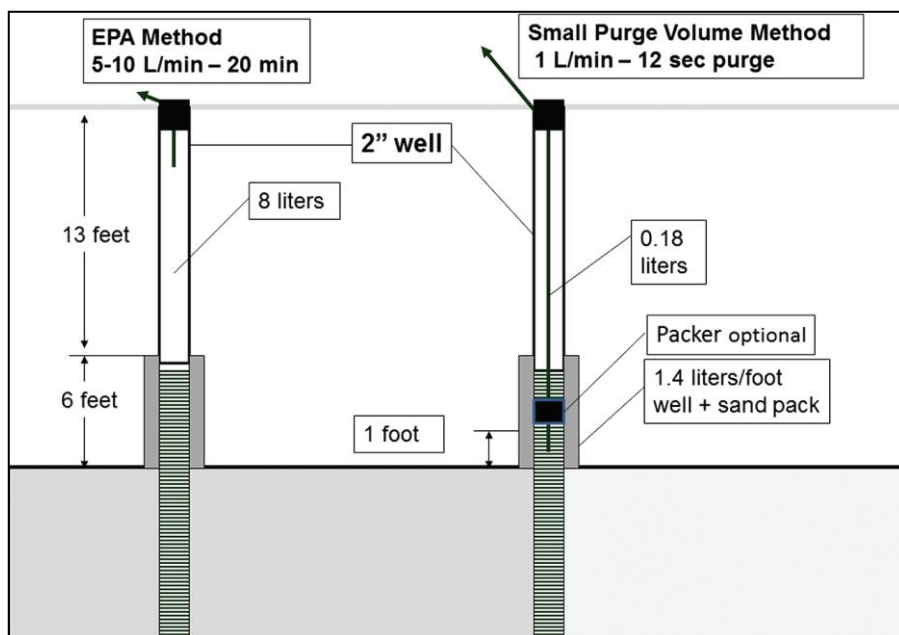


Figure D.4-1. Comparison between EPA and the smaller purge volume method for obtaining vapour samples from monitoring wells. *Reproduced with permission from Sweeney and Ririe (2017).*

Determine the limit of the volume of gas to remove from the well by adding the well casing volume to a multiplication of the surrounding volume of soil by the estimated air-filled porosity. The time it would take for a significant increase in O₂ concentration (greater than 2%v) to be observed would be the volume limit divided by the pumping rate. Samples are collected in Tedlar® bags for vapour concentration analysis and subsequent NSZD rate calculation using the gradient method.

The concentrations of O₂ and CO₂ at the ground surface at most exterior locations can be reasonably approximated by those of ambient air. Soil gas concentrations at the ground surface (zero depth) can be assumed to be in equilibrium with the concentrations in ambient air: O₂ at 20.9%, and CO₂ at 0.03%. These are the upper boundary control points for the gradient method. In combination with using the ground surface as the upper boundary control point, a single probe at the right subsurface depth (i.e. at the lower boundary control point) can define a gradient with reasonable accuracy (API 2017). Thus, an existing groundwater monitoring well screened across the right subsurface depth can be used to estimate dC/dz .

Considerations

Ensure existing monitoring wells have at least 0.3 m of screen that is open to the vadose zone.

Locate some wells over the LNAPL footprint (over the petroleum hydrocarbon-impacted soils, but not near release location) and others outside the LNAPL footprint (background wells).

If the site presents different soil conditions, select existing wells that are located over the different soil types. Different site conditions, e.g. a dramatic change in the ground cover, can impact the deep vadose zone soil vapour concentrations and affect NSZD rates.

The low purge volume method is recommended over the large purge method for sampling at sites where low permeability soils exist in and around a LNAPL source zone.

Sampling from an existing monitoring well

For the large purge volume method, use a pump that removes the gas at 10 L/min. For testing the small purge volume method, use a field instrument to pump the gas at a rate of 1 L/min.

Determine the limit of the volume of gas to remove from close to the LNAPL source zone by the time (volume) it would take for a significant increase in O₂ concentration (greater than 2%v).

Use the following procedures to collect a soil vapour sample (CSIRO 2016):

1. Put on nitrile gloves.
2. Start up the field gas analyser, allow to warm up for 90 seconds before use.
3. Ensure that the instrument is in the correct measuring mode.
4. Note: calibrate the instrument and zero it prior to commencing work.
5. Measure and record the time and fluid levels in the well with an interface probe.
6. Record well details, condition, materials, diameter, odours, groundcover and any other pertinent observations.
7. Select appropriate end-cap to seal the top of well and adjust tubing length by loosening the cable gland on the end-cap and drawing the tubing through. Tighten the cable gland around the tubing so that the length of tube on the underside of the well cap positions the intake 300 mm above the fluid level. Double check this measurement to avoid contaminating the end of the tube with hydrocarbon.
8. Lower the weighted tubing into well. Place end-cap on well stickup and ensure a tight seal Tape join with PVC tape if necessary.
9. Connect the field gas analyser to the tubing.
10. Pump vapour from well and record gas composition (O₂, CO₂, CH₄, volatile organic compounds (VOC) (may also include hydrogen sulphide (H₂S), nitrogen (N₂)). Minimum response time is 30 seconds for the combined MX4 and MX6 sensors or 25 seconds for the RKI Eagle 2. Record gas concentration data every 30 seconds to indicate when purging is complete and gas compositions are most representative of equilibrated soil gas. If possible, use a N₂ analyser as a check-sum on the other gas results (the sum of O₂, CO₂, CH₄, N₂ and total volatile organic compounds (VOCs) should approach 100%).
11. If the pump starts to strain the formation or well screens may be blocked, there will then be no flow of gas into the well and measurements, stop the pump. Document the action in the field notes.
12. All data will be recorded in a field note book including: date, time, operators, instrument details, well name and location, results, fluid levels and interface, gas concentrations and observations.

Because data from sampling existing monitoring wells is typically used for screening-level purposes, leak tests are not always necessary. However, for higher data quality purposes, refer to appendix C.3 for leak detection test and soil gas samples collection process.

D.5 – Example gradient method-based NSZD rate calculations

A case study with example calculations is presented in this section to illustrate how this guidance for NSZD rate measurement using the gradient method can be applied. It is based on a real setting where NSZD monitoring was performed.

Site background

The gradient method was employed, in conjunction with the dynamic closed chamber (DCC) technology, at a former natural gas well site that was co-located compressor station in central Alberta, Canada in 2015. Six vapour monitoring probe clusters were installed with five to eight probes at varying depths per location in April 2015. Soil vapour data was collected in April, August and October. Additionally, the site was divided into two areas based on surface cover: gravel and vegetated.

Vapour monitoring probes installation

Vapour monitoring probes (VMPs) were installed on the site as follows (figure D.5-1):

- Four vapour monitoring probes to measure soil gas concentrations within the LNAPL plume footprint:
 - On vegetated area (southern portion): TC13 and TC16
 - On gravel pad cover (northern portion): TC09 and TC25
- Two vapour monitoring probes in background locations (outside the LNAPL plume footprint):
 - On vegetated area (southern portion): TC06
 - On gravel area (northern portion): TC07

The lower section of the VMPs consisted of an expendable stainless steel implant anchor connected to a 152 mm long and 6.4 mm diameter (stainless steel) mesh screen (0.15 mm pore openings). The clusters consisted of five to eight depth-discrete sampling probes, depending on the locations, distributed from approximately 0.4 mbg to slightly above the average water table, which ranged from 1.41 to 2.79 mbg.

Soil vapour sampling and in-situ tracer test

1. A negative-pressure leak test was conducted on the sampling train. A helium (He) leak test was also performed on each sample probe. Results of the field tests and analytical data indicated no significant leaks in the sampling train and all He detections were within specifications.
2. Soil gas samples were collected into Tedlar® bags using the vacuum box method and field-screened with a landfill gas analyser to measure concentrations of O₂, CO₂, CH₄, H₂S and VOCs. A Landtec GEM™2000 was used to measure O₂, CO₂, CH₄, H₂S and a RKI Eagle II was used to measure VOCs and O₂ (used for a QC check).
3. Soil gas sampling results were summarised and presented in table D.5-1.
4. Following collection of the soil gas samples, in-situ soil vapour diffusivity testing was conducted in twelve sampled soil gas probes using He as the tracer gas. The tests were conducted according to the procedures outlined in Johnson *et al* (1998)

and API 2017. He diffusion data was excluded from calculations if methane is detected at the same location/depth due to interference of CH₄ with the field He detector instrument. In-situ soil vapour diffusivity testing results are presented in table D.5-2.

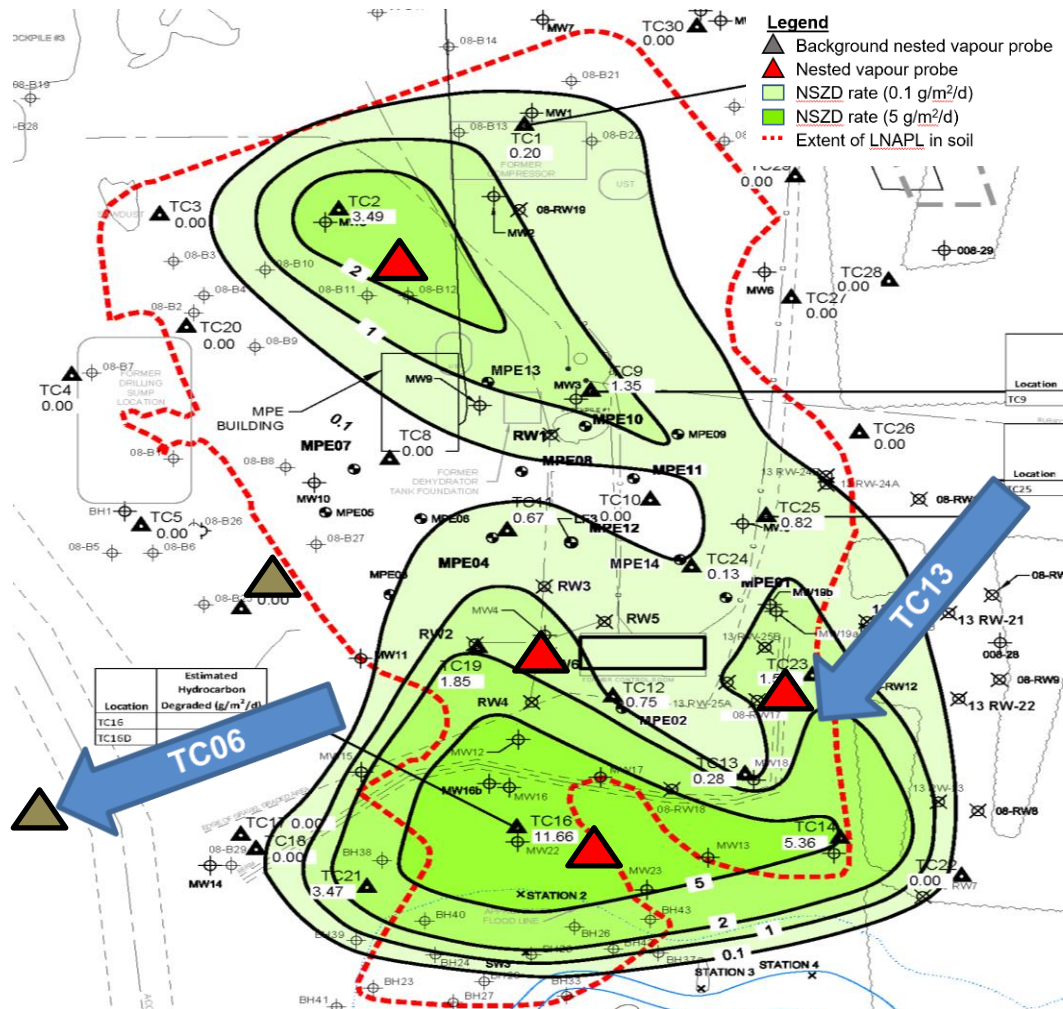


Figure D.5-1. Gradient method case study site plan.

Effective soil vapour diffusion coefficient calculation, D_{He}^{eff}

For each location, the value of the effective diffusion coefficient for the tracer gas He (D_{He}^{eff}) was determined using equation D.1.

$$\text{Equation D.1: } D_{He}^{eff} = \left[\frac{\theta_V^{1/3}}{\beta} \right] \left[\frac{1}{4t_s} \right] \left[\frac{3V_S}{4\pi} \right]^2$$

where θ_V is the air-filled porosity (cm³-vapour/cm³-soil), t_s is the residence time of the tracer in the subsurface (s), and V_S is the volume of vapour extracted at the end of the test (cm³).

1. The air-filled porosity θ_V for the site has been assumed to be 0.3 cm³/cm³ (per justification provided by Johnson *et al* 1998).

The value of β has been determined using the graphic shown in figure D.1-3, excerpted from Johnson *et al* (1998), where η is the fraction of mass recovered, calculated as the measured concentration of the recovered gas (ppmv) divided by the initial injected concentration of the gas (ppmv).

- For location TC13, at 0.4 mbg:

$$\eta_{0.4mbg}^{TC13} = \frac{14850 \text{ ppmv}}{48600 \text{ ppmv}} = 0.31$$

- For location TC13, at 1.2 mbg:

$$\eta_{1.2mbg}^{TC13} = \frac{27000 \text{ ppmv}}{48600 \text{ ppmv}} = 0.56$$

- V_o is the volume of the injected gas (L) and V_s is the volume of the injected gas extracted at the end of the test (L).

- For location TC13, at 0.4 mbg:

$$\frac{V_o^{TC13}}{V_{s0.4mbg}} = \frac{1 \text{ L}}{1 \text{ L}} = 1$$

- For location TC13, at 1.2 mbg:

$$\frac{V_o^{TC13}}{V_{s1.2mbg}} = \frac{1 \text{ L}}{1 \text{ L}} = 1$$

- With the values calculated above, using the graphic shown in figure D.1-3 (Johnson *et al* 1998), the values of β are:

- For location TC13, at 0.4 mbg:

$$\beta_{0.4mbg}^{TC13} = 1.1$$

- For location TC13, at 1.2 mbg:

$$\beta_{1.2mbg}^{TC13} = 3$$

2. The values of t_s , the sampling times, are:

$$t_{s0.4mbg}^{TC13} = 960 \text{ s}$$

$$t_{s1.2mbg}^{TC13} = 840 \text{ s}$$

Table D.5-1 Soil gas sampling results

Ground cover type	Location	Depth (mbg)	GEM2000					RKI Eagle II			
			O ₂ (%)	CO ₂ (%)	CH ₄ (%)	H ₂ S (ppmv)	Barometric pressure (kPa)	VOCs (HEX) (ppmv)	VOCs (IBL) (ppmv)	O ₂ (%)	
Grass	TC06 background	0.4	20.3	0.8	0.0	0.0	89.4	0	0	20.9	
		0.8	18.9	2.8	0.0	0.0	89.4	0	0	19.1	
		1.2	19.1	2.7	0.0	0.0	89.4	0	0	19.3	
		1.6	18.6	3.3	0.0	0.0	89.7	0	0	18.6	
		2.0	17.7	4.3	0.0	0.0	89.7	0	0	17.8	
		2.4	17.8	4.5	0.0	0.0	89.7	0	0	17.4	
	TC13	0.4	20.3	0.9	0.1	0.0	90.8	35	74	20.4	
		0.8	17.9	4.0	0.2	0.0	90.8	30	35	17.7	
		1.2	15.5	6.2	0.1	0.0	90.8	25	83	15.4	
		1.6	9.9	11.8	0.3	0.0	90.8	0.0	50	10.1	
		TC16	0.4	19.7	0.7	0.2	0.0	90.8	105	150	20.9
			0.8	15.0	4.9	0.2	0.0	91.1	80	130	15.6
1.2	14.5		7.2	0.2	0.0	90.8	70	142	14.5		
Gravel	TC07 background	0.8	11.9	7.0	0.0	0.0	90.1	0.0	10	12.4	
		1.2	11.6	7.4	0.0	0.0	90.1	0.0	4.0	11.0	
		1.6	11.1	8.0	0.0	0.0	90.1	0.0	3.0	10.7	
		2.0	9.6	9.5	0.0	0.0	90.1	0.0	3.0	9.3	
		2.4	9.5	9.7	0.0	0.0	90.1	0.0	3.0	9.1	
		2.8	10.2	9.1	0.0	0.0	90.1	0.0	3.0	9.9	
	TC09	0.4	20.9	0.3	0.0	0.0	90.4	0.0	4.0	20.9	
		0.8	1.3	15.9	2.3	0.0	90.4	540	472	1.3	
		1.2	0.6	17.4	5.5	1.0	90.4	1250	884	0.4	
		1.6	1.0	17.5	4.9	1.0	90.4	1150	794	0.6	
		2.0	0.6	18.4	9.3	0.0	90.4	1500	959	0.6	
	TC25	0.4	19.8	0.2	0.0	0.0	90.1	0.0	2.0	20.1	
		0.8	19.3	0.3	0.0	0.0	90.1	0.0	2.0	19.3	
		1.2	18.6	0.2	0.0	0.0	90.1	0.0	2.0	18.5	
		1.6	18.4	0.2	0.0	0.0	90.1	0.0	2.0	18.5	
		2.0	18.2	0.4	0.0	0.0	90.1	0.0	3.0	18.5	
		2.4	15.1	0.2	0.0	0.0	90.1	0.0	3.0	15.3	
		2.8	13.6	0.2	0.0	0.0	90.1	0.0	3.0	13.8	

Table D.5-2. Soil Vapour Diffusivity Testing Results

Location	Depth (mbg)	Date	Injection				Extraction			
			Injected He conc. (ppm)	Volume (L)	Injection start time (hr:mm)	Injection duration (min)	Extraction start time (hr:mm)	Volume (L)	Extraction duration (min)	Equilibrium extracted He conc. (ppm)
TC07	0.4	15/10/2015	48600	1	17:45	-	17:58	1	-	10000
TC07	1.2	15/10/2015	48600	1	18:03	-	18:16	1	-	5600
TC07	2.0	15/10/2015	48600	1	18:20	-	18:34	1	-	9000
TC07	3.2	15/10/2015	48600	1	18:38	-	18:53	1	-	24000
TC13	0.4	16/10/2015	48600	1	8:22	-	8:38	1	-	14850
TC13	1.2	16/10/2015	48600	1	8:41	-	8:55	1	-	27000
TC16	0.4	16/10/2015	48600	1	9:02	-	9:16	1	-	8600
TC16	1.2	16/10/2015	48600	1	9:21	-	9:35	1	-	26000
TC25	0.4	16/10/2015	48600	1	10:25	-	10:39	1	-	10200
TC25	1.2	16/10/2015	48600	1	10:42	-	10:55	1	-	12950
TC25	2.0	16/10/2015	48600	1	10:58	-	11:12	1	-	39000
TC25	2.8	16/10/2015	48600	1	11:15	-	11:27	1	-	30000

3. The values of V_s , the volumes of vapour extracted at the end of the test, are:

$$V_{s,0.4mbg}^{TC13} = 1000 \text{ cm}^3$$

$$V_{s,1.2mbg}^{TC13} = 1000 \text{ cm}^3$$

Thus, the values of the effective diffusion coefficient for the tracer gas He (D_{He}^{eff}) at TC13 are:

$$D_{He,0.4mbg}^{eff,TC13} = \left[\frac{0.3^{\frac{1}{3}}}{1.1} \right] \left[\frac{1}{4 \times 960s} \right] \left[\frac{3 \times 1000 \text{ cm}^3}{4\pi} \right]^{\frac{2}{3}}$$

$$D_{He,0.4mbg}^{eff,TC13} = 0.0061 \frac{\text{cm}^2}{s}$$

$$D_{He,1.2mbg}^{eff,TC13} = \left[\frac{0.3^{\frac{1}{3}}}{3} \right] \left[\frac{1}{4 \times 840s} \right] \left[\frac{3 \times 1000 \text{ cm}^3}{4\pi} \right]^{\frac{2}{3}}$$

$$D_{He,1.2mbg}^{eff,TC13} = 0.0026 \frac{\text{cm}^2}{s}$$

The approach chosen to estimate NSZD rates at this site was based on calculating the flux of O_2 consumption, therefore $D_{O_2}^{eff}$ is substituted for D_v^{eff} in equation 9 (Fick's first law of diffusion) and is calculated from D_{He}^{eff} by correcting for their difference in molecular diffusion coefficients in air (D_v^{air}) using equation D.2:

$$\text{Equation D.2: } D_{O_2}^{eff} = D_{He}^{eff} \left(\frac{D_{O_2}^{air}}{D_{He}^{air}} \right)$$

where $D_{O_2}^{air}$ is the molecular diffusion coefficient for O_2 ($0.21 \text{ cm}^2/s$) and D_{He}^{air} is the molecular diffusion coefficient for the tracer gas He ($0.70 \text{ cm}^2/s$).

$$D_{O_2,0.4mbg}^{eff,TC13} = 0.0061 \frac{\text{cm}^2}{s} \left(\frac{0.21 \frac{\text{cm}^2}{s}}{0.70 \frac{\text{cm}^2}{s}} \right)$$

$$D_{O_2,0.4mbg}^{eff,TC13} = 0.0018 \frac{\text{cm}^2}{s}$$

$$D_{O_2,1.2mbg}^{eff,TC13} = 0.0026 \frac{\text{cm}^2}{s} \left(\frac{0.21 \frac{\text{cm}^2}{s}}{0.70 \frac{\text{cm}^2}{s}} \right)$$

$$D_{O_2,1.2mbg}^{eff,TC13} = 0.00078 \frac{\text{cm}^2}{s}$$

The average $D_{O_2}^{eff}$ for location TC13 is calculated using:

$$D_{O_2,average}^{eff} = \frac{\sum_{i=1}^n D_{O_2,i}^{eff}}{n}$$

Where n is the number of values of $D_{O_2}^{eff}$ at each location, or number of diffusivity tests conducted at each location.

$$D_{O_2 \text{ average}}^{eff TC13} = \frac{0.0018 \frac{cm^2}{s} + 0.00078 \frac{cm^2}{s}}{2}$$

$$D_{O_2 \text{ average}}^{eff TC13} = 0.0013 \frac{cm^2}{s}$$

The same procedure was followed for each of the four locations where the soil vapour diffusivity test was conducted. The lowest average value was for TC13 (0.0013 cm²/s) and the highest value was for TC07 and TC29 (0.0038 cm²/s). Thus, the range of D_{O₂}^{eff} used for the follow-on calculations at this site was:

$$D_{O_2 \text{ low}}^{eff} = 0.0013 \frac{cm^2}{s} = 1.3 \times 10^{-7} \frac{m^2}{s}$$

$$D_{O_2 \text{ high}}^{eff} = 0.0038 \frac{cm^2}{s} = 3.8 \times 10^{-7} \frac{m^2}{s}$$

The lowest and highest values of D_{O₂}^{eff} were used to estimate the range of possible NSZD rates at the site.

Background correction and concentration gradient estimation, dC/dZ

The concentrations of the analysed gases, presented in table D.5-1, were plotted to obtain the soil gas concentration profiles for each location. For example, in the grass area, the results for the background location TC06 and the impacted location TC13 were paired and are shown on figure D.5-2.

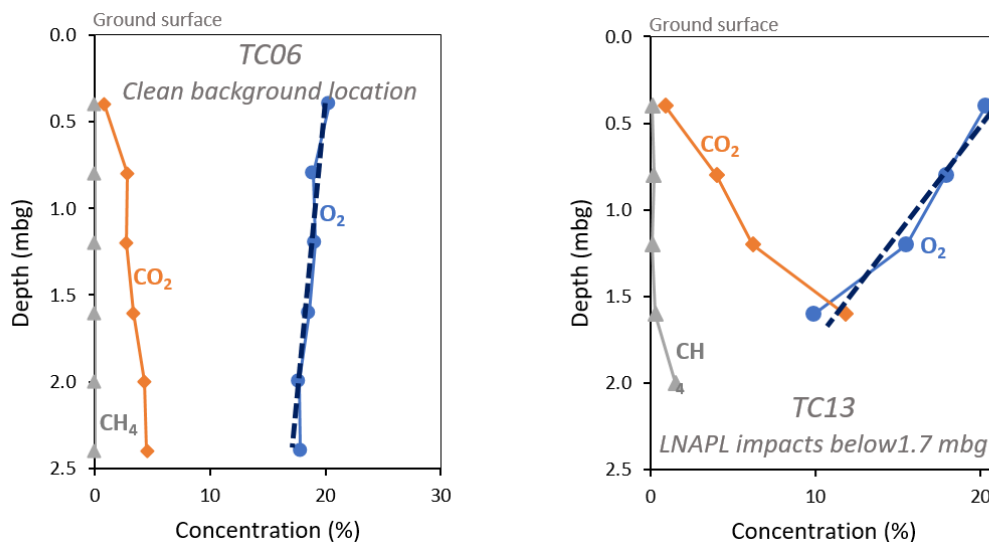


Figure D.5-2 Field monitoring results at background location TC06 and impacted location TC13

The approach chosen to estimate NSZD rates at this site was based on calculating the flux of O₂ consumption in the subsurface. The decision to use O₂ was a site-specific judgment based on review of the site-specific soil gas profiles. Table D.5-3 shows the selected upper (green shaded) and lower (beige shaded) boundary control points of measurement at TC06 and TC13. The lower boundary control point is the apparent depth to maximum O₂ depletion.

Table D.5-3. Upper and lower boundary control points for gradient calculations.

Ground cover type	Location	Depth (mbg)	GEM2000 O ₂ (%)
Grass	TC06 background	0.4	20.3
		0.8	18.9
		1.2	19.1
		1.6	18.6
		2	17.7
		2.4	17.8
	TC13	0.4	20.3
		0.8	17.9
		1.2	15.5
		1.6	9.9

The difference in concentration between the upper and lower boundary control points of measurement, divided by the vertical distance between the control points, gives an estimate of the vertical O₂ concentration gradient as shown in equation D.4.

$$\text{Equation D.4: } \frac{dC}{dz} = \frac{C_2 - C_1}{z_2 - z_1}$$

where, for this application, C₁ and C₂ are the O₂ concentrations at depths z₁ and z₂, respectively. Subscript 2 is for the lower boundary control point. Concentration values from the field are in % of O₂ by volume.

To estimate the mass consumed per year, it is necessary to convert the value of O₂ in % by volume to grams of O₂ per unit of volume using equation D.5.

$$\text{Equation D.5: } \frac{mg}{m^3} = ppmv \times \frac{MW}{0.08205 \times T}$$

where T is the ambient temperature in °K (°K = 273.15 + °C) and 0.08205 is the Universal gas constant in atm·m³/(kmol·K) The molecular weight (MW) of O₂ is 32 grams per mole (g/mol).

The values of T were assumed to be 25 °C at 0.4 mbg and 15 °C at 2.4 mbg. For the grass, background location TC06:

$$C_1^{TC06} = 20.3 \% = 203000 \text{ ppmv (0.4 mbg depth)}$$

$$C_1^{TC06} = 203000 \text{ ppmv} \times \frac{32 \frac{g}{mol}}{0.08205 \frac{atm \cdot m^3}{kmol \cdot oK} * (273.15 + 25)oK}$$

$$C_1^{TC06} = 266,000 \frac{mgO_2}{m^3}$$

$$z_1^{TC06} = 0.4 \text{ m}$$

$$C_2^{TC06} = 17.8 \% = 178000 \text{ ppmv (2.4 mbg depth)}$$

$$C_2^{TC06} = 178000 \text{ ppmv} \times \frac{32 \frac{g}{mol}}{0.08205 \frac{atm \cdot m^3}{kmol \cdot K} * (273.15 + 15)K}$$

$$C_2^{TC06} = 241,000 \frac{mgO_2}{m^3}$$

$$z_2^{TC06} = 2.4 \text{ m}$$

The concentration gradient at TC06 is then calculated as:

$$\frac{dC^{TC06}}{dz} = \frac{241000 \frac{mg}{m^3} - 266000 \frac{mg}{m^3}}{2.4 \text{ m} - 0.4 \text{ m}}$$

$$\frac{dC^{TC06}}{dz} = -12,500 \frac{mgO_2}{m^3m}$$

$$\frac{dC^{TC06}}{dz} = 12 \frac{gO_2}{m^3m}$$

Same calculations for the grass, impacted location TC13:

$$C_1^{TC13} = 20.3 \% = 203000 \text{ ppmv (0.4 mbg depth)}$$

$$C_1^{TC13} = 203000 \text{ ppmv} \times \frac{32 \frac{g}{mol}}{0.08205 \frac{atm \cdot m^3}{kmol \cdot K} \times (273.15 + 25)K}$$

$$C_1^{TC13} = 266,000 \frac{mgO_2}{m^3}$$

$$z_1^{TC13} = 0.4 \text{ m}$$

$$C_2^{TC13} = 9.9 \% = 99000 \text{ ppmv (1.6 mbg depth)}$$

$$C_2^{TC13} = 99000 \text{ ppmv} \times \frac{32 \frac{g}{mol}}{0.08205 \frac{atm \cdot m^3}{kmol \cdot K} \times (273.15 + 15)K}$$

$$C_2^{TC13} = 134,000 \frac{mgO_2}{m^3}$$

$$z_2^{TC13} = 1.6 \text{ m}$$

The concentration gradient at TC13 is then calculated as:

$$\frac{dC^{TC13}}{dz} = \frac{134000 \frac{mg}{m^3} - 266000 \frac{mg}{m^3}}{1.6 \text{ m} - 0.4 \text{ m}}$$

$$\frac{dC^{TC13}}{dz} = -110,000 \frac{mgO_2}{m^3m}$$

$$\frac{dC^{TC13}}{dz} = -110 \frac{gO_2}{m^3m}$$

The background O₂ flux was subtracted from the total flux measured above the source zone to estimate the NSZD rate in order to eliminate flux contributions from non-NSZD processes. Thus, at location TC13, the estimated concentration gradient was:

$$\frac{dC_{corrected}^{TC13}}{dz} = \frac{dC^{TC13}}{dz} - \frac{dC^{TC06}}{dz}$$

$$\frac{dC_{corrected}^{TC13}}{dz} = 110 \frac{gO_2}{m^4} - 12 \frac{gO_2}{m^4}$$

$$\frac{dC_{corrected}^{TC13}}{dz} = 98 \frac{gO_2}{m^3m}$$

NSZD rate calculation, J_{NSZD}

The steady-state diffusive flux of O_2 is calculated using Fick's first law of diffusion as shown in equation 9.

$$\text{Equation 9: } J_{O_2} = D_{O_2}^{eff} \left(\frac{dC}{dz} \right)$$

$$J_{O_2\ low}^{TC13} = D_{O_2\ low}^{eff} \times \left(\frac{dC_{corrected}^{TC13}}{dz} \right)$$

$$J_{O_2\ low}^{TC13} = 1.3 \times 10^{-7} \frac{m^2}{s} \times 98 \frac{gO_2}{m^3m} \times \frac{86400s}{d}$$

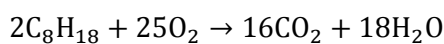
$$J_{O_2\ low}^{TC13} = 1.1 \frac{gO_2}{m^2 \cdot d}$$

$$J_{O_2\ high}^{TC13} = D_{O_2\ high}^{eff} \times \left(\frac{dC_{corrected}^{TC13}}{dz} \right)$$

$$J_{O_2\ high}^{TC13} = 3.8 \times 10^{-7} \frac{m^2}{s} \times 98 \frac{gO_2}{m^3m} \times \frac{86400s}{d}$$

$$J_{O_2\ high}^{TC13} = 3.2 \frac{gO_2}{m^2 \cdot d}$$

LNAPL loss rates are calculated based on the O_2 flux values by first selecting a representative hydrocarbon composition of C_8H_{18} (octane). The balanced oxidation equation for C_8H_{18} is:



The MW of C_8H_{18} is 114 g/mol and MW of O_2 is 32 g/mol. The balanced stoichiometric equation indicates that 2 moles of C_8H_{18} react with 25 moles of O_2 . Using the MWs:

$$2\ mol \times MW\ C_8H_{18} = 2 \times 114 \frac{g}{mol} C_8H_{18} = 228\ g\ C_8H_{18}$$

$$25\ mol \times MW\ O_2 = 25 \times 32 \frac{g}{mol} O_2 = 800\ g\ O_2$$

This means that when 228 g of C_8H_{18} are consumed, 800 g of O_2 are depleted. Thus, the stoichiometric conversion ratio for $C_8H_{18} : O_2$ is:

$$\text{Stoichiometric Ratio } C_8H_{18} : O_2 = \frac{228\ g\ C_8H_{18}}{800\ g\ O_2} = 0.285 \frac{g\ C_8H_{18}}{g\ O_2}$$

This stoichiometric ratio is then used to convert the O_2 flux into an NSZD rate as follows:

$$J_{NSZD\ low}^{TC13} = J_{O_2\ low}^{TC13} \times \text{Stoichiometric Ratio } C_8H_{18} : O_2$$

$$J_{NSZD_{low}}^{TC13} = 1.1 \frac{gO_2}{m^2 \cdot d} \times 0.285 \frac{g C_8H_{18}}{g O_2}$$

$$J_{NSZD_{low}}^{TC13} = 0.31 \frac{g C_8H_{18}}{m^2 \cdot d}$$

$$J_{NSZD_{high}}^{TC13} = J_{O_2_{high}}^{TC13} \times \text{Stoichiometric Ratio } C_8H_{18} : O_2$$

$$J_{NSZD_{high}}^{TC13} = 3.2 \frac{gO_2}{m^2 \cdot d} \times 0.285 \frac{g C_8H_{18}}{g O_2}$$

$$J_{NSZD_{high}}^{TC13} = 0.91 \frac{g C_8H_{18}}{m^2 \cdot d}$$

The estimated mass-based NSZD rates at grass location TC13 using the gradient method ranged from approximately 0.31 to 0.91 grams octane per day by square metre ($g C_8H_{18}/m^2/d$).

Applying an LNAPL density of 0.85 gram of hydrocarbon per cubic centimetre (g/cm^3), the NSZD rate can be expressed the volumetric units of litre per hectare per day (L/ha/d):

$$J_{NSZD_{low}}^{TC13} = 0.31 \frac{gHC}{m^2 \cdot d} \times \frac{1}{\frac{0.85gHC}{cm^3}} \times \frac{0.001L}{cm^3} \times \frac{10000m^2}{ha} = 3.6 \frac{L}{ha \cdot d}$$

$$J_{NSZD_{high}}^{TC13} = 0.91 \frac{gHC}{m^2 \cdot d} \times \frac{1}{\frac{0.85gHC}{cm^3}} \times \frac{0.001L}{cm^3} \times \frac{10000m^2}{ha} = 11 \frac{L}{ha \cdot d}$$

The estimated volumetric-based NSZD rates at grass location TC13 using the gradient method ranged from approximately 3.6 to 11 L/ha/d.

APPENDIX E.

Passive flux trap-based NSZD evaluation procedures

This appendix contains procedures useful for practitioners to reference when implementing the passive flux trap method for NSZD evaluation. The following procedures are included herein:

E.1 – Procedure for passive flux trap method data analysis (including background correction)

E.2 – Manufacturer-recommended passive flux trap field procedures

E.3 – Example passive flux trap method-based NSZD rate calculations

E.1 – Procedure for passive flux trap method data analysis (including background correction)

The information presented in this section was extracted from the following source(s):

- API 2017, *Quantification of vapor phase-related NSZD processes*, Publication No. 4784.
- ASTM International 2002, *Standard test method for rapid determination for carbonate content of soils*, D4373-02.
- ASTM International 2016, *Standard test methods for determining the biobased content of solid, liquid, and gaseous samples using radiocarbon analysis*, D6686-16.
- Hua, Q, Barbetti, M & Rakowski, AZ 2013, 'Atmospheric radiocarbon for the Perdio 1950-201', *Radiocarbon*, vol. 55, no. 4, pp. 2059–2072.
- McCoy, K, Zimbron, J, Sale, T & Lyverse, M 2014, 'Measurement of natural losses of LNAPL using CO₂ traps', *Groundwater*, vol. 53, no. 4, pp. 658–667.
- Stuiver, M & Polach, HA 1977, 'Discussion – reporting of ¹⁴C data', *Radiocarbon*, vol. 19, no. 3, pp. 355–363.

Purpose and scope

The passive flux trap method is composed of a chemical trap to collect CO₂ gas moving from the subsurface to the atmosphere. As described in detail in section 4.4 of the main text, the amount of CO₂ collected on a sorbent over a known cross-section area and period of time can be used to calculate the CO₂ efflux. The rate of NSZD can then be estimated with a representative petroleum hydrocarbon and stoichiometric conversion. This appendix describes the application of passive CO₂ flux traps to estimate a site-wide NSZD rate.

This procedure provides step-by-step instructions, ranging from the installation of the CO₂ flux traps through to the calculation of the NSZD rate. Appendix E.2 provides specific procedures for execution of the field work. Example passive flux trap method-based NSZD rate calculations are included in Appendix E.3.

Prerequisites

It is assumed that the following prerequisites have been met prior to use of this procedure:

- Data needs, objectives, and quality levels are established to appropriately scope the effort
- An appropriate number of monitoring locations was selected for passive flux trap analysis, adequate to meet the data objectives and represent the potential range of NSZD rates at the site.

Equipment

- Personal protective equipment
- CO₂ Traps (receiver pipes, trap body, protective cover)
- Rubber sleeves and hose clamps for connecting the trap bodies to the receiver pipes
- Rubber mallet
- Flathead screwdriver or nut driver tool
- 15 cm diameter post-hole digger or drain spade
- Hand trowel
- 19 L bucket(s) and/or plastic sheeting for soil storage
- ASTM International D-698 Standard Proctor Compaction Hammer (2.5 kg with 30 cm drop)
- Field logbook

Procedures and guidelines

Use of the passive flux trap method to estimate the rate of NSZD involves the following steps:

1. Install/deploy the passive flux traps
2. Retrieve the traps, pack, and return ship them to a specialty laboratory
3. Perform laboratory analysis of carbon and radiocarbon 14 (¹⁴C)
4. Assess the modern (background) and fossil fuel (NSZD) carbon fractions to compensate for background flux
5. Calculate the NSZD rate

The following sections detail how to accomplish each step.

Install/deploy the passive flux traps

The procedure provided below describes protocols for installation of passive CO₂ traps. CO₂ traps are used to evaluate NSZD rates of LNAPL in soil. The CO₂ traps measure flux of CO₂ migrating out through the ground surface. This appendix presents a list of tools required for installation, deployment timing, associated QA/QC, and CO₂ trap retrieval and shipping procedures.

Location selection

The CO₂ traps are used to investigate the CO₂ efflux that originates from a subsurface petroleum hydrocarbon source at locations across the LNAPL footprint. Spatial distribution of the CO₂ traps is limited since they can be costly to install and analyse. Analysis requires an off-site laboratory and the ¹⁴C analysis greatly impacts the cost. The use of ¹⁴C analysis is considered valuable since it eliminates the need for additional background measurement locations. The number of traps needed to obtain a representative spatial distribution needs to be determined on a site-specific basis by taking into account the objectives of the NSZD monitoring program along with other site constraints.

Information such as the LNAPL distribution, local site geology, and release locations obtained from site investigations can be used to aid in the selection of CO₂ efflux measurement locations. It is recommended that CO₂ traps are located near

groundwater monitoring wells or soil borings, thus known subsurface information can be used to help interpret the NSZD measurement results.

At the lowest recommended frequency, generally assign an individual CO₂ trap to all distinct areas of LNAPL consistency, geologic, and hydraulic characteristics. Therefore, CO₂ trap measurements will be obtained from each unique source area at the site barring site-specific conditions that require otherwise. Typically, more than one trap will be installed in each distinct area to improve understanding of the geospatial heterogeneity.

Ground surface conditions also influence the selection of the CO₂ trap locations. Surface or shallow subsurface staining associated with recent spills can cause CO₂ efflux values to be anomalously high and thus the measured efflux would overestimate the efflux due to the LNAPL body of interest typically spread deeper in the formation within the capillary fringe and zone of water table fluctuation. An additional site-specific consideration for the passive flux method is impediments to gas flow between the subsoil and atmosphere. Impervious zones and surface amendments (e.g. concrete foundations or parking lots), compacted areas (e.g. heavily used dirt roads), or low permeability zones can act as a confining layer to the subsurface soil vapour. If this layer is broken by the installation of a CO₂ trap, then this may channel the soil vapour through the trap creating a chimney effect and high-bias the results. Therefore, do not install the traps in concrete or asphalt pavement, or very hard compacted soils without a pressure compensation device. For example, E-Flux, LLC has initiated development of a trap for impervious ground cover that utilises a cap for the top of the trap with a tube that vents beneath the low permeability ground cover.

Avoid surface vegetation when possible as it can also cause the allowable deployment time of the CO₂ trap to be drastically reduced as it will increase the quantity of CO₂ efflux. Without significantly disturbing the subsoil, remove any vegetation at the selected installation location from beneath the trap location prior to installation.

Receiver pipe installation

Impact the soil vapour gas flow as little as possible when installing the receiver pipes. Directly push the receiver pipe into the ground surface where the surface soil is soft enough, in order to minimise the amount of soil removal necessary and potential bias introduced with replacing/recompacting the soils. Prior to installation, ensure that the majority of surface vegetation is removed from the area to minimise the influence of modern sources of CO₂. In some cases, the soil conditions may not allow for the direct push methodology and a more intrusive soil removal procedure is needed as discussed below:

1. If soil is removed from the receiver pipe installation location, segregate it so that only the soil removed is replaced in order to re-establish pre-installation conditions as best possible and attain representative soil efflux results. Plastic sheeting or a 19 L bucket can be used to isolate the removed soils.
2. Prior to installation of the receiver pipe, set aside large particles (i.e. anything 5 cm or larger in diameter). Large particles such as rocks, will inhibit the ability to adequately compact smaller soil particles and may result in nesting or voids below these larger particles. Additional smaller particulate materials may be gathered from surrounding soil for replacement, if required. If, during initial excavation, it is determined that greater than 50% of the soil removed consists of large particles

- and those conditions appear to match the surrounding soil conditions, selectively replace all materials to match the thickness of the largest particle.
3. During removal, if soils are mostly clay/silt, it will be important to break up clods larger than 5 cm in diameter before materials are backfilled.
 4. If soil is saturated, do not install the receiver pipe. Allow the soil to drain and dry out after a rain event prior to installation. High moisture content can reduce the movement of soil vapour and thus result in a low bias efflux measurement.
 5. Once the receiver pipe is installed, the process of replacing the soils within the area inside and outside the pipe can begin and those soils can be compacted to closely match the surrounding soil conditions based on the field observations. Replace the soil from the 19 L bucket or the plastic sheeting in an even horizontal loose layer, both inside the pipe and outside of the pipe.
 6. After the soil is replaced both inside and outside of the receiver pipe, secure the trap receiver with stakes to the ground surface.
 7. Next, compact the soil to a consistent compaction. This can be accomplished with a standard drop hammer. Start compaction in the centre of the receiver pipe and move outward, finishing with compaction on the outside of the receiver pipe.

To reiterate, the primary goal of installation is to match the soil conditions with the surrounding in-place soils so that the soil vapour flow is not impacted by the installation of the receiver pipe and the measured soil efflux is as close to pre-existing conditions as possible. Where possible, push the receiver pipe directly into the ground in order to minimise the amount of soil removal necessary and potential bias introduced with replacing/recompacting the soils to as close to pre-installation conditions as possible.

Allow the receiver pipe to set undisturbed for 12 to 24 hours prior to installation of the trap body to allow for any settling that may occur.

Trap installation

Prior to installation, remove the ship caps on both sides of the trap and store them for the duration of trap deployment. Attach the bottom of CO₂ trap body to the receiver pipe using a rubber sleeve and hose clamps. The rubber sleeve is placed on the receiver pipe followed by the hose clamps. The bottom of the trap body is then slipped into the rubber sleeve and the hose clamps are tightened to create a connection impermeable to gas flow. Lastly, thread on the protective rain cover to protect the top of the trap assembly from weather elements. The basic set-up of a passive flux trap is presented in figure 4-2.

After installation is complete, take photographs to document the trap and ground conditions and the surrounding environment, which can be useful when interpreting measurement results.

For the duration of the trap deployment, place the trip blank (TB), provided with end caps by the trap supplier, in a plastic, zip-lock bag and keep it in an area protected from weather elements near the deployed traps.

Deployment time period

Determine the deployment time period prior to field mobilisation, design it to allow sufficient time, based on the anticipated CO₂ efflux, for collection of enough CO₂ to avoid non-detectable measurements. In addition, do not deploy the traps for a duration in which the sorbent material would exceed saturation and not be capable to capturing all the CO₂ emitted from the subsurface. A typical time period for deployment is 10 to

20 days, but can be adapted for site-specific scheduling and logistical needs. Discuss site conditions with the flux trap supplier in advance; they can provide some additional guidance on deployment duration. It will be based on NSZD rate assumptions and may be founded on existing known site information. Note that it is rare to exceed the saturation limit of the trap sorbent within the above stated deployment duration.

Retrieval and shipping

At the conclusion of the deployment time, collect the CO₂ traps, replace the top and bottom shipping caps, and ship the CO₂ traps, along with the TB after removal from the plastic bag, back to the specialty laboratory for carbon and ¹⁴C analysis. No special preservatives or packaging are required, except to protect them from damage during shipment. The traps are typically shipped to and from the site in a cooler provided by the trap supplier.

The laboratory typically requires between two to four weeks to complete the analysis. During the lab analysis, provide the lab with the preferred site-specific representative hydrocarbon compound for the stoichiometric analysis and the LNAPL density for volumetric NSZD rate conversion. In this way, the results will be reported in custom units. The trap supplier will typically provide a lab report that performs the site-specific NSZD rate calculations. This is very useful to help minimise the subsequent data analysis.

Background correction using ¹⁴C

Background correction is needed to remove modern carbon contributions associated with plants/vegetation and other natural organic matter in the ecosystem from the total CO₂ efflux which also includes the gaseous expression of NSZD. The quantification of unstable ¹⁴C isotope composition is an established quantitative basis (ASTM International Method D6866-16) that is used to differentiate between old sources of fossil fuel-based carbon from modern biogenic sources. Modern carbon is distinct from carbon derived from LNAPL NSZD as it is significantly younger than carbon from fossil fuel-based petroleum hydrocarbon that originate from deep geologic reservoirs millions of years in age. ¹⁴C is an unstable carbon isotope and is used for background correction using the radiocarbon technique. ¹⁴C is generated by cosmic rays in the atmosphere. ¹⁴C is absent from petroleum, but is present in all living things. Living organisms interact with the atmosphere, which is the source of ¹⁴C causing the modern sources of carbon to have a higher concentration of the ¹⁴C isotope. Petroleum, on the other hand, does not readily interact with the atmosphere. The half-life of approximately 5,600 years causes petroleum derived carbon to have a concentration of ¹⁴C significantly less than modern sources of carbon. Thus, modern organic carbon is ¹⁴C-rich, while fossil-based carbon is ¹⁴C-depleted.

The use of accelerator mass spectrometry (AMS) to detect ¹⁴C allows for the quantification of the amount of modern carbon in a solid, liquid, or gas sample (Stuiver and Polach 1977). Therefore, AMS analysis of ¹⁴C can be performed on carbon extracted from a CO₂ trap or a gas sample extracted from the ground surface and the ¹⁴C with known CO₂ content, can be attributed to modern or petroleum hydrocarbon-derived sources. Once analysed the laboratory reports the modern carbon fraction in the sample ($F_{m_{\text{sample}}}$). Thus, with the assumption that the carbon is only comprised of modern and fossil-based isotopes, a two-source mass balance can be used to calculate the fossil fraction ($F_{f_{\text{sample}}}$) (API 2017). $F_{m_{\text{sample}}}$ can be estimated using equation E.1:

$$\text{Equation E.1: } Fm_{\text{sample}} = (Ff_{\text{sample}} \cdot Fm_{\text{sample}}) + [(1 - Ff_{\text{sample}}) \cdot Fm_{\text{atm}}]$$

where Fm_{atm} is the fraction of modern carbon in the contemporary living material and is equal to 1.05 (Hua *et al* 2013). Fm_{fossil} is the fraction of modern in the fossil-based carbon which is equal to zero as discussed above. Substituting these values into equation D.1, gives a solution for Ff_{sample} as shown on equation E.2:

$$\text{Equation E.2: } Ff_{\text{sample}} = 1 - \frac{Fm_{\text{sample}}}{1.05}$$

Note that counter-intuitively, Fm_{atm} is larger than 1 since ^{14}C analysis reports based on a 1950 National Bureau of Standards oxalic acid standard, synthesised when the ^{14}C atmospheric levels were lower than current due to nuclear testing. Due to reporting conventions, Fm_{sample} is reported as if the analysis was done in 1950 and Fm_{atm} is larger than 1.

Calculate the NSZD rate

The following section walks through calculation of the NSZD rate. These calculations are typically performed by the trap supplier and analytical laboratory. It is prudent to comprehend the calculation basis so that the laboratory results can be checked. An example excerpt from an actual passive CO_2 flux trap laboratory report (E-Flux, LLC) is provided as table E.1-1 along with a lab report legend/key that explains each field of the report table.

The CO_2 mass ($M_{\text{CO}_2\text{-sample}}$ in g) sorbed to the bottom sorbent layer of the CO_2 trap is first analytically measured by the laboratory using ASTM D4373. This bottom sorbent is exposed to the gaseous efflux from the subsurface, while the upper sorbent layer is exposed to atmospheric CO_2 . Typically, only the bottom sorbent element is analysed.

Next, the calculated sorbed CO_2 mass is corrected ($M_{\text{CO}_2\text{-TB-corrected}}$ in g) for manufacturer- and travel-related sorbent contamination by subtracting the CO_2 mass in the TB ($M_{\text{CO}_2\text{-TB}}$ in g) as shown on equation E.3.

$$\text{Equation E.3: } M_{\text{CO}_2\text{-TB-corrected}} = M_{\text{CO}_2\text{-sample}} - M_{\text{CO}_2\text{-TB}}$$

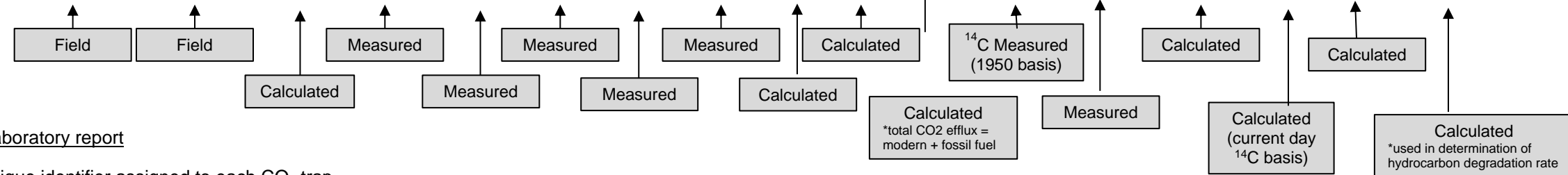
After TB correction, the mass of CO_2 is converted into a total CO_2 efflux (J_{Total} in $\frac{\mu\text{mol}}{\text{m}^2\text{s}}$) using equation E.4.

$$\text{Equation E.4: } J_{\text{Total}} = \frac{M_{\text{CO}_2\text{-TB-corrected}} \cdot \left(\frac{1 \text{ mol CO}_2}{44 \text{ g CO}_2}\right) \cdot \left(\frac{1000000 \mu\text{mol CO}_2}{\text{mol CO}_2}\right)}{\text{days deployed} \cdot 24 \frac{\text{hr}}{\text{day}} \cdot 3600 \frac{\text{s}}{\text{hr}} \cdot 8.11 \times 10^{-3} \text{ m}^2}$$

where the cross-sectional area of the receiver pipe is $8.11 \times 10^{-3} \text{ m}^2$ and the remainder of the parameters are standard conversion factors.

Table E.1-1. Example passive CO₂ flux trap laboratory data report from E-Flux, LLC

Sample ID	Deployment Dates			Raw Results (not blank corrected)					Blank Corrected Results ^a and ¹⁴ C Analysis (Fossil Fuel)								
	Deployed	Retrieved	Days	Moisture	Dry Sorbent Mass (g)	Num. of Repts. ^b	Avg CO ₂ ^b	CV CO ₂ ^c	Carbon Content ^d		CO ₂ Flux ^e (microM/m ² .sec)	Modern Carbon, As Reported ^f	Std. Dev. Modern	Modern CO ₂ Flux (microM/m ² .sec)	Adjusted Fossil Fuel Carbon ^h	Grams Of Fossil Fuel CO ₂ (g)	Fossil Fuel CO ₂ Flux (microM/m ² .sec)
									%	(g)							
PUEPM-R1-CO2-TB	NA	NA	0.00	17.8%	42.777	2	1.31%	1.61%	0.0%	-	-	77.2%	0.27%	-	26.5%	-	-
PUEPM-R1-CO2-01	6/18/14 16:33	7/7/14 11:35	18.79	13.5%	51.257	2	26.72%	3.26%	25.4%	13.03	22.45	37.1%	0.25%	8.3	64.6%	8.67	15
PUEPM-R1-CO2-02	6/18/14 16:27	7/7/14 11:30	18.79	19.1%	50.087	2	23.92%	0.05%	22.6%	11.33	19.56	42.4%	0.42%	8.2	59.6%	8.97	12
PUEPM-R1-CO2-03	6/18/14 16:20	7/7/14 11:25	18.80	20.8%	48.464	2	20.85%	2.92%	19.5%	16.35	16.35	50.1%	0.28%	8.1	52.3%	5.12	8.8



Explanation of the laboratory report

1. Sample ID: a unique identifier assigned to each CO₂ trap

2. Deployment Dates:

- Deployed: Date and time CO₂ trap is deployed
- Retrieved: Date and time CO₂ trap is retrieved
- Days: Number of days the CO₂ trap was deployed, calculated from the deployment and retrieval dates.

3. Raw Results (not blank corrected):

- Moisture: This is the amount of moisture that sorbed to the sorbent material, gravimetric lab analysis.
- Dry sorbent mass: This is the mass in g of the sorbent material minus the mass of the measured moisture.
- Number of replicates: The number of carbon analyses performed per trap. This is normally conducted in duplicate, however if the coefficient of variation (cv) is greater than 5%, then the carbon content is analysed in triplicate.
- Average CO₂: This is the % of total sorbent mass that is CO₂. The average %CO₂ is calculated without performing blank correction.
- CV CO₂: The cv is equal to the standard deviation of the replicate CO₂ measurements over the average CO₂. If the cv is greater than 5% a third replicate is performed.

4. Blank Corrected Results:

- Carbon content (% and g CO₂): This is the total amount of CO₂ in a trap after subtraction of CO₂ contained in the trip blank. The trip blank (TB) results are the first row of data in the lab report (i.e. PUEPM-R1-CO2-TB).
- CO₂ flux: the total CO₂ flux is calculated by dividing the trip blank-corrected CO₂ mass (that sorbed to the bottom sorbent layer) by the cross-sectional area of the receiver pipe ($8.11 \times 10^{-3} \text{m}^2$ for a 8 cm diameter) and the deployment time.

- Modern carbon, as reported: Based on calculations described in previously, this is the radiocarbon ¹⁴C analysis result. This is the fraction of carbon that is derived from modern sources and it is found through ¹⁴C analysis by AMS. These results are as reported by the AMS lab, which means using standard 1950 atmospheric content.
- Standard deviation modern CO₂: This is a ¹⁴C lab result obtained from the difference in the replicate measurements by the AMS.
- Modern CO₂ flux: Calculated by multiplying the total CO₂ flux by the % modern carbon, as reported.
- Adjusted fossil fuel carbon: the modern carbon (as reported) AMS results are transformed to present day ¹⁴C levels as described.
- Grams of fossil fuel CO₂: This is calculated using equation E.3.
- Fossil fuel CO₂ flux: The fossil fuel CO₂ efflux is calculated by multiplying adjusted % fossil fuel carbon by TB-correct CO₂ flux following equation E.5.

The passive flux trap laboratory can also report one additional column in the lab report, entitled Equivalent Fossil Fuel NAPL Loss Rate. Provide the lab with an LNAPL density (e.g. 0.75 g/cm³) and a representative hydrocarbon (e.g. octane, C₈H₁₈). Through stoichiometry as described in section 4.1, the molar ratio can be determined for conversion. For example, a conversion factor of $1 \frac{\mu\text{mol}_{\text{CO}_2}}{\text{m}^2 \cdot \text{s}} = 3.8 \frac{\text{g}_{\text{CO}_2}}{\text{m}^2 \cdot \text{d}}$ is obtained when assuming a stoichiometric relationship of C₈H₁₈ + 12.5 O₂ → 8 CO₂ + 9 H₂O, MW of octane of 114.23 grams per mole (g/mol), and an LNAPL density of 0.75 grams per cubic centimetre (g/cm³). The lab will calculate and report these values.

The ¹⁴C results from the AMS and two-source mass balance analysis are used to convert the total CO₂ efflux (J_{total}) into a fossil fuel (or background corrected) CO₂ efflux ($J_{NSZD-ff}$) as shown in equation E.5.

$$\text{Equation E.5: } J_{NSZD-ff} = J_{Total} * Ff_{sample}$$

Lastly, the background corrected CO₂ efflux is used to estimate the NSZD rate (R_{NSZD}) through the stoichiometric conversion discussed in section 4.1.

$$R_{NSZD} = \left[\frac{J_{NSZD-ff} m_r MW}{10^6} \right] \times \frac{86400s}{d}$$

where R_{NSZD} is the total hydrocarbon degraded or NSZD rate (g/m²/d), $J_{NSZD-ff}$ is the background corrected soil gas flux measurement (micromoles per square metre per second (μmol/m²/s)), m_r is the stoichiometric molar ratio of hydrocarbon degraded in equation 7 (unitless), and MW is the molecular weight of the representative hydrocarbon (g/mol).

An example set of calculations to demonstrate use of the above equations is presented in Appendix E.3.

Site-wide NSZD rate estimation

In some cases, it may be useful to combine all the NSZD rate data from various locations around the site, and estimate a site-wide total NSZD rate.

Area determination

The spatial location (i.e. northing and easting coordinates) of each NSZD measurement point can be used to generate Thiessen polygons. The Thiessen polygons are used to estimate the area associated with each NSZD measurement location.

The extent of a Thiessen polygon is defined by lines separating measurement locations that are equidistant from each adjacent measurement point. In so doing, any point within a polygon is closest to its central measurement location than any other adjacent location. Thiessen polygons are generated geometrically by the intersecting perpendicular lines that run through the midpoints of a line connecting two measuring locations. Figure E.1-1 presents a simple example with six measuring points and six Thiessen polygons. It can be assumed that the outer measurement locations are within the NSZD influenced efflux area, therefore a buffer is used to extend the calculated Thiessen area. This buffer length from the outer points is user defined (i.e. typically a 10% extension).

Geospatial integration

Estimating the site-wide NSZD rate is a simple summation of the product of the NSZD rate and their respective Thiessen polygon area for all Thiessen polygon areas (e.g. six areas in figure E.1-1) over the LNAPL footprint at the site (equation E.6).

$$\text{Equation E.6: } R_{NSZD-site} = \left(\sum_{i=1}^n R_{NSZD-i} * A_i \right) * \left(\frac{1 \text{ kg}}{1000 \text{ g}} \right) * \left(\frac{365 \text{ d}}{1 \text{ yr}} \right)$$

where $R_{NSZD-site}$ is the site-wide total NSZD rate (kg/yr), R_{NSZD-i} is the NSZD rate for Area i ($\frac{g}{m^2 d}$), A_i is the area of the Thiessen polygon Area i (m^2) associated with R_{NSZD-i} , and n is the number of Thiessen polygon areas.

Further, with multiple events of site-wide measurements made throughout the year, the individual event site-wide NSZD rate estimates can be integrated over the year (including seasonal fluctuation, if any) to develop an annual average site-wide NSZD rate.

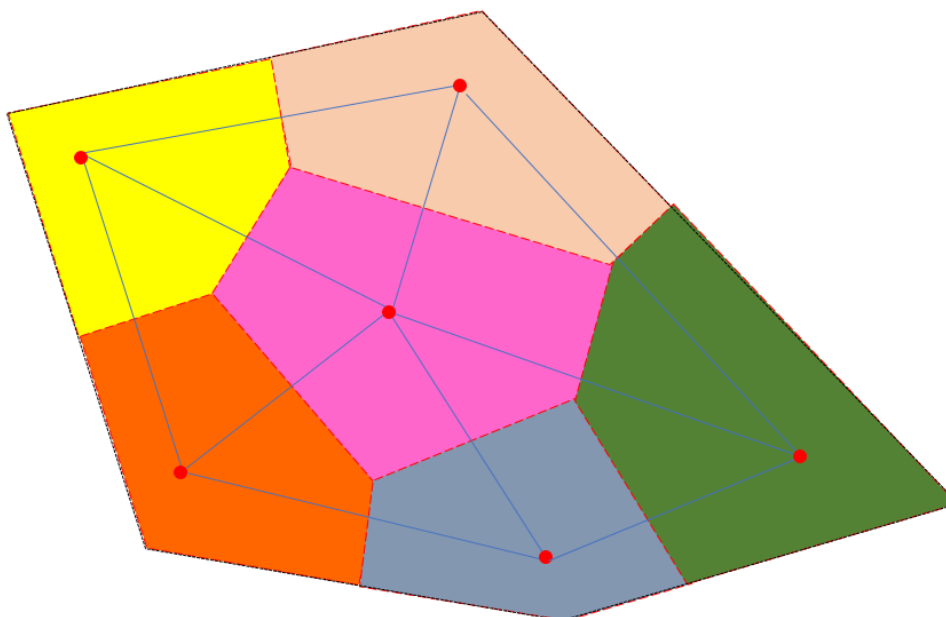


Figure E.1-1 Example Thiessen polygon arrangement on a site with six NSZD measurement locations

Passive flux trap method quality assurance/quality control

QA/QC procedures are important in evaluating the accuracy and precision of the data collected. One duplicate trap location every 10 locations is recommended to evaluate consistency between installation procedures and replication of results. Place the duplicate trap approximately 0.3 m from the parent location and install it in an area of similar ground cover. Statistics such as the calculation of a relative percent difference (RPD) from the parent and duplicate sample data can be performed to assess data quality. An elevated RPD of greater than 30% is typically used as a criterion to re-evaluate the soil receiver pipe installation procedures to ensure a good seal with the subsurface was attained. However, heterogeneities in the subsurface impact the ability to achieve an RPD of less than 30% at many sites, therefore the 30% criterion may not be achieved in all cases.

As discussed above, a TB must be provided by the passive flux trap supplier and analysed along with the samples for each field event. The TB accounts for CO_2 not associated with flux from the subsurface that either came from manufacturing or sorbed from atmosphere (through the caps) during the shipment.

The detection limit of a passive CO₂ trap is dictated by the detection limit of the analytical method. The detection limit of the analytical method is found by multiplying a typical coefficient of variation of 3% on trap CO₂ analyses, and a typical blank trap CO₂ content of 1% by weight by five (i.e. 3% cv * 1% CO₂ by weight * 5). The detection limit of the analytical method of CO₂ trap is approximately 0.15% CO₂ by weight of the sorbent (API 2017). Then using deployment time, the area exposed to efflux, and the quantity of sorbent material the detection limit of the CO₂ trap can be determined. The detection limit is typically 0.1 μmol/m²/s for a 15-day deployment time, a cross-sectional diameter of 10.16 cm of the Schedule 40 polyvinyl chloride (PVC) receiver pipe, and 40 g of sorbent material. A decrease in deployment time of 4 days would result in approximately a 5-fold increase in the detection limit (0.5 μmol/m²/s). Note that if laboratory results are less than the specified analytical detection limit, the resulting detection limit of the CO₂ traps must be considered non-detect.

Consider the following when designing a field program and obtaining efflux measurements:

- A review of historical documentation and photo documentation of each CO₂ trap location is used to ensure that locations are as expected.
- If snowfall occurs after a receiver pipe is installed, remove as much snow as possible prior to the data collection.
- If vegetation grows or vegetation deadfall collects in the receiver pipe after installation, the vegetation needs to be removed prior to completing the measurements(s).

E.2 – Manufacturer-recommended field procedures

The information presented in this section was extracted from the following source(s):

- E-Flux 2018 *Manufacturer-recommended field procedures*, E-Flux, Colorado USA, available at <www.soilgasflux.com/ff2>.

E.3 – Example passive flux trap method-based NSZD rate calculations

The information presented in this section was extracted from the following source(s):

- API 2017, *Quantification of vapor phase-related NSZD processes*, Publication No. 4784.
- E-Flux 2018 *Manufacturer-recommended field procedures*, E-Flux, Colorado USA, available at <www.soilgasflux.com/ff2>.
- Gorder, K & Holbert, C 2010, 'Thiessen area and mass calculator for assessment of plume dynamics', Poster presentation at the Seventh Annual Conference on the Remediation of Chlorinated and Recalcitrant Compounds, California, USA, May 24–27.

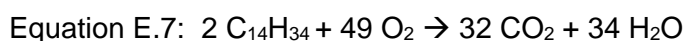
An example case study of the passive flux trap method is presented in this section to show how measurement of CO₂ efflux using passive CO₂ flux traps can be conducted and calculation performed to obtain a site-wide estimate of the NSZD rate. It is based on a real setting where NSZD monitoring was performed.

Study details

Three quarterly CO₂ efflux surveys were conducted at a 100-year old active railyard site located in a temperate, semi-arid region where a large quantity of diesel fuel was released. The efflux surveys were conducted in June, September, and December of 2014. A site map is presented in figure E.3-1. Passive flux traps supplied by E-Flux, LLC were deployed for approximately 18 days during each event. The traps were then collected and shipped for laboratory analysis, including ¹⁴C isotope analysis. The light non-aqueous phase liquid (LNAPL) of concern had a density of 0.92 g/cm³ and gas chromatogram reviews indicated that the residual LNAPL was best represented by hexadecane (C₁₆H₃₄).

Calculation of the NSZD rate

Laboratory reported results, including the estimate NSZD rates, are presented in table E.3-1. As a QA/QC measure, the laboratory reported NSZD rates were checked for accuracy. To convert the background corrected CO₂ efflux (J_{NSZD-ff}) to the estimated NSZD rate, C₁₆H₃₄ was the assumed representative hydrocarbon for the aged diesel fuel that was released at the site.



As shown in equation E.7, two moles of hexadecane (MW= 226.45 g/mol) is degraded through the microbial mediated processes to form 32 moles of CO₂. Below is an example calculation for location CO2-01 for the flux trap measurement on 18 June 2014:

$$R_{NSZD} = 15.0 \frac{\mu\text{mol CO}_2}{\text{m}^2\text{day}} \cdot \frac{2 \text{ mol C}_{16}\text{H}_{34}}{32 \text{ mol CO}_2} \cdot \frac{226.45 \text{ g C}_{16}\text{H}_{34}}{1 \text{ mol C}_{16}\text{H}_{34}} \cdot \frac{86400 \text{ s}}{1 \text{ d}} \cdot \frac{1 \text{ mol}}{1000000 \mu\text{mol}}$$

$$R_{NSZD} = 18 \frac{\text{gC}_{16}\text{H}_{34}}{\text{m}^2\text{d}}$$

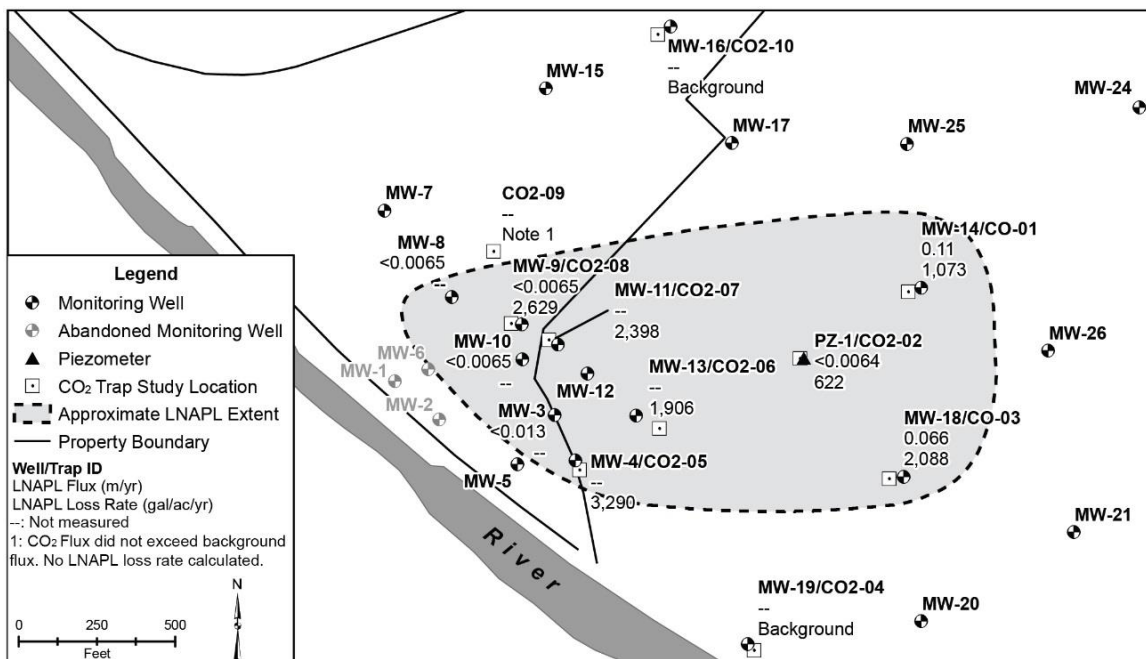


Figure E.3-1 – Sampling locations and estimated LNAPL extent based on in-well LNAPL measurements

Thiessen polygons

A spreadsheet Thiessen polygon calculator developed for evaluating groundwater plume mass and the plume centre of mass (Gorder & Holbert 2010) was adapted to calculate Thiessen polygon areas for estimating the site-wide NSZD rate. The Thiessen polygons are accepted as a mathematically discrete technique of handling environmental data and are free from subjectivity that may be introduced with interpolation programs. Table E.3-2 presents the areas of the Thiessen polygons.

Seasonally corrected site-wide NSZD rate

The areas of each polygon were multiplied by the estimated NSZD rate at each respective location. It was assumed that the June and September 2014 rates are representative of three months each and account for half of the NSZD per year. The estimated rate of NSZD in December 2014 was assumed to attribute for the hydrocarbon degradation over the remaining 6 months of the year. The rates obtained during the June, September, and December 2014 events were multiplied by 91, 92, and 182 days respectively, to obtain the seasonal total NSZD for each. These estimated rates of NSZD per polygon were then summed to get an estimated site-wide rate of NSZD per event. The degradation rates per event were summed to obtain the annual estimated seasonally corrected NSZD loss rate. The estimated seasonally corrected annual NSZD loss rate using the passive CO₂ flux trap method was approximately 36,800 kg/yr.

Table E.3-1. Laboratory efflux results and estimated hydrocarbon degraded calculation

Sample Location	Deployment dates			Raw results (not blank corrected)					Blank corrected results										
									Carbon content		CO ₂ efflux	Modern carbon, as reported	Standard deviation modern CO ₂	Modern CO ₂ efflux	Contemporary fossil fuel carbon %	Grams Of fossil fuel CO ₂	Fossil fuel CO ₂ efflux	Estimated hydrocarbon degraded, NSZD rate	
	Deployed	Retrieved	Days	Moisture	Dry sorbent mass (g)	Number of replicates	Average % CO ₂	CV % CO ₂	% CO ₂	g CO ₂	µmol/m ² /s	% Mod	%	µmol/m ² /s	%	g CO ₂	µmol/m ² /s	g/m ² /d	
PUEPM-R1-CO2-TB	NA	NA	NA	17.8%	42.777	2	1.31%	1.61%	0.0%	-	NA	77.2%	0.27%	-	26.5%	-	-	-	
PUEPM-R2-CO2-TB	NA	NA	NA	15.5%	42.712	2	1.16%	1.21%	0.0%	-	NA	72.3%	0.31%	-	31.1%	-	-	-	
PUEPM-R3-CO2-TB	NA	NA	NA	15.2%	44.604	2	1.15%	0.05%	0.0%	-	NA	74.5%	0.21%	-	29.0%	-	-	-	
CO2-01	18/6/14	7/7/14 11:35	18.79	13.5%	51.257	2	26.72%	3.26%	25.4%	13.03	22.49	37.1%	0.25%	8.3	64.6%	8.67	15.0	18	
	5/9/14	23/9/14 9:35	17.88	14.1%	48.130	2	16.63%	0.76%	15.5%	7.44	13.50	66.3%	0.36%	8.8	36.9%	2.79	5.1	6.2	
	5/12/14	23/12/14 9:42	17.92	15.9%	46.427	2	10.93%	0.29%	9.8%	4.54	8.22	22.8%	0.52%	1.8	78.3%	3.81	6.9	8.4	
CO2-02	18/6/14	7/7/14 11:30	18.79	20.8%	50.087	2	23.92%	0.05%	22.6%	11.33	19.56	42.4%	0.42%	8.2	59.6%	6.97	12.0	15	
	5/9/14	23/9/14 9:40	17.90	13.1%	48.582	2	23.09%	0.25%	21.9%	10.65	19.31	47.3%	0.33%	9.0	54.9%	5.99	10.9	13	
	5/12/14	23/12/14 9:37	17.92	16.5%	46.040	2	11.51%	1.83%	10.4%	4.77	8.64	21.8%	0.41%	1.9	79.3%	4.04	7.3	8.9	
CO2-03	18/6/14	7/7/14 11:25	18.79	11.9%	48.464	2	20.85%	2.92%	19.5%	9.47	16.35	50.1%	0.28%	8.1	52.3%	5.12	8.8	11	
	5/9/14	23/9/14 9:45	17.92	10.2%	47.225	2	16.59%	0.44%	15.4%	7.29	13.19	67.7%	0.29%	8.8	35.5%	2.62	4.7	5.8	
	5/12/14	23/12/14 9:32	17.92	11.3%	45.504	2	8.23%	3.40%	7.1%	3.22	5.83	30.7%	0.33%	1.8	70.7%	2.49	4.5	5.5	
CO2-04	18/6/14	7/7/14 11:20	18.79	21.7%	47.118	3	7.63%	6.63%	6.3%	2.98	5.14	99.3%	0.40%	5.0	5.4%	0.03	0.1	0.07	
	5/9/14	23/9/14 9:50	17.94	25.9%	45.220	2	3.27%	0.62%	2.1%	0.95	1.73	98.9%	0.44%	1.7	5.8%	-0.07	-0.1	0	
	5/12/14	23/12/14 9:27	17.93	21.2%	45.837	2	2.05%	0.96%	0.9%	0.41	0.75	99.7%	0.32%	0.7	5.0%	-0.11	-0.2	0.	
CO2-05	18/6/14	7/7/14 11:05	18.79	9.4%	54.516	2	38.51%	0.73%	37.2%	20.28	35.03	24.4%	0.20%	8.5	76.8%	15.93	27.5	34	
	5/9/14	23/9/14 9:55	17.97	14.7%	49.976	2	23.56%	0.71%	22.4%	11.19	20.21	45.4%	0.31%	9.1	56.8%	6.51	11.8	14	
	5/12/14	12/23/14 9:23	17.93	15.2%	56.756 *	2	33.69%*	0.47%*	32.5%*	18.47 *	33.43 *	6.5%*	0.27%*	2.1 *	93.8%*	17.75 *	32.1 *	39 *	
CO2-06^	18/6/14	7/7/14 11:10	18.79	18.8%	46.171	2	13.46%	1.55%	12.2%	5.61	9.69	81.1%	0.43%	7.8	22.7%	1.25	2.2	2.6	
	5/9/14	23/9/14 10:05	17.89	35.4%	45.149	2	7.40%	2.73%	6.2%	2.82	5.11	158.0%^	0.29%	8.0	-50.5%^	-1.84 ^	-3.34 ^	0	
	NM	NM	NM	NM	NM	NM	NM	NM	NM	NM	NM	NM	NM	NM	NM	NM	NM	NM	
CO2-07	18/6/14	7/7/14 11:00	18.79	19.2%	52.242	2	27.88%	1.55%	26.6%	13.88	23.96	35.0%	0.33%	8.3	66.7%	9.53	16.4	20	
	5/9/14	23/9/14 10:20	18.00	9.4%	51.679	2	26.98%	0.99%	25.8%	13.35	24.06	38.4%	0.27%	9.2	63.4%	8.66	15.6	19	
	5/12/14	23/12/14 9:15	17.92	15.2%	49.235	2	18.24%	0.34%	17.1%	8.42	15.23	13.1%	0.27%	2.0	87.5%	7.69	13.9	17	
CO2-08	18/6/14	7/7/14 11:55	18.83	25.5%	49.073	2	16.34%	0.13%	15.0%	7.38	12.71	63.3%	0.41%	7.9	39.7%	3.01	5.2	6.3	
	5/9/14	23/9/14 10:25	18.03	10.6%	46.568	2	15.59%	1.33%	14.4%	6.72	12.10	73.4%	0.34%	8.8	30.1%	2.03	3.6	4.5	
	5/12/14	23/12/14 9:03	17.92	14.9%	46.113	2	7.87%	1.72%	6.7%	3.10	5.61	31.8%	0.37%	1.8	69.7%	2.37	4.3	5.2	
CO2-09	18/6/14	7/7/14 10:45	18.79	13.9%	54.206	2	35.11%	2.18%	33.8%	18.33	31.64	26.9%	0.30%	8.4	74.4%	13.97	24.1	29	
	5/9/14	23/9/14 10:30	18.04	19.2%	54.173	2	26.18%	1.68%	25.0%	13.55	24.38	38.0%	0.26%	9.2	63.8%	8.86	15.9	19	
	5/12/14	23/12/14 8:55	17.92	19.1%	48.027	2	9.76%	3.56%	8.6%	4.14	7.49	25.0%	0.38%	1.8	76.2%	3.41	6.2	7.5	
CO2-10	18/6/14	7/7/14 10:30	18.79	24.2%	47.250	2	13.45%	2.71%	12.1%	5.74	9.90	99.1%	0.27%	9.7	5.6%	0.19	0.3	0.41	
	5/9/14	23/9/14 10:35	18.05	20.9%	49.287	2	18.29%	2.44%	17.1%	8.44	15.17	99.4%	0.36%	14.9	5.3%	0.31	0.6	0.68	
	5/12/14	23/12/14 8:47	17.92	21.5%	46.556	2	3.40%	0.13%	2.3%	1.05	1.90	98.2%	0.28%	1.8	6.5%	-0.06	-0.1	0	

* %CO₂ for sample PUEPM-R3-CO2-05 is 33.69%. Sorbent saturation is 30%. As such, results from this sample may be conservative; ^ = an error in efflux measurement was made at CO2-06 in September 2014 and was not sampled in December 2014; % Mod = percent modern carbon; NA = not applicable

Table E.3-2. Thiessen polygon areas and site-wide annual rate of NSZD

Location	Coordinates		Area	14 June 2014		5 September 2014		15 December 2014		Annual NSZD rate
	Northing	Easting		(g/m ² /d)	kg over 3 months	(g/m ² /d)	kg over 3 months	(g/m ² /d)	kg over 6 months	(kg/yr)
	(m)	(m)	(m ²)							
CO2-01	481,862.09	992,472.86	652	18	1,090	6.2	368	8.4	999	
CO2-02	481,853.15	992,428.10	2,137	15	2,874	13	2,593	8.9	3,473	
CO2-03	481,810.47	992,458.89	877	11	866	5.8	464	5.5	879	
CO2-05	481,830.23	992,375.71	1,513	34	4,651	14	1,988	39	10,799	
CO2-07	481,856.36	992,338.92	750	20	1,377	19	1,307	17	2,317	
CO2-08	481,864.02	992,328.80	177	6.3	102	4.5	72	5.2	169	
CO2-09	481,868.57	992,315.39	75	29	203	19	134	7.5	103	
Total					11,200		6,900		18,700	36,800

APPENDIX F.

Dynamic closed chamber-based CO₂ NSZD evaluation procedure

This appendix contains procedures useful for practitioners to reference when implementing the dynamic closed chamber (DCC) method for NSZD evaluation. The following procedures are included herein:

F.1 – Procedure for DCC method implementation and data analysis (including background correction)

F.2 – Example DCC method-based NSZD rate calculations

1.2 F.1 – Procedure for DCC method implementation and data analysis (including background correction)

The information presented in this section was extracted from the following source(s):

- API 2017, *Quantification of vapor phase-related NSZD processes*, Publication No. 4784.
- Jassal, RS, Black, TA, Nestic, Z & Gaumont-Guay, D 2012, 'Using automated non-steady-state chamber systems for making continuous long-term measurements of soil CO₂ efflux in forest ecosystems', *Agricultural and Forest Meteorology*, vol. 161, pp. 57–65.
- LI-COR 2014, *Testing the limits with the LI-8100A*, LI-COR Biosciences Inc. Nebraska, USA, available at <www.licor.com/env/newsline/2014/07/testing-the-limits-with-the-li-8100a/>.
- LI-COR Biosciences, Inc. 2015, *Using the LI-8100A soil gas flux system & the LI-8150 multiplexer*, LI-COR Biosciences Inc. Nebraska, USA.
- Sihota, NJ, Singurindy, O & Mayer, KU 2011, 'CO₂-efflux measurements for evaluation source zone natural attenuation rates in a petroleum hydrocarbon aquifer', *Environment, Science and Technology*, vol. 45, pp. 482–488.

1.3 I. Purpose and scope

The DCC method is composed of a chamber, a circulation pump, and a field gas analyser to measure CO₂ gas moving from the subsurface to the atmosphere. From the time rate of change in measured CO₂ concentrations over a known area and amount of time, the CO₂ flux from the subsurface can be calculated. The rate of NSZD can then be estimated with a representative site LNAPL and stoichiometric conversion. In addition to the CO₂ efflux and NSZD rate calculations, this appendix also describes the application of the DCC method to estimate a site-wide NSZD rate.

The procedures provided below describe how to implement the DCC method for measurement of CO₂ efflux and calculate NSZD rates. This appendix presents a list of equipment required for installation, procedures for measurement, associated QA/QC, and data management and analysis.

Prerequisites

It is assumed that the following prerequisites have been met prior to use of this procedure:

- Data needs, objectives, and quality levels are established to appropriately scope the effort
- An appropriate number of monitoring locations were selected for DCC analysis, adequate to meet the data objectives and represent the potential range of NSZD rates at the site

Equipment

- DCC soil flux system including chamber, circulation pump, CO₂ gas analyser, and software/controller
- 20 cm diameter collars
- hand trowel
- rubber mallet
- personal protective equipment
- ASTM D-698 Standard Proctor Compaction Hammer (2.5 kg with 30 cm drop)
- Field logbook and camera

Procedures and guidelines

The procedure provided below describes protocols for installation, measurement, data analysis, and associated QA/QC. Use of the DCC method to estimate the rate of NSZD involves the following steps:

1. Install the collars and allow re-equilibrium
2. Perform the CO₂ efflux survey using the DCC soil gas flux system a minimum 16 hours after collar installation
3. Conduct data validation and visualisation
4. Assess the background and NSZD fractions of CO₂ efflux
5. Calculate the NSZD rate

The following sections detail how to accomplish each step.

Install the DCC collars

The following describes selection of locations and collar installation.

Location selection

Performing a CO₂ efflux survey using the DCC method results in the mapping of the geospatial distribution of CO₂ efflux across the LNAPL footprint and distinguishing efflux between hydrocarbon impacted and background source areas. The density of collar locations is dependent on site specific needs and requirements. However, in general, space soil collars so that the appropriate interpolation of efflux and extent of the NSZD can be performed to meet the data quality objectives. Existing guidance on the selection of sampling locations that can be used to guide this effort includes Schedule B2 of National Environment Protection Council, National Environment Protection (Assessment of Site Contamination) Measure 1999 2013 amendment.

Site specific LNAPL distribution data from sources such as historical release records, soil boring logs, monitoring wells, and aerial photos with visible vegetation coverages can be used to aid the selection of survey locations and the understanding of the CO₂ efflux data. Locating survey points, both influenced by petroleum hydrocarbon and background locations, near monitoring wells containing measurable LNAPL, is a first step in identifying survey points.

Because the DCC field methodology measures only total CO₂ efflux, it cannot distinguish between modern sources of CO₂ efflux (e.g. from plant and natural organic matter) and petroleum hydrocarbon derived CO₂ efflux (e.g. from NSZD). As such, the

selection of background locations is critical background locations are needed from each specific vegetative cover type, since vegetative cover and the underlying soil can significantly impact the measured CO₂ efflux. A sufficient number of background locations are needed from each vegetative cover type to accurately estimate the background CO₂ efflux. Locate background locations in areas with no underlying petroleum hydrocarbons in the soil. Since ¹⁴C analysis on passive CO₂ flux traps can distinguish between modern and petroleum derived carbon through isotope analysis, pairing of the two methods (DCC and passive CO₂ traps) can be used to verify DCC background correction.

In many cases, the geospatially interpolated, background corrected, CO₂ efflux values may mimic the footprint of the LNAPL as indicated by other site data. Therefore, a higher density of DCC CO₂ efflux survey locations as compared to monitoring wells may be used as evidence of the presence or absence of LNAPL in areas without monitoring wells (Sihota *et al* 2016).

Collar installation

After the selection of survey locations, an 11 cm length of 20 cm diameter polyvinyl chloride (PVC) soil collar is embedded into the ground at a shallow depth of approximately 3- to 8-cm to provide a stable surface that the chamber can be placed upon. The exact installation depth depends on site conditions and the length of time the collars will be deployed at the site (LI-COR 2015). The collar needs to be installed at a depth that provides a solid foundation so the collar does not move when placing the chamber on it. Ensure the installation depth is deep enough to form a seal with the ground surface to prevent lateral gas exchange from the atmosphere (i.e. chamber leakage). In instances where soil conditions prevent the use of direct push methodology, surface soils can also be manually scored using a hand tool to install the collar, where care is taken to minimise soil disturbances inside and outside the collar. Significant soil disturbances may cause preferential gas flow resulting in a measured efflux that is not representative.

Similar to the installation of receiver pipes for the passive flux traps, prior to installation, remove surface vegetation from the installation to minimise the influence of modern sources of CO₂. Additionally, the lowest possible impact to the soil vapour gas flow is targeted when installing soil collars. Therefore, it is desired to directly push the soil collar into the ground surface where the surface soil is soft enough, in order to minimise the amount of soil removal necessary and potential bias introduced with replacing/recompacting the soils. However, the soil conditions may not allow for the direct push methodology and a more intrusive soil removal procedure is needed as discussed below:

1. Prior to installation, remove surface vegetation from the installation area to minimise the influence of modern sources of CO₂ (e.g. natural soil respiration (NSR)).
2. If soil is removed from the collar installation location, it needs to be segregated so that only the soil that is removed is replaced in order to achieve post-installation conditions that are as close to pre-existing conditions as possible. Plastic sheeting or a 19 L bucket can be used to isolate the removed soils.
3. Prior to installation of the collar, discard large particles (i.e. anything 5 cm or larger in diameter). Large particles such as rocks, will inhibit the ability to adequately compact smaller soil particles and may result in nesting or voids below these larger

particles. Additional smaller particulate materials may be gathered from surrounding soil for replacement, if required. If, during initial excavation, it is determined that greater than 50% of the soil removed consists of large particles and those conditions appear to match the surrounding soil conditions, selectively replace all materials to match the thickness of the largest particle.

4. During removal, if soils are mostly clay/silt, it will be important to break up clods larger than 5 cm in diameter before materials are backfilled.
5. If soil is saturated, do not install the collar and allow soil to drain and dry out to at least field capacity after a rain event prior to installation. High moisture content can reduce the movement of soil vapour and thus create a low bias of the efflux measurements.
6. Once the soil vapour efflux measurement collar has been put in place, the process of replacing the soils within the area inside and outside the pipe can begin and those soils can be compacted to closely match the surrounding soil conditions based on the field observations. Replace the soil from the 19 L bucket or the plastic sheeting in an even horizontal loose layer, both inside the pipe and outside of the pipe.
7. After the soil is replaced, secure the collar by backfilling around the edges to slightly above the surrounding ground surface elevation.

Once the soil collars are installed, the soil inside and outside the collar is re-compacted to pre-existing conditions using a manual standard compaction slide hammer or other standard procedure. Consistency of installation of all collars is critical to obtain representative and comparable CO₂ soil efflux measurements. In order to provide comparable data across the survey network at the site, install soil collars to a consistent depth. If collars are installed at different depths, some can penetrate through soil that act as confining layers. These layers can restrict movement of underlying soil vapour to the ground surface, thus creating a preferential gas pathway, or chimney, when the collars are installed and breach the layer. As a result, this may create inconsistent and variable results. Differences in the re-compaction may also cause biased efflux measurements that are not representative of actual conditions.

Install soil collars a minimum of approximately 16 hours prior DCC efflux measurement to allow for CO₂ vapour in the shallow soil to stabilise and minimise effects from soil disturbance occurring as a result of setting the collars in the soil. Label soil collars and photograph them after installation to document the condition of the soil collars prior to the collection of efflux measurements.

The offset (e.g. the height of the collar top lip above ground surface) is measured in three locations within the inner diameter of an individual soil collar and recorded, to be used to estimate the average collar/chamber volume estimate. This measurement is used to determine the total volume inside the chamber and collar and is important in the calculation of the efflux. If multiple survey events are planned, leave the soil collars in place (with a rain/debris cover if necessary) in order to prevent changes between survey events.

If multiple measurements at the same collar are within an individual day, allow a minimum of 20 minutes between measurements. This delay between measurements is to allow re-equilibration of vapours within the shallow soil.

To reiterate, the primary goal is to match the soil conditions inside the collar with the surrounding in-place soils so that the soil vapour flow is not impacted. In the situation

where the surface soil is soft enough, directly push the collar into the ground by hand to minimise the amount of soil removal necessary and minimise the potential bias introduced.

1.3.1 Perform the gas efflux survey using DCC soil gas flux system

The following parameters are used by the DCC system to calculate the soil CO₂ efflux:

- changes in concentration of CO₂
- chamber volume
- soil collar area and height above ground surface (i.e. the offset)
- temperature
- pressure
- initial water vapour mole fraction, and
- water-corrected CO₂ mole fraction.

The DCC system chamber is set on the collar to provide a direct conduit for soil gas migration into the chamber and field gas analyser during the measurement period. A laptop or smart phone application allows communication with the controller and programming of the measurement sequence. Once initiated, the controller automatically communicates with the chamber, vapour pump, and the infrared gas analyser (IRGA) and performs a series of efflux measurements. The vapour pump begins circulation of gas from the chamber to the analyser unit for the measurements of CO₂, temperature, and water vapour. A purge cycle ensues for a relatively short duration to flush stagnant gases from the system. The chamber then closes onto the soil collar and measurement of CO₂ concentrations by the IRGA begins. The basic set-up of a DCC system is presented in figure 4-3.

A period of time to allow for steady mixing in the chamber after it closes can be set to neglect the earliest time change in CO₂ concentration data. This is referred to as a deadband (the duration of which is defined by the user and is approximately 10 to 20 s). After this deadband period the change in CO₂ concentrations over time is used to estimate the CO₂ efflux. The measured CO₂ concentrations are corrected to a dry basis prior to the estimation of the CO₂ efflux using water and temperature data. Once the pre-defined measurement period ends, the bellows deflates, the chamber is raised off the collar, and a post-measurement purge cycle is initiated. This measurement cycle of pre-purge and chamber closure, CO₂ efflux measurement, and post purge continues until the preset number of measurements are collected at a particular location. After the completion of the preset number of measurements, the user evaluates the data to assess whether additional measurements are needed at the same location or whether measurements are complete at that location. When it is determined that no additional measurements are needed at a location, the user lifts the chamber off the collar, and moves the chamber and analyser unit to the next location and the process is repeated.

The measurement obtained using the DCC method is of short duration (approximately 90 s). As a result of the short measurement timeframe, a minimum of three sequential total CO₂ efflux measurements are made at a single location. Thus, CO₂ efflux measurements are made over a total period of approximately 5 minutes at each location. For planning purposes, a network of 30 collars typically can be measured in a one day field effort.

Note: The soil collar height above ground (offset) is the only parameter that needs to be routinely measured in the field, all other parameters are automatically calculated or measured by the LI-COR unit.

Conduct data validation and visualisation

Data QA/QC consists of the following three steps:

1. establishing a detection limit
2. data validation, and
3. data visualisation.

Establishing the limit of detection

A field blank measurement is collected during each field event. A collar with a sealed bottom cap is used for the field blank. The chamber is set upon the sealed collar in the field and allowed to run a total of 60 measurements. The results of the field blank are then averaged, three times the standard deviation is added, and the resulting value is assigned the limit of detection for the particular measurement event. This measurement protocol is described in detail by LI-COR (2014).

Data validation

After tabulation of the raw field data, data validation occurs. The process of validating the DCC field measurement data is as follows:

1. Tabulate the data from the CO₂ efflux field survey
2. Assign non-detect values by comparison of raw results to the field blanks
3. Optimise the CO₂ concentration curve fits. Adjust the deadband and observation time in order to optimise the curve fit parameter (R^2) and evaluate the validity of the individual efflux measurements
4. Eliminate data that are outliers, poor curve fit correlations, results from poor field procedures, or outside the manufacturer's recommended operating limits (i.e. IRGA bench temperature of 50 degree Celsius (°C) and minimum of 90 recorded data points)

The LI-COR 8100A DCC system automatically plots the dry CO₂ concentration, which is the water vapour dilution corrected CO₂ mole fraction, over time. Data to be used for curve fitting can be bound using a deadband setting (i.e. the time before the vertical green line in figure F.1-1) and an observation time setting (time at the vertical red line in figure F.1-1). The deadband and observation times can be adjusted to optimise the R^2 after measurements are obtained and do not need to be correctly chosen in the field. An observation length of 90 seconds is typically long enough to achieve a good curve fit.

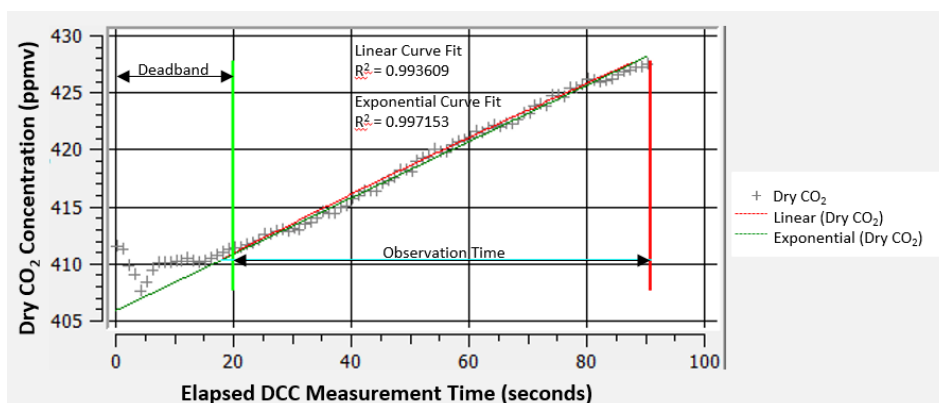


Figure F.1-1. Example output from a CO₂ efflux measurement using a DCC soil flux system.

With the software supplied by LI-COR, Inc. (SoilFluxPro version 4.1 in 2017) the rate of CO₂ increase in the chamber is fit using either a linear or exponential regression. In general, the difference between linear and exponential curve fits is typically small. However, Jassal *et al* (2012) found that a simple linear regression best represented an imposed CO₂ efflux. If R² value is low (<0.95) and/or large differences between the linear and exponential curve fits occur, further scrutinise the data for a problem. Poor quality data points include less than 90 readings per measurement (a reading is one individual measurement of the CO₂ concentration, multiple readings over time are used to calculate an efflux), an optimised R² less than 0.5, a flux of less than -0.2 micromole per square metre per second (μmol/m²/s), an IRGA temperature of less than 50° C, and outliers (data points found to have greater than a 100% difference of the average efflux measurements made at an individual location).

After optimisation of R², the time rate of change in the CO₂ concentration is used to estimate the efflux as shown in equation F.1.

$$\text{Equation F.1: } J_{Total} = \frac{10 \cdot V \cdot P_0}{R \cdot S \cdot (T_0 + 273.15)} \frac{dC}{dt}$$

where J_{Total} is the soil CO₂ efflux (μmol/m²/s), V is volume of the chamber headspace above ground surface (m³), P_0 is the initial pressure (pascal (Pa)), S is soil surface area (m²), T_0 is initial air temperature (°K), R is the universal gas constant, and dC/dt is the initial rate of change in CO₂ mole fraction (μmol/m²/s).

Data visualisation

After data validation is complete, a geospatial mapping of the CO₂ efflux survey results can be used to further validate the results. Mapping of the total CO₂ efflux and overlay it on existing maps which contain other LNAPL information such as in-well LNAPL presence/absence or soil boring LNAPL observations such as headspace or visual occurrence, can be used to further validate the results of the DCC survey. Generally, the zones of elevated total CO₂ efflux should correspond to areas of LNAPL occurrence. If they do not, then further data scrutiny is warranted to reconcile the data.

Assess the background and NSZD fractions of CO₂ efflux

Prior to the analysis and interpretation of the data, background correction must be performed. This is a critical step in calculating rates of degradation of LNAPL. Measurements obtained with the DCC method do not distinguish the source of the CO₂ as derived from modern sources or older fossil-fuel sources. The modern CO₂ efflux is

determined by the emplacement of background locations, where it is believed CO₂ derived from petroleum is not encountered. Segregation of the background locations within the same soil and surface vegetative cover is often difficult due to the relative size and surface limitations of sites impacted with LNAPL. When measurement locations are determined in the planning phase, locations that are thought to potentially be used as background are identified. However, once efflux measurements are obtained, the CO₂ may or may not be as expected. Look at the total CO₂ efflux values, and compare it to the assumed LNAPL footprint. If a correlation is observed, then particular locations can be assigned to be background and all the CO₂ efflux measured at these locations can then be assigned as derived from modern sources. However, background CO₂ can differ based on the vegetative cover, thus in order to perform this background correction in more complex settings, locations need to be separated into different vegetative cover types. Vegetative cover types are determined visually when installing the soil collar and when evaluating patterns observed in the total CO₂ efflux measurements. The separation of certain effluxes within different vegetative cover designations is then confirmed using the non-parametric analysis of variance (ANOVA) statistical analysis. When background locations are identified, the effluxes are averaged for a particular surface vegetation cover, and the average is then subtracted from the non-background locations with the same surface vegetation to perform the correction to obtain the CO₂ efflux only attributed to the degradation of the LNAPL.

In some cases, no discernable background can be determined from the comparison of the total CO₂ efflux and the LNAPL footprint. In these cases, investigate using other techniques to determine the background CO₂ efflux. Such as, in the case where a passive CO₂ trap is deployed adjacent to a DCC location, the results can be compared and, if comparable, the modern flux found with a passive CO₂ trap can be used as background to correct the DCC measurements. Alternatively, the assigned surface vegetation cover may be incorrect and may need to be changed.

Although, it is not always possible, it is recommended that at least two background locations per vegetative cover are identified and thus used for correction.

Calculate the NSZD rate

During the background correction process, each location is assigned a surface vegetative cover type. Background locations are identified within the vegetative designations and the average CO₂ efflux at these background locations are subtracted from all measurements taken in the area, thus reducing the CO₂ efflux to that derived only from the LNAPL source. Based on the assumed hydrocarbon stoichiometry of the LNAPL source (e.g. tetradecane C₁₄H₃₀) the CO₂ efflux is converted and the NSZD rate is calculated.

The NSZD rates at all locations can then be mapped and contoured. The areas of each contoured region are used to estimate the total NSZD for that contoured interval. The NSZD rates per interval are summed to obtain the total site-wide estimate of NSZD.

The degradation rate may vary seasonally if the site is located in a temperature latitude and the LNAPL smear zone is relatively shallow. If seasonal changes are suspected, the annual degradation rate requires seasonal corrections. This can be accomplished through the collection of efflux measurements at various times throughout the year to evaluate how the CO₂ efflux changes over time. From this data set, a more accurate site-wide annual NSZD rate can be obtained.

A second geospatial mapping, this time of the corrected CO₂ efflux or calculated NSZD rates at each monitoring location, may be useful to help further assess the DCC monitoring results. Contouring and geospatial integration of the NSZD rates across the site at all locations can be performed to estimate the site-wide, total NSZD rate.

DCC method quality assurance/quality control

QA/QC measures are critical in evaluating the accuracy and precision of the efflux measurements obtained using the DCC methodology. Manufacturers of the DCC systems commonly periodically perform a thorough and intensive calibration under controlled conditions in a laboratory setting. In addition, calibration of the instrument in the field using a span gas is recommended to set the instrument to atmospheric conditions encountered in the field. This field calibration involves calibration to a 0 parts per million by volume (ppmv) CO₂ standard (zero gas) and a span gas cylinder with a 500 ppmv CO₂ concentration.

It is also recommended that a duplicate collar be installed and duplicate efflux measurements be made at a frequency of one for every 10 locations. Collect the duplicate location measurement during the same time of day as the normal (parent) sample location. Locate the normal and the duplicate locations less than 0.3 metres (m) apart and within the same ground cover. General statistics such as relative percent difference (RPD) between normal and duplicate sample locations are performed to assess data quality and identify potential differences in soil collar installation, ensure a good seal with the subsurface was attained, and evaluate any heterogeneities in the subsurface. Generally, an RPD greater than 30% indicates that the practitioner should evaluate installation procedures and influences of soil heterogeneities. The 30% RPD is a target only and may not be achievable at many sites due to soil heterogeneities.

Variability in sequential measurements may be observed greater than 10% of each other. If this situation arises, it is recommended to perform a second round of measurements at the same location. If efflux measurements are to be repeated at the same collar within an individual day, delay the subsequent measurement by 20 minutes to allow re-equilibration of vapours in the soil.

In addition, a field blank measurement comprised of 60 readings, is collected during each field event. A collar with a sealed bottom cap is used for the field blank. The field blank is used to estimate the detection limit of the DCC system as described in the next section.

Detection limit

The detection limit of the DCC method is dictated by the detection limit of the IRGA. The IRGA of the LI-COR 8100A has an accuracy of 1.5% of the measured CO₂ concentration, with a peak to noise ratio of approximately 2 ppmv. Under a controlled experiment by LI-COR, the limit of detection of the analyser was found to be 0.01 $\mu\text{mol}/\text{m}^2/\text{s}$ (LI-COR 2014).

Atmospheric conditions influence the limit of detection of the LI-COR 8100A analyser. Therefore, atmospheric differences (e.g. changes in barometric pressure) influence the limit of detection. To account for this, collect a CO₂ flux field blank during each individual field event to determine a limit of detection for the particular atmospheric conditions encountered during a particular event. This is performed by collecting efflux measurements on a completely sealed collar that is impermeable to gas flow into the

chamber (LI-COR 2014). Typically, the detection limit found with a field blank is composed of the average of 60 readings and the addition of three times the standard deviation. Measured efflux values below the field limit of detection are considered non-detect.

Consider the following when designing a field program and obtaining efflux measurements:

- A review of historical documentation and photo documentation of each collar location is used to ensure that locations are as expected.
- If snow occurs after a collar is installed, remove as much snow as possible prior to the data collection. If snow melt and refreezing occurred, then re-install the collar.
- If vegetation grows or vegetation dead collects in the collar after installation, the vegetation needs to be removed prior to completing the measurements(s).

F.2 – Example DCC method-based NSZD rate calculations

An example case study of the DCC method and calculations is presented in this section to show how measurements of CO₂ efflux can be used to obtain a site-wide NSZD rate. It is based on a real setting where NSZD monitoring was performed.

Study details

During the fall of 2015 and spring of 2016 CO₂ efflux surveys were conducted at a natural gas compressor station in an arid temperate region where various condensate releases and a flare pit historically served as LNAPL sources to the subsurface. The LI-COR 8100A unit was employed to measure CO₂ efflux over two opposing seasons to estimate the range in site-wide NSZD rates at the site. In addition, a select number of locations were also co-located with the passive CO₂ trap efflux method for comparison purposes against the DCC method results. The subsurface is primarily composed of a heterogeneous sand and silty sand material with clay.

Installation of soil collars

Installed soil collars at 34 normal and three duplicate locations and re-compacted the soil to pre-installation conditions with a 25 cm slide hammer weighing 2.5 kg. Soil collars were set in place a minimum of approximately 12 hours before the first measurement to allow for CO₂ vapour in the shallow soil to stabilise and minimise effects from soil disturbance occurring as a result of setting the collars in the soil.

CO₂ efflux measurement

The LI-COR controller was set up with the following parameters:

- Chamber offset = Average collar height above soil
- Observation delay = 0 s
- Deadband = 20 s
- Observation rate = 90 s
- Post-purge = 30 s

After the collar and LI-COR 8100A controller were set up, the CO₂ efflux survey measurements were collected at the 34 normal and 3 duplicate locations. A minimum of three observations (CO₂ efflux measurements) were recorded at each soil collar location. On occasion, five to seven measurements were collected at collar locations in order to attempt to obtain three measurements with less than 10% variance. Collected data were stored on the memory card in the LI-COR instrument and were directly transferred to a laptop computer at the end of each day and reviewed for accuracy with the recorded field notes.

Data optimisation

The data was then optimised as described in appendix F.1 to optimise the curve fit (R²) by adjusting the deadband and observation time using the current version of software provided by LI-COR, Inc.

Data evaluation

Once the data was optimised, it was loaded into an Excel table and measurements removed from average efflux calculation based on poor quality and outlier identification. Poor quality data designations include less than 90 readings per measurement (a reading is one individual measurement of the CO₂ concentration, multiple readings over time are used to calculate an efflux), an optimised R² less than 0.5, a flux of less than - 0.2 μmol/m²/s, and an infrared gas analyser (IRGA) temperature of less than 50 degree Celsius (°C). Outliers were identified if they were found to have greater than a 100% difference of the average efflux measurements made at an individual location. Efflux values that were found to be less than field detection limit (the field blank average plus 3 times the standard deviation ($0.03 \mu\text{mol}/\text{m}^2/\text{s} + 3 \cdot 0.09 \mu\text{mol}/\text{m}^2/\text{s} = 0.3 \mu\text{mol}/\text{m}^2/\text{s}$)) were assigned a non-detection designation.

Total CO₂ efflux

The three to seven CO₂ efflux measurements obtained at each location, that passed the data validation process, were averaged to obtain the total CO₂ efflux at a particular location for each measurement event. The total CO₂ efflux values can be viewed in the Total CO₂ efflux column of table F.2-1.

Vegetation surface cover determination

Through field notes on surface vegetation per location, areal imagery, and evaluation of significant differences in measured effluxes (performed using a non-parametric t-test), it was found that there were two types of surface vegetation coverage: none/little vegetation and vegetated.

Background location identification and calculation

The total CO₂ efflux values at all locations were plotted and contoured (figure F.2-1). Locations SC-1, SC-4, and SC-12 (measured during September 2015, but was removed from the measurement program prior to the March 2016 survey) within the non to little vegetation area and SC-29 and SC-32 within the vegetated area were assigned as background locations because they were located outside of the LNAPL footprint and possessed lower CO₂ effluxes. The effluxes from each of the different vegetation surface covers were then averaged. The average background effluxes measured during the 23 March 2016 event were 0.38 and 1.2 μmol/m²/s for the none/little vegetation and vegetated areas, respectively.

Corrected CO₂ efflux

Following the determination of background values, corrected CO₂ efflux values were calculated. The correction was performed by subtracting the average background total CO₂ efflux for a specific vegetative ground cover from the total CO₂ efflux at locations above the LNAPL footprint within the same vegetative ground cover. The results are listed in the corrected efflux column in table F.2-1.

Hydrocarbon degraded per location

To convert the corrected CO₂ efflux, or the NSZD-derived CO₂ efflux, to an NSZD rate, octane (C₈H₁₈) was assumed the representative hydrocarbon for the condensate that was released at the site.

Equation F.2: $\text{C}_8\text{H}_{18} + 12.5 \text{O}_2 \rightarrow 8 \text{CO}_2 + 9 \text{H}_2\text{O}$

As shown in equation F.2, one mole of octane (MW 114.23 g/mol) is degraded through the microbial mediated processes to form eight moles of CO₂. Below is an example calculation for location SC-3DUP for DCC measurement on 17 September 2015:

$$R_{NSZD} = 8.8 \frac{\mu\text{mol CO}_2}{\text{m}^2\text{day}} \cdot \frac{1 \text{ mol C}_8\text{H}_{18}}{8 \text{ mol CO}_2} \cdot \frac{114.23 \text{ g C}_8\text{H}_{18}}{1 \text{ mol C}_8\text{H}_{18}} \cdot \frac{86400 \text{ s}}{1 \text{ d}} \cdot \frac{1 \text{ mol}}{1000000 \mu\text{mol}}$$

$$R_{NSZD} = 11 \frac{\text{gC}_8\text{H}_{18}}{\text{m}^2\text{d}}$$

A tabulation of the NSZD rates is presented in table F.2-1.

Site-wide rate of natural source zone degraded

The hydrocarbon degraded rates were plotted and contoured as shown in figure F.2-2. The contours indicate various intervals of NSZD rates across the site. The areas defined by these contours were multiplied by the average NSZD rate in each contour interval and then summed to obtain a site-wide rate of estimated NSZD. The site-wide NSZD rates were calculated as shown in table F.2-2. The loss rate found in the September 2015 was 15,800 kg/yr, which was found to be 70% larger than the loss rate of 9,300 kg/yr found in March/April of 2016.

Table F.2-1 Summary of LI-COR efflux measurements

Location	Date	Season	Surface cover	Type of product	Pressure (kPa)	Temperature (°C)	Total CO ₂ efflux (μmol/m ² /s)	Standard deviation	% of Average	Corrected CO ₂ efflux (μmol/m ² /s)	Estimated NSZD rate (g/m ² /d)
Little to No Vegetation											
SC-1	2/9/2015	(Sept. 2015)	Silty sand/gravel	--	80.58	32.84	1.3	0.08	6%	--	--
	16/9/2015				80.31	21.11	2.0	0.06	3%	--	--
	23/3/2016	(March/April 2016)	Silty sand	--	80.48	12.31	0.61	0.03	5%	--	--
	13/4/2016				80.38	20.00	0.79	0.05	7%	--	--
SC-4	2/9/2015	(Sept. 2015)	Silty sand/gravel	--	80.72	31.36	0.31	0.00	0%	--	--
	17/9/2015				81.01	12.40	0.74	0.05	7%	--	--
	23/3/2016*	(March/April 2016)	Gravel/sand (non-native)	--	80.43*	12.15*	0.15 (ND)*	0.00*	0%*	--	--
	13/4/2016				80.51	23.16	0.20	0.01	7%	--	--
SC-12	2/9/2015*	(Sept. 2015)	Silty sand	--	80.47*	32.48*	0.39*	0.04*	9%*	--	--
	17/9/2015				81.04	17.06	0.76	0.04	5%	--	--
Little to no vegetation background average CO ₂ efflux (2/9/2015 – 4/9/2015):							0.68				
Little to no vegetation background average CO ₂ efflux (17/9/2015):							1.2				
Little to no vegetation background average CO ₂ efflux (23/3/2016):							0.38				
Little to no vegetation background average CO ₂ efflux (13/4/2016):							0.50				
SC-2	2/9/2015	(Sept. 2015)	Gravel	Liquid Natural Gas	80.74	30.08	0.41	0.03	7%	0.0	0.0
	16/9/2015				80.32	19.01	0.47	0.02	3%	0.0	0.0
	23/3/2016	(March/April 2016)	Gravel/Sand (non-native)	Liquid Natural Gas	80.47	10.02	0.41	0.02	6%	0.030	0.037
	13/4/2016				80.50	21.83	1.2	0.06	5%	0.71	0.88
SC-3	2/9/2015	(Sept. 2015)	Silty sand	Liquid natural gas	80.73	34.22	32	1.14	4%	32	39
	17/9/2015				80.98	12.81	18	0.69	4%	17	21
	23/3/2016	(March/April 2016)	Silty sand/gravel	Liquid natural gas	80.45	12.25	1.5	0.02	2%	1.2	1.4
	13/4/2016				80.35	19.05	1.4	0.07	5%	0.86	1.1
SC-3DUP	2/9/2015*	(9/16/15)	Silty sand	Liquid natural gas	80.61*	32.05*	13*	0.33*	2%*	13*	16*
	17/9/2015				80.92	15.06	9.9	0.11	1%	8.8	11
	23/3/2016	(March/April 2016)	Silty sand/gravel	Liquid natural gas	80.46	11.43	0.95	0.03	3%	0.57	0.70
	13/4/2016				80.36	19.14	12	0.50	4%	11	14
SC-5	2/9/2015	(Sept. 2015)	Silty sand/gravel	Liquid natural gas	80.70	32.73	0.78	0.02	2%	0.10	0.13
	17/9/2015				80.85	15.92	0.56	0.02	4%	0.0	0.0
	23/3/2016	(March/April 2016)	Silty sand/gravel	Liquid natural gas	80.46	12.20	0.15 (ND)	0.01	0%	0.0	0.0
	13/4/2016*				80.35*	18.49*	0.28*	0.01*	3%*	0.0*	0.0*
SC-6	2/9/2015*	(Sept. 2015)	Silty gravel	Liquid natural gas	80.52*	31.63*	0.26*	0.00*	0%*	0*	0.0*
	16/9/2015				80.97	15.44	0.40	0.01	2%	0.0	0.0
	17/9/2015	(March/April 2016)	Silty sand	Liquid natural gas	80.44	13.42	0.25 (ND)	0.09	0%	0.0	0.0
	23/3/2016				80.41	23.00	0.31	0.02	7%	0.0	0.0
SC-7	2/9/2015	(Sept. 2015)	Silty sand	Liquid natural gas	80.63	33.26	0.72	0.05	7%	0.043	0.053
	16/9/2015				80.30	20.98	1.7	0.15	9%	0.57	0.70
	23/3/2016*	(March/April 2016)	Silty sand	Liquid natural gas	80.49*	13.79*	0.15 (ND)*	0.00*	0%*	0.0*	0.0*
	13/4/2016				80.37	20.21	0.34	0.01	2%	0.0	0.0
SC-8	2/9/2015	(Sept. 2015)	Silty sand/gravel	Liquid natural gas	80.56	33.03	0.59	0.03	5%	0.0	0.0
	16/9/2015				80.30	21.00	0.92	0.07	7%	0.0	0.0
	23/3/2016	(March/April 2016)	Silty sand	Liquid natural gas	80.49*	13.43*	0.15 (ND)*	0.00*	0%*	0.0*	0.0*
	13/4/2016				80.39	22.08	0.33	0.03	9%	0.0	0.0
SC-9	2/9/2015	(Sept. 2015)	Silty sand/gravel with little vegetation	Liquid natural gas	80.63	21.53	8.7	0.21	2%	8.1	9.9
	17/9/2015				80.58	23.21	8.3	0.21	3%	7.2	8.9
	23/3/2016	(March/April 2016)	Silty sand	Liquid natural gas	80.49	12.58	4.3	0.09	2%	3.9	4.8
	13/4/2016				80.72	19.53	4.7	0.26	6%	4.2	5.1
SC-10	2/9/2015*	(Sept. 2015)	Silty sand/gravel	Liquid natural gas	--*	--*	--*	--*	--*	--*	--*
	17/9/2015*				80.75*	22.08*	1.2*	0.06*	5%*	0.55*	0.68*
	23/3/2016				80.45	13.05	0.15 (ND)	0.00	0%	0.0	0.0

	13/4/2016	(March/April 2016)	Silty sand	Liquid natural gas	80.53	23.58	0.25	0.02	6%	0.0	0.0
SC-11	2/9/2015	(Sept. 2015)	Silty sand/gravel	Liquid natural gas	80.46	32.44	0.70	0.06	9%	0.023	0.028
	17/9/2015				80.75	19.95	0.30	0.01	4%	0.0	0.0
	23/3/2016	(March/April 2016)	Gravel/sand	Liquid natural gas	80.44	11.60	0.41	0.02	6%	0.030	0.037
13/4/2016	80.55				21.57	0.20	0.01	6%	0.0	0.0	
SC-13	3/9/2015	(Sept. 2015)	Silty sand/gravel	Liquid natural gas	80.61	23.81	0.81	0.06	8%	0.13	0.16
	17/9/2015				80.43	14.21	0.29	0.02	6%	0.0	0.0
	23/3/2016	(March/April 2016)	Silt	Liquid natural gas	80.05	9.94	0.15 (ND)	0.00	0%	0.0	0.0
	13/4/2016*				80.67*	20.83*	0.61*	0.03*	5%*	0.12*	0.14*
SC-14	2/9/2015	(Sept. 2015)	Silty sand/gravel	Liquid natural gas	80.54	18.75	0.50	0.02	4%	0.0	0.0
	17/9/2015				80.44	14.01	0.36	0.02	6%	0.0	0.0
	23/3/2016*	(March/April 2016)	Silt	Liquid natural gas	80.24*	3.84*	0.15 (ND)*	0.00*	0%*	0.0*	0.0*
	13/4/2016				80.69	21.85	0.62	0.05	8%	0.12	0.15
SC-15	2/9/2015	(Sept. 2015)	Silty gravel	Liquid natural gas	80.55	17.82	5.6	0.23	4%	4.9	6.1
	17/9/2015				80.42	15.68	5.2	0.25	5%	4.1	5.0
	23/3/2016	(March/April 2016)	Silty sand	Liquid natural gas	80.57	11.59	2.9	0.03	1%	2.6	3.2
	13/4/2016				80.72	21.98	3.8	0.13	3%	3.3	4.1
SC-17	2/9/2015	(Sept. 2015)	Silty sand/gravel	Liquid natural gas	80.51	20.11	2.1	0.10	5%	1.4	1.7
	17/9/2015				80.44	14.22	1.2	0.06	5%	0.087	0.11
	23/3/2016	(March/April 2016)	Silt/gravel	Liquid natural gas	80.20	1.99	0.79	0.04	5%	0.42	0.51
	13/4/2016				80.65	20.71	2.1	0.13	6%	1.6	2.0
SC-18	2/9/2015	(Sept. 2015)	Silty sand	Liquid natural gas	80.50	20.64	4.2	0.22	5%	3.5	4.3
	4/9/2015				80.54	25.56	5.1	0.20	4%	3.9	4.9
	17/9/2015	(March/April 2016)	Silt	Liquid natural gas	80.67	9.94	1.5	0.07	4%	1.2	1.4
	23/3/2016				80.91	-82.41^	2.7	0.23	8%	2.2	2.7
SC-19	2/9/2015	(Sept. 2015)	Silty sand	Liquid natural gas	80.50	19.42	3.0	0.22	7%	2.3	2.9
	17/9/2015				80.53	24.83	3.8	0.12	3%	2.7	3.3
	23/3/2016	(March/April 2016)	Silty	Liquid natural gas	80.67	10.00	2.2	0.01	1%	1.9	2.3
	13/4/2016				80.88	-82.83^	3.8	0.32	8%	3.3	4.1
SC-19DUP	2/9/2015	(Sept. 2015)	Silty sand	Liquid natural gas	80.49	18.34	3.6	0.08	2%	2.9	3.6
	17/9/2015				80.52	25.58	4.7	0.17	4%	3.5	4.4
	23/3/2016	(March/April 2016)	Silty	Liquid natural gas	80.70	9.52	2.2	0.06	3%	1.8	2.2
	13/4/2016				80.91	-83.36^	3.3	0.17	5%	2.8	3.5
SC-22	3/9/2015	(Sept. 2015)	Silty sand/gravel	Liquid natural gas	80.43	25.92	3.1	0.08	3%	2.4	3.0
	17/9/2015				80.39	18.02	2.7	0.15	5%	1.5	1.9
	23/3/2016	(March/April 2016)	Silt/gravel	Liquid natural gas	80.11	1.82	0.67	0.06	9%	0.29	0.36
	13/4/2016				80.87	-82.78^	0.95	0.06	6%	0.46	0.56
Vegetated											
SC-29	2/9/2015	(Sept. 2015)	Silty sand/vegetated	--	80.52	24.28	3.1	0.09	3%	--	--
	17/9/2015				80.44	18.01	2.9	0.12	4%	--	--
	23/3/2016	(March/April 2016)	Silt/vegetated	--	80.42	7.62	1.2	0.02	1%	--	--
	13/4/2016				80.86	17.32	2.6	0.06	2%	--	--
SC-32	2/9/2015	(Sept. 2015)	Silty sand/vegetated	--	80.47	26.92	3.6	0.08	2%	--	--
	17/9/2015				80.42	15.27	3.6	0.06	2%	--	--
	23/3/2016	(March/April 2016)	Silt/vegetated	--	80.42	10.08	1.2	0.03	3%	--	--
	13/4/2016				80.85	19.75	2.2	0.13	6%	--	--
Vegetated background average CO ₂ efflux (2/9/2015 – 3/9/2015):							3.4				
Vegetated background average CO ₂ efflux (17/9/2015):							3.2				
Vegetated background average CO ₂ efflux (23/3/2016):							1.2				
Vegetated background average CO ₂ efflux (13/4/2016):							2.4				
SC-16	3/9/2015	(Sept. 2015)	Silty sand/gravel/vegetated	Liquid natural gas	80.61	25.15	4.9	0.08	2%	1.6	1.9
	17/9/2015				80.56	25.27	6.8	0.17	2%	3.5	4.3
	23/3/2016	(March/April 2016)	Silty sand/vegetated	Liquid natural gas	80.57	12.49	2.6	0.01	0%	1.3	1.7
	13/4/2016				80.74	22.11	3.1	0.04	1%	1.9	2.4
SC-20	3/9/2015	(Sept. 2015)	Silty sand/gravel/vegetated	Liquid natural gas	80.60	26.69	8.4	0.25	3%	5.0	6.2
	17/9/2015				80.44	26.21	9.0	0.30	3%	5.8	7.2

	23/3/2016 13/4/2016	(March/April 2016)	Silty sand/vegetated	Liquid natural gas	80.59 80.88	11.06 15.23	3.1 2.2	0.01 0.19	0% 8%	1.9 1.0	2.3 1.2
SC-21	3/9/2015 17/9/2015	(Sept. 2015)	Silty sand/gravel/vegetated	Liquid natural gas	80.61 80.44	24.87 14.60	1.7 0.91	0.07 0.07	4% 8%	0.0 0.0	0.0 0.0
	23/3/2016 13/4/2016	(March/April 2016)	Silty soil	Liquid natural gas	80.26 80.74	5.23 21.74	0.73 1.4	0.01 0.04	1% 3%	0.0 0.13	0.0 0.16
	2/9/2015 17/9/2015	(Sept. 2015)	Silty sand/gravel/vegetated	Liquid natural gas	80.49 80.45	19.77 26.84	8.2 10	0.40 0.18	5% 2%	4.8 6.8	6.0 8.4
	23/3/2016 13/4/2016	(March/April 2016)	Silty/vegetated	Liquid natural gas	80.30 80.64	7.23 23.84	0.64 2.5	0.02 0.07	3% 3%	0.0 1.2	0.0 1.5
SC-23	2/9/2015 17/9/2015	(Sept. 2015)	Silty sand/gravel/vegetated	Liquid natural gas	80.50 80.44	19.75 26.60	9.2 11	0.42 0.24	5% 2%	5.8 7.7	7.2 9.5
	23/3/2016 13/4/2016	(March/April 2016)	Silty/vegetated	Liquid natural gas	80.30 80.91	6.93 -81.48^	2.7 3.2	0.03 0.03	1% 1%	1.5 1.9	1.8 2.4
	2/9/2015 17/9/2015	(Sept. 2015)	Silty sand/gravel/vegetated	Liquid natural gas	80.59 80.48	27.68 25.87	5.3 5.7	0.19 0.16	4% 3%	1.9 2.5	2.4 3.0
	23/3/2016 13/4/2016	(March/April 2016)	Silty sand/vegetated	Liquid natural gas	80.62 80.92	11.20 7.04	3.1 3.1	0.02 0.12	0% 4%	1.9 1.9	2.3 2.4
SC-24	3/9/2015 17/9/2015	(Sept. 2015)	Silty sand/gravel/vegetated	Liquid natural gas	80.60 80.50	27.64 21.85	6.5 3.3	0.35 0.10	5% 3%	3.1 0.053	3.9 0.065
	23/3/2016 13/4/2016	(March/April 2016)	Silty/vegetated	Liquid natural gas	80.65 80.91	11.00 -82.61^	0.41 0.69	0.02 0.06	4% 8%	0.0 0.0	0.0 0.0
	3/9/2015 17/9/2015	(Sept. 2015)	Sandy silt/vegetated	Liquid natural gas	80.53 80.41	28.93 19.82	5.7 2.9	0.10 0.13	2% 5%	2.3 0.0	2.9 0.0
	23/3/2016 13/4/2016	(March/April 2016)	Silty/vegetated	Liquid natural gas	80.18 80.89	2.40 -82.70	2.6 5.1	0.13 0.16	5% 3%	1.4 3.8	1.7 4.7
SC-25	3/9/2015 17/9/2015	(Sept. 2015)	Sandy silt/vegetated	Liquid natural gas	80.56 80.42	28.61 22.08	7.4 3.8	0.11 0.15	1% 4%	4.1 0.51	5.0 0.63
	23/3/2016 13/4/2016	(March/April 2016)	Silt/vegetated	Liquid natural gas	80.34 80.91	9.03 3.71	3.4 3.8	0.02 0.17	0% 5%	2.1 2.5	2.6 3.1
	2/9/2015 17/9/2015	(Sept. 2015)	Sandy silt/vegetated	Liquid natural gas	80.49 80.52	21.74 20.34	6.4 4.3	0.35 0.04	5% 1%	3.1 1.0	3.8 1.3
	23/3/2016 13/4/2016	(March/April 2016)	Silty/vegetated	Liquid natural gas	80.66 80.91	8.63 -83.36^	1.8 2.9	0.03 0.09	1% 3%	0.58 1.7	0.71 2.1
SC-26	3/9/2015 17/9/2015	(Sept. 2015)	Sandy silt/vegetated	Liquid natural gas	80.48 80.42	27.86 17.08	6.4 6.4	0.39 0.11	6% 2%	3.0 3.2	3.7 3.9
	23/3/2016* 13/4/2016	(March/April 2016)	Silty/vegetated	Liquid natural gas	80.38* 80.79	7.23* 19.41	2.9* 3.9*	0.12* 0.16	4%* 4%	1.7* 2.7	2.1* 3.3
	2/9/2015 17/9/2015	(Sept. 2015)	Sandy silt/vegetated	Liquid natural gas	80.47 80.43	27.97 16.35	6.3 2.7	0.32 0.17	5% 6%	3.0 0.0	3.7 0.0
	23/3/2016 13/4/2016+	(March/April 2016)	Silty/vegetated	Liquid natural gas	80.40 --	10.75 --	1.4 --	0.02 --	1% --	0.18 --	0.23 --
SC-27	3/9/2015 17/9/2015	(Sept. 2015)	Sandy silt/vegetated	Liquid natural gas	80.48 80.39	33.56 17.05	3.5 4.5	0.16 0.11	5% 3%	0.16 1.2	0.20 1.5
	23/3/2016 13/4/2016	(March/April 2016)	Silty/vegetated	Liquid natural gas	80.13 80.90	1.49 3.15	0.95 1.3	0.61 0.06	64% 5%	0.0 0.11	0.0 0.14
	23/3/2016* 13/4/2016	(March/April 2016)	Silt/vegetated	Liquid natural gas	80.57* 80.73	13.75* 21.10	2.2* 2.6	0.00* 0.09	0%* 4%	0.95* 1.4	1.2* 1.7
	23/3/2016* 13/4/2016	(March/April 2016)	Silt/vegetated	Liquid natural gas	80.57* 80.73	13.75* 21.10	2.2* 2.6	0.00* 0.09	0%* 4%	0.95* 1.4	1.2* 1.7

* Did not acquire three readings within 10%; + the SC-31 location was damaged due to cattle and was not measured during the 13 April 2016 event; ^ temperature measurement is not consistent with observed ambient temperatures; depth to groundwater based on the closest well with available information to the monitoring location; octane (C8H18) was used as the representative hydrocarbon; -- not sampled; NA not applicable; ND not detected; NM not measured; NT no groundwater temperature acquired due to presence of light non-aqueous phase liquid in well.

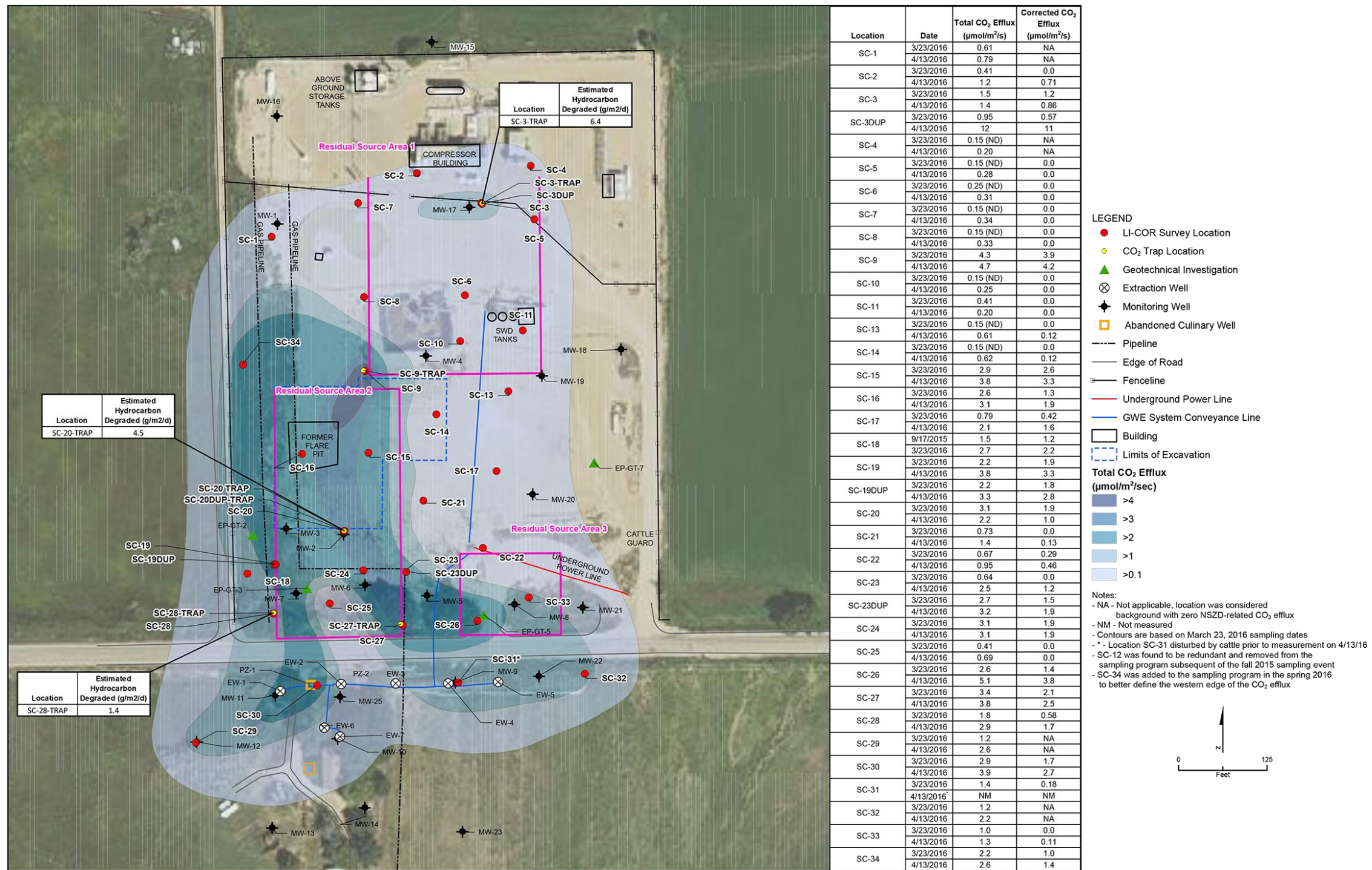


Figure F.2-1 Total CO₂ efflux measurement results, March and April 2016

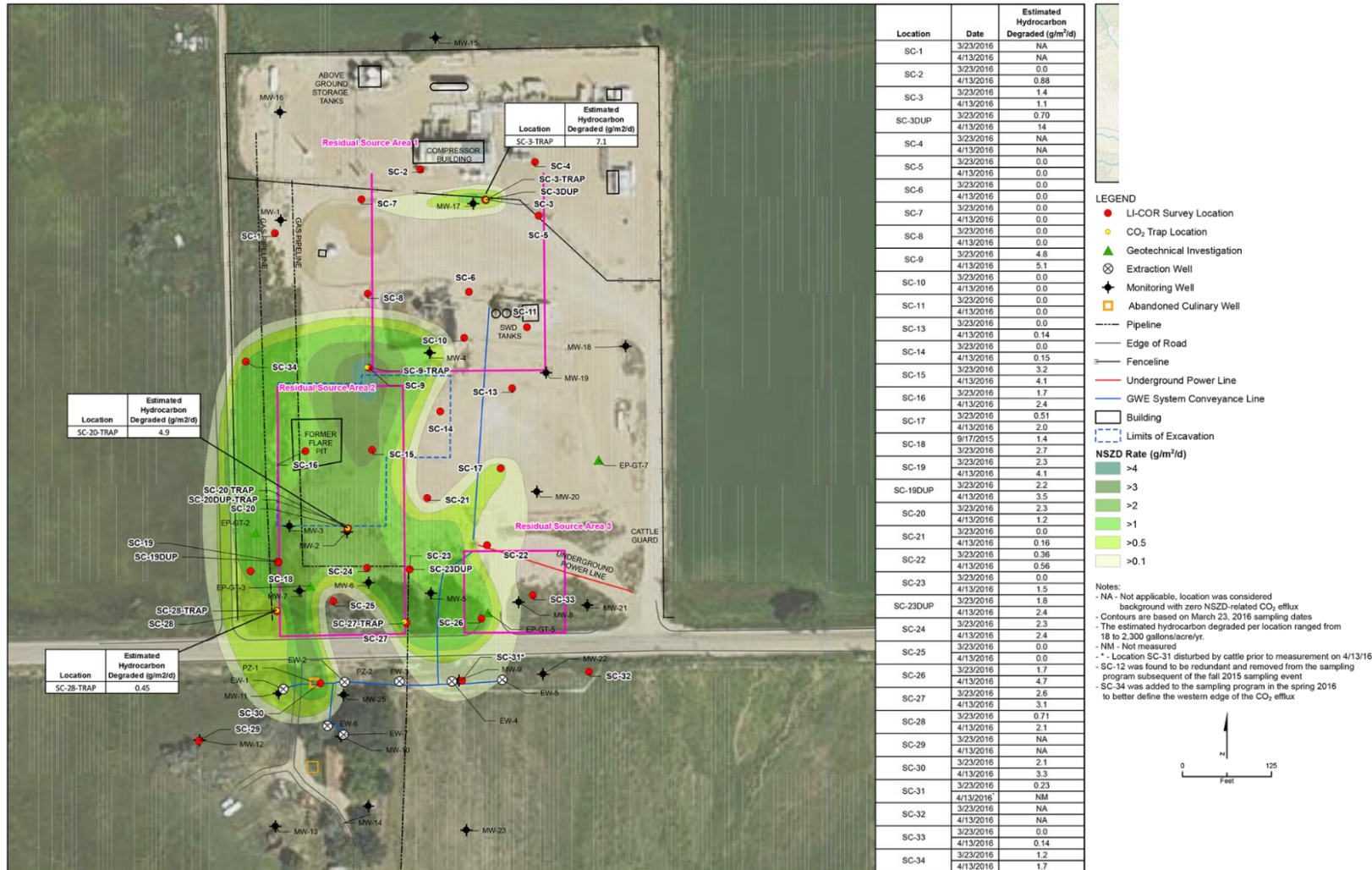


Figure F.2-2 NSZD rates, March and April 2016

Table F.2-2 Calculation of estimated site-wide NSZD rate based on March/April 2016 CO₂ effluxes

Isoconcentration level (g/m²/d)	Average rate (g/m²/d)	Area (m²)	Annual extrapolation (kg/yr)
>4	4.4	165	266
3–4	3.5	708	905
2–3	2.5	3790	3459
1–2	1.50	5879	3219
0.5–1	0.75	3715	1017
0.1–0.5	0.3	4282	469
Total NSZD	12.9	18,500	9,300

APPENDIX G.

Biogenic heat method-based NSZD evaluation procedures

This appendix contains procedures useful for practitioners to reference when implementing the biogenic heat method for NSZD evaluation. The following procedures are included herein:

G.1 – Technical summary table of published approaches to estimate NSZD from temperature measurements

G.2 - Procedure for biogenic heat method data analysis (including background correction)

G.3 – Example biogenic heat method-based NSZD rate calculations

G.1 – Technical summary table of published approaches to estimate NSZD rates from temperature measurements

This table summarises the copious amount of information that was available on using subsurface temperature measurements as a basis for estimating NSZD rates. Petroleum hydrocarbon biodegradation reactions associated with NSZD are often manifested as increases in soil temperature. Various entities have developed theoretical bases, analytical and numerical methods, and monitoring approaches for estimation of NSZD rates using biogenic methods. In summary, a literature review identified seven different approaches that have been proposed in the literature. They range from simple screening methods to numerical modelling using Monod kinetics. To help understand them better, table G.1-1 presents a summary of the identified biogenic heat-based NSZD evaluation approaches, key assumptions, and data input. Table G.1-1 can be used to help practitioners select which approach may best suit their needs by matching data objectives, available data, and site conditions that may or may not match key assumptions.

Table G.1-1. Attributes of available tools to estimate NSZD rates from subsurface temperature monitoring.

Name/source	Johnston <i>et al</i> (2008)	Sweeney and Ririe (2014)	Sweeney and Ririe (2014)	Warren and Bekins (2015)	Warren and Bekins (2015)	ThermaINSZD® (2017)	BioTherm® (2015)
Threshold attributes							
Overview	Quantitative Heat flux analysis. Sensitive to soil thermal properties and estimated air flux. Site-specific measure of soil properties suggested along with thermal characteristics of biodeg reactions.	Screening Option 1 – hybrid thermal and soil gas approach, uses in-well temperature measurement to identify depth to aerobic/anaerobic (A/A) interface, then applies gradient method using soil gas data	Quantitative Option 2 – thermodynamic approach, Van Wijk and de Vries (WV) (1963) equation to estimate ΔT and SF (heat flux), curve fits to measured temp data to separate heat from NSZD and background	Quantitative Option 1 – saturated and unsaturated zone temperature measurements used to determine microbial heating rates in unsaturated zone estimated by averaging measured temperature increase over one year, produced heat is used to estimate the NSZD rate	Screening Option 2 – rough estimate, measure groundwater temperature (in situ, not flow through) at depth to water, difference between ambient and temperature at groundwater table is ΔT , this closely approximates NSZD rate without the thermal anomalies associated with the vadose zone	Quantitative Energy flows from conduction, convection, and the change in storage of energy within the NAPL impacted area, to determine the rate of energy released during NAPL biodegradation. Includes a series of thermodynamic equations to estimate the value of heat released (enthalpy) from biodeg reactions. (CSU patent pending)	Screening, quantitative if calibrated to field data A one-dimensional transient heat equation for coupled heat transfer and heat generation in soils. Calculates NSZD rates from Monod kinetics NSZD _{monod} and thermal gradients NSZD _{TG} using multiple modalities including no, ideal, or non-ideal background correction and instantaneous or annual term. (E-Flux LLC patent-pending)
Peer reviewed	No, conference paper	Yes, in peer reviewed journal	Yes, in peer reviewed journal	Yes	No, put forth as an option in the paper, but not fully vetted	No, only presented in CSU thesis	No, not yet published
Relative use	Deployed on <5 sites	>10 sites	>10 sites	Deployed on one site	Deployed on one site	Deployed on <10 sites	Applied on <5 sites
Basic attributes							
Heat balance dimension	1D	1D	1D	1D	1D	1D	1D
Steady state/transient	Steady-state	Steady-state	Transient	Steady-state	Steady-state	Transient	Transient
Background correction	No	Yes	Yes	Yes, and normalised for variable unsaturated zone thicknesses (to average depth to water) and segregated for other heat sources	Same as Warren and Bekins (2015) Option 1, except only correct groundwater temperatures	Same as Sweeney and Ririe (2014) Option 2	Optional, uses standard approach, but also a long-term mass balance that does not need background correction
Analytical/numerical	Numerical (simple vertical heat conduction equation)	Analytical	Analytical	Analytical	Analytical	Analytical	Numerical
Inherent assumptions							
Boundary conditions	Constant temperature at ground surface and within groundwater (~1.5 m below water table)	See API 2017 for gradient method assumptions, zero O ₂ at A/A interface	Annual WV model, no net heating of soil, biodegradation heat = heat flux to groundwater and atmosphere	Same as Sweeney and Ririe (2014) Option 2	Same as Warren and Bekins (2015) Option 1	Same as Sweeney and Ririe (2014) Option 2	Transient ambient temperatures on top side of the control plane, transient groundwater temperatures on bottom plane, no lateral heat transport
Exclusions	No vertical flow or heat from of liquid water of VOCs, no vapour dispersion, no difference in thermal properties of LNAPL/water	See API 2017 for gradient method assumptions	Lateral heat loss from gw flow, convection, water vapour (latent heat of vaporisation)	Same as Sweeney and Ririe (2014) Option 2	Same as Warren and Bekins (2015) Option 1	See Sweeney and Ririe (2014) Option 2, except has site-specific biodegradation reactions for heat production term	Soil gas transport, heat loss from biomass growth
Inclusions	Conduction, air convection, and water vapour	Instantaneous reaction (Davis <i>et al</i> 2009b) – all O ₂ use goes to hydrocarbon biodegradation and creates a thermal signature, see API 2017 for gradient method assumptions	Heat loss to atmosphere and groundwater through conduction	Heat loss via vertical conduction only to land surface, uniform thermal conductivity in soil (comparable between LNAPL and background locations)	Same as Warren and Bekins (2015) Option 1	All reactions go to completion – i.e. CO ₂ and H ₂ O	Monod kinetics apply, steady-state biomass, all biodegradation reactions go to completion – i.e. CO ₂ and H ₂ O

Isotropic/homogeneous	Yes	Yes	Yes	Yes	Yes	Yes	Yes, but option to include multiple soil layers pending
Other assumptions	100% RH soil vapour, constant vertical air flux, constant depth-distribution of water saturation	API 2017 for gradient method assumptions	Constant biogenic heat source	Same as Sweeney and Ririe (2014) Option 2, no biomass growth	Same as Sweeney and Ririe (2014) Option 2, groundwater is better buffered from temperature variations and is representative because it's warmed by the overlying CH ₄ oxidation reaction	Same as Sweeney and Ririe (2014) Option 2	The user is encouraged to test the sensitivity of the model solution to all inputs
Governing equation #1	Heat balance → $H_{\text{internal}} = H_{\text{stored}} + \int \{J_{z\text{-top}} - J_{z\text{-bot}}\} dt$	Fick's Law, $J = D_v^{eff} \frac{dC}{dz}$	WV equation, $T(z,t) = T_o + A_o \cos(\omega z/D) \sin(\omega t - \omega z/D)$	Maximum annual average temperature for each monitoring location used to determine heat from CH ₄ oxidation (Fourier's first law) $q_H = K * \Delta T / \Delta x$	$q_H = K * \Delta T / \Delta x$, where ΔT is the change in temperature between land surface and groundwater and Δx is half this distance from land surface to water table	Fourier's first law, $q_h = -K_T (\Delta T / \Delta z)$	Fourier heat equation, $\partial T / \partial t = \alpha (\partial^2 T / \partial z^2) + (q_i / \rho c_p)$; $\alpha = k / (\rho * C_p)$
Governing equation #2	$H_{\text{internal}} = H_{\text{bio}} + H_{\text{latent}}$, assumes a secondary source of heat from vaporisation and mass flux of water vapour out of control volume	None	$H_{\text{bio}} = G_{\text{bio}} / H_{\text{hydrocarbon}}$	NSZD = q_H / H^0 , stoichiometric conversion to CO ₂ efflux for comparison to other methods	Same as Warren and Bekins (2015) Option 1	NSZD = q_H / H^0	Monod kinetics equation, $-dC/dt = (k_{max}C) / (C + C_m) = (k_0C) / (C + C_m)$
Required data input							
Continuous temperature	Yes	No, not necessary	Yes, at least daily measurements for one year	Yes (e.g. hourly in water-filled tube in vadose zone for one year)	Yes	Yes	No, model generates soil temperature profiles that can be compared to field measurements, but does not accept them as input
Thermal conductivity	Yes, based on Zhang <i>et al</i> 2007 (3D)	No	Yes	Yes	Yes	Yes	Yes
Heat of biodegradation	Yes, based on Tissot 1999	No	Yes, assumed 48 kJ/gPHC oxidation (average gasoline and kerosene range)	Used methane and hexadecane as representative hydrocarbon for Bemidji crude, assumes all heat reactions occur in the aqueous phase (not in the LNAPL)	Yes	Yes (patented series of thermodynamic equations)	Yes (Monod and Arrhenius equations)
Groundwater temperature	Yes	Yes	Yes	Yes	Yes	Yes	Yes
Lab analysis – heat of bioreaction	No	No	No	No	No	No	No, calculated or literature based
Ambient temperature	Yes	Yes	Yes	Yes	Yes	Yes	Yes
Soil PHC concentrations	No	No	No	No	No	No	Yes

G.2 – Procedure for biogenic heat method data analysis (including background correction)

The information presented in this section was extracted from the following source(s):

- Sweeney, RE & Ririe, GT 2014, 'Temperature as a tool to evaluate aerobic biodegradation in hydrocarbon contaminated soil', *Groundwater Monitoring & Remediation*, vol. 34, no. 3, pp. 41–50.
- Warren, E & Bekins, BA 2015, 'Relating subsurface temperature changes to microbial activity at a crude oil-contaminated site', *Journal of Contaminant Hydrology*, vol. 182, pp. 183–193.
- API 2017, *Quantification of vapor phase-related NSZD processes*, Publication No. 4784.
- Sass, JH, Kennelly, JP, Smith, EP & Wendt, WE 1984, *Laboratory line-source methods for the measurement of thermal conductivity of rocks near room temperature*, Open-file report 84-91, US Department of the Interior Geological Survey.
- Van Wijk, WR & de Vries, DA 1963, 'Periodic temperature variations in a homogeneous soil', in WR Van Wijk (ed) *Physics of Plant Environment*, North-Holland Publishing Company, Amsterdam.

Purpose and scope

The purpose of this procedure is to provide practical guidelines for the implementation of the biogenic heat method to estimate the rate of NSZD in the subsurface. As described in detail in section 5 of the main body of this document, this procedure assumes that conduction is the dominant heat transport mechanism in the soil and the site conditions vetted and the method determined applicable.

This procedure provides step-by-step instructions, ranging from installation of the soil temperature monitoring probes through to the calculation of the NSZD rate. Section III of this appendix provides specific procedures for execution of the field work. Example NSZD rate calculations are included in appendix G.3.

The biogenic heat method is based on Fourier's first law of conduction as shown in equation 10.

$$\text{Equation 10: } q_H = K_T \left(\frac{\Delta T}{\Delta Z} \right)$$

where q_H is the steady-state conductive heat flux ($\text{J/m}^2\text{-soil/s}$), which is proportional to the temperature gradient, $\Delta T/\Delta Z$ ($^\circ\text{K/m}$). K_T is the thermal conductivity of the soil ($\text{J/m/s/}^\circ\text{K}$), that is specific to the soil within the zone of the thermal anomaly. This equation will be cited throughout this procedure because it is a fundamental basis for the calculations.

Prerequisites

It is assumed that the following prerequisites have been met prior to use of this procedure:

- An appropriate number of monitoring locations were selected for soil temperature profiling, adequate to meet the data objectives and represent the potential range of NSZD rates at the site.
- Monitoring locations include areas both atop the LNAPL footprint and in background (non-impacted) areas. If an adequate background location is not feasible, then a mathematical approach may be used.
- The various temperature measurement and biogenic heat calculation options were reviewed and a preferred approach selected based on the data needs and site constraints.

Procedures and guidelines

Use of the biogenic heat method to estimate the rate of NSZD involves the following steps:

1. Install soil temperature measurement devices or establish alternative means for temperature monitoring as discussed below
2. Log soil temperatures
3. Estimate the soil thermal conductivity
4. Tabulate the data and calculate the average temperature
5. Plot the average data and account for background
6. Estimate the thermal gradient
7. Calculate the NSZD rate

The following sections detail how to accomplish each step.

Install soil temperature measurement devices

As discussed in section 5.1.2, the depth and intervals of temperature measurements depend upon the site conditions. At a minimum, measurements are needed within and above the hydrocarbon oxidation zone so that an accurate estimate of the upward thermal gradient can be made. Measurements below the oxidation zone and into the groundwater table may also be valuable to assess the downward heat flux and impacts to the shallow groundwater. Review site climatology and groundwater temperatures to assess the ideal measurement depths. Because the incremental added cost to add measurement depths to a thermistor string, for example, is relatively small, at times it makes sense to monitor the entire thickness of the vadose zone and the upper portion of the groundwater at an evenly spaced interval with a maximum of 1 metre (m) spacing to avoid missing thermal peaks useful for gradient estimates.

There are several options to monitor soil temperature profiles and estimate thermal gradient ($\Delta T/\Delta z$) as described in equation 10. Temperature profiles are measured atop and aside the LNAPL footprint and used as a basis to estimate the NSZD rate using the biogenic heat method using various techniques including:

- Dedicated nested string of thermistor or thermocouples
- Existing monitoring wells – thermocouple and reel, and

- Existing monitoring well – dedicated string of button-type temperature loggers.

Temperature monitoring devices should be capable of 0.1 °C) accuracy and resolution in order to adequately measure soil temperature increases as low as 1 °C.

Figures G.2-1 through G.2-4 show examples of each type of temperature measurement technique. The most direct measurement is dedicated thermistor strings, solid rod with multiple thermocouples or thermistors attached to it, installed and backfilled in soil boreholes (figure G.2-1). They can be installed using conventional drilling. The backfill typically consists of dry medium-fine sand to ensure efficient thermal connectivity with the surrounding formation. Thermistors are wired to an at-grade datalogger that is set to record temperatures at least twice daily, once at a time of maximum temperature (e.g. 2 PM) and once at the lowest (e.g. 2 AM). The datalogger can be manually downloaded or connected to the internet for remote data access and periodic download. A similar string of thermistors can also be dropped into a small diameter, solid casing installed using conventional drilling (figure G.2-2). The string can be left in-place if using wired thermistors or temporarily removed and manually downloaded if using wireless button-type temperature data loggers.

When installing temperature monitoring equipment, it is important to limit convective pathways between loggers at separate depths in the same borehole or well.

Sweeney & Ririe (2014) proposed using existing monitoring wells to measure subsurface temperatures. An existing monitoring well with a sealed wellhead can be used as a screening tool to assess subsurface soil temperatures. As shown on figures G.2-3 and G.2-4, this can be performed using either a thermocouple on a reel or a dedicated string of button-type loggers. The reel method requires sequential drop of the thermocouple probe and a wait time of at least 3-minutes at each stop depth before taking a measurement in the vadose zone and at least a 1-minute wait time before taking groundwater temperatures. The wireless button-type temperature data logger strings are typically left in-place for a year or more and periodically removed and manually downloaded.

Biogenic heat flux can be affected by conditions above and below the vadose zone, including atmospheric and groundwater. To support data evaluation efforts after the field measurement program, it is typically prudent to synoptically monitor and record atmospheric conditions such as temperature, barometric pressure, wind speed, and precipitation. This can often be done remotely using data from a local meteorological data station that posts their data on a publicly available website or onsite using a weather monitor. Likewise, synoptic measurements of the groundwater level and temperature can also help inform data evaluation efforts.

Scrutinise the validity of the measurement methods through close inspection of the LCSM including the vadose zone properties (e.g. boring logs, soil samples, soil vapour measurements) and it may be useful to confirm results with at least one nested soil temperature measurement probe installation.

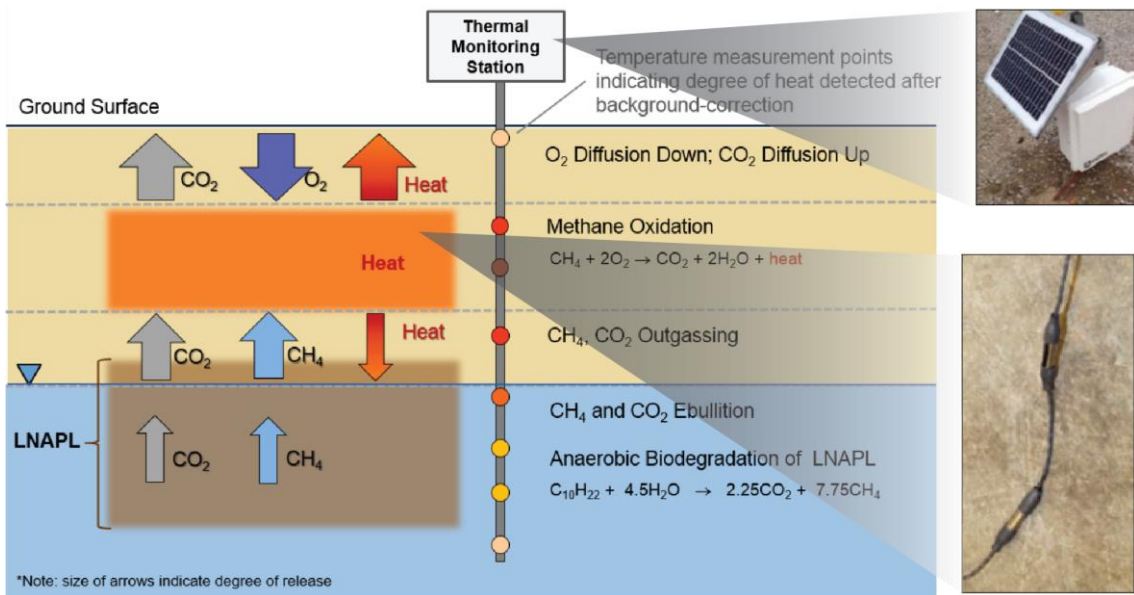


Figure G.2-1. Dedicated nested thermistor string for soil temperature profiling. *Courtesy of ThermalNSZD 2017, www.thermalnszd.com)*

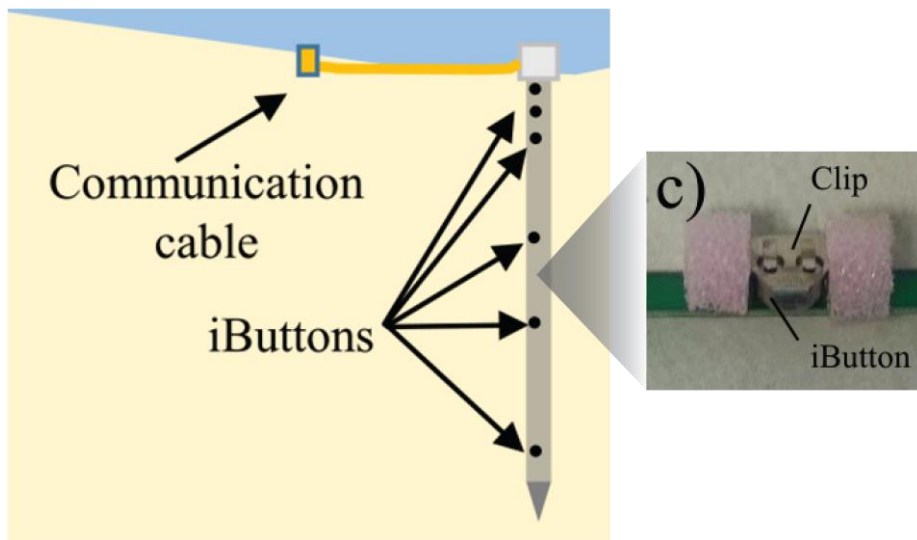


Figure G.2-2. Discrete subsurface temperature profiling probe (TROD). *Used with permission from Naranjo & Turcotte (2015).*



Figure G.2-3. Thermocouple reel to measure adjacent soil temperature profile. *Courtesy of Ririe & Sweeney 2016)*



Figure G.2-4. Use of existing monitoring well and dedicated temperature logger string for approximation of the adjacent soil temperature profile. Courtesy of Ririe & Sweeney (2016) and Maxim Integrated, (www.maximintegrated.com)

Log soil temperatures

The technique for temperature logging depends on the selected measurement device. An automatic data logger with hourly recording frequency, for example, is useful to track transient trends and derive robust daily, monthly, and/or annual average temperatures. Measurement devices with manual snap-shot in time recorded temperatures are also acceptable as long as the data quality is consistent with the data use.

The duration of monitoring is a site-specific judgment and based on the magnitude of soil temperature variability due to seasonality. Warmer climates or deeper oxidation zones with a relatively uniform temperature within the zone of the thermal anomaly may only need a month or two of monitoring. Other sites may require up to a year or more. In general, longer monitoring durations improve the representativeness of the data. One-time or routine temperature measurements may be collected, but the data quality may be qualified as screening-level if not collected when conditions are near an average condition. As detailed in section 5.1.1, the use of long-term averaged temperature data results in a more representative, time-weighted average NSZD rate.

Estimate the soil thermal conductivity

Thermal conductivity (K_T) can be estimated using either lab testing, calculations, or literature sources. A volume-weighted average value (or geometric mean) should be used that is representative of all different lithologies within the oxidation zone (Warren & Bekins 2018).

Literature means to estimate thermal conductivity

The thermal conductivity of most earth materials is between 0.1 to 4 J/m/s/°K. Considering this relatively small range, empirical estimates of K_T using literature values based on known soil conditions are feasible without significantly compromising data quality level. Table G.2-1 presents typical thermal conductivity and thermal diffusivity values based on soil type (Sweeney & Ririe 2014).

Table G.2-1. Thermal properties of air, water, and soil. *Reproduced with permission from Sweeney & Ririe (2014).*

Thermal Properties of Air, Water, and Soil Types*				
Material	Heat Capacity		Thermal Conductivity	Thermal Diffusivity
	C _g (J/kg-K)	C _v ((10 ⁶ J/m ³ -K)	k (J/m-s-K)	α (10 ⁻⁸ m ² /s)
Air	1004	0.001	0.03	1938
Water	4181	4.18	0.60	14
Soil	800	1.44	0.17–3.98	12–276
Sand (saturated)	1257	2.64	2–4	76–152
CTS	1089	1.76	1.67	95
M-FTS	1508	2.14	1.26	59
Sand (dry)	794	1.27	0.15–0.25	12–20
CTS (dry)	838	1.34	0.17	13
M-FTS (dry)	838	1.09	0.10	10

CTS = coarse-textured soil; M-FTS = medium to fine-textured soil.

Note: De Vries and Afgan (1975).

*Modified from Wisconsin.edu—soils website.

Site-specific measurement of thermal conductivity

A laboratory method (Sass *et al* 1984) is available to measure the thermal conductivity of soil near room temperature using a line-source method. A probe is inserted into either unconsolidated soil or drilled into more competent rock. A constant current source is applied to the probe and the temperature drift rate of the apparatus is monitored and equated to a material thermal conductivity. This method is commercially available at large geotechnical laboratories.

Tabulate the data and calculate average temperatures

After the desired temperature data is logged and downloaded, it can be entered into a database for statistical analysis. Quite simply, for each measurement location and depth, the average (or mean) value is calculated. The period of which the average is calculated is a site-specific judgment, but will determine the time period over which the NSZD rate can be stated. For example, if a day or year period of data are averaged, then the NSZD rate can be stated in terms of gram per square metre per day (g/m²/d) or kilogram per square metre per year (kg/m²/yr), respectively.

Plot the average data and account for background

Plotting the average temperature profiles at the measurement locations is a useful exercise to observe the difference between soil temperatures atop and aside the LNAPL footprint. As discussed in section 1.5.3, the temperature of the soil above the LNAPL will often be warmer than its surroundings and a depth profile plot can visually illustrate the magnitude of the difference.

The authors that describe the methods summarised on table G.1-1 noted the large variations in subsurface temperatures can be numerically managed through averaging of depth temperature profiles to provide a more representative time-integrated thermal gradient. Figure G.2-5 presents the results of 8-month averaging at two temperature profile measurement locations (DBT1 and DBT2) at a warm climate site near Perth, Western Australia. The average background soil temperature is also plotted. The background location ranges between 18 degrees °C and 20 °C while the thermal signature from oxidation of gases generated by underlying NSZD has a distinct peak with a ΔT of approximately 13 °C at 3 metre below grade (mbg). This is the data that is carried forward into the calculations.

Estimating NSZD-related heat fluxes is complicated by non-petroleum related variations in soil temperature. In this document, background is considered heat that is unrelated to the presence of the petroleum hydrocarbon LNAPL source. This includes contributions from atmosphere or groundwater. The effects from background heat tend to be most significant at sites with a shallow LNAPL smear zone and/or groundwater table, but are variable from site to site. Selection of high quality background monitoring locations is vital to the success of the biogenic heat method.

There are numerous challenges with background correction using temperature monitoring results from outside the LNAPL footprint, especially at sites with:

- diverse ground cover (e.g. that can have differing insulating properties)
- subsurface utility presence
- active natural soil processes (for the same reason as discussed for the gradient method – see appendix D.1)
- variable depth to LNAPL source zones, or
- surface water drainage pattern.

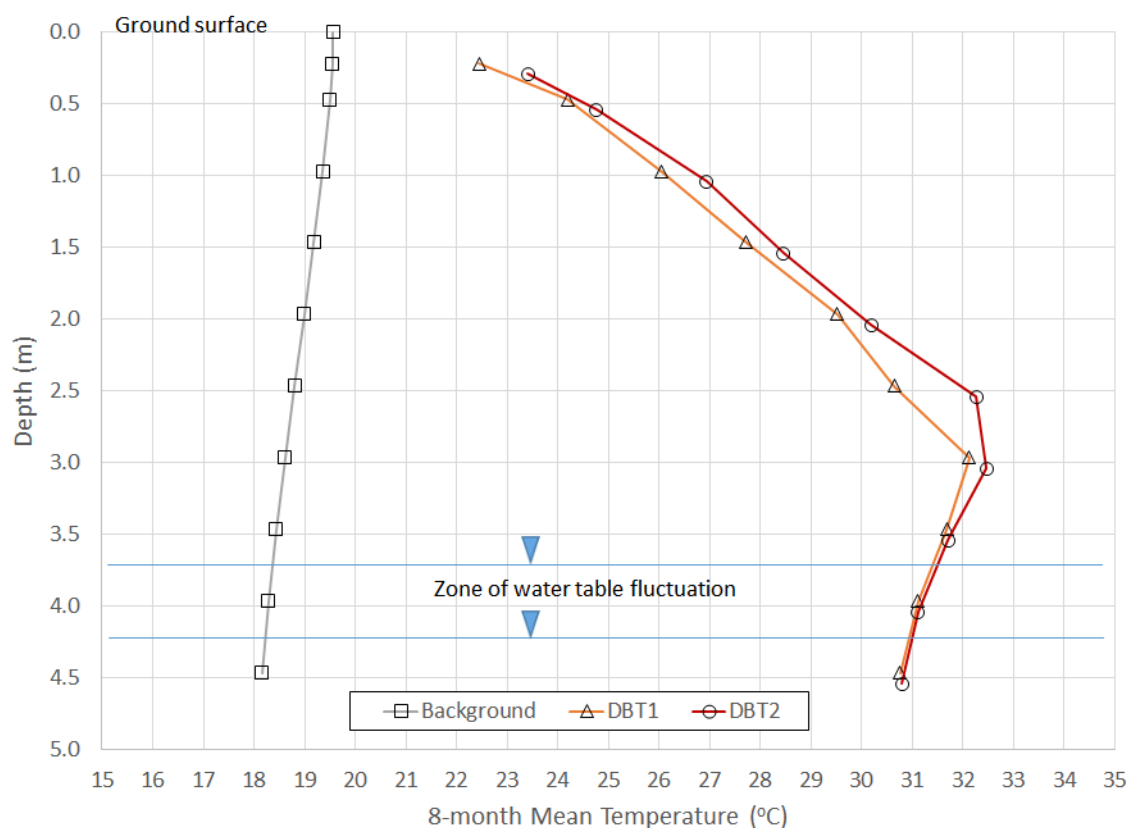


Figure G.2-5. 8-month average temperature profile at a background and LNAPL-impacted locations.

Therefore, it is important to determine which method of background correction will be used as part of the NSZD program design stage because it will affect the number of locations to be measured.

If additional sources of heat are identified (e.g. subgrade pipelines), then it is important to account for this additional heat source otherwise NSZD rates will be over-estimated

(Warren & Bekins 2018). Preference is to monitor biogenic heat distal from any additional sources of heat that may confound the data evaluation.

There are two different approaches to eliminate heat flux contributions from non-NSZD processes: install temperature measurement locations in a nearby uncontaminated setting with similar surface and subsurface conditions and use mathematical means. Background temperature measurement is preferred, but this guidance offers an alternative because complexities commonly exist at remediation sites that may preclude this.

Direct measurement of background temperature

Temperature measurements and data averaging are performed for a background location in the same way as done for the locations overlying the LNAPL footprint. As shown on figure G.2-5, the background and LNAPL locations can be compared to visually assess temperature differences. Next step is to subtract the background temperatures from the measurement locations atop the LNAPL. Figure G.2-6 shows the results of background correction using measured data.

As discussed above, the number of background locations will be driven by the diversity in site conditions. Ideally the background temperatures are measured in each significantly unique soil condition. If large variability in background measurements are observed, then a statistical approach may be useful (e.g. based on pre-established confidence limits).

Mathematical estimation of background temperature

If background soil temperatures are not measurable (e.g. offsite in areas without legal access permission) or site conditions are relatively uniform and free from potential interference listed above, then mathematical means can be used to estimate background soil temperatures. Note that this background correction option neglects the effects that groundwater temperature has on the overlying soil. Therefore, if groundwater temperatures depart from the annual average ambient/atmospheric temperature, then reconsider using this approach.

Depending upon the depth to the hydrocarbon oxidation zone and the seasonal changes in the ambient and groundwater temperatures, the temperature profile can vary with time. The sinusoidal Van Wijk & de Vries (1963) function was proposed as an analytical solution to estimate subsurface temperatures based on ambient temperature variation, key soil properties, and curve fitting constants as shown in equation G.1 (Sweeney & Ririe 2014).

$$\text{Equation G.1: } T_{(z,t)} = T_o + A_o * \left(e^{-\frac{z}{D}} * \sin \left(w * t - \frac{z}{D} + \psi \right) \right)$$

where $T_{(z,t)}$ is the soil temperature ($^{\circ}\text{K}$) at depth z (m) and time t (s), T_o is the mean annual ambient temperature ($^{\circ}\text{K}$), A_o is the amplitude of the sinusoidal curve ($^{\circ}\text{K}$), w is the angular frequency (s^{-1}) equal to $\frac{2\pi}{P}$ where P is the period of the sinusoidal curve (s) typically set to 365 days, D is equal to $\frac{2 * \alpha^{0.5}}{w}$ where α is thermal diffusivity of the soil (m^2/s), and Ψ is a phase shift curve fit parameter (s).

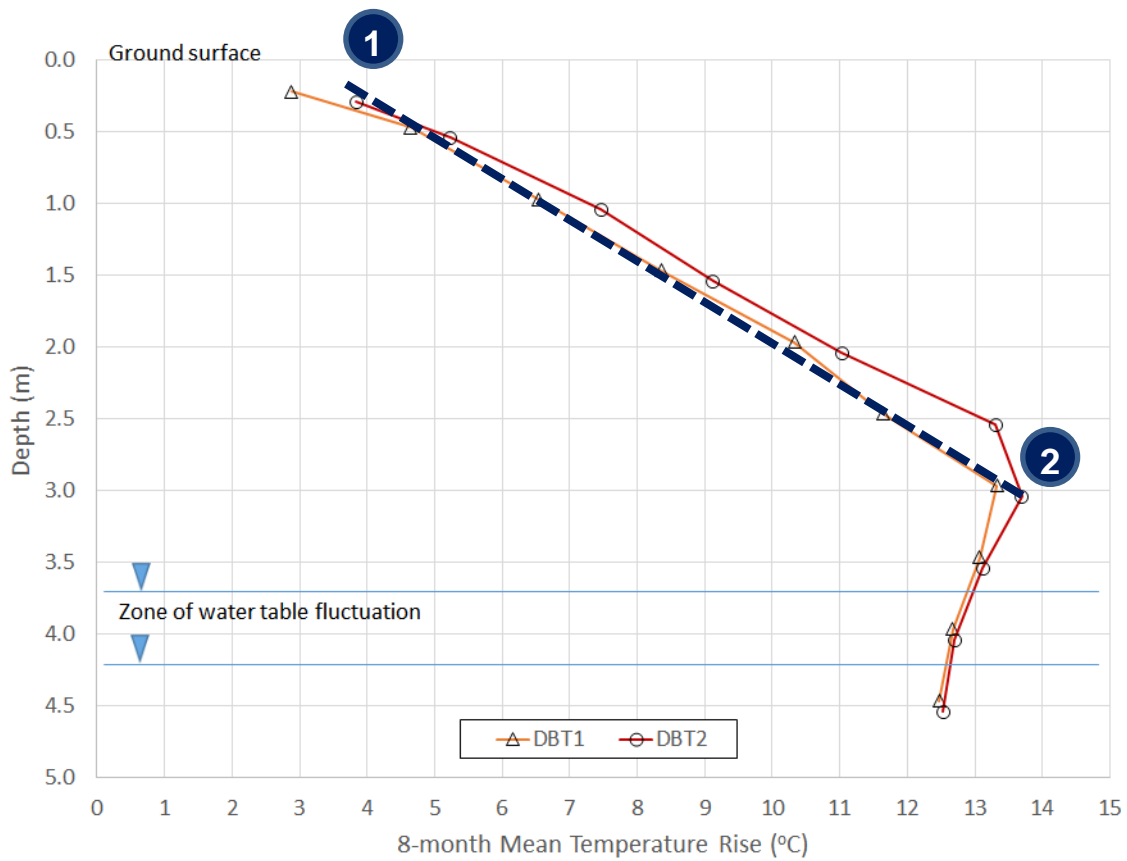


Figure G.2-6. Background corrected 8-month average temperature profile at a location atop LNAPL-impacts. Upper (1) and lower (2) control points shown with estimated thermal gradient in dashed line.

Figure G.2-7 presents an example temporal change in ambient and subsurface temperatures at a moderately temperate site (i.e. approximately 10 °C seasonal mean daily temperature swing). The ambient temperature is plotted over a two year period of time with a curve fit using the modified Van Wijk and de Vries function. Subsurface temperatures are shown for a silty, clayey sand with a thermal diffusivity (α) of $5.0 \times 10^{-7} \text{ m}^2/\text{s}$, phase shift Ψ is $-3.1 \times 10^4 \text{ s}$, sine wave amplitude is 4.7 °K, and mean annual temperature is 292.9 °K (19.75 °C).

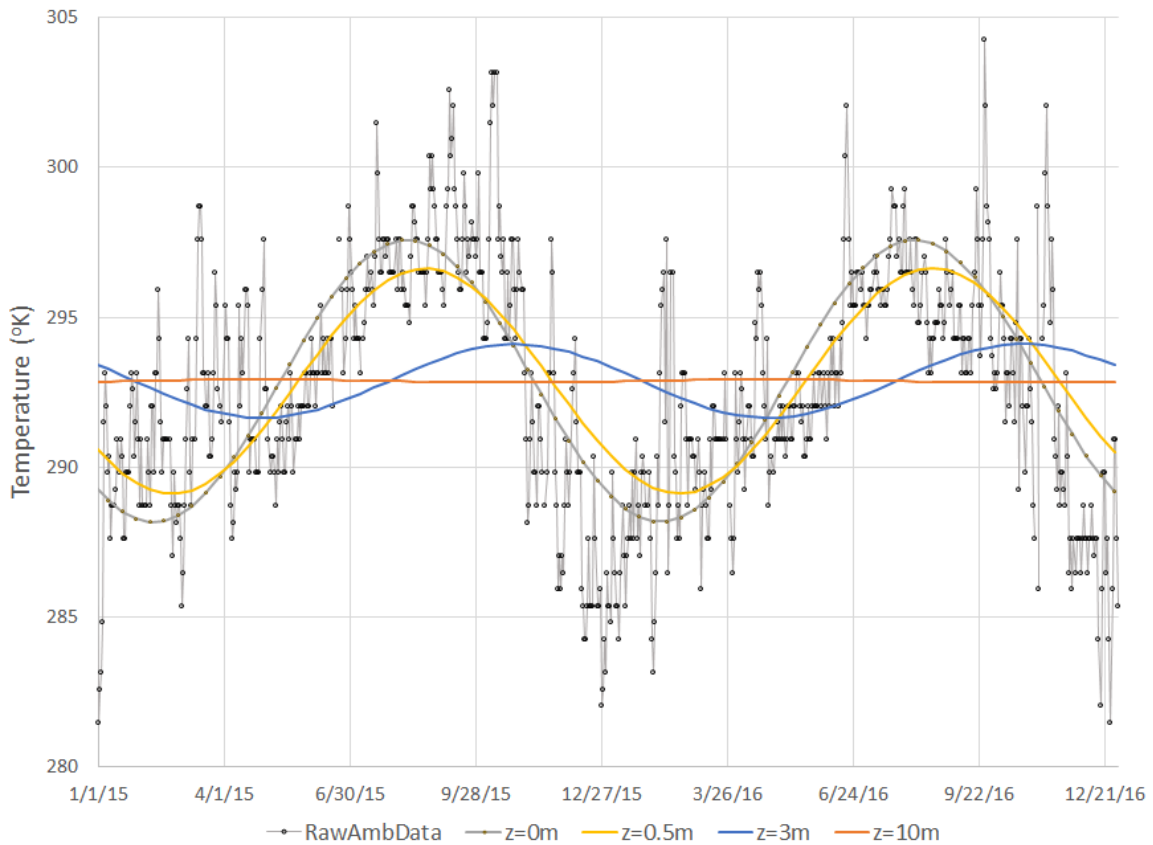


Figure G.2-7. Temporal change in subsurface temperatures as they relate to ambient temperature.

Of note on figure G.2-7 are a more significant temperature variation in shallow soils. At a depth of 10 m, little discernible change in soil temperature is evident. Additionally, there is a lag in time between ambient temperature change and subsurface temperatures, up to three months at a depth of 3 m. The mean annual temperature is observed in early February and early August at this site. This is significant in that NSZD monitoring may be optimally performed when temperatures within the smear are near average ambient temperature.

Using the Van Wijk and de Vries function (equation G.1), the background soil temperatures can be estimated and tabulated for each measurement depth interval. The average background temperature profile for the period of interest can be calculated and plotted as shown on figure G.2-5 and used to correct the measurements collected over the LNAPL footprint as shown on figure G.2-6.

Estimate thermal gradient of NSZD

The difference in temperature between the upper and lower boundary control points of measurement, divided by the vertical distance between the control points, gives an estimate of the vertical thermal gradient as shown in equation G.2.

$$\text{Equation G.2: } \frac{\Delta T}{\Delta z} = \frac{T_2 - T_1}{z_2 - z_1}$$

where T_1 and T_2 are the background corrected soil temperatures at depths z_1 and z_2 , respectively. Subscript 1 represents the upper control point and 2 the lower as shown on figure G.2-6. The corresponding temperatures and depths are picked off the figure and a thermal gradient is estimated.

The shapes of the corrected thermal profiles from NSZD can be variable. The temperature of the groundwater may or may not be similar to the thermal maxima. As a result, it is important to inspect the thermal profiles and assess whether an added thermal gradient is necessary to more accurately account the total heat flux. As discussed in section 7.1 of API (2017), the total heat flux theoretically equals a summation of losses from the temperature peak to atmosphere (upper) and groundwater (lower). In practice, measurement of the heat flux to groundwater has not been rigorously analysed. Because the net effect of neglecting it results in a conservative estimate of NSZD (i.e. an under-estimate), it is the prerogative of the practitioner to assess the need and value of including it in the calculations.

Calculate the NSZD rate

After the thermal conductivity (K_T) and thermal gradient ($\Delta T/\Delta z$) are estimated, the heat flux is calculated. The last step is then to calculate the NSZD rate. As specified in section 5.1.2, the enthalpy of methane (CH_4) oxidation (ΔH°) can be used in this calculation. Simple division to obtain the NSZD rate (R_{NSZD}).

Gradient method quality assurance/quality control

Appropriate QA/QC measures are essential to assess the accuracy and precision of the data collected. Use proper, manufacturer-recommended calibration procedures for all field instruments. A minimum two-point calibration is typically prudent with a span calibrated to the range of expected soil temperatures.

G.3 – Example biogenic heat method-based NSZD rate calculations

A case study with example calculations is presented in this section to illustrate how this guidance for NSZD rate measurement using the biogenic heat method can be applied. It is based on a real setting where NSZD monitoring was performed.

Site background

The biogenic heat method was employed at a major industrial facility in the Perth coastal plain in Western Australia. It is situated in a warm climate zone with hot summers and mild wet winters. Gasoline and diesel releases impacted the calcareous fine to medium dune sands. Depths to water range from 3 to 5 metre below grade (mbg).

Use of the biogenic heat method to estimate the rate of NSZD involves the following steps:

1. Install soil temperature measurement devices or establish alternative means for temperature monitoring as discussed herein
2. Log soil temperatures for an extended period of time as discussed below
3. Estimate the soil thermal conductivity
4. Tabulate the data and calculate the average temperature
5. Plot the average data and account for background
6. Estimate the thermal gradient, and
7. Calculate the NSZD rate.

The following sections detail each of these steps was accomplished on this site.

Thermistor string installation

Two temperature monitoring clusters were installed (figure G.3-1) with ten thermistors at varying depths per location. The thermistor strings were installed for the purposes of monitoring the baseline effectiveness of NSZD prior to start-up of an air sparging system. Specifically, they provided the temperature data needed to assess thermal gradients in the vadose zone.

Temperature logging

The thermistor strings were manually downloaded on 23 occasions between 30 November 2005 and 18 July 2006. Temperatures at each of the thermistor locations was recorded. Table G.3-1 presents the data collected at location DBT1 during this approximate eight-month period.

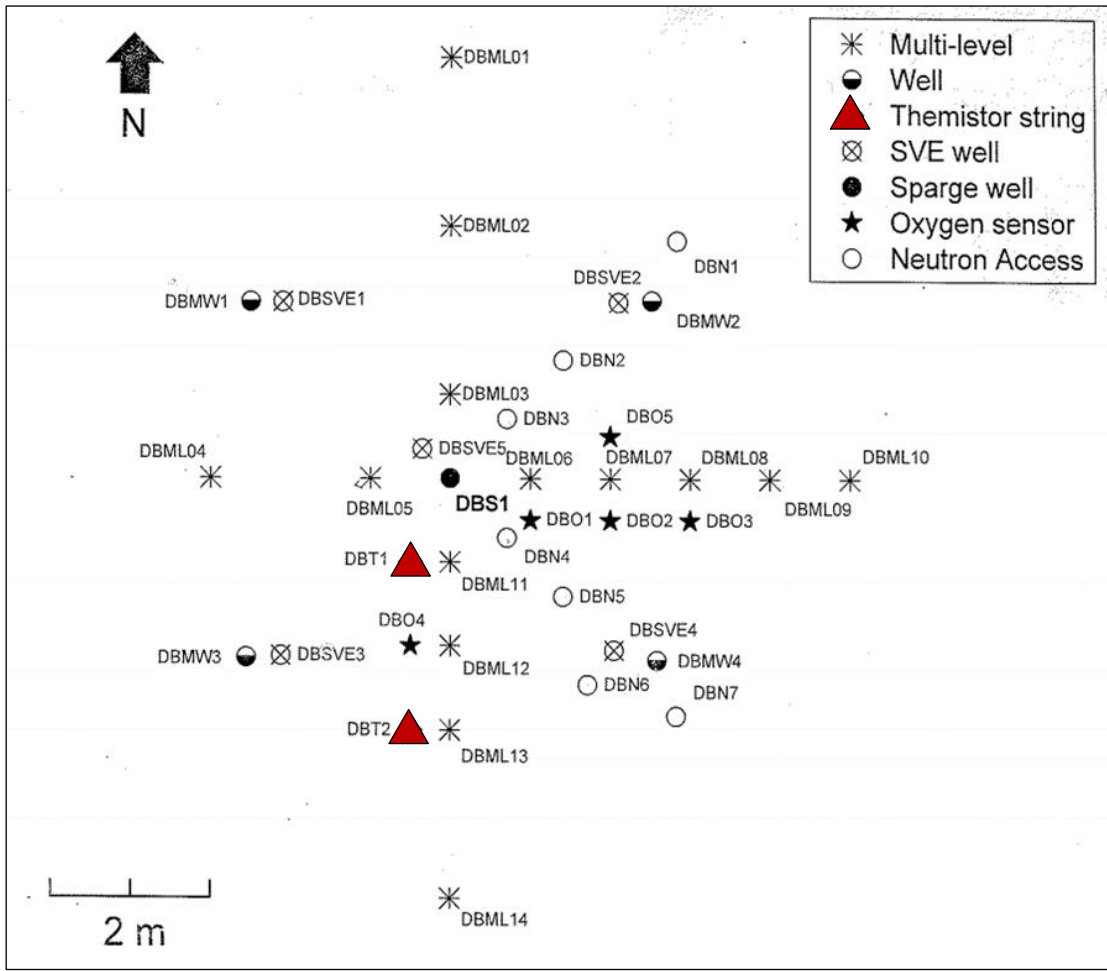


Figure G.3-1. Temperature monitoring locations and other site monitoring stations.

Soil thermal conductivity

The effective soil thermal conductivity was calculated from a quadratic, parallel model of multiple constituent conductivities (Johnston *et al* 2007). The thermal conductivity of the soil formation was estimated to be 1.86 J/m/s/°K. As discussed in appendix G.2, no lab analysis was performed since it is a relatively insensitive parameter and the soil horizon across the depth interval of concern is relatively uniform sand.

Data tabulation and temperature averaging

All temperature data was entered into a simple Excel worksheet. For each depth interval, an average temperature was calculated as shown on the bottom row of table G.3-1.

Background correction

The most complex element of this case study was background correction. No background temperature measurements, in similar faceted locations, could be taken due to the complexities of working around the major industrial site. Therefore, the Van Wijk and de Vries mathematical solution was used instead.

Table G.3-1. Raw temperature measurements at thermistor monitoring location DBT1.

		DBT1 - measured									
Depth below ground, z =		0.22	0.47	0.97	1.47	1.97	2.47	2.97	3.47	3.97	4.47
	Date	T (°C)	T (°C)	T (°C)	T (°C)	T (°C)	T (°C)	T (°C)	T (°C)	T (°C)	T (°C)
	11/30/05	24.0	24.7	24.9	25.2	26.7	27.1	28.9	29.1	29.4	29.8
	12/7/05	23.5	24.0	25.0	25.7	26.8	27.9	29.8	29.6	29.3	29.8
	12/13/05	23.2	24.3	25.1	26.0	27.2	28.5	30.2	29.7	29.6	29.8
	12/23/05	24.2	26.0	26.0	26.7	28.0	29.3	30.9	30.1	29.8	29.9
	1/13/06	25.0	27.4	27.9	28.3	29.2	30.1	31.6	30.8	30.3	30.1
	1/17/06	27.5	27.6	27.6	28.5	29.5	30.5	31.7	30.9	30.3	30.1
	1/19/06	27.3	28.3	27.8	28.6	29.6	30.5	31.9	31.0	30.4	30.2
	2/1/06	24.9	26.7	28.1	29.1	30.1	30.9	32.3	31.3	30.6	30.3
	2/9/06	26.6	28.0	28.6	29.3	30.3	31.2	32.6	31.6	31.4	30.5
	2/16/06	27.4	29.2	29.2	29.7	30.7	31.5	32.7	31.8	31.3	30.5
	3/1/06	29.4	29.7	29.4	30.1	31.5	31.9	33.0	32.0	31.1	30.7
	3/13/06	26.4	28.8	30.2	30.9	31.7	32.2	33.4	32.3	31.4	30.8
	3/22/06	27.9	28.7	29.7	30.7	32.3	32.4	33.5	32.5	31.6	30.9
	4/4/06	21.9	24.7	27.9	30.1	31.9	32.6	33.5	32.8	31.8	31.2
	4/11/06	23.0	24.9	27.4	29.6	31.6	32.4	33.6	32.9	31.8	31.2
	4/21/06	22.2	23.2	26.4	29.0	31.2	32.2	33.6	32.9	31.9	31.3
	5/5/06	19.3	21.5	25.2	28.0	30.7	31.9	33.1	32.9	32.0	31.4
	5/11/06	18.5	21.0	24.6	27.6	30.0	31.7	33.1	32.8	32.0	31.4
	5/25/06	15.4	19.6	23.8	26.8	29.4	31.1	32.6	32.5	31.9	31.4
	6/9/06	14.0	17.2	21.8	25.4	28.4	30.3	32.2	32.3	31.8	31.4
	6/26/06	16.4	17.1	20.8	24.3	27.5	29.6	31.6	31.9	31.6	31.3
	7/6/06	14.7	17.4	21.0	24.2	27.6	29.8	32.1	33.1	32.4	31.7
	7/18/06	13.3	16.2	20.3	23.8	26.9	29.0	31.1	32.0	31.9	31.7
Average		22.4	24.2	26.0	27.7	29.5	30.6	32.1	31.7	31.1	30.7
ΔT from background		3.8	5.8	7.9	9.9	12.0	13.3	14.8	14.4	13.8	13.5

Daily average temperature meteorological data was downloaded from a nearby weather station in Perth for the duration of the thermistor monitoring. It was tabulated in an Excel worksheet.

A sinusoidal curve was fit to the data using the Excel Solver add-in. The curve fit equation is shown in equation G.3.

$$\text{Equation G.3: } T = T_o + A_0 \sin(\omega t + \varphi)$$

where T_o is the mean atmospheric temperature (°K), A_0 is amplitude of the sine wave (°K), $\omega = 2\pi/P$ (1/d), P is the sine wave period (d), and φ is a phase shift, curve fit parameter (d).

The Excel Solver was used to iteratively solve for the best fit solution. Under the Data menu, Solver was selected. In the Solver parameter box, an empty cell was set as the Set Objective and the Min value selected. A value of 1 was set for both A and ψ . The mean ambient temperature of the data set, or a value of 291 °K, was entered for T_o . P was assigned the standard value of 365 d. By Changing Variable Cells data range was set to include A , ψ , and T_o . A constraint was set to include the A value to be greater than or equal to 0. The Make Unconstrained Variables Non-Negative box was left unchecked. After setting these parameters, the Solver was run. The resultant curve fit parameters were as follows:

- $A = 5.68$ °K
- $\Psi = 0.59$ d
- $T_o = 291.0$ °K
- $P = 365$ d
- $w = 0.017$ /d

A graphical check of the success of the curve fit was also performed. Figure G.3-2 shows that the Solver produced reasonable results and thus the parameter values were carried through to the next step of the process.

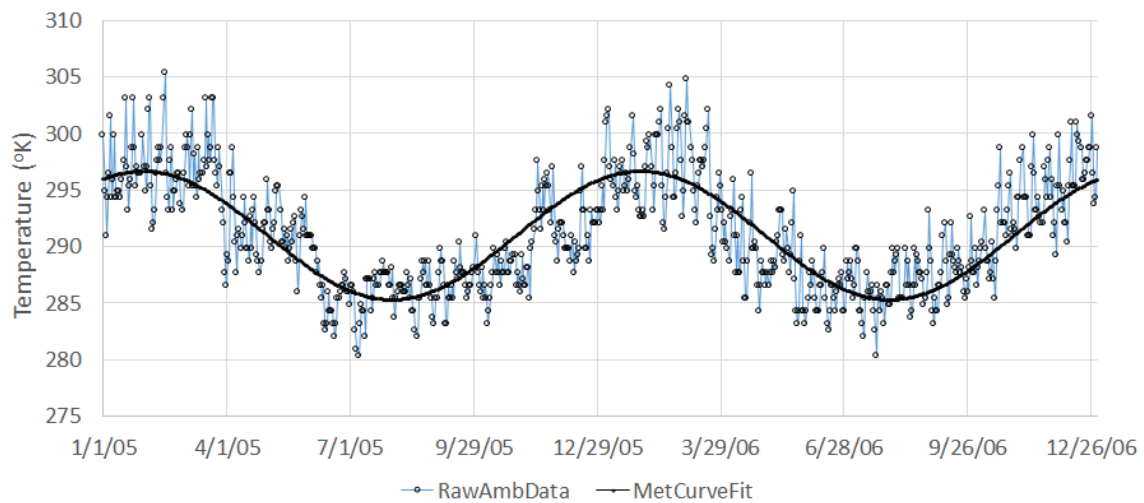


Figure G.3-2. Graphical check of the meteorological data curve fit results.

Next, the curve fit parameters were used in equation G.1 to estimate the background soil temperatures at all the monitored depths.

$$\text{Equation G.1: } T_{(z,t)} = T_o + A_o * \left(e^{\frac{-z}{D}} * \sin \left(w * t - \frac{z}{D} + \psi \right) \right)$$

where $T_{(z,t)}$ is the soil temperature (°K) at depth z (m) and time t (s), T_o is the mean annual ambient temperature (°K), A_o is the amplitude of the sinusoidal curve (°K), w is the angular frequency (1/s) equal to $\frac{2\pi}{P}$ where P is the period of the sinusoidal curve (s) typically set to 365 days, D is equal to $\frac{2 * \alpha^{0.5}}{w}$ where α is thermal diffusivity of the soil (m^2/s), and Ψ is a phase shift curve fit parameter (s).

With the exception of D and α , all values were carried over from the meteorological data curve fit and units were converted. α was estimated to be $8.0 \times 10^{-7} \text{ m}^2/\text{s}$ based on the geologic data (moist fine-medium sand) provided in Johnston *et al* (2007), table G.2-1, and figure G.3.3 which shows some additional typical values and correlation with thermal conductivity, K_T (E-Flux, LLC 2017). D was then calculated to be 2.83 metre (m).

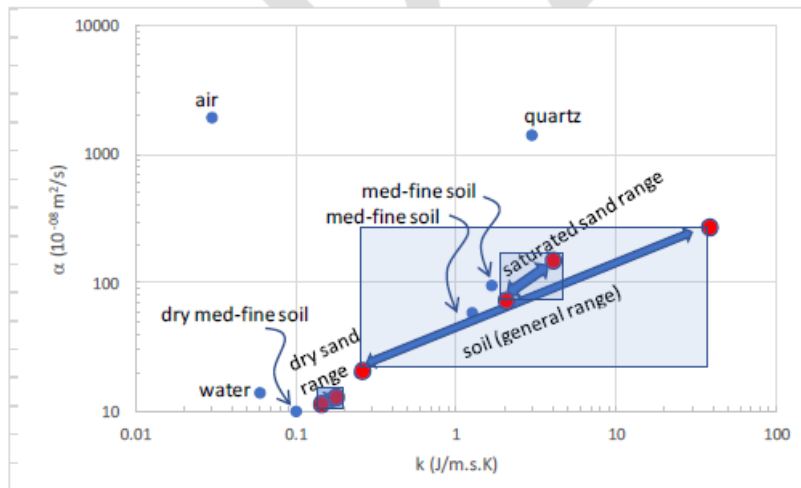


Figure 2. Values and ranges for different soil types (values from Chiasson et al., 1999; Bristow, 1997; Sweeney and Ririe, 2014). Ranges are shown with blue arrows and red circle limits. Note red circle extremes are shown assuming highs and lows of both properties plotted are paired - no correlation is implied by the arrow shown (although some is expected based on Equation 4). A light-blue shaded box is shown to represent a hypothetical lack of correlation. Note logarithmic scales on both axes.

Figure G.3-3. Graphical check of the meteorological data curve fit results. *Reproduced with permission from E-Flux, LLC (2017).*

With all values known, the equation G.1 was entered into a matrix in Excel to solve for background temperatures at all monitoring locations and depths. Table G.3-2 shows the computed background temperatures for thermistor location DBT1.

The 8-month averaged temperature profile values for both thermistor monitoring locations (DBT1 and DBT2) and the calculated background were plotted to visually assess differences in locations and background (figure G.3.4).

The background temperatures were then subtracted from the DBT1 and DBT2 measurements to derive the background-corrected temperature profiles shown on figure G.3.5. These charts were used to estimate the thermal gradients in the next step.

Table G.3-2. Calculated background temperatures at thermistor monitoring location DBT1.

Depth below ground, z =	DBT1 Background - calculated											
	0	0.22	0.47	0.97	1.47	1.97	2.47	2.97	3.47	3.97	4.47	
Date	T (°C)	T (°C)	T (°C)	T (°C)	T (°C)	T (°C)	T (°C)	T (°C)	T (°C)	T (°C)	T (°C)	T (°C)
11/30/05	12.2	12.6	13.0	13.9	14.7	15.4	16.1	16.6	17.1	17.4	17.7	17.7
12/7/05	12.3	12.7	13.0	13.8	14.6	15.3	15.9	16.4	16.9	17.2	17.5	17.5
12/13/05	12.5	12.8	13.1	13.8	14.5	15.1	15.8	16.3	16.7	17.1	17.4	17.4
12/23/05	12.9	13.1	13.3	13.9	14.4	15.0	15.6	16.1	16.5	16.9	17.2	17.2
1/13/06	14.3	14.2	14.3	14.4	14.7	15.1	15.5	15.9	16.2	16.6	16.9	16.9
1/17/06	14.6	14.5	14.5	14.6	14.8	15.1	15.5	15.8	16.2	16.6	16.9	16.9
1/19/06	14.8	14.7	14.6	14.6	14.8	15.1	15.5	15.8	16.2	16.5	16.8	16.8
2/1/06	15.9	15.7	15.5	15.3	15.3	15.4	15.6	15.9	16.2	16.5	16.7	16.7
2/9/06	16.7	16.4	16.1	15.7	15.6	15.6	15.7	15.9	16.2	16.4	16.7	16.7
2/16/06	17.3	17.0	16.6	16.2	15.9	15.8	15.9	16.0	16.2	16.4	16.7	16.7
3/1/06	18.6	18.1	17.7	17.0	16.6	16.3	16.2	16.3	16.4	16.5	16.7	16.7
3/13/06	19.7	19.2	18.7	17.8	17.2	16.9	16.6	16.5	16.5	16.6	16.7	16.7
3/22/06	20.6	20.0	19.4	18.5	17.8	17.3	17.0	16.8	16.7	16.7	16.8	16.8
4/4/06	21.6	21.0	20.4	19.3	18.5	17.9	17.5	17.2	17.0	17.0	16.9	16.9
4/11/06	22.1	21.5	20.8	19.8	18.9	18.2	17.8	17.4	17.2	17.1	17.0	17.0
4/21/06	22.7	22.1	21.5	20.4	19.5	18.7	18.2	17.8	17.5	17.3	17.2	17.2
5/5/06	23.2	22.7	22.1	21.0	20.1	19.3	18.7	18.2	17.9	17.6	17.5	17.5
5/11/06	23.4	22.9	22.3	21.3	20.4	19.6	19.0	18.4	18.1	17.8	17.6	17.6
5/25/06	23.5	23.1	22.6	21.7	20.8	20.1	19.4	18.9	18.4	18.1	17.9	17.9
6/9/06	23.3	23.0	22.6	21.9	21.1	20.4	19.8	19.3	18.8	18.5	18.2	18.2
6/26/06	22.6	22.4	22.2	21.8	21.2	20.7	20.1	19.6	19.2	18.8	18.5	18.5
7/6/06	22.0	21.9	21.8	21.5	21.1	20.7	20.2	19.7	19.3	18.9	18.6	18.6
7/18/06	21.1	21.2	21.2	21.1	20.9	20.6	20.2	19.8	19.4	19.1	18.8	18.8
Average	18.6	18.4	18.2	17.8	17.5	17.4	17.3	17.3	17.3	17.3	17.3	17.3

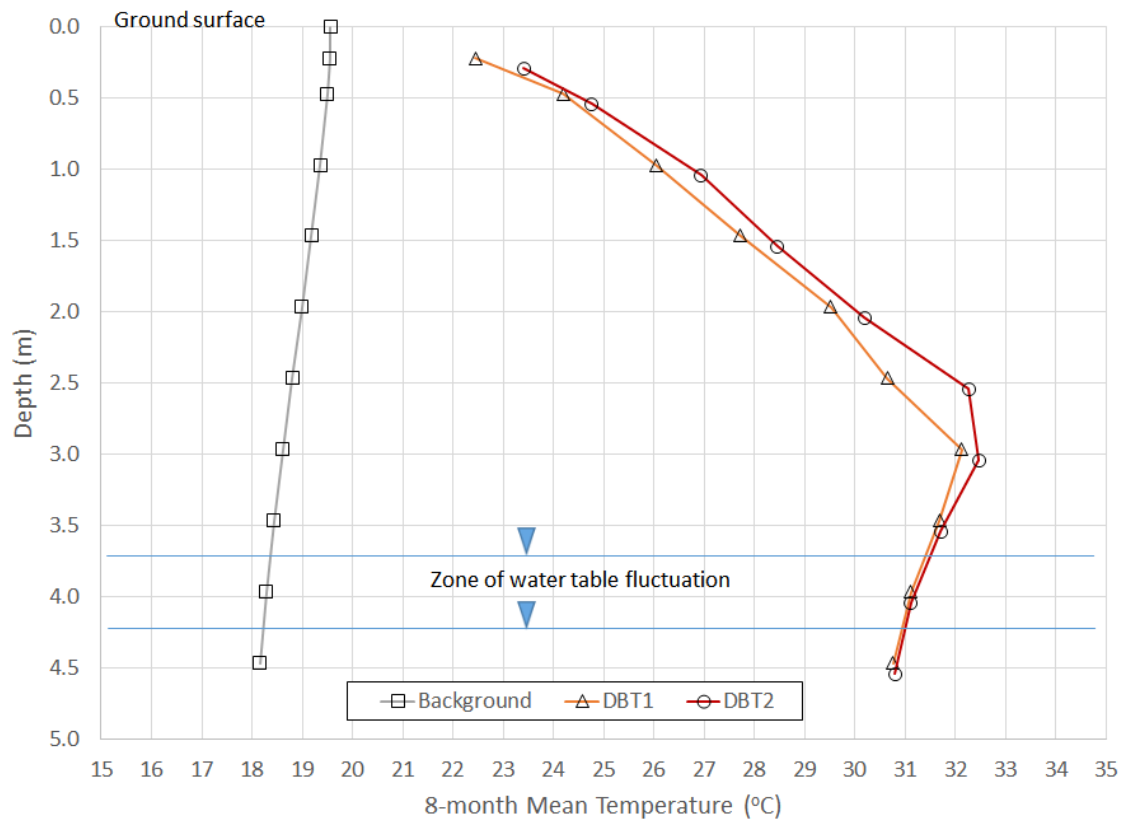


Figure G.3-4. 8-month average temperature profiles at a background and light non-aqueous phase liquid (LNAPL)-impacted locations.

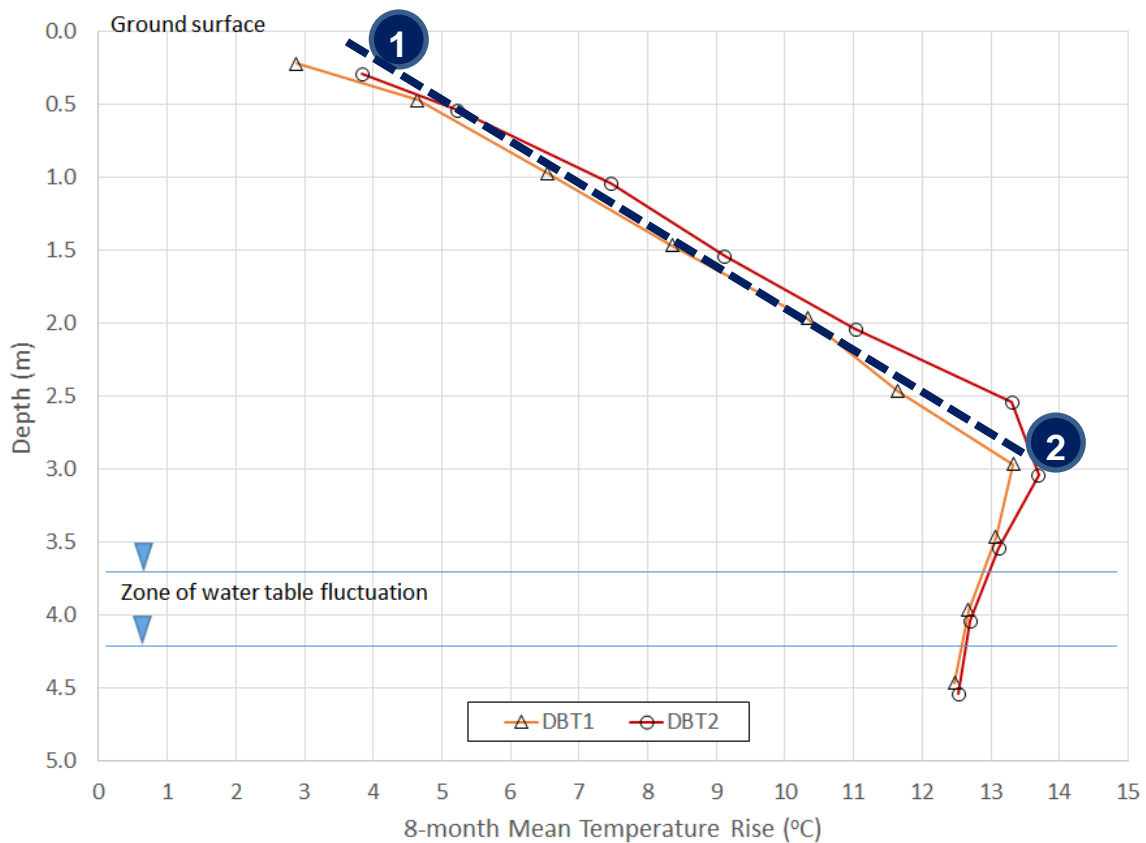


Figure G.3-5. Background corrected 8-month average temperature profiles at DBT1 and DBT2. Upper (1) and lower (2) control points shown with estimated thermal gradient in dashed line.

Estimate the thermal gradient

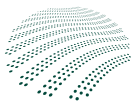
The thermal gradient is one of the key parameters in the equation to calculate the heat flux as shown in equation 10. $\Delta T/\Delta z$ is visually evident on figure G.3.5 between controls points 1 and 2. The upward thermal gradient at both DBT1 and DBT2 appears consistent; therefore, only one gradient will be calculated. As discussed in the text, taking a conservative method approach, the downward gradient will be ignored. Following equation G.2, the thermal gradient is estimated as follows:

$$\text{Equation G.2: } \frac{\Delta T}{\Delta z} = \frac{13.5-4}{3-0.2} = 3.4 \frac{^{\circ}\text{C}}{\text{m}} = 3.4 \frac{^{\circ}\text{K}}{\text{m}}$$

Multiplying the thermal gradient by the prior modelled thermal conductivity (1.86 J/m/s/°K), the heat flux, q_H , is estimated to be 6.3 Joules per square metre per second (J/m²/s).

NSZD rate calculation, J_{NSZD}

The last step in the process is use of equation 11 to calculate the NSZD rate. The remaining parameter is ΔH° , which is the heat of reaction (J/mol). As discussed in detail in section 5.1.2 of the main body text, sole use of the methane (CH₄) oxidation heat of $\Delta H^{\circ} = 43,900$ Joules per gram (J/g CH₄) is adequate to account for 98% of the mass of all hydrocarbons (e.g. volatile organic compounds and CH₄) that are oxidised (API 2017).



CRC CARE

*A safer, cleaner
environmental future*

CRC CARE

ATC Building
University of Newcastle
Callaghan NSW 2308
Australia

Postal

C/- Newcastle University LPO
PO Box 18
Callaghan NSW 2308
Australia

Contact us

P: +61 2 4985 4941
E: admin@crccare.com

www.crccare.com



Australian Government
Department of Industry,
Innovation and Science

Business
Cooperative Research
Centres Programme